The role and function of microRNAs in the nervous system

Development, nociception, and aging

Thesis submitted for the degree of Doctor of Philosophy

Clare Alice Martin, BSc (Hons)

Student ID: 4235046

September 2018





Declaration

I confirm that the work in this thesis is my own. Images from other sources, or work that has been generated through collaborative projects, have been otherwise acknowledged in the text.

Signed:

Clare Alice Martin

Acknowledgements

Firstly, I would like to thank my supervisors: Dr Federico Dajas-Bailador for his patience and guidance throughout my PhD, and Dr Marios Georgiou for his introduction to *Drosophila* work. In addition, I would like to acknowledge everyone else who I have worked with in both the Dajas-Bailador and Georgiou Labs both past and present. I would particularly like to thank Dr Alex Rathbone and Raquel Ribeiro for the last 4 years, and their invaluable advice and support. I would also like to thank Dr Gareth Hathway, Dr Tomas Bellamy, and the members of their labs for their help and guidance in pain research and calcium imaging, particularly the work of Dr James Spalton on hyperalgesic priming. The members of the Ronshaugen lab in Manchester, in particular Dr Tom Pettini, have also proved invaluable in supporting me. I am also grateful to Chris Gell and Ian Ward from SLIM for their training and support on the microscopes.

I would like to thank all the people who work on QMC D floor, for providing friendly faces in the corridor and being accepting of any unsolicited calls for advice, reagents and equipment, or trips to the pub. Particularly the members of the Layfield lab, who have always been supportive of all members of the Dajas-Bailador lab.

I would like to thank all of my friends, particularly my Sci-comm family, Bright Club members, and the Holibobs group, who have been with me since my first year of university. Rob, thank you for keeping me and Coco alive for these past few months, hopefully living with at least one of us will become easier now!

Finally, I reserve my biggest thanks to my family, particularly my Mum, Dad, Lee and Mark for always being there for me, even in my absence.

Abstract

In this thesis, novel functions for miRNAs in nervous system processes are characterised. It has been shown that miRNAs have the potential to play an important role in all aspects of the nervous system, from development and function to neurodegeneration. Reflecting on this breadth of possible roles for miRNAs, this is a thesis of two interconnected projects. Firstly, miRNAs with possible novel roles in inflammatory nociceptive processes were identified, and secondly, miRNAs with novel functions in nervous system development and function are investigated through the model system of *Drosophila*.

The work carried out demonstrates that miRNAs are dysregulated in the rat model of inflammatory pain, hyperalgesic priming. One miRNA, miR-138, has a distinctive expression profile that correlates with the pain behaviour. It is shown that miR-138 can potentially mediate inflammatory pain processes through direct targeting of the key inflammatory mediator MYD88. In order to investigate the molecular mechanisms of miRNA function in nociceptive processes, novel *in vitro* models were established. In these models, functional and molecular characteristics of sensory neuron cultures can be assessed within compartmentalised culture system, allowing a more accurate recapitulation of *in vivo* cellular environments.

The second part of this thesis focused first on the investigation of the effects that individual miRNAs can have on the development and function of the nervous system. The model of the *Drosophila* compound eye allowed for the identification of several miRNAs that can control crucial aspects of the development of these nervous system structures. One candidate miRNA which arose from this study, miR-190, was selected for further investigation. The expression pattern of miR-190 within the developing embryo of *Drosophila* was shown here through a modified *in situ* hybridisation protocol. Overexpression of miR-190 was found to cause detrimental effects in both *Drosophila* and mammalian neuron development, and a predicted conserved target for miR-190 which may explain this effect was identified, the transcription factor Dac/DACH1. An additional function for miR-190 was also proposed in this work in the mature nervous system. Inhibition of miR-190 in the neurons of adult *Drosophila*, leads to defects in the aged climbing ability and reduces lifespan of the adult. Bioinformatics analysis allowed for the proposal of a mechanism through which miR-190 exerts these effects, as predicted targets for the miRNA suggest a role in the modulation of the cholinergic system.

Overall, this work demonstrates the potential and breadth of miRNA functions in the nervous system, and characterises the role of two specific miRNAs within nociception, development, and aging. This work broadens our knowledge of the functioning of miRNAs themselves, and also of processes of the nervous system.

Contents

Chapter 1. General Introduction 1

1.1 The nervous system 1

1.2 Cell types of the nervous system 1

1.3 The neurone 2

1.4 The synapse 4

1.5 Protein homeostasis in the nervous system 7

1.6 Translation in the nervous system 8

1.7 Translational control 11

1.8 miRNAs 12

1.9 miRNA biogenesis 13

1.10 miRNA function 14

1.11 miRNA expression profiling methods 18

1.12 miRNA molecular tools for functional studies 20

1.13 miRNA target identification 21

1.14 miRNAs and the nervous system 24

1.15 Identified functions of miRNAs in nervous system development 26

1.16 miRNAs in nervous system differentiation 26

1.17 miRNAs in polarisation and neurite pathfinding 27

1.18 miRNAs in synapse formation and function 29

1.19 Summary 33

1.20 Hypothesis and aims 33

Chapter 2. Materials and methods 35

2.1 Identification of miRNAs which may play a role in pain processes 35

2.1.1 Hyperalgesic priming and Dorsal Root Ganglion extraction 35

2.1.2 RNA extraction from fixed DRG tissue 35

2.1.3 TRIzol extraction of RNA 35

2.1.4 miRNA microarray 36

2.1.5 qPCR 36

2.1.6 Bioinformatics 37

2.1.7 Cloning of miRNA target sites into luciferase construct 37

2.1.8 Site-directed mutagenesis of miRNA target constructs 38

2.1.9 Seeding and transfection of HEK293T cells for luciferase assay 39

2.1.10 Luciferase reporter assay 39

2.2 *In vitro* modelling of nociception 40

2.2.1 Dissociation of DRG 40

2.2.2 Bath culture of dissociated DRG 40
2.2.3 Calcium imaging 40
2.2.4 Microfluidic device culture 41
2.2.5 Immunofluorescence 42
2.2.6 Lipophilic tracer dye 42
2.2.7 Culture of DRG on porous membranes 42
2.2.8 Extraction of cell fractions from porous membrane culture 43
2.3 Identification of miRNA which may play a role in nervous system development 43
2.3.1 *Drosophila* stocks 43
2.3.2 *Drosophila* husbandry and crosses 45
2.3.3 *Drosophila* eye imaging 45
2.3.4 *Drosophila* eye size measurement 46
2.3.5 *Drosophila* eye ommatidia disorder scoring 46
2.4 Investigation of miR-190 in nervous system development 46
2.4.1 Embryo collection and fixation 46
2.4.2 smiFISH miRNA probe design and preparation 47
2.4.3 smiFISH 47
2.4.4 Embryo immunostaining 48
2.4.5 *Drosophila* embryo imaging 48
2.4.6 Viability assay 49
2.4.7 Cortical cultures 49
2.4.8 Cortical transfections 49
2.4.9 Target predictions 50
2.4.10 *Drosophila* brain immunostaining 50
2.5 Investigation of miR-190 in nervous system function 50
2.5.1 Collection of age matched flies 50
2.5.2 Climbing assays 51
2.5.3 Longevity assays 51
2.6 Data analysis and statistics 51

PART I – INVESTIGATION OF MIRNA IN NOCICEPTION 53

Chapter 3. Identification of miRNAs which may play a role in pain processes 53
3.1 Introduction 53
3.1.1 The nervous system and pain 53
3.1.2 The sensory circuit 53
3.1.3 The sensory neuron 54
3.1.4 Nociceptive sensitisation 56

3.1.5 Central sensitisation 56
3.1.6 Peripheral sensitisation 57
3.1.7 Control of protein translation and sensitisation 59
3.1.8 miRNA and sensitisation 59
3.1.9 Hyperalgesic priming 63
3.1.10 Experimental aims 66
3.2 Results and discussion 67
3.2.1 Microarray to assess deregulated miRNAs in chronic pain 67
3.2.2 qPCR investigation of miR-138 through the priming protocol 72
3.2.3 Identification of functionally relevant targets for miR-138-5p 74
3.2.4 Validation of MYD88 as a target for miR-138-5p 79
3.3 Conclusions and future directions 81

Chapter 4. *In vitro* modelling of nociception 82
4.1 Introduction 82
4.1.1 *In vitro* assessment of nociception 82
4.1.2 Modelling of the nociceptive circuit 83
4.1.3 Microfluidic devices 84
4.1.4 Culture of DRG on porous membranes 85
4.1.5 Experimental aims 86
4.2 Results and discussion 87
4.2.1 Embryonic DRG cultures demonstrate subtypes relevant to nociception through calcium imaging 87
4.2.2 Microfluidic devices allow for the culture and functional analysis of DRG neurons 90
4.2.3 Culture of DRG on porous membrane allows for the extraction of RNA from cell body and axon 93
4.3 Conclusions and future directions 95

PART II – INVESTIGATION OF MIRNAS AND THEIR ROLE IN THE DEVELOPMENT AND AGEING IN THE NERVOUS SYSTEM OF *DROSOPHILA* MELANOGASTER 98

Chapter 5. Identification of miRNAs with a role in nervous system development 98
5.1 Introduction 98
5.1.1 *Drosophila* melanogaster as an experimental model 98
5.1.2 Gal4/UAS 99
5.1.3 Nervous system development in *Drosophila* melanogaster 100
5.1.4 Differentiation of nervous system cells 102
5.1.5 Axon growth and pathfinding 102

5.1.6 Synapse development 103
5.1.7 Using *Drosophila* to investigate non-conserved biological paradigms 104
5.1.8 The *Drosophila* compound eye 105
5.1.9 *Drosophila* melanogaster as a model to study miRNA 107
5.1.10 Experimental aims 110
5.2 Results and discussion 111
5.2.1 Eye size defects after overexpression of miRNAs in the developing eye 111
5.2.2 Defects in ommatidia patterning after overexpression of miRNA in the developing eye 113
5.2.3 Conservation of miRNA sequences 117
5.3 Conclusions and future directions 120

Chapter 6. Investigation of miR-190 in nervous system development 122
6.1 Introduction 122
6.1.1 miR-190 conservation 122
6.1.2 Identified functions of miR-190 123
6.1.3 Identified target genes of miR-190 125
6.1.4 Expression pattern of miR-190 126
6.1.5 Experimental aims 127
6.2 Results and discussion 129
6.2.1 smiFISH of miR-190 in *Drosophila* embryos 129
6.2.2 Modulation of miR-190 effect on *Drosophila* development 132
6.2.3 Effect of miR-190 modulation on murine cortical cultures 135
6.2.4 Identification of conserved miR-190 targets 137
6.2.5 Functional validation of predicted miR-190 target sites 139
6.2.6 Indications of conserved targeting of *dac* by miR-190 in *Drosophila* 141
6.3 Conclusions and future directions 147

Chapter 7. Investigation of miR-190 in mature nervous system function 149
7.1 Introduction 149
7.1.1 The mature nervous system of *Drosophila* 149
7.1.2 Adult behavioural assays in *Drosophila* 151
7.1.3 Experimental aims 152
7.2 Results and Discussion 153
7.2.1 miR-190 inhibition in neurons leads to a reduction in *Drosophila* lifespan 153
7.2.2 Inhibition of miR-190 in the nervous system and assessment of climbing ability 154
7.2.3 Inhibition of miR-190 within the nervous system and assessment of lifespan 157
7.2.4 Identification of targets of miR-190 which may indicate a role in nervous system function 159
7.3 Conclusions and future directions 163

Chapter 8. Final Conclusions **164**

8.1 Identification of miRNAs which could regulate nervous system function in chronic nociception and pain 164

8.2. Investigation of individual miRNAs that control nervous system processes in *Drosophila* melanogaster 167

8.3 Future directions 169

8.4 General findings 170

9. BIBLIOGRAPHY 172

10. APPENDICES 203

Appendix I. Plasmid maps 203

Appendix II - Hyperalgesic priming protocol 204

Appendix III. Chronic stage DRG microarray results 207

Appendix IV. UAS-miRNA *Drosophila* stock list 218

Appendix V. smiFISH probe sequences 220

Appendix VI. miR-190 role in *Drosophila* larval NMJ assessment 222

Appendix VII. Professional internship for DTP student's reflection 224

Figures and Tables

Table 1.1 Summary of nervous system cell types 2
Figure 1.1 Example diagram of a neuron. 3
Figure 1.2 A chemical synapse 5
Figure 1.3 Canonical miRNA biogenesis 14
Figure 1.4 miRNA mediated gene silencing 15
Figure 1.5 Luciferase reporter assay 22
Table 2.1.1 miRNA target site oligonucleotides 38
Table 2.1.2 Primers for site-directed mutagenesis 38
Table 2.3.1 *Drosophila* stocks 44
Table 2.3.2. Balancer Chromosomes and Markers 44
Table 2.3.3. Genetic Constructs 45
Figure 3.1.1 Schematic of the sensory circuit. 54
Table 3.1.1 Summary of peripheral sensory fibre subtypes originating from within the DRG 55
Figure 3.1.2 Published studies of miRNA levels within sensory ganglia in models of pain. 62
Figure 3.1.3. Hyperalgesic priming. 65
Figure 3.2.1 Microarray assessment of miRNA which show change in levels in the chronic pain state 67
Figure 3.2.2. Differentially expressed miRNA from microarray assessment at day 14 of the priming protocol 68
Figure 3.2.3. Published studies of miRNA levels within sensory ganglia in models of pain, and comparison to the microarray of miRNA levels in hyperalgesic priming. 71
Figure 3.2.4. Levels of miR-138-5p as assessed through microarray and qPCR throughout the hyperalgesic priming protocol. 73
Figure 3.2.5 Bioinformatics workflow for miRNA target identification. 75
Figure 3.2.6 MYD88 as a central node in inflammatory signalling 77
Figure 3.2.7. Luciferase assay confirmation of MYD88 as a target of miR-138-5p 79
Figure 4.1.1 Microfluidic devices 85
Figure 4.1.2 Porous membrane culture inserts. 86
Figure 4.2.1 Subsets of cells relevant to pain processes are present in embryonic DRG cultures based on their calcium responses 88
Figure 4.2.2 Microfluidic devices 91
Figure 4.2.3 Capsaicin responsive DRG cells extend functional axons through microgrooves 92
Figure 4.2.4 Porous membrane cultures show effective physical separation of DRG axons from cell bodies to allow for RNA extraction 93
Figure 5.1.1 The Gal4/UAS enhancer trap system 100
Figure 5.1.2 Nervous system development in *Drosophila* 101

Figure 5.1.3 The *Drosophila* compound eye 105
Figure 5.1.4 The *Drosophila* retinal determination network 106
Figure 5.2.1 Overexpression of miRNA can produce defects in eye size 112
Figure 5.2.2 Overexpression of miRNA can produce defects in ommatidia patterning 114
Figure 5.2.3 Summary of the miRNA overexpression screen in the developing eye 115
Figure 5.2.4 Conservation of miRNA sequences of those miRNA which produced a significant result in the *Drosophila* eye screen. 119
Figure 5.2.5 Summarisation of conserved miRNA results from the eye screen 120
Figure 6.1.1 Sequence conservation of miR-190 from *Drosophila* to human 122
Table 6.1.1 Summary of targets previously identified for miR-190 validated through luciferase assay 125
Figure 6.2.1 Confirmation of specific hybridisation of miR-190 probes 130
Figure 6.2.2 smiFISH of miR-190 in *Drosophila* embryos 131
Figure 6.2.3 Developmental effects due to miR-190 level modulation in the nervous system 134
Figure 6.2.4 Effect of miR-190 mimic and inhibitor in mouse cortical cultures 136
Figure 6.2.5 Identification of relevant conserved targets of miR-190 139
Figure 6.2.6 Luciferase assays to determine probable novel targets of miR-190a-5p 140
Figure 6.2.7 Effect of miR-190 overexpression on mushroom body development 142
Figure 6.2.8 miR-190 expression suggests conserved targeting of DACH1 145
Figure 7.2.1 Inhibition of miR-190 throughout the nervous system leads to a reduction of lifespan 153
Figure 7.2.2 miR-190 inhibition effect on climbing ability in adult flies 156
Figure 7.2.3 miR-190 sponge effect on lifespan expressed in nervous system subsets 159
Figure 7.2.4 Identification of predicted target genes for miR-190 which can modulate neuronal function 162

Abbreviations

Ago	Argonaute
CNS	Central Nervous System
Ct	Cycle Threshold
DAPI	4’,6-diamidino-2-phenylindole
DH	Dorsal Horn
DMEM	Dulbecco's modified eagle medium
DNase	Deoxyribonuclease
DRG	Dorsal Root Ganglia
FBS	Fetal Bovine Serum
GDNF	Glial cell derived neurotrophic factor
HEK293T	Human Embryonic Kidney 293T cells
HEPES	4-(2-hydroxyethyl)-1-piperazineethanesulfonic acid
IB4	Isolectin B4
KO	Knockout
LNA	Locked Nucleic Acid
LPS	Lipopolysaccharide
LTP	Long-term potentiation
miRNA (miR)	Micro Ribonucleic acid
MRE	miRNA recognition element
mRNA	Messenger Ribonucleic acid
MYD88	Myeloid differentiation primary response 88
NGF	Nerve growth factor
NGS	Normal Goat Serum
NMJ	Neuromuscular Junction
NTC	Non Template Control
Oligos	Oligonucleotides
p bodies	Processing bodies
PABP	Polyadenylate binding protein
PBS	Phosphate-buffered saline
PET	polyethylene terephthalate

PFA	Paraformaldehyde
PGE2	Prostaglandin E2
PNS	Peripheral nervous system
polyA	Polyadenylate
poly-T	Poly Thymine
pre-miRNA	precursor micro ribonucleic acid
pri-miRNA	primary micro ribonucleic acid
PS	Penicillin Streptomycin
qPCR	Quantitative Polymerase Chain Reaction
RISC	RNA-induced silencing complex
RNA	Ribonucleic acid
RNAPol	RNA polymerase
RNase	Ribonuclease
RNP	Ribonucleoprotein
SDS	Sodium Dodecyl Sulphate
smiFISH	Small Molecule Inexpensive Fluorescent In Situ Hybridisation
SNOR	Small Nucleolar RNA
SSC	Saline Sodium Citrate
TLR	Toll Like Receptor
UAS	Upstream activating sequence
UTR	Untranslated Region
WBR	Western Blocking Reagent

Chapter 1. General Introduction

1.1 The nervous system

The nervous system is a highly complex and precisely controlled network of circuits. This system is responsible for the sensing of external cues, processing of information, and relay of responses throughout the entire body. The nervous system is both a self-governing and consciously controllable system, with somatic and autonomic contributions leading to the correct function of the nervous system, and ultimately the survival of the individual. It has been quantified that the human brain contains, on average, 86.1 billion neuronal cells (Azevedo et al. 2009) and these specialised cells have the ability to communicate with each other in a highly regulated, yet dynamic circuit. This finely tuned complexity must first be established during nervous system development, and then maintained throughout the life of the organism. When the nervous system either develops improperly, or is not maintained, this can lead to life limiting disorders such as Schizophrenia (Owen et al. 2011; del Pino et al. 2018) or degenerative disorders such as Alzheimer's disease (Sanabria-Castro et al. 2017; Maccioni et al. 2001). The study of the biological processes, gene expression profiles, and molecular networks which underlie the correct development and function of the circuitry of the nervous system is therefore integral to the understanding of these disorders, and the generation of novel therapies (Murray et al. 2017).

1.2 Cell types of the nervous system

The general structure of the nervous system is comprised of the processing bodies of the Central Nervous System (CNS), the brain and the spinal cord; and the Peripheral Nervous System (PNS), which relays information both to and from the body. The nervous system is comprised of multiple cell types, which can be broadly characterised into neuronal and non-neuronal cells, with further subdivisions based upon the cell locations and functions (Table 1.1). Each cell type possesses important biological characteristics which allows the cells to carry out their specialised functions (Table 1.1). The distinctive characteristics of these multiple cell types are

specified during development, and their function can be regulated throughout the life of the organism by complex cell intrinsic and extrinsic signalling cascades.

Table 1.1 Summary of nervous system cell types

Cell type		Location	Function
Neuronal	Receptors	PNS	Sensation and perception
	Interneurons	CNS	Receive and send signals from/to other neurons
	Effectors/motor neurons	PNS	Send signals from the nervous system to other systems
Non-neuronal/glia	Astrocytes	CNS	Structural support and reguation of ion flow in synapses
	Oligodendrocytes	CNS	Production of myelin to form myelin sheath
	Microglia	CNS	Immune defence in the CNS
	Ependymal cells	CNS	Generation of CSF and regneration of neurons
	Satellite cells	PNS	Regulation of the "neuronal microenvironment"
	Schwann cells	PNS	Myelin sheath formation in the PNS

An introduction to the cell types of the nervous system is outlined in the above table. The Peripheral Nervous System (PNS) and Central Nervous system (CNS) are made up of multiple cell types. These can be broadly characterised into neuronal and non-neuronal/glia cells. These can then be further subcategorised based upon their morphology, location, and function. All are specialised throughout development and maintained throughout the life of the organism to perform their function within the nervous system.

The neuronal cells are the focus of this thesis, however it is important to note that non-neuronal cells also contribute to the development and function of the nervous system (Reemst et al. 2016; Bouvier & Murai 2015). Estimates of the abundance of these non-neuronal cells suggest that they account for around 50% of the brain's weight, and are in ten times more abundance in cell number than the neuronal cells (Azevedo et al. 2009). Non-neuronal cells have also been shown as key players in the progression of disorders of the nervous system, such as the role of microglia in Alzheimer's disease (Clayton et al. 2017). As such, their role and presence must be acknowledged when considering the processes of the nervous system.

1.3 The neurone

The neurone is a highly polarised cell, with somatic, dendritic and axonal compartments that are morphologically distinct, and specialised to carry out specific functions (Figure 1.1). Classically, the soma and dendrites are understood to be the cell compartments which receive and process information, while the axon carries out the delivery of electrochemical impulses to the synaptic target.

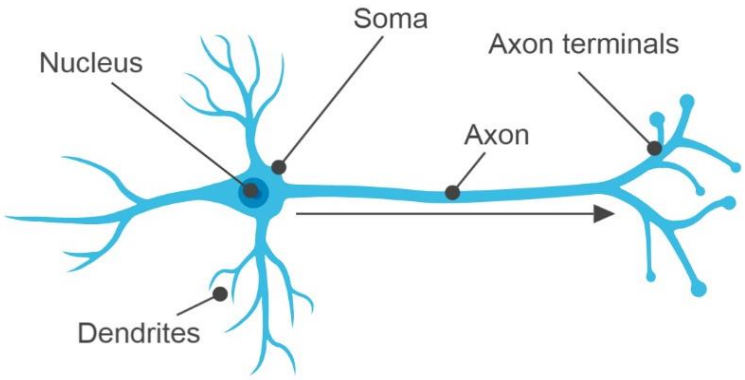


Figure 1.1 Example diagram of a neuron.
The schematic of a typical neuron shows the basic cell compartments. During neuronal communication it is mainly the cell body/dendrites that receives most synaptic inputs from axon terminals and process the accordingly to generate signalling cascades and resulting changes in membrane potential. This information is then integrated by the neurons and transmitted along the axon in the form of an electrochemical action potential to the axon terminals. Arrow demonstrates direction of electrochemical action potential transmission. Diagram in the figure is not to scale as the axon is typically many orders of magnitude longer than dendrites.

Whilst this classical dogma of neuron function remains true, the axon does not simply function as a cable through which electrical impulses can be passed. The supporting structure of the axonal cytoskeleton functions as a platform through which cargoes can be transported as an additional form of cell signalling (Kevenaar & Hoogenraad 2015). Like the neuron itself, the microtubule cytoskeleton is polarised, allowing the directional transport of cargoes such as mRNA (Sotelo-Silveira et al. 2006) along the axon length through the use of motor proteins such as dynein and kinesin (Maday et al. 2014). This bi-directional transport of cargoes is critical to the nervous system function, and disruption in the cytoskeletal structure, or the axonal transport machinery, has also been implicated in various neurodegenerative diseases and nervous system disorders (Kevenaar & Hoogenraad 2015; Maday et al. 2014).

Endosomal trafficking for example is a communication mechanism used by neurons to respond to a diverse range of signals (Cosker & Segal 2014). Sensory neurons, upon application of Nerve Growth Factor (NGF) to the peripheral axon, demonstrate retrograde signalling of early endosomes (Delcroix et al. 2003). These endosomes allow for the transport of NGF, TrkA, and activated signalling peptides (such as p-ERK1/2 and p-p38) to the cell body (Delcroix et al. 2003). This example demonstrates how the axon is an important mediator of signalling as these endosomes are

directionally trafficked to the cell body as a means of communicating the peripheral environment.

It is important to note that there are also multiple subtypes of neuron, each specialised morphologically and biochemically to carry out a specific function. For example, the sensory neurons of the Dorsal Root Ganglion (DRG) possess a unique pseudounipolar structure, whereby the cell possesses a single long axon which extends one branch to the periphery and another to the CNS (Marmigère & Ernfors 2007). This distinct morphology allows the sensory neuron to carry out its function of the relay of sensory information from the periphery of the organism to the CNS for subsequent information processing. Sensory neurons can also be further subdivided into subtypes which express a wide range of receptors and associated proteins, allowing these neurons to sense and respond to the full range of stimuli an organism can experience (Marmigère & Ernfors 2007).

1.4 The synapse

The function of the nervous system is underpinned by the formation of the correct circuitry, and the appropriate communication through, and modulation of this circuitry throughout the lifespan of an organism. The connections between neurons within the nervous system circuitry are called synapses, and the formation and maintenance of these, and their adaptability, allows the nervous system to function. The majority of synapses are axodendritic, formed between the axon of one neuron and the dendritic spines/cell body of downstream neurons. Synapses can however also form between two axons, or two dendrites. Synapses can also connect neurons with non-neuronal receiving cells or tissues, for instance at the NMJ. A single neuron can possess thousands of synapses, and these synaptic connections provide yet another layer of complexity to the circuitry of the nervous system.

There are two major types of synapse communication in the nervous system: electrical and chemical, and a single synapse can communicate through one or both of these methods (Pereda 2014). Electrical synapses require direct cell-cell contact as they are mediated by gap junctions. As such, they are bi-directional, and, as the

same electrochemical signal is passed between cells, this makes electrical synapses sensitive to degradation of the signal as it is passed directly between cells. These synapses do however allow for more rapid transmission of signals, due to the direct signal transmission between cells (Miller & Pereda 2017). Chemical synapses rely on the diffusion of neurotransmitters, these synapses are slower in action than electrical synapses, and are unidirectional. However, as they signal through evoking a new action potential in the post-synaptic neuron, they are not as sensitive to the degradation of signals as the electrical synapse.

In the presynaptic cell, neurotransmitters are packaged into vesicles which, in the absence of an action potential, remain docked intracellularly at the presynaptic membrane (Bajjalieh 1999). Upon the arrival of an action potential at the presynapse, calcium ion influx triggers the fusion of the vesicles with the membrane, and the release of contained neurotransmitters into the synaptic cleft (Figure 1.2). The synaptic cleft is a tightly controlled short distance between cells (Dani et al. 2010), which allows for rapid targeted diffusion of neurotransmitters to the post synaptic membrane. Released neurotransmitters bind to their cognate receptors on the postsynaptic membrane, and these receptors can then initiate a series of diverse

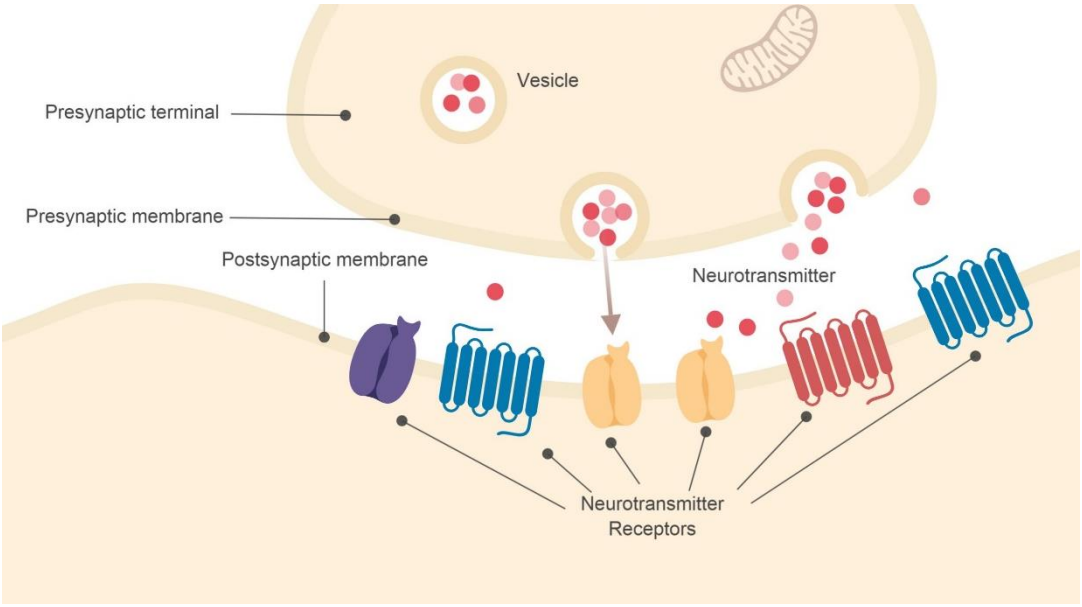


Figure 1.2 A chemical synapse
Neurotransmitters are packaged into vesicles in the presynaptic terminal and are docked at the presynaptic membrane. Upon arrival of an action potential, these vesicles fuse with the membrane, releasing the neurotransmitter into the synaptic cleft. This allows the neurotransmitter to diffuse and bind to its cognate receptors on the postsynaptic membrane.

signalling cascades, including the initiation of the flow of ions into the postsynaptic cell for the creation of a new action potential (Figure 1.2).

There are multiple types of chemical synapses, characterised by the neurotransmitter, and neurotransmitter receptors, with which they communicate. Synapses can be either excitatory or inhibitory, dependent on the signalling cascades triggered by the arrival of the neurotransmitter at the post synaptic membrane. Individual synapses can also communicate with multiple neurotransmitters, and individual synaptic vesicles can contain more than one type of neurotransmitter. For example, many cholinergic synapses in the brain are also glutamatergic (El Mestikawy et al. 2011). All of these characteristics of synaptic communication adds again yet another layer of complexity to the circuitry of the nervous system.

In addition to the transmission of action potentials through neurotransmitter release, the release of subthreshold levels of neurotransmitter is required for the maintenance of the synapse. These subthreshold events (or minis) were first observed in the frog Neuromuscular Junction (The chemical synapse between a motor neurone and a muscle fibre, NMJ), where they were demonstrated to be unrelated to neuronal stimulation (Fatt & Katz 1952). It has since been shown that these events serve to maintain the synapse in the absence of activity, and without them the synapse diminishes (Sutton et al. 2006). Due to their role in neurotransmission, and synapse maintenance, the levels of neurotransmitter and their cognate receptors therefore must be tightly controlled in order for the adequate function and maintenance of the nervous system.

The architecture of the synapse is also key to its function (Lin & Koleske 2010). The previously mentioned synaptic cleft can be as little as 20nm wide, with the synapse occupying a membrane area as little as 10nm (Dani et al. 2010). The supporting cytoskeletal architecture therefore must be very tightly controlled in order to maintain this contact. The precise control of synaptic structure is also extremely important when the density of synapses within a dendritic arbour is considered,

where even slight alternations could cause misalignment of the synapse and therefore incorrect signalling between cells.

As well as maintenance of the existing synapse, a key feature of the synapse is the ability to adapt and change in response to stimuli. The strength of a synapse can be defined as the change in transmembrane potential as a result of postsynaptic receptor activation, or the post-synaptic potential. Changes in synapse strength can be short term, lasting only seconds to minutes, or long term. Long term changes in synapse strength are a result of Long Term Potentiation (LTP), where repeated or continuous stimulus of a synapse leads to second messenger cascades resulting in alterations to the synapse (Nicoll 2017). LTP underpins the processes of learning and memory, and is therefore indispensable for the survival of the organism.

1.5 Protein homeostasis in the nervous system

The development, maintenance and function of nervous system circuits is supported by the control of protein levels in a time and space-dependent manner. Whilst the focus of this thesis, miRNAs, are regulators of protein expression at the level of specific mRNA translation, it is important to note that protein levels can be controlled through multiple mechanisms which govern the synthesis, assembly, activation and degradation of proteins (Hetz & Glimcher 2011). All of these mechanisms must work in concert with each other to maintain systemic protein homeostasis.

The disruption of protein homeostasis at any level can be deleterious to the nervous system. Disrupted regulation of protein synthesis for instance has been shown to be linked to neurodegenerative disease (Kapur et al. 2017). As an example, elevated levels of phosphorylated eukaryotic initiation factor (p-eIF) 2 are associated with a reduced general rate of translation. Elevated levels of p-eIF2 are observed in multiple neurodegenerative disorders, including Huntington's disease (Leitman et al. 2014) and the associated reduced rate of translation is thought to be a contributing factor to the pathogenesis of these neurodegenerative disorders (Kapur et al. 2017).

As a further example, the disruption of protein folding and protein degradation in the nervous system has also been shown to be detrimental to its function, particularly in regard to the processes which lead to protein aggregation and resulting toxicity (Douglas & Cyr 2010). For instance E3 Ubiquitin ligases play a role in the development, maintenance and degradation of cells of the nervous system (Upadhyay et al. 2017). The E3 Ubiquitin ligases play a critical role in Ubiquitin (Ub) recruitment to proteins, mediating the final stage of Ub transfer to the target substrate, and govern the specificity of the Ub transfer (Zheng, N et al. 2017). It has been shown that the levels of the E3 Ub ligase E6-AP are raised under stress conditions, where E6-AP interacts with Hsp70, and preferentially targets aggregatory proteins for clearance by the Ub-Proteasome System (Mishra et al. 2009). E6-AP is encoded by the UBE3A gene, and mutations in this gene are associated with the neurological disorder Angelman Syndrome (Kishino et al. 1997), demonstrating the key role E6-AP plays within the nervous system.

Whilst systemic alterations to proteostasis in the nervous system can have deleterious effects, the focus of this thesis, miRNA, are regulators of translation at a mRNA specific level. As such the remainder of this introduction will focus on the role of translational control and miRNA in the nervous system.

1.6 Translation in the nervous system

More than any other cell type, the highly polarised structure of the neuron, and the subsequent specialised functions of the resulting neuronal compartments, means that the levels of proteins within these domains demonstrate marked differences and therefore must be differentially regulated. Localised translation of proteins is a key mechanism of protein level control which contributes to this (Di Liegro et al. 2014). It has been demonstrated, and is now well accepted, that differential mRNA localisation and local protein translation must occur, and plays a critical role in the establishment and function of the nervous system (Jung et al. 2012; Sotelo-Silveira et al. 2006). The disruption of which can lead to neurological disorders such as spinal muscular atrophy (Wang et al. 2007).

Translational control also provides the temporal regulation of protein expression required by the developing nervous system. Changes in the mRNA content which correspond to different developmental stages have been observed within the localised environment of the axon (Gumy et al. 2011), and mRNA content differs even to the subcellular level of the growth cone (Zivraj et al. 2010), suggesting the involvement of local protein translation in axon growth and guidance. Indeed, *X.laevis* retinal ganglion cell axons retain the ability to respond to guidance cues even after the loss of somatic contribution (Harris et al. 1987). This is most likely due to local translation which can occur in the axon during growth (Campbell & Holt 2001), and demonstrates the ability of the axon to partially function independently from the cell body as a result of this. These studies demonstrate that local translation of proteins, and its temporal control systems are central in the development of the nervous system.

Localised protein translation also plays a key role in the maintenance of the mature nervous system. Throughout the length of mature vertebrate axons, periodic structurally defined domains which contain translational machinery have been identified (Koenig et al. 2000). These domains contribute to the ability of the mature axon to carry out translation independently of the cell body (Lee & Hollenbeck 2003). These domains are associated with cytoskeletal mRNAs such as beta actin (Sotelo-Silveira et al. 2008). The protein products of neurofilament mRNAs which have been shown to be present throughout the mature sciatic nerve, are upregulated in response to injury (Sotelo-Silveira et al. 2000). This demonstrates the importance of localised translation of proteins throughout the axon for the maintenance and regeneration of the neuron.

As with other aspects of the nervous system, synapse function and maintenance is dependent on the existence of a complex protein network. In both the presynaptic terminal (Siksou et al. 2011) and the postsynaptic target (Sheng & Kim 2011) proteins are expressed at specific locations in controlled amounts in order to carry out specialised functions. These proteins can serve as machinery controlling neurotransmitter release and reception, the subsequent downstream signalling

cascades, or serve as the scaffold for the synapse structure. Local translation provides a mechanism through which these proteins can be tightly controlled spatially and temporally in response to internal or external stimuli. It has been shown that proteins in both the synaptic axon terminal (Batista & Hengst 2016) and within dendrites (Steward & Schuman 2001) are locally translated, and that this is crucial to synapse function (Thomas et al. 2014).

Local translation of proteins within the synapse microenvironment also underpins synapse function, with protein translation machinery (Steward & Levy 1982) and a distinct population of mRNAs (Cajigas et al. 2012) known to be localised within the synapse. Translation for instance has for many years been known to be key in LTP and the formation of memory. It was shown in 1963 that mice which have protein translation inhibited through puromycin treatment demonstrate reduced ability to form memories in the shocked arm Y maze test (Flexner et al. 1963). Puromycin application following the test does not however lead to memory loss (Flexner et al. 1963). As memory formation is underpinned by LTP, this indicates the importance of translation in synaptic plasticity. Currently, the knowledge of the complete mechanisms underlying the control of LTP by translation is however incomplete (Bliim et al. 2016).

This local translation is controlled in an activity dependent manner, as demonstrated by the recruitment of polyribosomes to active dendritic spines during LTP in rat hippocampal slices (Ostroff et al. 2002). The dysregulation of mediators of this localised translation in the synapse has also been implicated in various developmental, degenerative and psychiatric disorders (Swanger & Bassell 2013).

Translational control of protein levels in a spatial and temporal manner, therefore underpins the processes of development, maintenance, and function of the nervous system. It is therefore important to investigate the multiple mechanisms and cellular processes that can regulate translation in neurons.

1.7 Translational control

The synthesis rate of a protein is, in general, proportional to the translational efficiency and concentration of its mRNA, and as such the mechanisms which control mRNA translation efficiency (Hershey et al. 2012) and mRNA decay (Wu & Brewer 2012; Thapar & Denmon 2013) are central to the correct levels of protein synthesis in a controlled spatial and temporal manner.

Control of translation efficiency is governed by a number of cis acting regulatory sequences within the mRNA and trans acting RNA binding proteins which interact with the mRNA itself (Hershey et al. 2012). One common process in translational silencing and mRNA decay is the recruitment of mRNAs to p-bodies (Parker & Sheth 2007). P-bodies are aggregates of mRNA, associated translational silencing proteins, and mRNA decay protein machinery (Luo et al. 2018). mRNAs which are recruited to p-bodies can be either translationally repressed and stored for a later return to the available pool of mRNA in the cytoplasm, or degraded. The repressive transient storage of mRNA in p-bodies has been demonstrated as a protein expression control mechanism in multiple cellular processes (Kedersha et al. 2005), for instance the transient repression of protein translation in hypoxic conditions (Koritzinsky et al. 2006).

Regulation of mRNA decay is important for controlling the availability of transcripts from which protein can be translated. mRNA degradation can occur through several processes, the most common of which is the shortening and removal of the poly(A) tail, and decapping of the mRNA by ribonucleases, this makes the resulting RNA fragment vulnerable to exonuclease attack (Wiederhold & Passmore 2010). The degradation of mRNAs can be facilitated, or prevented, through specific pathways. For example, the deadenylation of the poly(A) tail has been shown to be coupled to the level of translation of a mRNA, this is a mechanism to remove unrequired mRNA transcripts (Funakoshi et al. 2007).

Alternatively, mRNA decay can also be mediated by systemic signalling pathways such as hormonal changes (Guhaniyogi & Brewer 2001). For instance, the stability of

the type I procollagen mRNA (which encodes for the primary structural protein in bone and skin) is effected by levels of the steroid hormone class of glucocorticoids. It has been shown that glucocorticoids can downregulate procollagen type I mRNA in fibroblasts through post-transcriptional mechanisms (Linquist et al., 2000). This mechanism is thought to be a contributing factor to Glucocorticoid-induced osteoporosis, demonstrating that the effect hormonal changes can have on the stability of mRNA can lead to significant disorders.

The control of translational availability of mRNA is particularly important in the nervous system, where the need to not only temporally control protein expression is required, but also spatial regulation of mRNA available for translation. It has been shown for example, that in order for a mRNA to localise to the axon terminal of a neuron the associated proteins not only translationally repress the mRNA, but associate with the cytoskeletal motor proteins which allow for the directed transport of the mRNA to the required location (Di Liegro et al. 2014).

The focus of this thesis, microRNAs (miRNAs), have been identified as a class of regulatory molecules that can modulate mRNA translational efficiency and stability. Their characteristics and ability to regulate the translation of mRNA in the temporal and spatial manner required by the nervous system will be discussed in the following sections.

1.8 miRNAs

MicroRNAs are a family of small (~22 nucleotide), non-coding, RNAs. miRNAs regulate the level of protein expression through facilitating translation repression or degradation of target mRNAs. The first miRNA was discovered in *C.elegans* as the Lin-14 regulator, Lin-4, and this was thought to be an isolated regulatory event (Lee 1993; Wightman et al. 1993). The first evolutionarily conserved miRNA was not reported for another seven years, Let-7 (Pasquinelli et al. 2000). At the time of writing, there are now 2654 mature miRNA sequences identified for humans in the miRBase miRNA database (Kozomara & Griffiths-Jones 2014). microRNAs have been shown to play roles in many processes and diseases, including cancer (Romero-Cordoba et al. 2014), pain (Andersen et al. 2014; Sakai & Suzuki 2014), and the

development of the nervous system (Meza-Sosa et al. 2014; Iyer et al. 2014). In addition to the interest in understanding their physiological role, an important part of interest in the research of miRNA is also due to their potential use as therapeutic targets or agents (van Rooij & Kauppinen 2014).

1.9 miRNA biogenesis

The miRNA genes are located throughout the genome, either individually, or as clusters of miRNA genes. These genes can be positioned at their own specific locus, or within an intron of a protein coding gene (Poliseno et al. 2010). The majority of miRNAs are generated from these through the canonical biogenesis pathway (figure 1.3).

In brief, a primary-miRNA (pri-mRNA) transcript is produced from the gene by RNA Polymerase II (RNAPolII) (Lee et al. 2004) and subsequently processed in the same way as protein coding RNA transcripts (Cai et al. 2004). The pri-miRNA forms a characteristic stem-loop structure, flanked by sequences of yet unknown function. The flanking sequences are cleaved from the stem loop by the concerted action of Drosha and DGCR8 within the microprocessor complex, to form the precursor-miRNA (pre-miRNA, figure 1.3). The pre-miRNA is exported from the nucleus, and the loop region is then cleaved in the cytoplasm by the Dicer ribonuclease, producing a short (~22nt, dependant on specific miRNA) RNA duplex (figure 1.3).

The process described here is the canonical pathway of miRNA biogenesis (figure 1.3), however alternative pathways employ other mechanisms of miRNA processing. For instance, those miRNA which are contained within the introns of a protein coding genes undergo initial processing by the spliceosome complex to produce the pre-miRNA, allowing them to bypass microprocessor cleavage (J Graham Ruby et al. 2007). It is important to consider the existence of these alternative miRNA biogenesis pathways when considering the significance of studies such as those which concern the knockout or inhibition of miRNA processing proteins. For a

detailed review of miRNA biogenesis, and non-canonical pathways of miRNA processing the reader is directed to (Ha & Kim 2014).

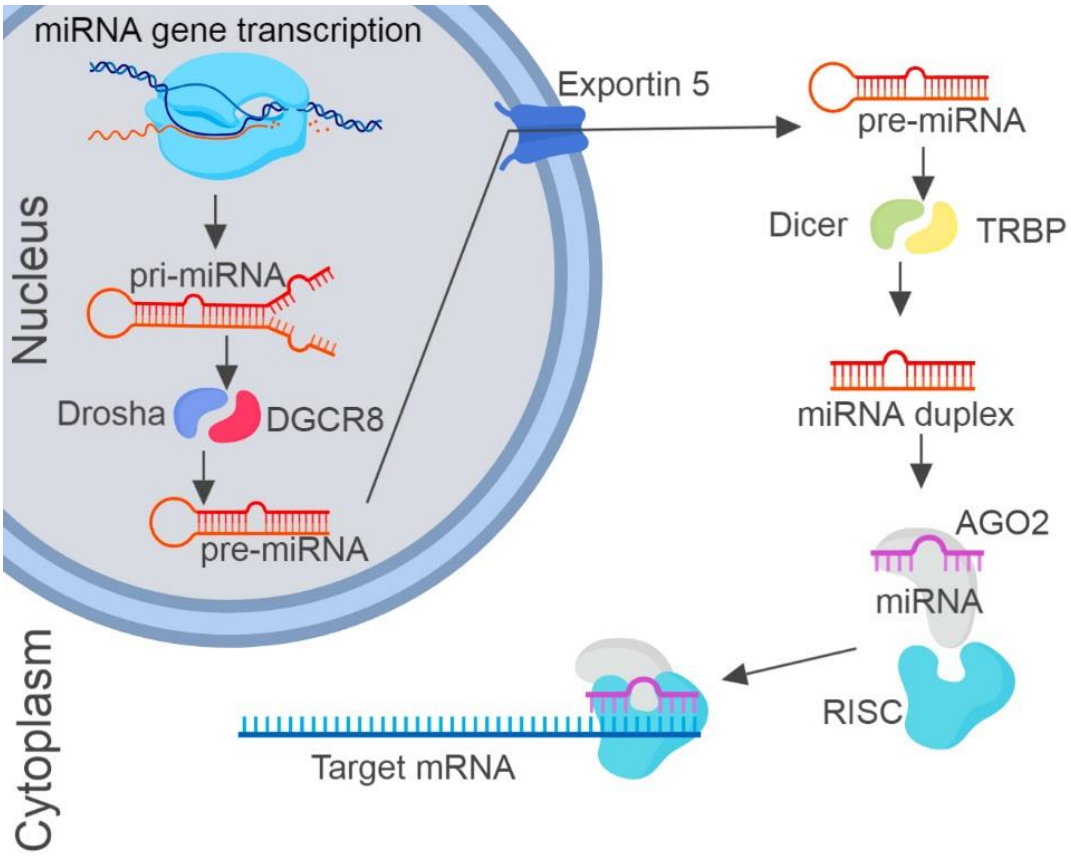


Figure 1.3 Canonical miRNA biogenesis
miRNA genes are transcribed within the nucleus resulting in the pri-miRNA, a hairpin structure with extended 5' and 3' overhangs. The pri-miRNA is cleaved by the Drosha/DGCR8 microprocessor complex into the pre-miRNA hairpin. This is exported from the nucleus by exportin 5 into the cytoplasm. The pre-miRNA is further cleaved in the cytoplasm by TRBP associated Dicer to the miRNA duplex. Either strand of this duplex can associate with AGO to be recruited into the RISC complex which facilitates miRNA binding to a target mRNA. (Figure constructed in Biorender)

1.10 miRNA function

miRNAs are mediators of mRNA silencing, serving as the targeting guide for the miRNA induced silencing complex (miRISC). miRISC, or RISC, is a protein complex which can inhibit translation and/or promote mRNA degeneration. The core of RISC is comprised of the argonaute (Ago) and GW182 proteins (figure 1.4).

Stereotypically, one strand of the miRNA duplex is loaded via Ago association into the multiprotein RNA-Induced Silencing Complex (RISC) and the other is degraded. However, dependent on the context the miRNA is being expressed within, either

strand can be loaded preferentially into RISC (Khvorova et al. 2003). Previous naming convention of the miRNA dubbed the less preferentially loaded strand as the miRNA* strand. These are now named based upon their position in the miRNA precursor (e.g., miR-184-5p is the 5' strand of the miR-184 miRNA).

Ago facilitates recognition of the mRNA by the miRNA through complementary sequence binding (figure 1.4). This miRNA:mRNA interaction is not absolutely required for Ago repression of protein synthesis, as Ago protein artificially tethered to the 3'Untranslated Region (UTR) of an mRNA still leads to a downregulation of protein levels (Pillai et al. 2004) reinforcing the role of the miRNA as a targeting RNA. However, it has been shown that the level of miRNA:mRNA duplex stability correlates negatively with mRNA repression by miRNA (Kozomara et al. 2014), suggesting a further functional influence of the miRNA. Ago interacts with, and recruits the GW182 protein to the RISC complex, an interaction which is essential to miRNA mediated gene silencing (Yao et al. 2011).

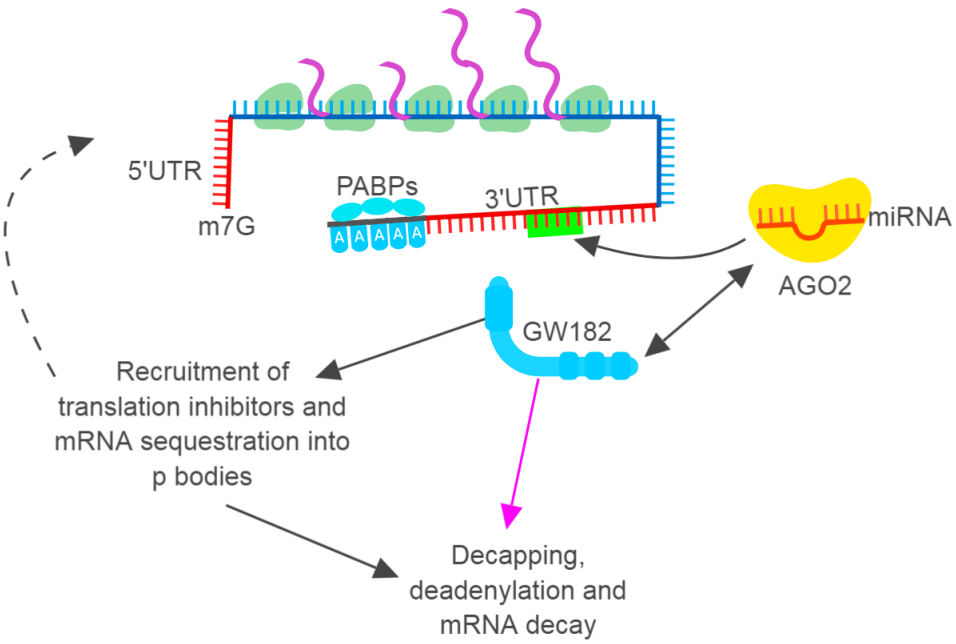


Figure 1.4 miRNA mediated gene silencing
miRNA serves as a guide for the targeted association of AGO with the 3'UTR of a mRNA. AGO recruits GW182 which, through protein-protein interactions, leads to the recruitment of translation inhibitors and sequestration of the target mRNA into p bodies, and the subsequent decapping, deadenylation and mRNA decay. The targeting of a 3'UTR could also lead to the immediate decay of an mRNA without transient inhibition of translation (pink arrow). The inhibition of translation initiated through miRNA association can also be reversed (dashed arrow).

As with Ago (Pillai et al. 2004), GW182 artificially tethered to the 3'UTR of a mRNA is sufficient to induce silencing of the target mRNA (Eulalio, Helms, et al. 2009) demonstrating the importance of GW182 in RISC complex mediated gene silencing. GW182 consists of specialised domains which facilitate the recruitment of effector proteins which mediate translation inhibition and mRNA decay.

GW182 possesses N-terminal ubiquitin associated, and glutamine-rich domains which are responsible for the localisation of GW182 to the p-bodies (Eulalio et al. 2008). An additional N-terminal effector domain has also been identified, which may play an endogenous role in gene silencing, which as of yet, has not been fully defined (Fabian & Sonenberg 2012). The GW182 C-terminal silencing domain alone is however sufficient for GW182 mediated silencing of a target mRNA independent of the N-terminal sequences (Eulalio, Helms, et al. 2009).

The C-terminal silencing domain of GW182 functions through the binding and recruitment of multiple effector proteins. One such protein is Poly(A)-Binding protein (PABP) (Derry et al. 2006), which is recruited via interaction with a PAM domain within the GW182 C-terminal (Fabian et al. 2009). The exact mechanism of this interaction leading to gene silencing is unclear, as the interaction of GW182 with PABP alone is not sufficient, or absolutely necessary, for miRNA mediated gene silencing (Zipprich et al. 2009). The PAM domain can also interact with the E3 Ubiquitin ligase, EDD (Su et al. 2011). EDD facilitates gene silencing through a ubiquitin independent mechanism, possibly through the recruitment of the decapping enhancer p54, promoting mRNA decay (Su et al. 2011). The C-terminal of GW182 can also associate with deadenylases such as CCR4-NOT (Fabian et al. 2011). It has been demonstrated that alongside a role in recruitment of deadenylases to the target mRNA, GW182 can act as a co-activator of CCR4-NOT to promote mRNA deadenylation upon association (Fabian et al. 2011). miRNA mediated RISC association with an mRNA therefore leads to gene silencing, through recruitment of proteins by GW182 which either impair translation of the mRNA (Bhattacharyya et

al. 2006), or enhance the degeneration of the mRNA (Eulalio, Huntzinger, et al. 2009).

Individual miRNAs are able to function through either the translational repression or mRNA decay pathways, or both. For instance, in pancreatic cancer cells, miR-143 was demonstrated to lower protein levels to a greater extent than expected from the observed reduction in mRNA levels (Yang et al. 2010), indicating that both translation repression and mRNA decay were occurring as a result of miR-143 gene silencing. Translation repression mediated by miRISC can also be reversed (Bhattacharyya et al. 2006), further demonstrating that miRISC association does not absolutely lead to mRNA degeneration. It has been suggested however, that translation inhibition will proceed to RNA decay through a cap-dependent, polyA-independent, mechanism (Fabian & Sonenberg 2012). The result of miRNA mediated association of the RISC complex with a target mRNA is therefore variable, and the mechanisms which govern this choice have not yet been fully elucidated.

Whilst the canonical miRNA function of interaction with the 3'UTR is described here (figure 1.4), alternative mechanisms of miRNA mediated translational repression and mRNA decay have been suggested. For instance, sequence features of miRNA which promote 5'UTR binding as opposed to 3'UTR binding have also been identified (Lee et al. 2009). Ago association guided by a miRNA with the 5'UTR of an mRNA can also lead to repression of translation (Lytle et al. 2007). As this study was based upon mRNA containing an internal ribosome entry site (IRES), this mechanism of translational repression is believed to be through a mechanistic function distinct from steric hindrance of translation initiation factors by the RISC complex (Lytle et al. 2007). However the exact mechanism of action of 5'UTR miRNA association leading to translational repression is not yet known.

In addition to miRNA functioning to inhibit translation of mRNA, additional work has been published which demonstrates the ability of miRNA to interact directly with proteins to exhibit an effect. The RNA-sensing Toll-like receptor 7 (TLR7) for example, has been shown to be activated by the miRNA lethal-7 (let-7) located in the

extracellular environment to induce neurodegeneration, suggesting a role for miRNAs as signalling molecules (Lehmann et al. 2012). This highlights the diverse range of functional mechanisms through which a miRNA can act.

1.11 miRNA expression profiling methods

A common approach to the study of miRNA is to first profile miRNA expression changes in a system of interest before drilling down into the results of profiling to classify a miRNA of interest. There are multiple tools available with which to view the miRNA profile within a system, including microarray profiling and next generation sequencing (Svoboda 2015, Pritchard et al. 2012). In microarray profiling, an array of probes complementary in sequence to a range of miRNAs are mounted on the microarray chip, and detection of a miRNA within a sample relies on the complementary annealing of the miRNA with its cognate probe. Before annealing to the chip, the miRNA containing sample of interest will be labelled, so that the expression profile can be analysed via imaging of the chip. Multiple chips have been developed in order to assess miRNA expression profiles across different species, and with different arrays of miRNA of interest mounted upon them (Liu, C. G. et al. 2004, Thomson et al. 2004, Nelson et al. 2004) . A consideration to hold when using this method of miRNA profiling is that the profile will only provide results regarding those miRNAs with probes mounted on the array, and will therefore not assist with the identification of novel transcripts. Additionally, the efficiency of the specific array being used must also be considered (Sato et al. 2009), including implications of the possibility for cross-reactivity between similar miRNA sequences, and any variations in optimal hybridisation temperatures of the probes and the target miRNA.

An alternative miRNA profiling method, next generation sequencing (NGS) begins with the creation of a small RNA cDNA library from the sample of interest, followed by parallel sequencing of the individual cDNA molecules. Significant computational analysis of the resulting data is then required to produce the expression profile of the small RNAs within the sample (Metzker 2010). Next generation sequencing of miRNA provides a method of high sensitivity and accuracy, which (conversely to microarray profiling) can identify novel miRNAs within a sample. There are however

significant costs associated with this profiling method which may make this inaccessible to the researcher, although the availability and costs of these methods are rapidly improving due to their high demand (Bahassi & Stambrook 2014).

In regards to the detailed investigation of individual miRNA expression patterns, the methods of Northern blotting and qPCR are widely used to track changes in an individual candidate miRNAs. Northern blotting is the oldest method of miRNA detection, and whilst the method itself is relatively labour intensive, the resulting insight into the biogenesis and degeneration of a miRNA is invaluable. As such, northern blotting results formed the basis for the standard identification of novel miRNAs (Ambros et al. 2003). In a single Northern blot the relative pri-miRNA and miRNA levels in a sample can be revealed, alongside any length variations and possible covalent modifications, and the sensitivity of this method has been improved through the use of LNA probes (Várallyay 2008). This method provides the ability to construct a comprehensive picture of a miRNA within a sample within a single experiment.

More common in recent years the approach of qPCR is used to reveal levels of individual miRNA, and a number of protocols and commercially available kits have been developed for this purpose, including qPCR array formats which allow for the simultaneous quantification of many miRNAs in multiple samples (Svoboda 2015). As the RNA sample undergoes an initial cDNA amplification step prior to qPCR analysis, this method allows for a high degree of sensitivity in the qPCR reaction and in fact it has been shown that miRNA profiles can be created even at a single cell level using qPCR (Tang et al. 2006). This method is less labour intensive than that of Northern Blotting and as such provides a relatively simple method through which to identify the levels of an individual miRNA within a sample.

Another common individual miRNA detection approach is in situ hybridisation (ISH). This approach allows for the spatial and time sensitive detection of a miRNA within a fixed sample. As miRNAs are short by nature this produces difficulties in optimising traditional RNA ISH methods, however the use of LNA in probe design in order to

increase the melting temperature of the duplex has proved useful in the improvement of this. Recently, an optimised RNA ISH protocol was developed, small molecule inexpensive fluorescent ISH (smiFISH) (Tsanov et al. 2016) and this is used within this thesis. This protocol uses a sequence specific primary probe which is annealed to a secondary fluorescent probe, this use of primary and secondary probes significantly decreases the cost of primary probe synthesis, therefore decreasing the cost of probe synthesis and allowing for an increase in the detection efficiency of the target RNA through the use of higher probe concentrations (Tsanov et al. 2016).

1.12 miRNA molecular tools for functional studies

There are a battery of tools available to the researcher in order to experimentally investigate the functional role of an individual miRNA (Svoboda 2015). These tools include classical targeted gene knockouts, or genetic modifications, for instance those which have been developed in *Drosophila* (Chen et al. 2014). Whilst these models are valuable in the identification of miRNA function at the level of the whole organism, more sophisticated genetic modifications can be used to identify the tissue or cell specific function of miRNAs. For instance there are a number of lines in Drosophila which exploit the Gal4 UAS system to allow for targeted overexpression or downregulation of a miRNA (these are discussed in more detail in sections 5.1.2 and 5.1.9).

It is now also possible to either mimic or inhibit the action of an individual miRNA through the use of synthetic RNA oligonucleotides. These can contain modified Locked Nucleic Acid (LNA) moieties which are designed to enhance binding of the oligonucleotide to its corresponding sequence and therefore LNA modifications can therefore help to overcome the short length, and variable melting temperatures of miRNA (Hutvagner et al. 2004; Meister et al. 2004). These synthetic oligonucleotides allow for the assessment of the effect modulations of miRNA levels may have in the context of interest, for instance on cell morphology, behavioural assays, or on gene/protein expression profiles. Whilst these tools allow for the assessment of

changes which may be induced through alterations to miRNA activity, they do not identify the direct functional targets of a miRNA.

1.13 miRNA target identification

The most common approach to identify possible miRNA targets is through the use of target prediction algorithms. As previously stated, the miRNA itself primarily functions as a targeting guide for the RISC complex through complementary sequence binding. At the molecular level, miRNA targeting is governed by classical Watson-Crick base pairing. Early analysis of miRNA target sites demonstrated highly conserved base pairing of the miRNA Recognition Elements (MREs) within the target mRNA with 6-8 nucleotides from position 2 of the miRNA (Bartel 2004). These nucleotides within the miRNA are called the "seed region". The seed region complementarity with the 3'UTR of an mRNA formed the basis of the first target prediction algorithms, and still features in the most used databases today (Betel et al. 2008; Thadani & Tammi 2006). The functional targeting of an mRNA by a miRNA is also governed by a set of promiscuous rules which go beyond the base pairing of the seed sequence, including binding of the 3' region of the miRNA (Bartel 2009), imperfect complementarity of the central region of the miRNA (Shin et al. 2010; Martin et al. 2014) and sequence features of the 3'UTR beyond the MRE (Grimson et al. 2007). The seed sequence however, prevails as the most crucial aspect of miRNA complementarity (Agarwal et al. 2015; Steinkraus et al. 2016).

It is predicted that at least a third of human mRNAs are targeted by miRNAs (Lewis et al. 2005). Single nucleotide polymorphism (SNP) analysis of mutations within predicted target sites for miRNA, demonstrates a low level of tolerance for inheritance, compared to SNPs present in other conserved 3'UTR sequence motifs (Chen & Rajewsky 2006). This demonstrates the importance of miRNA mediated translation regulation and conservation of the MRE.

Although many aspects of the miRNA-MRE sequence complementarity have now been uncovered, target prediction still leads to a high rate of false positives and negatives (Rajewsky 2006; Lee et al. 2015). For instance in one study the efficiency of

target predictions was assessed based on one miRNA, miR-22 (Lee et al. 2015). In this study SILAC-based proteomics was used to quantify protein expression in the presence and absence of miR-22 in metastatic melanoma cells, revealing a false positive rate of 46-71% and a false negative rate of 44-82% dependent on the prediction algorithm used (Lee et al. 2015). These high false rates are most likely due to secondary interactions that are independent of sequence complementarity (Afonso-Grunz & Muller 2015; Didiano & Hobert 2006; Kertesz et al. 2007). This produces a requirement for the validation of complementary sequence binding of a miRNA to any predicted target site within the desired context.

There are several strategies which can aid in the confirmation of a predicted miRNA target or experimentally identify miRNA targets (Svoboda 2015). The luciferase reporter assay (Jin et al. 2013) is the most widely used, and is an accepted method to confirm miRNA association with a specific predicted target site. This assay is based upon the co-transfection of a miRNA mimic alongside a luciferase reporter construct, which contains the predicted miRNA target site within the 3'UTR of luciferase. If the miRNA does indeed associate with its predicted target site, luciferase activity will be reduced within the resulting cell lysate (figure 1.5).

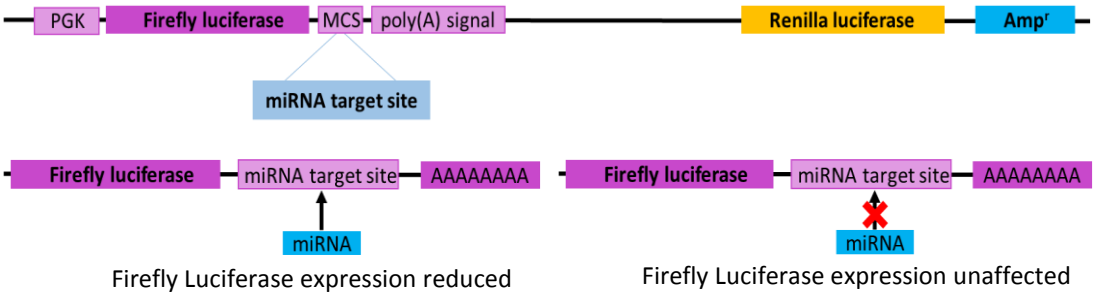


Figure 1.5 Luciferase reporter assay
Schematic of the luciferase reporter assay used in this work. pmiRglo vector allows for the expression of Firefly and Renilla Luciferase within mammalian cells. The predicted miRNA target site is inserted within the 3'UTR of firefly luciferase. Renilla luciferase serves as a transfection efficiency control. If the predicted target site is a true target of the miRNA, firefly luciferase activity in relation to Renilla luciferase activity will be reduced in the presence of a miRNA mimic. If the miRNA does not recognise the site, the level of firefly luciferase activity will be unaffected.

It is however important to further assess miRNA targeting within the system of interest. For example, it has been shown that 3'UTR binding proteins exist which can

mediate the association of a miRNA with its target site in a given biological context. It was demonstrated for instance that miR-221 and miR-222 require the presence of the RNA binding protein pumilio to allow their association with and subsequent repression of p27 (Kedde et al. 2010). This is due to pumilio binding to a hairpin structure within the 3'UTR, which changes the confirmation, and exposes the miRNA target site, allowing complementary sequence binding (Kedde et al. 2010). A separate study demonstrated that the presence of binding sites for the HuR protein in close proximity to a miRNA binding sites inhibits miRNA binding at a whole system level (Y. C. Lu et al. 2014). Dependent on the presence or absence of these proteins, the miRNA function can therefore be enhanced or attenuated. This emphasises the importance of miRNA targeting confirmation within the context of interest, or within a suitable model of this context.

Individual miRNA have also been shown to mediate multiple processes through different targets dependent on the context which they are expressed. For instance, one of the first discovered miRNA, let-7, modulates a diverse range of biological processes dependant on its expression context, from tumour suppressor and promoter of cell differentiation in development (Lee et al. 2016), to regulator of glucose metabolism in the adult (Frost & Olson 2011).

Experimental techniques have therefore been developed in order to identify miRNA targets within the context of interest, these techniques can also simultaneously identify multiple targets of miRNA. One such technique is through High-Throughput Sequencing of RNA isolated by Crosslinking Immunoprecipitation (HITS-CLIP)(Chi et al. 2009). RNAs are first crosslinked with their associated proteins in the context of interest through UV treatment (Chi et al. 2009). This then allows for the subsequent immunoprecipitation of RISC complex proteins, alongside associated miRNAs and mRNAs (Chi et al. 2009). RNA can then be assessed, for instance through high-throughput sequencing (Chi et al. 2009). If this technique is combined alongside inhibition or overexpression of a miRNA of interest, the global changes in miRNA:mRNA associations can be determined, alongside possible confirmation of an expected target mRNA. Techniques such as HITS-CLIP whilst powerful, do however

demonstrate technical problems to the researcher. These include issues such as the requirement for large quantities of initial cell lysates, and the requirement for advanced technologies (for instance high-throughput sequencing technologies) which may not currently be widely available or affordable (Svoboda 2015).

1.14 miRNAs and the nervous system

As potential regulators of translation, and therefore protein synthesis, miRNAs have been shown to play an important role in the growth and function of the neuron (Iyer et al. 2014; Meza-Sosa et al. 2014; Schratt 2009; Rajman & Schratt 2017; Hu & Li 2017). Key studies which indicate the role of the whole miRNA family in the nervous system are outlined here. Most of these initial papers concern the targeted knockout or inhibition of miRNA processing enzymes such as dicer, and it is important to highlight the possibility of alternative miRNA biogenesis pathways when validating these (Ha & Kim 2014) and also alternative systems which utilise the same machinery. For instance, dicer is known to be involved in the processing of other small non-coding RNAs (siRNA for example (Sakurai et al. 2011)).

The first *in vivo* indication for a role of miRNAs in nervous system development came from a Dicer knockout in zebrafish (Giraldez et al. 2005). This was shown to cause severe malformations in the brain and spinal cord, which were rescued through application of pre-processed miRNAs (Giraldez et al. 2005). A later study in a mouse model of schizophrenia provided evidence for a more miRNA specific role (Stark et al. 2008). The study demonstrated that the deletion which occurs in this model contains a gene which is believed to be specifically involved in miRNA processing, *DGCR8* (Stark et al. 2008). It is believed that the loss of *DGCR8* contributes to the neural disruptions seen in the model due to developmental defects (Stark et al. 2008). These studies demonstrate the importance of miRNAs as a whole in the development of the nervous system, but do not point to the function of specific miRNAs, their localisation, or the developmental time point at which they act.

In addition to the developmental role of miRNAs in the nervous system, they are also important regulators in the mature nervous system. Directed ablation of dicer in

postmitotic Purkinje neurons leads to their degeneration, and associated development of ataxia (Schaefer et al. 2007). The targeted inducible disruption of dicer in adult mouse hippocampal neurons leads to an initial increase in neuronal activity, which eventually induces excitotoxic neurodegeneration (Fiorenza et al. 2016). Whilst these studies demonstrate a neuronal cell type specific action of the miRNA family, they do not indicate which miRNAs are driving these downstream effects.

As further evidence of the relevance of miRNAs in the functioning of the nervous system, multiple studies have demonstrated neuronal activity dependant changes in miRNA expression (Sim et al. 2014). For instance, mice which have undergone nervous system stimulation with electroconvulsive shock demonstrate significant transient changes in miRNA expression in the hippocampus (Eacker et al. 2011). Specific stimulation of receptor subtypes can also lead to modulation in the levels of miRNA expression, for instance NMDA-mediated stimulation of *in vivo* and *in vitro* hippocampal neurons drives miRNA expression changes (Kye et al. 2011; van Spronsen et al. 2013). These modulations in miRNA levels as a result of neuronal activation demonstrate the relevant role of miRNAs in mature nervous system function, but do not characterise the specific individual miRNA which may be producing downstream effects.

Alterations to miRNA levels in neurological disorders, or disease states, have also been observed, highlighting their relevance in health and disease. For example, miRNA level dysregulation in brains of Alzheimer's disease patients (Cogswell et al. 2008) or in the sensory neuron in mouse models of chronic pain (Kusuda et al. 2011) suggest an important endogenous role for miRNA in the proper maintenance and function of the mature nervous system and progression of neurological disorders.

Although these studies highlight the importance of the regulation of the miRNA family of transcriptional regulators in the development, maintenance and function of the nervous system. The specific miRNA which govern this, and their functional targets is not always been fully elucidated.

1.15 Identified functions of miRNAs in nervous system development

The development of the nervous system occurs through a complex series of intrinsic and adaptive processes. These rely on multiple stages of cell and tissue development in order for the correct connections to form, and the nervous system to achieve its functional properties. Individual miRNAs have been identified as regulators of multiple stages of neuronal development, from differentiation, to axon growth and synapse formation and function (Iyer et al. 2014; Meza-Sosa et al. 2014; Schratt 2009; Rajman & Schratt 2017; Hu & Li 2017). Some examples of this are described below.

1.16 miRNAs in nervous system differentiation

The process whereby neurons differentiate from precursor stem cells is termed neurogenesis. Neural progenitors in the early mammalian embryo are formed from the ectoderm (de Vellis & Carpenter 1999). A complex system of signalling gradients and intrinsic signalling cascades within the ectoderm during gastrulation leads to the formation of neural stem cells from migrating cells, and these form the structures of the neural tube and the neural crest (de Vellis & Carpenter 1999). The cells of the neural tube and crest are further specified and organised throughout development, to form the cells of the mature nervous system (de Vellis & Carpenter 1999). As regulators of protein translation, miRNAs possess the potential to control the gene expression networks required during differentiation of cells in the nervous system.

It has been observed for example that differentiating photoreceptors in the *Drosophila* eye require repression of miR-7 by the transcription factor Yan to be lifted (Li & Carthew 2005). A further study demonstrated the importance of miR-7 in the control of cell fate determination, which is especially required under temperature stress conditions (Caygill & Brand 2017). miR-7 was shown to promote the transition of neuroepithelial precursor cells to neuroblasts, through the limitation of Notch signalling (Caygill & Brand 2017). This demonstrates the ability of a single miRNA to regulate neuronal cell fate differentiation. miR-7 is also of particular importance in the development of the *Drosophila* eye under temperature

stress (Caygill & Brand 2017), demonstrating the capacity of miRNAs to act as layers of regulatory control for biological networks.

In mouse neural stem cells, miR-34a overexpression has been shown to increase the proportion of post-mitotic neurons and increase the length of neurites, whereas inhibition of miR-34a produced the opposite effect (Aranha et al. 2011). The effect on neurite length was believed to be through the action of miR-34a on the already confirmed targeting of SIRT1 deacetylase, whereas the effect on differentiation was postulated to be controlled through the modulation of p53 activity (Tarantino et al. 2010). In a separate study by the same lab, they found that miR-34a expression was lowered during neurogenesis, and that the synapse formation and electrophysiological maturation of *in vitro* mouse neural stem cells was impaired with miR-34a overexpression (Morgado et al. 2015). These effects were shown to be through the targeting of Synaptotagmin 1 (Syt1) and Autophagy-related 9a (Atg9a) by miR-34 (Morgado et al. 2015). Taken together, these studies emphasise the capacity of a single miRNA to control multiple functional processes in various cellular and developmental contexts via the regulation of different targets.

1.17 miRNAs in polarisation and neurite pathfinding

Once neuronal cells are specified, the cells must polarise into their mature morphologies, and this is crucial to their function. The establishment of this polarised morphology has been extensively studied (Schelski & Bradke 2017; Lewis et al. 2013; Polleux & Snider 2010). The classical model system for the study of neuron polarisation is the *in vitro* culture of dissociated rodent Pyramidal Neurons (PNs), established in the late 1980s (Dotti et al. 1988). It is important to note however, that this model essentially captures the redevelopment of polarisation, as PNs develop their polarity from leading and trailing processes during migration from the ventricular zone to the cortex (Barnes & Polleux 2009). It is also important to note that not all neurons establish their polarity in the same manner. Retinal ganglion cells for example have been shown *in vivo* to polarize from the apical basal polarity of their progenitors (Zolessi et al. 2006). The *in vitro* culture of PNs has however

proven critical in building current understanding of the mechanisms underlying the establishment of polarity (Takano et al. 2015).

The growth and guidance of the axon, and the subsequent formation of correct synaptic contacts during development, is crucial to the function of the nervous system. Once established during neuronal polarisation, the axon rapidly extends towards its target, with the growth cone comprising both the “vehicle” and “navigator” of the extending process (Lowery & Van Vactor 2009). The discovery of the growth cone by Ramon y Cajal in 1890 was a huge leap forward in neuroscience, and to this day the understanding of the growth cone structure and function is one of the most important aspects of both developing and regenerative neuroscience (Tamariz & Varela-Echavarría 2015). Relevant to our work, the polarisation of neurons and subsequent pathfinding of the growing axon requires specific spatiotemporal expression of proteins, which can be controlled by miRNAs (Iyer et al. 2014).

For example, the Bantam locus in *Drosophila* encodes a miRNA which demonstrates developmentally controlled expression levels, and is associated with tissue growth and apoptosis (Hipfner et al. 2002; Brennecke et al. 2003). Bantam has been shown as a regulator of dendrite outgrowth of *Drosophila* sensory neurons. Bantam expression in epithelial cells of the larval body wall modulates Extracellular Matrix (ECM) contacts of the epithelium, which dampen Akt activity in the sensory neuron dendrites (Parrish et al. 2009; Jiang et al. 2014). Bantam mutants also demonstrate enhanced regeneration of dendrites in *Drosophila* sensory neurons, thought to be through the disruption of this pathway (Song et al. 2012). This miRNA has been further implicated in axonal growth during development; with bantam mutants showing severe alterations in axon structures in the brain (Banerjee & Roy 2018). These mutants also show an increased level of the actin modulator enabled in the brain, which is thought to be the cause of the aberrant axon development (Banerjee & Roy 2018). This demonstrates the ability of Bantam to regulate the correct development of nervous system connections through differential pathway modulation in neighbouring cells, and the neurons themselves.

Levels of Map1b in developing mouse cortical axons both *in vitro* and *in vivo* can be regulated by miR-9 targeting (Dajas-Bailador et al. 2012). Map1b has been shown to play a role in microtubule dynamics in the growing axon, supressing axon branching, and promoting axonal growth (Tymanskyj et al. 2012). Downregulation of Map1b through transfection of a miRNA-9 precursor in cortical neurons leads to a decrease in overall axon length, and a promotion of branching (Dajas-Bailador et al. 2012). Short two hour treatment of cortical axons with the neurotrophic growth factor BDNF decreases miRNA-9 presence in developing axons; miR-9 has therefore been proposed as a regulator through which elongation and branching of axons can be regulated in response to BDNF (Dajas-Bailador et al. 2012). This demonstrates the ability of a miRNA to control biological processes such as axon growth in response to external stimuli such as trophic factors.

1.18 miRNAs in synapse formation and function

The development of correct synaptic contacts is crucial to maturation of the nervous system. Again, this is a process which requires specific patterns of protein expression, under tight regulation, to form a functional mature synapse and miRNAs have been heavily implicated in this (Hu & Li 2017). Logically, due to their function as adaptive regulators of protein translation, miRNAs have also been shown to play a critical role in the formation and functioning of the synapse (Hu & Li 2017; Fiore & Schratt 2007). A subset of miRNA precursors have been shown to be enriched within synaptic fractions of the forebrain compared to whole tissue lysate (Lugli et al. 2008) and differential expression of miRNAs has been shown within synaptic fractions of the nucleus accumbens compared to the forebrain (Saba et al. 2012). This demonstrates the regulatory potential of miRNAs in synapse formation and the specification of synaptic subtypes.

Cytoskeletal modelling of the synapse for example is regulated by miRNAs. In hippocampal neurons *in vitro* miR-29a/b has been shown to inhibit the formation of dendritic spines, and instead promote the formation of filipodial outgrowths through cytoskeletal remodelling (Lippi et al. 2011). The action of miR-29a/b in dendritic

spine formation was shown to be through the targeting of the actin nucleation factor Actin-related protein 2/3 complex subunit 3 (Arpc3) by miR-29 (Lippi et al. 2011). Overexpression of another miRNA, miR-125b, in hippocampal neurons leads to elongation of dendritic protrusions (Edbauer et al. 2010). The action of miR-125b is believed to be, in part, due to the targeting of NR2A, a NMDA receptor subunit leading to downstream cytoskeletal remodelling (Edbauer et al. 2010). These examples demonstrate the ability of miRNAs to regulate synapse formation, and therefore potential synaptic plasticity, at the level the cytoskeleton.

A key aspect of synapse development and function is the activity dependent maturation and plasticity of the synapse (Yao et al. 2006; Ataman et al. 2008). It has been demonstrated that the levels of a number of miRNAs can be modulated through the activity of neurons (Sim et al. 2014). In one study, the model system of the *Drosophila* larval NMJ was used (Nesler et al. 2013). Several miRNAs were found to be downregulated in the larval CNS following light stimulation of ChR2 expressing motor neurons: miR- 1, -8, -289, -314, and -958 (Nesler et al. 2013). Further to this, miR-8 was suggested to be involved in the restriction of NMJ growth through the downregulation of its target, wingless (Nesler et al. 2013). A subsequent study then demonstrated the role of miR-8 in the formation of the NMJ through targeting of multiple cell adhesion molecules, allowing their correct localisation at both the pre- and post-synapse (C. S. Lu et al. 2014). These studies are a demonstration of how miRNAs which can be modulated by neuronal activity may exhibit downstream effects on the architecture of the synapse.

As well as miRNAs role in the formation of the synapse architecture in response to neuronal activity, miRNAs also play a role in the plasticity of the mature synapse in response to neuronal activity. A key paper which demonstrated the role of miRNAs in the activity dependant plasticity of the nervous system centred on the activity dependant maturation of miR-181 in dendrites (Sambandan et al. 2017). In this study, a fluorescent reporter construct was used to demonstrate that miR-181 is processed from pre-miRNA into mature miRNA in a spatially and activity dependent manner within the dendrites of hippocampal neurons (Sambandan et al. 2017). This

activation of miR-181 was associated with its localised targeting of the synaptic regulator CamKIIa (Sambandan et al. 2017). This shows how miRNAs can be locally activated in response to neuronal activity and how this allows miRNAs to exhibit targeted precise effects.

Along with the activity dependent production of mature miRNAs described in (Sambandan et al. 2017), the reversible miRNA mediated silencing of transcription allows for fast temporal control of gene expression. For example, miR-134 is a negative regulator of dendritic spine size through dendrite localised targeting of the mRNA encoding for the actin polymerisation regulator LIM domain kinase 1 (LIMK1) (Schratt et al. 2006). This is an activity dependent mechanism, as it has been shown that application of BDNF (which is endogenously released in response to synaptic stimulation) can remove miR-134 mediated repression of LIMK1 translation (Schratt et al. 2006). This example demonstrates how miRNA mediated repression can be lifted in response to synaptic activity, allowing for appropriate maturation of the synapse.

In a screen for miRNAs involved in *Drosophila* olfactory memory, miR-974 and miR-31a appeared as regulators of memory formation (Busto et al. 2015). The specific neuronal subtypes through which these miRNAs act were then identified, with miR-31a shown to be required in cholinergic neurons for the correct formation of memory (Busto et al. 2015). Whereas inhibition of miR-974 in the olfactory receptor neurons and the mushroom body V2 neurons led to the enhanced performance of memory (Busto et al. 2015). Predicted targets for these miRNAs were identified, but the exact mechanism through which they act in the process of memory formation was not defined.

Models of developmental neurological disorders also provide us with miRNAs which modulate synapse formation. For instance, in the amygdala of rat models of autism, miR-181 shows increased levels (Olde Loohuis et al. 2015), as well as in cell lines derived from human Autism spectrum disorder samples (Ghahramani Seno et al. 2011). This suggests the relevance of miR-181 in neurological disorders. Inhibition of

miR-181c increased axon growth in rat cortical neurons *in vitro*, but lowered dendritic spine density, demonstrating the possibility of miR-181 playing multiple roles in neuronal development (Kos et al. 2016). Moreover, RNA sequencing following miR-181c inhibition in cortical primary cultures showed significant alterations in the expression of neurodevelopmental genes which possess predicted miR-181c target sites within their 3'UTR (Kos et al. 2016). The exact mechanisms of miR-181 action within autism however are yet to be shown.

One particular example of the modulation of synaptic activity by miRNAs in the context of this work is the *Drosophila* miRNA, miR-1000, and its mammalian homologue, miR-137. Reduced levels of miR-1000 expression are observed in aged adult *Drosophila* heads, and miR-1000 knock out flies demonstrate a significantly reduced lifespan (Verma et al. 2015). This miR-1000 knockout leads to increased levels of apoptosis in the brain of *Drosophila*, believed to be due to its roles in regulating glutamate excitotoxicity of neurons (Verma et al. 2015). The mammalian homologue of miR-1000, miR-137, is believed to play an equal role in the regulation of glutamate excitotoxicity in mice (Verma et al. 2015). In a separate study, it was shown that an increase in levels of miR-137 can lead to aberrant synaptic function in reprogrammed human fibroblasts *in vitro*, and overexpression of miR-137 in mice *in vivo* causes learning behavioural defects (Siegert et al. 2015). Some slight improvements in these deficits can be achieved through miR-137 sequestration (Siegert et al. 2015). This suggests that the mechanism of action of miR-137 may act in a different context to that of the *Drosophila* homologue, miR-1000, demonstrating the importance of considering the context through which a miRNA is being investigated.

miR-34, in addition to its role in nervous system development (Aranha et al. 2011; Morgado et al. 2015) has also demonstrated a role in aging and neurodegeneration in *Drosophila*. miR-34 is upregulated in the *Drosophila* brain during ageing, and miR-34 mutant flies show a reduced lifespan (Liu et al. 2012). This lifespan reduction is accompanied by a transcriptional profile which associated with accelerated aging in miR-34 mutants, suggesting miR-34 is a master regulator of neurodegeneration

associated genes, either through direct targeting of the miRNAs or indirect pathway modulation (Liu et al. 2012). miR-34 has additionally been implicated in the pruning of axons during mushroom body remodelling in *Drosophila* through targeting the ecdysone receptor EcR-B1 (Lai et al. 2016), this could suggest a further role for miR-34 in nervous system and synaptic contact remodelling within the mature nervous system.

1.19 Summary

The nervous system is a complex network of multiple cell types, with neurons and supporting non-neuronal cells. Neurons are highly specialised cells, both in terms of morphology and function. Control of protein homeostasis, and particularly the spatial and temporal control of translation of proteins, has been shown to play an important role in the development and function of the nervous system. As regulators of protein translation, miRNAs have become accepted as important regulators of the development, maintenance, and function of the nervous system. The expression and action of several miRNAs such as those described above have been associated with processes of the nervous system. However, the full repertoire of miRNAs that are able to be involved in these processes, and the exact molecular mechanisms of their functions, has not been fully elucidated.

1.20 Hypothesis and aims

We believe, based on the assessment of previous research outlined above, that there is still much scope for the identification and classification of individual miRNAs, and the investigation of their individual functions within processes of the nervous system. This overarching hypothesis was investigated in two separate parts using independent experimental paradigms:

1. Identification of miRNAs which could regulate nervous system function in chronic nociception and pain

2. Investigation of individual miRNAs that control nervous system development and function in *Drosophila melanogaster*

Chapter 2. Materials and methods

Methods are described as per the order of appearance in results chapters. Standard protocols are not repeated (i.e. Luciferase assay). Suppliers for all reagents are named in the first instance.

2.1 Identification of miRNAs which may play a role in pain processes

2.1.1 Hyperalgesic priming and Dorsal Root Ganglion extraction

The model of hyperalgesic priming was used to identify miRNA which may be relevant in the processes of inflammatory nociception sensitisation. Animal husbandry and hyperalgesic priming protocols were performed by James Spalton, (Appendix II). For all experiments performed on RNA extracted from Dorsal Root Ganglia (DRG), one affected DRG from each animal was used, therefore each DRG represents a separate animal. In the context of all data analysis each individual DRG represents an individual repetition.

2.1.2 RNA extraction from fixed DRG tissue

RNA was extracted from DRG in order to assess the levels of miRNA. The processing of fixed DRG tissue was carried out by A. Rathbone. PFA (Fisher Scientific) was removed from fixed DRGs through washing with 100% Ethanol twice, followed by air drying. Digesting buffer (50mM Tris-HCl, 75mM NaCl, 5mM $CaCl_2$, 0.5mg/ml proteinase K and 0.1%(w/v) SDS (all Sigma), pH7.5) was applied to the tissue followed by manual homogenisation with a sterile RNAse-free micro-homogeniser and incubated at 55°C for 3 hours. 1ml TRIzol reagent (Fisher scientific) was added per 50-100mg of tissue, followed by a secondary manual homogenisation with a sterile micro-homogeniser. The extraction then continued as outlined in 2.1.2.

2.1.3 TRIzol extraction of RNA

Samples were lysed and homogenised in one volume of TRIzol reagent, and incubated at room temperature for 5 minutes to allow dissociation of the ribonucleoprotein complexes. One fifth volume of chloroform was added to the sample, capped securely and vortexed, followed by a 5 minute incubation at room temperature. The sample was then centrifuged for 15 minutes 12,000xg at 4°C. The clear upper aqueous phase containing the RNA was transferred to a new tube, taking care not to disrupt the interphase or lower red phenol-chloroform phase. One half volume of isopropanol was added to the aqueous phase, and the sample was placed at -20°C overnight. Sample was centrifuged for 10minutes 12,000xg at 4°C, and the

supernatant removed from the RNA pellet. The RNA pellet was washed in one volume of 75% ethanol in Hyclone RNAse and DNAse free water (GE Healthcare) followed by centrifugation for 5minutes 7500xg at 4°C and removal of supernatant. The RNA pellet was allowed to air dry before resuspension in Hyclone. To aid RNA resuspension the sample was incubated at 55°C for 5minutes. RNA concentration and purity was then determined using a Nanodrop 2000c UV/Vis Spectrophotometer (Thermo Fisher Scientific), before storage at -80°C.

2.1.4 miRNA microarray

Extracted DRG RNA from two control and two primed animals was sent for microarray analysis by Toray industries. Due to sample integrity the data shown is as a result of analysis of one control and two primed samples. Data shown was obtained from the Toray 3D gene rat miRNA V20 chip (Toray Industries). In total 729 miRNAs are mounted on the array (Appendix III.) this represents 95.42% of the 764 mature miRNAs identified for rat on miRBase. Annotation and oligonucleotide sequences of the probes are conformed to the miRBase miRNA data base Release 19. Chips include a number of control and spike in probes. Spots with intensities above that of the blank are considered “present”.

Briefly, a hybridisation buffer was added to the RNA samples prior to injection into the chip. Chips were incubated at 32°C for 16 hours with agitation to allow for hybridisation. Chips were then washed, and scanned with 3Dgene Scanner® 3000 instrument (Toray) to measure fluorescence intensity of the array. Obtained images were analyzed with the 3D-Gene® Extraction software (Toray). Auto analysis files were delivered for further analysis.

2.1.5 qPCR

qPCR was carried out to determine the levels of miRNA within extracted RNA samples. miRNA cDNA was synthesised from total RNA using the miRCURY LNA Universal cDNA synthesis kit (Exiqon) using the supplied poly-T primer and following manufacturer’s instructions. ROX (Thermo Fisher Scientific) was added to the cDNA as a passive reference dye for normalisation of fluorescence. A non-template control (NTC) was included for each primer to confirm absence of background signal or contamination. Spike in samples containing Sp6 were used as confirmation of PCR efficiency and also as inter-plate calibrators where necessary. For each sample the

assay was repeated in duplicate within the same plate to produce on repetition of the assay. qPCR was performed using the ExiLENT SYBR Green master mix kit (Exiqon) using a StepOne Plus Thermocycler (Applied Biosystems) with the following cycling parameters: Polymerase Activation/Denaturation 95°C, 10 min; 40 amplification cycles of 95°C, 10 s then 60°C, 1 min, ramp-rate 1.6°C/s. StepOne software version 2.3 (Applied Biosystems) was used for data acquisition and cycle threshold (Ct) value calculation. Ct values were analysed for relative miRNA quantification using the comparative ΔCt method (Bustin 2002). miR-138 primers used were the hsa-miR-138-5p LNA PCR primer set (Exiqon) which are reported to be compatible with samples from rat. SNORD33_F: 5'-AGCTTGTGATGAGGATGTCTCC-3' SNORD33_R:5'-TGGTAGTGCATGTAGAGTCGTC-3' primers were designed with Primer3 software.

2.1.6 Bioinformatics

A bioinformatics approach was undertaken to identify relevant target genes for miR-138-5p. A list of predicted targets for miR-138-5p was generated through the miRgate database from known 3'UTRs of protein coding genes. The miRgate database is an online access target prediction database, curated from multiple prediction algorithms, including computational and validated target databases (Andrés-León et al. 2015). Transcript IDs were converted to gene IDs through Biomart (Ensembl). Resulting gene IDs were imported into PANTHER gene ontology database (Mi et al. 2013), to be sorted into relevant pathways.

2.1.7 Cloning of miRNA target sites into luciferase construct

In order to confirm the interaction of a miRNA with a predicted target site the method of luciferase assay is used. Oligonucleotide pairs were designed so that when annealed they contained the desired miRNA target region in the correct conformation. Here the miRNA target region is inserted into the pmiRglo vector, as opposed to the entire 3'UTR. Restriction sites were included on either end, so that overhangs created by oligonucleotide annealing are complementary to those generated by restriction enzyme digestion of the pmiRglo Vector (Promega, Appendix I). An internal *NotI* restriction site was added to oligonucleotides for clone confirmation.

Table 2.1.1 miRNA target site oligonucleotides

Oligo	Sequence (5'-3')
MYD88_138_1+2_F	CTAGCATGCGGCCGCAGACACTATAGAACAGGACCAGCTGAGACTAAGAAGGACCAGCAG
MYD88_138_1+2_R	TCGACTGCTGGTCCTTCTTAGTCTCAGCTGGTCCTGTTCTATAGTGTCTGCGGCCGCATG
MYD88_138_3_F	CTAGCATGCGGCCGCGAATGTACTCTCACACACACAGGCACCAGCATACACG
MYD88_138_3_R	TCGACGTGTATGCTGGTGCCTGTGTGTGTGAGAGTACATTCGCGGCCGCATG
Pax6_190_F	CTAGCGGCGGCCGCTTTTGACAAGCAATTTACATATCTG
Pax6_190_R	TCGACAGATATGTAAATTGCTTGTCAAAAGCGGCCGCCG
DACH1_190_S1_F	CTAGCGCGGCCGCATGAAATAACATTTTGCATATCTG
DACH1_190_S1_R	TCGACAGATATGCAAAATGTTATTTCATGCGGCCGCG
DACH1_190_S2_F	CTAGCGCGGCCGCTCTCTTTGTTTTTTGCATATCTG
DACH1_190_S2_R	TCGACAGATATGCAAAAAACAAAGAGAGCGGCCGCG

Oligonucleotides were delivered in a lyophilised state (Integrated DNA technologies), and suspended in hyclone to a concentration of 1µg/µl prior to annealing. pmiRglo vector was digested with *NheI*-HF (NEB) and *SalI*-HF (NEB) followed by alkaline phosphatase (NEB) treatment to prevent re-ligation of the linearized plasmid DNA. Annealed oligos were ligated into the pmiRglo vector with T4 DNA ligase (NEB). Resulting plasmid was transformed into XL10 gold high-efficiency competent cells through heat shock, and cultured on an LB agar (Sigma) Ampicillin (Sigma) plate overnight at 37°C. Colonies were picked, and cultured for miniprep (Qiagen) extraction of the plasmid following manufacturer's instructions. Efficient cloning was confirmed through *NotI* (NEB) digestion of plasmid followed by agarose gel visualisation of excised fragment bands. Plasmid sequence was then confirmed through sequencing.

2.1.8 Site-directed mutagenesis of miRNA target constructs

Primers were designed in order to generate through PCR a mutant strand where the four nucleotides which represented the 2^{nd}-6^{th} nucleotides of the miRNA target site seed sequence were altered.

Table 2.1.2 Primers for site-directed mutagenesis

Primer	Sequence (5'-3')
MYD88_S3_SDM_F	TACTCTCACACACACAGGCAAACACATACACGTCGACCTG
MYD88_S3_SDM_R	CAGGTCGACGTGTATGTGTTTGCCTGTGTGTGTGAGAGTA
Pax6_190_SDM_F	GCCTGCAGGTCGACATGCCTGTAAATTGCTTGTC
Pax6_190_SDM_R	GACAAGCAATTTACAGGCATGTCGACCTGCAGGC
DACH1_S2_SDM_F	CCTGCAGGTCGACATGCCTGCAAAATGTTATTTC
DACH1_S2_SDM_R	GAAATAACATTTTGCAGGCATGTCGACCTGCAGG

PCR reaction was carried out within Phusion reaction buffer (NEB). Mutant strand synthesis cycle was as follows: 95°C for 30 seconds; 18 cycles of 95°C for 30 seconds, 55°C for 1 minute, 68°C for 9 minutes; hold at 4°C. PCR product was subsequently DpnI (NEB) digested to remove the parental dsDNA prior to transformation into XL10 gold cells, and confirmation of mutagenesis as in 2.1.6.

2.1.9 Seeding and transfection of HEK293T cells for luciferase assay

HEK293T cells were seeded at a density of $0.8x10^5$ cells per well in a 24 well plate, with 1ml media volume per well (DMEM, 10% FBS, 2% Pen Strep (all Sigma)). 24 hours after seeding, cells were transfected with Lipofectamine2000 following manufacturer's instructions (Fisher Scientific). 50ng of the appropriate reporter plasmid containing the predicted target site per well, plus either the miRNA mimic or miRNA mimic control at a final concentration of 50nM was transfected. For miR-138 luciferase: hsa-miR-138-5p miRCURY LNA™ microRNA Mimic and Negative Control Scramble4 miRCURY LNA™ microRNA Mimic (both Exiqon). For miR-190-5p luciferase: miRIDIAN microRNA Human hsa-miR-190a-5p mimic, and miRIDIAN microRNA mimic negative Control #1 (Both Dharmacon) were used. Cells were then incubated at 37°C 5% CO_2 for 48 hours prior to luciferase reporter assay. Three separate transfections per condition were performed per replicate of the assay, and the resulting luciferase reporter assay results of these were combined into one replicate. Each replicate of the assay was performed on a separate day with cells which were independently split and seeded.

2.1.10 Luciferase reporter assay

The luciferase reporter assay allows for confirmation of the miRNA targeting of a predicted target site (figure 2.1.1). Luciferase reporter assay was carried out using the luciferase reporter assay system (Promega) following the manufacturers protocol. Briefly, cells were washed with ice cold sterile PBS (Sigma). Cells were then lysed in 100µl passive lysis buffer for 30minutes at room temperature. Lysed cultures were agitated by pipetting until complete lysis was achieved. 10µl of lysed cells per each transfection was assayed in triplicate per repetition of the assay. Luciferase activity of the lysed cells was assessed in a white 96 well plate (Greiner) with an

automatic luminometer (Berthold), the outer wells of the plate were not used to prevent any distortion of the light signal produced.

2.2 *In vitro* modelling of nociception

2.2.1 Dissociation of DRG

In order to culture the DRG cells within the microfluidic device, the ganglia must be dissociated into individual cells. DRG were extracted from E18 Wistar rats and transferred into L15 medium (Gibco) on ice until the required quantity of DRG were extracted. Following extraction, DRG were treated for 10 minutes with 0.025% trypsin (Sigma) in calcium and magnesium free PBS (Sigma) followed by 15 minutes collagenase (Gibco) digestion at 37°C. Collagenase was removed through pipetting and DRG were mechanically dissociated in DMEM (Gibco). Cell suspension was centrifuged for 5 minutes at 1000xg and the resulting cell pellet suspended in the appropriate volume of DRG growth media (DMEM (Gibco), 2% B27(Invitrogen), 1% Penicillin Streptomycin (Sigma), 2mM Glutamax (Gibco), 50ng/ml GDNF (Invitrogen), 50ng/ml NGF (Invitrogen) 4uM Aphidocolin (Sigma)). The anti-mitotic Aphidocolin is included within the DRG growth media in order to restrict the proliferation of non-neuronal cells.

2.2.2 Bath culture of dissociated DRG

A 50µl droplet of 20µg/ml laminin (Sigma) in DMEM was applied to the centre of an ibiTreat precoated µ-dish (ibidi) for at least one hour prior to cell seeding. Laminin solution was removed, and 50µl of DRG cell suspension containing 2 ganglia was applied to the centre of the dish in a droplet. Cells were allowed to attach overnight, and 1.5ml of DRG growth media was added to the cells the following morning. Media was completely replaced every 3-4 days of culture.

2.2.3 Calcium imaging

To assess the activity of the neurons *in vitro* here the method of calcium imaging was used. The Fluo-5 calcium indicator dye (Fisher Scientific) was suspended in pluronic (Fisher Scientific) at a concentration of 10µM and stored in aliquots at -20°C. Fluo-5 in pluronic was then diluted to 100nM concentration in imaging buffer (135mM NaCl, 3mM KCl, 10mM HEPES, 15mM glucose, 1mM $MgSO_4$, 2mM $CaCl_2$, (all Sigma)) immediately prior to calcium imaging.

Media was removed from cultured cells, and cells were washed in imaging buffer. Cells were loaded through incubation in 100nM Fluo5 calcium indicator dye in

imaging buffer for thirty minutes. Excess Fluo5 was washed from the cells with imaging buffer, followed by incubation of the cells in imaging buffer for thirty minutes to allow de-esterification of the indicator dye.

Loaded cells were then imaged using a Nikon Eclipse T*i* inverted microscope. Cells were excited at 450/20 nm with an exposure of 50 ms. Fluorescence emission of calcium bound dye at 535/50 nm was detected with a Zyla 4.2 sCMOS camera (Andor Technology, Belfast, UK) and recorded in Micromanager (Edelstein et al. 2014). Image analysis was carried out using Fiji software (Schindelin et al. 2012). Multiple ROI were selected, and simultaneous mean fluorescence levels of individual cells were measured. Change in fluorescence is shown as normalised to a baseline of culture without stimulus for 15 seconds.

2.2.4 Microfluidic device culture

Microfluidic device culture of DRG cells allows for the physical and environmental separation of neuronal cell bodies and axons. Microfluidic devices (Xona) were prepared for cell culture through soaking overnight in DMEM at 37°C. Devices were then washed twice in sterile water and once in 70% ethanol before being allowed to air dry. Nunclon (Thermo scientific) dishes were coated in 0.1mg/ml poly-L-lysine (Sigma) in sterile water for at least one hour, before being washed twice with sterile water and allowed to completely dry. Microfluidic devices were then applied with gentle pressure to the NUNC dishes, microgroove side down. Once secure, devices were washed through with DMEM and careful pipetting was used to gently force media flow through the channels and microgrooves. Media was then removed from the wells of the device and replaced by DRG growth media containing 20µg/ml of laminin. This laminin suspension was allowed to coat the inside of the device for at least 1 hour at 37°C and removed immediately prior to cell seeding. Dissociated DRG cell suspension was applied through smooth and slow pipetting into the culture channels to allow cells to enter the channel of the device 20µl of suspension was applied per device, 10µl each side of the channel to prevent excessive flow through. Once cell suspension was applied, cells were allowed to attach for 1-2hours before additional DRG growth medium was added to the wells of the device, typically 200µl per well. Media was topped up every 2-3 days as required. If high levels of media evaporation were observed, water was placed around the device to provide extra

humidity to the culture. In experiments where fluidic isolation of the axon was required, a media difference between channels of at least 50µl was created and monitored.

2.2.5 Immunofluorescence

In order to assess the morphology of the DRG neurons growing within the microfluidic devices, the cells were imaged following immunofluorescent staining. Dissociated DRG cells were cultured within a microfluidic device as described. Following 5 days of culture the device was removed with forceps in a smooth upwards motion. The culture was washed once with PBS before fixation in PFA for 30 minutes. PFA was removed, and remaining was quenched in PBS with 0.3% 100x Triton (0.3% PBST) and 10mM Glycine (all sigma). Cells were permeabilised with 0.3% triton in PBS (0.3%PBST), then blocked for one hour at room temperature in 3% (w/v) BSA in PBS. Acetyl tubulin primary antibody was applied at a 1:500 concentration in 3% (w/v) BSA in PBS overnight at 4°C. Primary antibody was washed from the cells with 0.3%PBST before application of secondary antibody in 3% (w/v) BSA in PBS for 2 hours at room temperature. Excess antibody was washed from the cells with 0.3%PBST before one wash in PBS. A coverslip was placed over the cells with Vectashield hard set with DAPI. Cells were then imaged using a 200M microscope (Zeiss) mounted with a CoolSnap MYO camera (Photometrics).

2.2.6 Lipophilic tracer dye

Lipophilic tracer dye was applied to the microfluidic device culture in order to confirm fluidic isolation of the cell body and axonal chambers. Dissociated DRG cells were cultured within a microfluidic device as described. Following 2 days of culture, media was removed from the cell body channel, and attached media wells were filled with 200µl of fresh DRG growth media. Media was then removed from the axonal chamber, and replaced with 50µl fresh DRG growth media containing DiO lipophilic tracer dye (Thermo Fisher Scientific) at a concentration of 5µM. 12 hours following the application of the dye, cells were washed once with DRG growth media and then imaged live using a Zeiss 200M microscope mounted with a CoolSnap MYO camera (Photometrics).

2.2.7 Culture of DRG on porous membranes

Porous membrane culture of DRG allows for the physical separation of neuronal cell bodies and axons. Inserts used in this work were transwell permeable supports, with

PET membrane and pore size of 3µm (Corning). Culture method was developed from (Unsain et al. 2014). The inserts, when placed into the wells of a standard cell culture plate form two compartments. An upper compartment where the DRG explants are applied and a lower compartment where the DRG axons grow and extend. Culture inserts were coated through submersion in 0.1mg/ml poly-l-lysine for 1 hour, followed by washing twice in sterile water and being allowed to dry. Inserts were then coated by submerging in 20µg/ml laminin in DMEM for 1 hour. 2ml of DRG growth medium was added to each well of a six well plate, the culture inserts were then inserted into the wells, and a further 1ml of DRG growth medium was applied to the upper compartment. DRG were extracted from E18 Sprague Dawley rats into L15 medium on ice. 15 explants were transferred onto the upper side of each culture insert through pipetting. The plate was gently tapped on a flat surface to encourage DRG sinking and attachment to the filter. Media was exchanged every 3 days of culture.

2.2.8 Extraction of cell fractions from porous membrane culture

In order to assess the physical separation of neuronal cell bodies and axons the expression of nuclear RNA was assessed in the RNA extracted from either side of the culture. All media was aspirated from the culture, and both the explant and axon sides of the filter were washed with sterile PBS. Axonal RNA was first extracted: 1ml TRIzol reagent was washed over the axonal side of the culture, and the bottom of the filter was scraped with a sterile cell scraper. TRIzol was then repeatedly washed over the scraper and filter and collected. Once axonal RNA had been removed, 1ml TRIzol reagent was applied to the top of the filter, the filter was scraped with a sterile cell scraper, and the DRG explants were homogenised through pipetting up and down. RNA extraction then proceeded as outlined in 2.1.2. qPCR was carried out as outlined in 2.1.5.

2.3 Identification of miRNA which may play a role in nervous system development

2.3.1 *Drosophila* stocks

Table 2.3.1 contains a list of stocks used and where they originated. All stocks were obtained from the Bloomington *Drosophila* Stock Centre (BDSC, Indiana). A list of all Upstream Activation Sequence (UAS)-miRNA lines used for the initial investigation in

the *Drosophila* eye from (Bejarano et al. 2012) can be found in appendix IV. The balancer chromosomes, markers and genetic constructs contained within these lines are described in tables 2.3.2 and 2.3.3.

Table 2.3.1 *Drosophila* stocks

Stock descriptor	Genotype
Eyeless Gal4	w[*]; P{w[+m*]=GAL4-ey.H}4-8/CyO
Mushroom body Gal4	w[*]; P{w[+mW.hs]=GawB}OK107 ey[OK107]/In(4)ci[D], ci[D] pan[ciD] sv[spa-pol]
Pan neuronal Gal4	P{GawB}elav[C155]
Glutamatergic Gal4	w[1118]; P{w[+mW.hs]=GawB}VGlut[OK371]
Cholinergic Gal4	w[*]; Mi{Trojan-GAL4.0}ChAT[MI04508-TG4.0]/TM6B, Tb[1]
UAS miR-190 sponge	w[*]; P{y[+t7.7] w[+mC]=UAS-mCherry.mir-190.sponge.V2}attP40; P{y[+t7.7] w[+mC]=UAS-mCherry.mir-190.sponge.V2}attP2
UAS Scramble Sponge	w[*]; P{y[+t7.7] w[+mC]=UAS-mCherry.scramble.sponge}attP40; P{y[+t7.7] w[+mC]=UAS-mCherry.scramble.sponge}attP2

Table 2.3.2. Balancer Chromosomes and Markers

Symbol (name)	Chromosome	Type	Phenotype
CyO (Curley of Oster)	2	Balancer	Curly Wings
Ln(4)ci[D], ci[D] pan[ciD] sv [spa-pol]	4	Balancer	Shortened wing vein
TM6B, Tb[1]	3	Balancer	Tubby larvae, Humeral adult

Table 2.3.3. Genetic Constructs

Genetic construct	Description
P{w[+m*]=GAL4-ey.H}4-8	Expresses GAL4 under the control of ey. Strong expresser.
P{w[+mW.hs]=GawB}OK107 ey[OK107]	GAL4 expressed in mushroom bodies.
P{GawB}elav[C155]	Expresses GAL4 in neurons under elav control. Expression begins in the embryonic nervous system at stage 12.
P{w[+mW.hs]=GawB}VGlut[OK371]	Expresses GAL4 in glutamatergic neurons from embryonic stage 15 to adult.
Mi{Trojan-GAL4.0}ChAT[MI04508-TG4.0]	Expresses GAL4 under the control of ChAT regulatory sequences.
P{y[+t7.7] w[+mC]=UAS-mCherry.***.sponge.V2}attP40	Expresses an antisense 'sponge' RNA under UAS control for knocking down miRNA expression

2.3.2 *Drosophila* husbandry and crosses

Drosophila stocks were maintained on standard cornmeal medium at 25 or 18°C as required. Stocks were maintained as received from Bloomington and not isogenised on receipt. An 8 litre batch of standard cornmeal medium consists of: 7340ml H2O, 565ml golden syrup, 127g yeast, 73g soya flour, 536g cornmeal, 42g agar and 35.4ml propionic acid.

The life cycle of the fly is on average 10 days at 25°C and 21 days at 18°C (Ashburner et al. 2005), stocks were flipped twice weekly when at 25°C or monthly at 18°C.

Flies were anaesthetised using CO_2 for virgin collection or phenotype assessment, using a CO_2 diffusion pad and M60 dissection microscope (Leica). Virgins were collected every 8 hours at 25°C and 16 hours at 18°C, based on standard timings (Ashburner et al. 2005). Crosses were set with an approximate female to male ratio of 3:1 with between 10 and 20 females per vial.

For all crosses, virgin females from the Gal4 driver were crossed with males from the desired UAS construct stock. Progeny were screened for the appropriate genetic markers and balancers to ensure the inheritance of desired constructs.

2.3.3 *Drosophila* eye imaging

To assess the effect of miRNA overexpression within the developing eyes of *Drosophila* the adult eye was imaged and scored on size and ommatidia patterning. Adult flies were euthanized through freezing at -80°C for at least 30minutes, and stored at -80°C until imaging. Flies were mounted whole on a glass slide on their

right side with double sided tape to allow imaging of the eye. Eyes were imaged using a 200M microscope (Zeiss) mounted with a CoolSnap MYO camera (Photometrics) using bright field illumination to allow visualisation of the eye structure and ommatidia centres. Z stacks of each eye were taken, with increments of 10μM, creating approximately 20 images per eye, these were then processed via maximum intensity projection to produce the final images. The number of animals imaged for each genotype ranged from 8 to 15, with a median of 12.

2.3.4 *Drosophila* eye size measurement

Eye size measurements shown are measurements of the area of the external eye structure taken from a maximum intensity projection of the eye z stack. Measurements were obtained by manually tracing the perimeter of the external eye structures using the freehand selection tool in Fiji (Schindelin et al. 2012). All measurements are shown as a percentage relative to the mean of the eyGal4 heterozygotes. The number of animals assessed per genotype ranged from 8 to 15 with a median of 12.

2.3.5 *Drosophila* eye ommatidia disorder scoring

The analysis of the disruption of ommatidia pattern was determined through a manual method of scoring. The maximum intensity projections of the eye z stacks were visually scored based on the patterning of the ommatidia. 0: No disruption in ommatidia pattern observed; 1: Some regions of disruption, however majority of ommatidia structures remain ordered; 2: The majority of ommatidia showing disorder, however some regions of organisation still observed; 3: No ordered regions visible in the eye, complete disorder. For images representative of these scores please see (figure 5.2.2). All scores are shown as the mean of the individual eye scores. The number of animals assessed per genotype ranged from 8 to 15, with a median of 12.

2.4 Investigation of miR-190 in nervous system development

2.4.1 Embryo collection and fixation

The patterning of miR-190 expression through embryonic development was to be assessed, as such *Drosophila* embryos of the correct stage were collected. Crosses were set and male and female flies were allowed to acclimatise to embryo laying cages with an apple juice agar plate and yeast paste for around 24 hours before

embryo collections began. Apple juice plates consist of (for around 60 50mm plates): 18g agar, 600ml water, 20g sucrose and 200ml apple juice. A fresh apple juice agar plate with yeast paste was transferred to the embryo collection cage for the required laying time. Embryos were then aged at 25°C as required. Embryos were then gently dislodged from the plate using water, and sieved from the yeast paste in a cell strainer. Embryos were dechorinated in 50% bleach for 3 minutes. Dechorionated embryos were rinsed with water and transferred to heptane in a glass vial. An equal volume of 5% PFA was added to the heptane, and embryos were fixed at room temperature on a shaking platform (250rpm) for 20 minutes. PFA:Heptane mixture was removed, and embryos were then vortexed for 2 minutes in a 50:50 methanol:heptane mixture. Dechorionated embryos then sink to the bottom of the vial, and are stored in 100% methanol at -20°C until required.

2.4.2 smiFISH miRNA probe design and preparation

The method of Small molecule inexpensive fluorescent in situ hybridisation (smiFISH) was used to visualise the expression pattern of miR-190 in *Drosophila* embryonic development. Probes were designed by the Ronshaugen lab at the University of Manchester (UK), using the Stellaris probe designer tool. The target Pri-miRNA sequence is selected from the Flybase Genome Browser and inserted into the probe designer tool. Probes were designed with a length of 19-21 nucleotides, with an average of 34 probes per Pri-miRNA. Probes were masked against the *Drosophila* genome in order to improve specificity of binding to the target sequence. Probe sets used in this project can be found in Appendix V. Probe sequences were all modified to include a FLAP sequence, which would allow for them to be hybridised with a fluorescent tag with an attached complementary FLAP tag. Probes were delivered lyophilised in 96 well plates (Integrated DNA Technologies). Probes were prepared through hybridisation of the gene specific probe and labelled FLAP sequence in 1x NEB buffer at 85°C for three minutes, 65°C for three minutes and cooling to room temperature. Probes were then stored at -20°C.

2.4.3 smiFISH

smiFISH protocol for *Drosophila* embryos was developed from that outlined in (Tsanov et al. 2016) by the Ronshaugen lab in Manchester. Fixed embryos stored in methanol were rehydrated in 0.05% PBS-Tween (Sigma) through three five minute

washes. Embryos were then transitioned into stellaris wash buffer (2x SSC, 10% deionized formamide (Sigma)) through one 50:50 wash for ten minutes then two five minute washes in wash buffer. Embryos were incubated in wash buffer for 30 minutes at 37°C in a water bath. Embryos were incubated overnight in 80nM probe mixture in Stellaris hybridisation buffer (2x SSC, 10% deionised formamide, 10% dextran sulphate). Embryos were then washed twice for fifteen minutes in Stellaris wash buffer at 37°C. This was followed by three 0.05% PBS-Tween washes at room temperature. Embryos were then washed once with PBS before being transferred to slides, and mounted with hard set Vectashield with DAPI (Vectorlabs) or proceeding to immunostaining.

2.4.4 Embryo immunostaining

If necessary, embryos were removed from methanol and rehydrated through washing 3 times for five minutes in 0.3% PBS-Triton (Sigma). Embryos were then blocked in 1x Western Blocking Reagent (WBR, Sigma) in PBS for 30 minutes at room temperature. Primary antibody mixes were applied in 1xWBR for 2 hours at room temperature, or overnight at 4°C. Anti-CNS axons (BP102), anti-Repo (8D12) and anti-Dachshund (mAbdac1-1) hybridoma supernatant antibody extracts (all DSHB) were used at a concentration of 2µg/ml. Primary antibody was washed from the embryos through 0.3% PBS-Triton washes at room temperature. Secondary antibody was applied for two hours at room temperature in 1xWBR. Secondary antibody was washed from the embryos through 0.3% PBS-Triton washes at room temperature. Embryos were then washed once with PBS, before being transferred to slides and mounted with hard set Vectashield with DAPI.

2.4.5 *Drosophila* embryo imaging

Embryos were visually assessed for developmental stage from guidelines contained within the Atlas of *Drosophila* development from the interactive fly online resource (Hartenstein & Brody 1999) or (Campos-Ortega & Hartenstein 1997). smiFISH and immunostained embryos were imaged with an LSM 880 laser scanning confocal microscope (Carl Zeiss), and resulting Z-stacks were processed with either Zen software version 2 (Carl Zeiss) or Fiji (Schindelin et al. 2012). smiFISH and imaging of embryos was carried out at least three times, from separation embryo collections,

and all possible embryos per slide were assessed to ensure certainty of expression patterns observed.

2.4.6 Viability assay

In order to assess the effect of miRNA expression modulation a viability assay of the developing *Drosophila* was carried out. The viability assay was modified from the method used in (Chen et al. 2014). First instar larvae were collected of the required genotype. Three crosses were performed per genotype and sets of 50 larvae from each cross were placed into fresh food vials and stored at 25°C, totalling 150 larvae. Number of pupae formed upon the side of the vials was recorded 8 days following. The number of emerged adult flies, and male/female percentage was counted 13 days following.

2.4.7 Cortical cultures

Mouse cortical cultures were transfected with miR-190 miRNA mimics and inhibitors in order to assess the effect of miR-190 modulation on their development. Cortical culture prior to miRNA transfection was carried out by R.Ribeiro and C.Lucci. Briefly, E16.5 mouse embryo cortices were removed, treated with trypsin EDTA (Sigma) and DNAse (Sigma) and manually dissociated. Dissociated cells were then cultured in Neurobasal media (Fisher Scientific) supplemented with 1xGlutamax (Gibco) and 2% B27 supplement (Fisher Scientific) on Poly-L-Ornithine (Sigma) coated glass coverslips.

2.4.8 Cortical transfections

24 hours following cell seeding, cortical cultures were transfected with Lipofectamine2000. miRNA mimics and inhibitors were transfected alongside pmaxGFP (Lonza, Appendix I) to allow for visualisation of successfully transfected cells and morphological assessment. Inhibitors were transfected at a final concentration of 25nM, the hsa-miR-190a-5p miRCURY LNA™ microRNA inhibitor and Negative control A miRCURY LNA™ microRNA inhibitor control (both Exiqon) were used. Mimics were transfected at a final concentration of 10nM, the miRIDIAN microRNA Human hsa-miR-190a-5p - Mimic, and miRIDIAN microRNA Mimic Negative Control #1 (Both Dharmacon) were used. 48 hours following transfection, cultures were fixed with PFA, followed by mounting of coverslips using hard set Vectashield with DAPI for imaging. Slides were imaged with 200M microscope (Zeiss) mounted with a CoolSnap MYO camera (Photometrics). Images were subsequently

processed, and analysed for axon length and live neuron number in Fiji. Data shown is as a result of three separate biological repeats, with at least 50 individual cells contributing to each repeat.

2.4.9 Target predictions

Predicted targets for miR-190-5p were generated from the miRanda database with default parameters and a mirSVR score cut of off 0.7. Subsequent processing of these targets was carried out as described in relevant results sections.

2.4.10 *Drosophila* brain immunostaining

The effect of miR-190 over expression in the developing mushroom body of the *Drosophila* brain was assessed. Adult *Drosophila* were submerged in 70% ethanol prior to dissection to allow disruption of the waxy layer. Heads were removed in ice cold PBS and the surrounding structures of the head removed with forceps. Brains were then fixed in 4% PFA for 30 minutes, followed by washing by 3 exchanges of 0.3%PBS-Triton and permeabilisation in PBS-Triton for 20 minutes. Brains were blocked in 5% Normal goat serum (NGS, Sigma) in 0.3% PBS-Triton for at least one hour at room temperature before primary antibody application. Primary antibody was applied to brains overnight at 4°C in 5% NGS in 0.3% PBS-Triton. Nc82 antibody (DSHB) was used at a concentration of 5ug/ml and FASII antibody (DSHB) was used at a concentration of 3ug/ml. Primary antibody was washed from the brains with 0.3% PBS-Triton before application of the secondary antibody in 5% NGS in 0.3% PBS-Triton for two to three hours at room temperature. Excess secondary antibody was washed from the brains by washes in 0.3% PBS-Triton. Brains were then washed in PBS 3 times before suspension in DABCO mounting media. Brains were mounted between two coverslips forming a bridge to prevent compression, with a third coverslip above, sealed with clear varnish. Brains were imaged with an LSM 880 laser scanning confocal microscope (Carl Zeiss), and resulting Z-stacks were processed with either Zen software version 2 (Carl Zeiss) or Fiji (Schindelin et al. 2012).

2.5 Investigation of miR-190 in nervous system function

2.5.1 Collection of age matched flies

In order to carry out the longevity and climbing assays age matched adult flies of the required genotype were created and collected. Crosses were set in order to obtain the desired genotypes, kept at 25°C and transferred to new food daily. Vials

containing cross progeny were monitored for emerging adults daily. Once the first adults were seen to emerge, these were discarded to avoid selection of early emergents. Each day male and female emergents were transferred to fresh food vials, and allowed to mate for a further 24 hours. Following this mating period, female flies which emerged within the same 24 hour period were assessed for the correct genotype, and transferred in groups of 10 into fresh food vials. These were transferred, without anaesthetic, to fresh food every day for the first 3 days to allow the laying of fertilised eggs. Then on the first, third and fifth day of the week (i.e. Monday, Wednesday, Friday) for the remainder of the assay.

2.5.2 Climbing assays

Climbing assays were carried out using a protocol adapted from (Madabattula et al. 2015). Flies of required age and genotype were anaesthetised with CO_2 and transferred to identical glass measuring cylinders. Twenty flies were assessed per cylinder. Following a recovery period from anaesthesia of at least 30minutes, flies were continuously tapped gently to the bottom of the cylinder for five seconds. Following the five seconds, flies climbing past a pre-determined benchmark were counted for 15 seconds. Assays of different genotypes were performed at the same time to avoid bias due to light and environmental conditions. Three cohorts of 20 flies from three separate parent crosses were assessed per genotype.

2.5.3 Longevity assays

Longevity assays were carried out using a protocol adapted from (Linford et al. 2013). Aged flies were monitored during each transfer to fresh food. During each transfer the number of dead flies was recorded, alongside the number of censored flies. A fly was classed as censored if their cause of death was not natural (e.g. became stuck in the food or housing) or if the fly escaped during the transfer to new food. For each assay at least 60 individuals were included in each cohort resulting from 3 separate parental crosses.

2.6 Data analysis and statistics

Graphs presented were created using GraphPad Prism 7.0. All quantification data are shown as mean ±SEM. P-values are included in the relevant figure legends alongside the statistical tests performed. In the context of this work, a $p<0.05$ was considered

significant. Normality of data was tested by Shapiro-Wilk test. Significance between two groups was typically determined with Student's t test, paired or unpaired as required. One or two way analysis of variance (ANOVA) was utilised when comparing multiple groups. ANOVA was followed by Dunnett's multiple comparisons to compare each mean with the mean of an identified control, or Bonferroni's multiple comparisons to compare multiple means without an identified control.

Part I – Investigation of miRNA in nociception

Chapter 3. Identification of miRNAs which may play a role in pain processes

3.1 Introduction

miRNAs have the potential to regulate, or be regulated by, multiple processes in the nervous system function (Chapter 1.12-16). Here, an animal model of chronic inflammatory pain, hyperalgesic priming, was utilised to investigate the role of miRNAs in the sensory mechanisms of the nervous system. miRNAs have previously been implicated in pain processes, however the identity and specific function of those miRNAs involved in inflammatory pain has not been fully elucidated.

3.1.1 The nervous system and pain

The sensing and processing of painful stimuli is one of the key functions of the nervous system. The pain response to injury and/or potential tissue injury is a critical process that can protect an organism, and allows for subsequent uninterrupted healing of the damaged tissue (McMahon et al. 2013). Persistent, or chronic, pain can however evolve from these original acute pain triggers, due to a range of underlying causes. Estimates from 2016 on the prevalence of chronic pain in the UK concluded that up to 50% of the population may be experiencing some form of chronic/persistent pain (Fayaz et al. 2016). The proportion of suffers is predicted to increase in the coming years, due to the aging population (Fayaz et al. 2016). Chronic pain is therefore an extremely prevalent disorder which can have life limiting consequences for sufferers (Fayaz et al. 2016). Understanding the underlying mechanisms of pain, and those cellular processes that might drive the transition from acute to chronic maladaptive pain, are key in the treatment of pain conditions, and this is a growing challenge in clinical practice (McMahon et al. 2013).

3.1.2 The sensory circuit

The sensing of painful stimuli involves a concerted action of peripheral primary sensory neurons that transmit information from the periphery to the processing bodies of the central nervous system (McMahon et al. 2013, Figure 3.1.1). Changes

in protein expression at all levels of this circuit can therefore contribute to the development and progression of chronic pain.

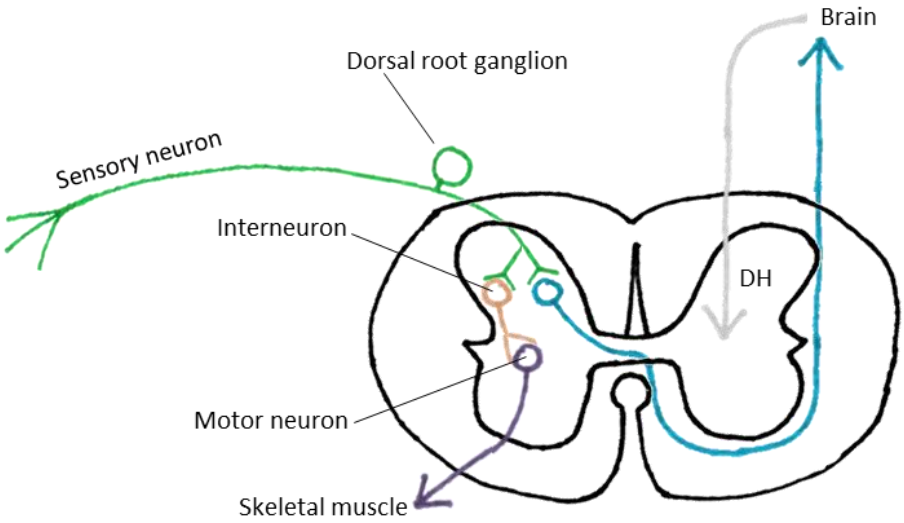


Figure 3.1.1 Schematic of the sensory circuit.
Sensory neuron cell bodies reside within the Dorsal Root ganglion (Green). These axons extend pseudounipolar axons, which relay information from the periphery to the Dorsal Horn (DH) of the spinal cord. In the DH the Sensory neurons synapse with interneurons, and these relay sensory information through ascending pathways (blue) to the brain. Sensory neurons can also synapse with interneurons (Orange) which can relay information directly to motor neurons (Purple) to activate the reflex response.

3.1.3 The sensory neuron

The cell bodies of the sensory neurons reside in Dorsal Root Ganglia (DRG) just outside of the spinal cord (figure 3.1.1). The unique pseudounipolar morphology of the sensory neuron allows the projection of axons to both the periphery and CNS of an organism (figure 3.1.1). The peripheral axon terminals are responsible for the generation of action potentials in response to sensory stimuli an animal may encounter. These axons therefore must have the ability to respond to a vast range of stimuli, which can be separated into three broad categories: mechanoreception (response to mechanical pressure), proprioception (sense of relative positioning and movement of the body) and nociception (response to harmful, or potentially harmful stimuli). Different subtypes of sensory neuron exist to allow for this, typically categorised by their diameter, conduction velocity and function (table 3.1.1).

Subtype	Function	Conduction velocity	Diameter	Myelination
Aβ	Innocuous sensory information	Fast (30-100m/s)	Large (10µm)	Myelinated
Aδi	Mechanical, Chemical and high threshold thermal stimulation	Slow (12-30m/s)	Small (2-6µm)	Thinly Myelinated
Aδii	Low threshold thermal stimulation			
C (Peptidergic)	Deep skin and visceral tissue nociceptors	Slow (0.5-2m/s)	Small (0.4-1.2µm)	Non-myelinated
C (non-peptidergic)	Skin nociceptors			

Table 3.1.1 Summary of peripheral sensory fibre subtypes originating from within the DRG
The Dorsal root ganglia (DRG) contains multiple subtypes of sensory neuron, which can be characterised by the physiological and morphological characteristics of the axons, or "fibres", they extend to the periphery. The table above describes the factors by which these can be classified.

An example of the diversity in membrane channel content and functional specificity seen in the sensory neuron population is given by those expressing the voltage gated sodium channel NaV1.8. Around 75% of total sensory neurons have been shown to express NaV1.8 (Shields et al. 2012). When these NaV1.8 expressing neurons are silenced through optogenetics (via the expression of an inhibitory light stimulated proton pump), pain response is alleviated, without disruption of low threshold mechanoreceptor responses (Daou et al. 2016). This demonstrates the specificity and importance of sensory neuron subtypes in the perception and processing of different sensory stimuli.

In addition to the sensory neurons functional specificity, the neurons also differentiate themselves with the location of their central projections within the dorsal horn. Sensory neurons project central axons into different regions of the dorsal horn in the spinal cord dependant on their function (Todd 2010). The interneurons present in these distinct regions of the dorsal horn (termed laminae) are specified for the processing of the stimulus they receive (Todd 2010). The combination of the sensory neuron peripheral fibre subtypes, and the projection of central sensory neuron axons into specific regions of the dorsal horn, is what allows processing of the broad spectrum of sensory capabilities required by an animal.

Given their role in the initial sensing of painful stimuli, sensory neurons have been the subject of much research in the field of pain. The TrkA positive, small cell body, Aδ and C fibres are traditionally regarded as the sensory neurons responsible for the rely of painful sensations (Lei et al. 2005). These fibres express a vast and variable array of receptors, which allow for the generation of an action potential from a wide range of painful stimuli. The transient receptor potential cation channel subfamily V member 1 (TRPV1) receptor is a cation channel present on the peripheral nociceptor fibres, which defines much of their functional properties. The pharmacology of the TRPV1 receptor has been studied in detail, and TRPV1 is activated by a range of stimuli, including heat, touch, and chemicals such as capsaicin (Gunthorpe et al. 2002). The entire range and complexity of the nociceptive system, with its peripheral and central nervous system components, is too broad to discuss in detail in this thesis (Woolf & Ma 2007; Carr & Zachariou 2014; Fenton et al. 2015), however specific examples will be given where appropriate.

3.1.4 Nociceptive sensitisation

Prolonged inflammation, or damage to the sensory circuit, can result in a decrease of nociceptive threshold which leads to an increase in pain sensation. This sensitisation is a key contributing factor in chronic pain conditions. This sensitisation of the pain circuit can be measured in a number of ways: either the painful response to a normally non-painful stimulus (allodynia); increased response to a painful stimulus (hyperalgesia); or the generation of spontaneous pain. Nociceptive sensitisation occurs through distinct mechanisms, involving both central and peripheral nervous system processing, however it is the sensory neuron which triggers both of these responses.

3.1.5 Central sensitisation

Changes within the CNS which lead to increased pain sensitivity are referred to as central sensitisation, a process which has shown to be crucial in the maintenance of chronic pain (Woolf 1983; Woolf 2011), and should therefore be considered in the context of the research or treatment of pain.

There are two different types of central sensitisation: homosynaptic and heterosynaptic. Homosynaptic sensitisation is the strengthening of a synapse through repeated stimulation, leading it to respond to normally sub-threshold stimuli, a process which is not dissimilar to long term potentiation (LTP) in memory formation (Ji et al. 2003). Homosynaptic sensitisation precedes heterosynaptic sensitisation, which is the subsequent strengthening of surrounding synapses, leading to the "spread" of pain from the initial site (Latremoliere & Woolf 2009). Both forms of sensitisation increase the input from the dorsal horn of the spinal cord to the ascending processes, and increases the sensation of pain. Central sensitisation is a field of much research and has implications to the understanding and treatment of chronic and spreading pain (Ji et al. 2018).

The mechanisms of central sensitisation should be considered when investigating the processes of chronic pain. However, the increased input from the peripheral neurons is the initial step in the advancement of acute pain to persistent chronic pain. The work in this thesis focuses on changes in the peripheral DRG neurons, and sensitisation of the peripheral terminals of these sensory neurons increases sensory inputs to the Dorsal Horn of the spinal cord. This increase in input can lead to the sensitisation of the central synapses of the sensory neurons with the interneurons in the dorsal horn responsible for the processing and potentiation of noxious stimuli (Latremoliere & Woolf 2009).

3.1.6 Peripheral sensitisation

Peripheral sensitisation is the sensitisation to pain due to changes in the peripheral nociceptor. Inflammatory sensitisation is produced due to the action of inflammatory mediators, while neuropathic sensitisation is generated in response to damage (Xu & Yaksh 2011). Independent of the origin, both of these lead to the lowering of the threshold required for activation of the neurons of the pain circuitry and a subsequent increase in nociception.

In neuropathic pain, damage to the peripheral sensory neuron can also lead to increased nociceptive input and sensitisation to pain (Xu & Yaksh 2011). One

clinically relevant example of this is nerve damage as a result of chemotherapy leading to neuropathic pain (Xiao & Bennett 2008). Again, the exact pathophysiology of this is yet to be completely uncovered, however various causes have been suggested. It has been shown that chemotherapeutic agent treatment can lead to degeneration in the peripheral nociceptive terminal structure, which may lead to spontaneous firing, or response to non-painful stimuli by nociceptive neurons (Xiao & Bennett 2008). One demonstrated cause of this spontaneous firing is an increased expression of low threshold calcium channels on the damaged nociceptive sensory neurons, leading to the generation of action potentials without stimulus, or to sub-threshold stimuli (Li et al. 2017).

As a cellular and physiological process, inflammation is an important mechanism which acts to prevent further tissue damage, protect from bacterial infection, and also remove damaged tissue from the site of initial injury. However, inflammation also contributes to the sensitisation of sensory neurons and the progression of chronic pain. Inflammation begins with an initial vasodilation, followed by infiltration of immune cells and production of inflammatory mediators (Zhang & An 2007). Released inflammatory mediators can then interact with receptors on the peripheral nociceptor terminal, which can sensitise these receptors to activate an action potential in response to stimuli which would otherwise be sub-threshold (Cheng & Ji 2008). Once the initial tissue damage has healed, the inflammatory mediators are removed, and the peripheral sensitisation is resolved. Maintained or repeated inflammation can however cause lasting damage, and long term peripheral sensitisation. For example, in conditions such as rheumatoid arthritis, where joint inflammation is a contributing factor to chronic pain (McWilliams & Walsh 2017).

The TRPV1 receptor can be sensitised during inflammation. The entire range of molecular and cellular mechanisms through which TRPV1 can be sensitised has not been fully elucidated, and a wide range of cellular signals and inflammatory mediators have been shown to have a role in this process (Adcock 2009). For example, TRPV1 can be phosphorylated by protein kinases leading to its sensitisation, and therefore any signalling pathways which lead to activation of these

kinases could potentially play a role in the sensitisation of TRPV1 (Adcock 2009). Protein kinases can be activated by many pro-inflammatory mediators, including TNFα, the Interleukins and LPS (Baud & Karin 2001).

3.1.7 Control of protein translation and sensitisation

The appropriate control of protein levels, and the ability to adjust protein expression in response to external stimuli, is important in the process of nociception, and also demonstrates a role in the dysregulation of nociception, and the progression into chronic pain. The importance of protein translation control in nociception, over other mechanisms of protein level control, was shown through the mechanism of enhanced action potential firing of sensory neurons caused by Nerve Growth Factor (NGF) injection (Kays et al. 2018). This NGF induced increased sensitivity of sensory neurons is blocked through injection to the same site of rapamycin (inhibitor of translation), but not application of actinomycin-D (inhibitor of transcription) (Kays et al. 2018). This is believed to be due, in part, to the decreased translation of the PKC variant PKMζ, which is associated with sustained nociceptive sensitisation (Kays et al. 2018). It has been further demonstrated that application of the translation inhibitor rapamycin to the peripheral tissues following tissue injury can attenuate persistent, but not acute pain (Jimé Nez-Díaz et al. 2008). This highlights the importance of local translation of proteins in the mechanisms of persistent, or chronic pain. It has also been shown that in an animal model of the transition from acute to chronic pain (hyperalgesic priming), peripheral application of the translation inhibitor anisomycin can interrupt the development of chronic pain (Ferrari et al. 2013). Therefore, peripheral protein translation can be seen as important in the processes of the establishment, and persistence, of chronic pain.

3.1.8 miRNA and sensitisation

As previously discussed, miRNAs are key regulators of translation, in particular in the nervous system (Chapter 1.12-16). As such, due to the importance of translation in the progression of chronic pain, it is a logical conclusion that miRNAs may play a role in these processes.

It has been shown that the Cre-Lox mediated deletion of dicer in mouse Nav1.8+ sensory neurons (which are important for inflammatory and neuropathic pain (Daou et al. 2016)), does not cause any significant abnormalities in animal development, or acute pain processing (Zhao et al. 2010). However, Dicer deletion in NaV1.8+ sensory neurons does lead to deficits in the progression of persistent inflammatory pain (Zhao et al. 2010). Dicer knockout will lead to the disrupted processing of small RNAs, including miRNAs. As an effect of this, the same study used miRNA-microarray analysis to identify a list of miRNAs which were significantly downregulated in the sensory ganglia following dicer knockout in NaV1.8+ sensory neurons (Zhao et al. 2010, figure 3.1.2). Whilst this study is pivotal in demonstrating the importance that miRNAs may hold in the progression of chronic pain, and identifies some miRNAs which may be key in this(figure 3.1.2), it does not demonstrate the roles or functions of these miRNAs.

The model of pain which is being used, and also the tissue being assayed, must be considered for studies of miRNAs role in chronification of pain. Review of previous studies demonstrates the variability of findings between models and tissues. For example, miR-1 has been shown to be downregulated in the DRG in two mouse models of inflammatory and neuropathic pain (Kusuda et al. 2011). While in a different, but similar, mouse neuropathic pain model, miR-1 showed an upregulation within the DRG (Kusuda et al. 2011). This study also demonstrated the importance of the tissue being assayed when comparing previous findings, as is demonstrated by the differential regulation of miR-1 shown in the Dorsal horn and DRG (Kusuda et al. 2011) and even between the DRG and the corresponding peripheral nerve in another study (Neumann et al. 2015).

A summary of previous studies of miRNA levels within the sensory ganglia of pain models is shown in figure 3.1.2, further demonstrating the variability of miRNAs observed in models of pain. This analysis of the literature demonstrated that there is not a great level of overlap between the studies, with 222 miRNAs being present across the studies shown, and 154 (69%) of these only appearing in one of the studies analysed (Figure 3.1.2). Only 8 (4%) of those miRNA present in these studies

demonstrated an overlap in more than two studies, with miR-181 being the only miRNA which was present in 4 studies. No miRNA were present in all studies assessed. It is important to note that in this comparison the directionality of the expression level change was not taken into account (as directionality is not applicable in the Dicer KO study), which no doubt would reduce the level of overlap between these studies.

Interestingly two separate studies from this analysis use the same model of pain, spinal nerve ligation (Sakai et al. 2013, Van Schack et al. 2011), however the two studies assess the levels of miRNA through different methods, Microarray (Sakai et al. 2013) and qPCR (Van Schack et al. 2011). The resulting overlap between these studies is 11 out of a potential 107 miRNA (10%). This low level of crossover may be a result of the different methods used, as by the nature of qPCR the researcher will only observe those miRNA that are selected for qPCR. However, there are a large proportion of those miRNA identified by qPCR (63%) which do not appear to demonstrate expression level changes when they are analysed by microarray.

With the variability observed in miRNA expression profiles between pain models it was therefore important to assess this the model which is being used here, hyperalgesic priming. Particularly as no previous studies of the miRNA expression profile in this model of pain had been conducted previously.

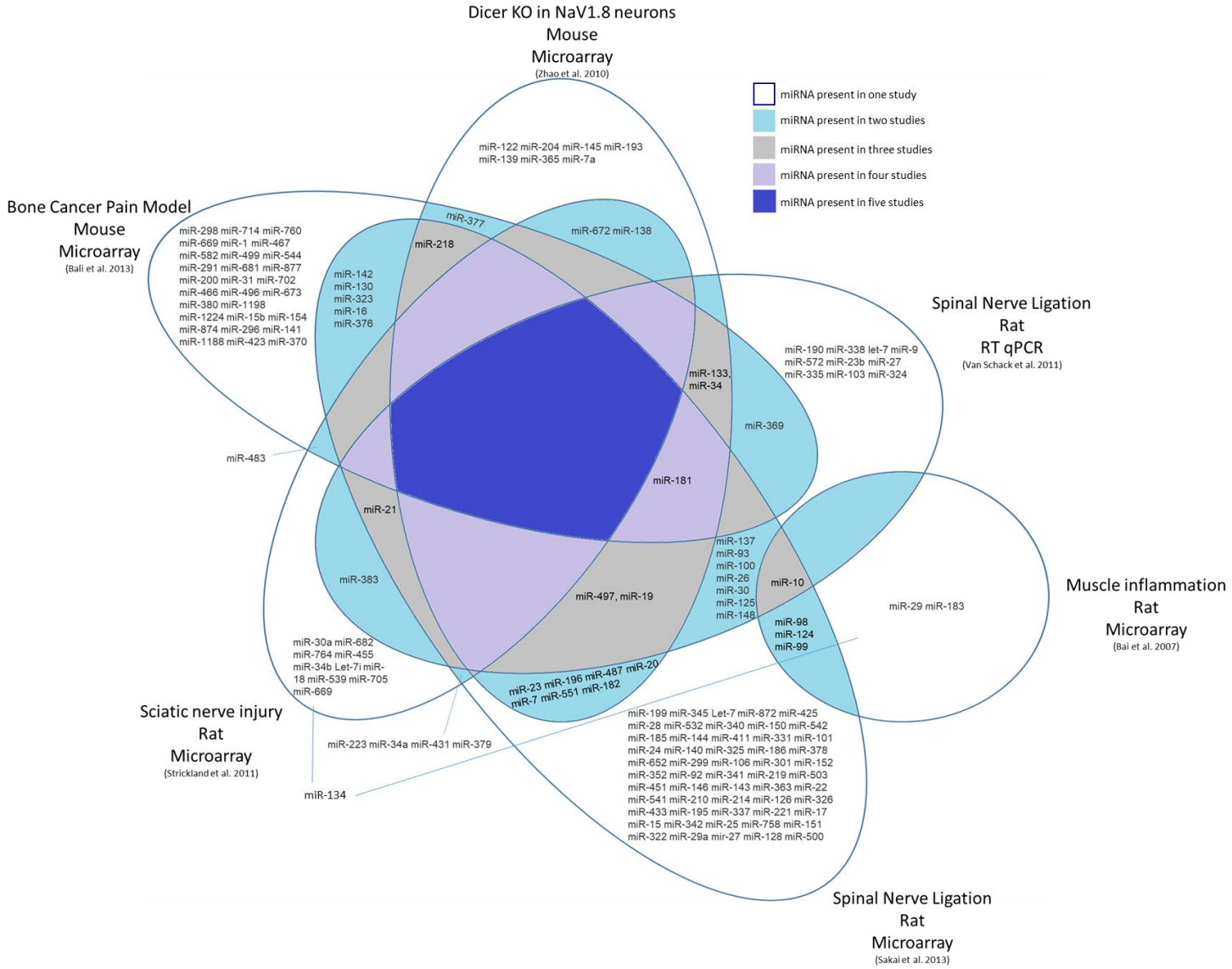


Figure 3.1.2 Published studies of miRNA levels within sensory ganglia in models of pain.
Available literature was searched for examples of extensive miRNA sequencing or arrays performed on the RNA extracted from sensory ganglia effected by models of pain. miRNA are shown as being "similar" between studies if the same miRNA family demonstrated changes in expression level (either up or down regulation) in the studies shown.

3.1.9 Hyperalgesic priming

The use of animal models of pain allow for the study of pain mechanisms and potential development of therapeutics. Both inflammatory and neuropathic pain models have been developed. Neuropathic pain can be modelled through either chemically induced (Byrne et al. 2015) or physically induced nerve injury (Austin et al. 2012). Inflammatory pain can be induced through the direct application of inflammatory mediators (Ren & Dubner 1999). These models will however directly induce chronic pain states, whereas in naturally occurring inflammatory pain, acute inflammatory pain will typically proceed chronic inflammatory pain.

In order to identify miRNAs which may be involved in the progression of acute to chronic pain, an animal model was used of the transition from acute to chronic inflammatory pain: hyperalgesic priming (Reichling & Levine 2009; Aley et al. 2000). In the hyperalgesic priming model, an initial inflammatory insult is injected into the rat hind paw, and the resulting inflammation and pain that lasts 2-3 days is allowed to resolve (figure 3.1.2, Appendix II). Control animals receive a primary injection of saline, as opposed to inflammatory agent (figure 3.1.2, Appendix II). A secondary inflammatory insult is then injected into the same site, and unlike the initial inflammatory insult, the pain response persists beyond the resolution of the inflammation (figure 3.1.2, Appendix II). This secondary stage is used as a model of chronic pain (Aley et al. 2000, figure 3.1.2).

In the protocol used in this work (Appendix II), the pain response is assessed through the use of Von Frey filaments (Chaplan et al. 1994). These are fibres which allow pressure of increasing weights to be applied to the paw of the animal, and the weight at which the animal displays a response (i.e. retraction of the paw) is recorded as the paw withdrawal threshold (Chaplan et al. 1994). This is a measure of allodynia, as animals experiencing inflammation typically show a response to a normally innocuous level of stimulus.

The hyperalgesic priming model has previously been shown to be regulated by local translation mechanisms (Ferrari et al. 2013). In this work they demonstrate that

application of either of the translation inhibitors rapamycin or cordycepin to the site of inflammation during either the initial priming inflammatory stimulus, or the secondary inflammatory stimulus can prevent the development of the prolonged secondary pain response (Ferrari et al. 2013). Importantly this may implicate a role or potential application of miRNAs in this model, due to the role of miRNAs in translation regulation.

As of yet however the expression patterns of miRNAs, or their specific roles or functions in the progression of hyperalgesic priming have not been studied. Hyperalgesic priming is a model of growing popularity which is proving applicable in many pharmacological contexts (Kandasamy & Price 2015), and therefore the work contained in this chapter is timely in the context of pain research, and relevant to further understanding of the model of hyperalgesic priming.

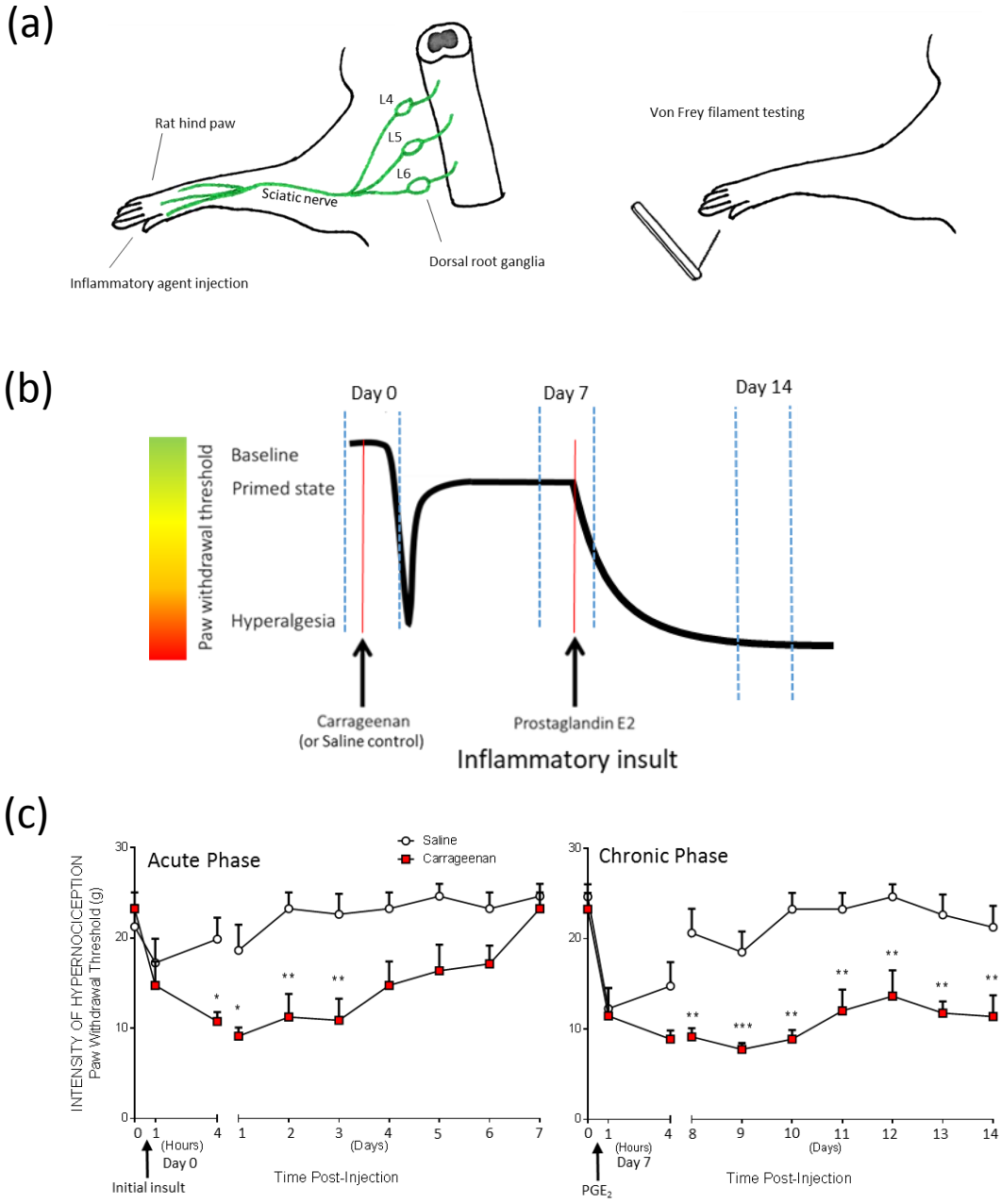


Figure 3.1.3. Hyperalgesic priming.
(a) Illustration of the rat hind paw, demonstrating the site of the inflammatory insult and subsequent Von Frey filament testing. **(b)** Schematic demonstrating the process of hyperalgesic priming. When the initial inflammatory insult is applied (Carrageenan at day 0) the paw withdrawal threshold lowers transiently, indicating hyperalgesia. This resolves to the baseline paw withdrawal threshold. When the secondary inflammatory insult is applied (Prostaglandin E2 at day 7), the paw withdrawal threshold lowers again, this time without resolution up to past day 14. **(c)** Representative readings from the Von Frey filament testing throughout the hyperalgesic priming protocol. Graphs in (c) were taken from "Investigation into the Mechanisms of Hyperalgesic Priming" Submitted by James Spalton to the University of Nottingham for the degree Doctor of Philosophy 2016. 2-way ANOVA test with a Bonferroni post hoc test *p<0.05, **p<0.01, ***p<0.001 (n=8 animals per group).

3.1.10 Experimental aims

The overall aim of the work contained within this chapter was to identify the miRNAs which might be dysregulated in hyperalgesic priming, and to determine what function these miRNA could have on the establishment and progression of chronic pain. For this, specific objectives were developed:

- To extract RNA from DRG neurons in the chronic stage of hyperalgesic priming and assess miRNA levels through a miRNA-microarray.
- A selected candidate miRNA from this was then further characterised within the model of hyperalgesic priming through qPCR.
- Relevant mRNA targets for the candidate miRNA were then predicted through bioinformatics which would further implicate the involvement the miRNA in chronic inflammatory pain. These were further validated through luciferase assay.

3.2 Results and discussion

3.2.1 Microarray to assess deregulated miRNAs in chronic pain

The hyperalgesic priming protocol provides us with a model through which the processes of acute and chronic inflammatory pain can be investigated. Following the secondary inflammatory insult, the subsequent pain persists up until, and past, day fourteen of the priming protocol (figure 3.2.1). To identify candidate miRNAs which may play a role in the processes of chronic inflammatory pain, a microarray was carried out on RNA extracted from DRG in this secondary chronic stage of hyperalgesic priming. Levels of miRNA in these DRG were compared to control animal DRG which had received an initial saline insult (figure 3.2.1).

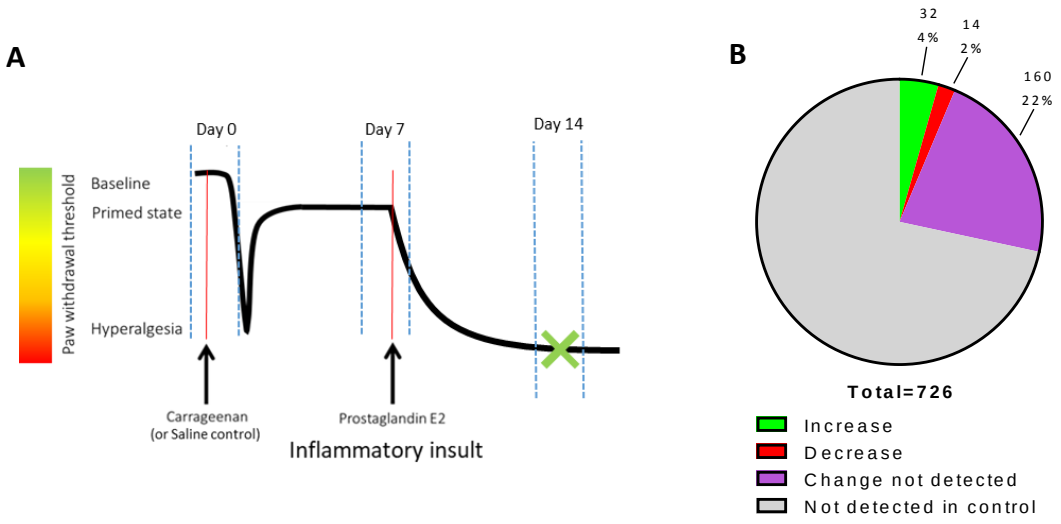


Figure 3.2.1 Microarray assessment of miRNA which show change in levels in the chronic pain state

(a)Schematic of the hyperalgesic priming process. DRG samples were collected at day 14 of the process as indicated by green cross. At this point the animals have received an initial inflammatory insult of carrageenan, or a saline control at day 0 and an inflammatory insult of Prostaglandin E2 at day 7. (b) Of a total of 726 miRNAs present on the array, 206 were detected in all of the DRG samples. 46 miRNAs were seen to have differential expression in the carrageenan primed DRG samples compared to the saline primed control. Saline primed control n=1. Carrageenan primed n=2. Differentially expressed miRNA were selected on having an average positive or negative 2 fold change compared to control sample.

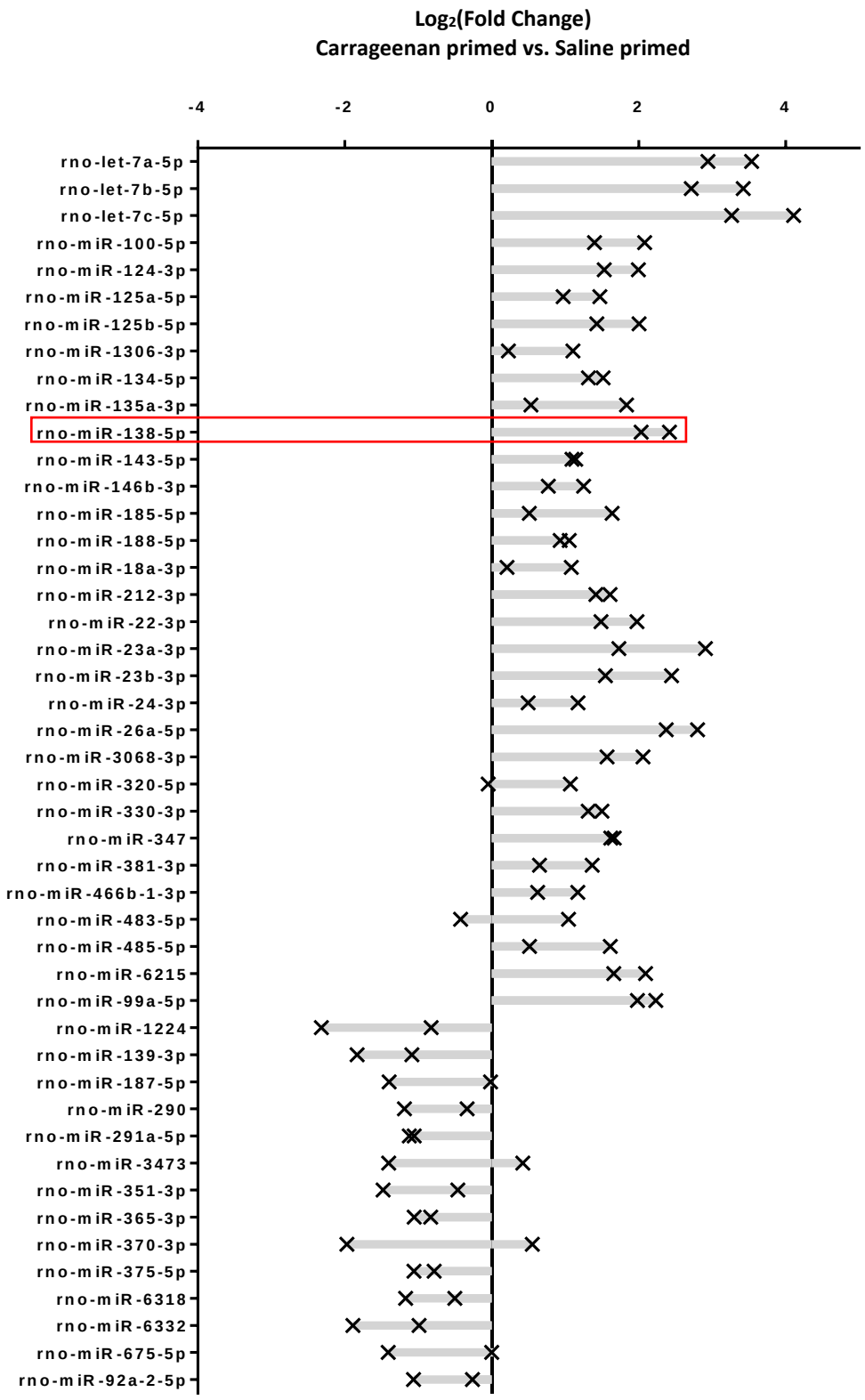


Figure 3.2.2. Differentially expressed miRNA from microarray assessment at day 14 of the priming protocol

Log_2(fold change) of miRNA levels within affected DRG from Carrageenan primed animals (n=2) comparative to Saline primed control animals (n=1). Differentially expressed miRNA were selected on having an average positive or negative 2 fold change compared to control sample. Each X represents a separate affected DRG from a separate carrageenan primed animal. Expression levels of miRNA are shown as Log_2(Fold change) compared to control, as this allows effective relative comparison between up and down regulated miRNA (N.B: $Log_2(1)=0$).

The microarray used here was the Toray 3D-Gene chip V20. This is reported to be one of the most reliable microarray technologies in regards to sensitivity, reproducibility and reliability in quantification of miRNA (Sato et al. 2009). From a total of 727 miRNAs which were present on the array, 206 were detected in both the saline control and experimental samples (figure 3.2.1, Appendix III). Of these, 32 demonstrated an increase, and 14 a decrease, in the experimental samples (Figure 3.2.1, Appendix III). Levels of the individual miRNAs which demonstrated at least a two fold up- or down-regulation in comparison to the control are shown (figure 3.2.2, Appendix III).

This initial microarray of the miRNA levels in the hyperalgesic priming model has provided us with a battery of candidates for further study. However, due to the low number of samples submitted for microarray, the microarray data constitutes only a first approach in the investigation of those miRNAs with a role in nociceptive processes. It can be seen from figure 3.2.2 that the experimental samples show a wide difference when compared to the control, with some miRNA (e.g. 483-5p) demonstrating different directionality of miRNA levels between the two samples. IT is therefore important to validate any conclusions from this work with an increased number of samples.

In comparison to the previous analysis of miRNA which were identified as demonstrating expression level changes in other models of pain (figure 3.1.2) 20 (43%) of the miRNA identified here are also present in those studies (figure 3.2.3).It is promising to note that a few of the miRNAs which were shown to be downregulated through the knockout of Dicer in NaV1.8 positive sensory neurons (Zhao et al. 2010) are present within the detected miRNAs in our microarray, as the study represents a clear indication of those miRNA which are specifically expressed within the nociceptive sensory neurons. Of these, miR-138, miR-23a and miR-23b were shown to be upregulated in our microarray, while miR-139 and miR-365 showed decreased levels in our microarray (figure 3.2.2 figure 3.2.3).

One of these upregulated miRNAs, miR-138-5p, (2.4 log2fold Change, respective to a 5.3 fold change, Figure 3.1.2), has been previously linked in other studies to nerve injury which may be linked to neuropathic pain (Liu et al. 2013). miR-138-5p acts as a negative regulator of regeneration of the sciatic nerve, in a negative feedback loop with SIRT-1, providing a clear role in response to peripheral nerve injury (Liu et al. 2013) and possibly neuropathic pain. In addition, miR-138-5p has been linked to inflammatory pathways in a model of periodontal inflammation (X. Zhou et al. 2016). In this model, miR-138-5p was shown to directly target and regulate levels of osteocalcin, and application of the inflammatory regulators IL6 and LPS increased miR-138 expression (X. Zhou et al. 2016). These studies, and the hyperalgesic priming microarray pointed towards miR-138 being a relevant candidate for further study in peripheral mechanisms regulating inflammatory pain. As such, the levels of the identified candidate for further study, miR-138-5p, were further validated through qPCR throughout the hyperalgesic priming protocol.

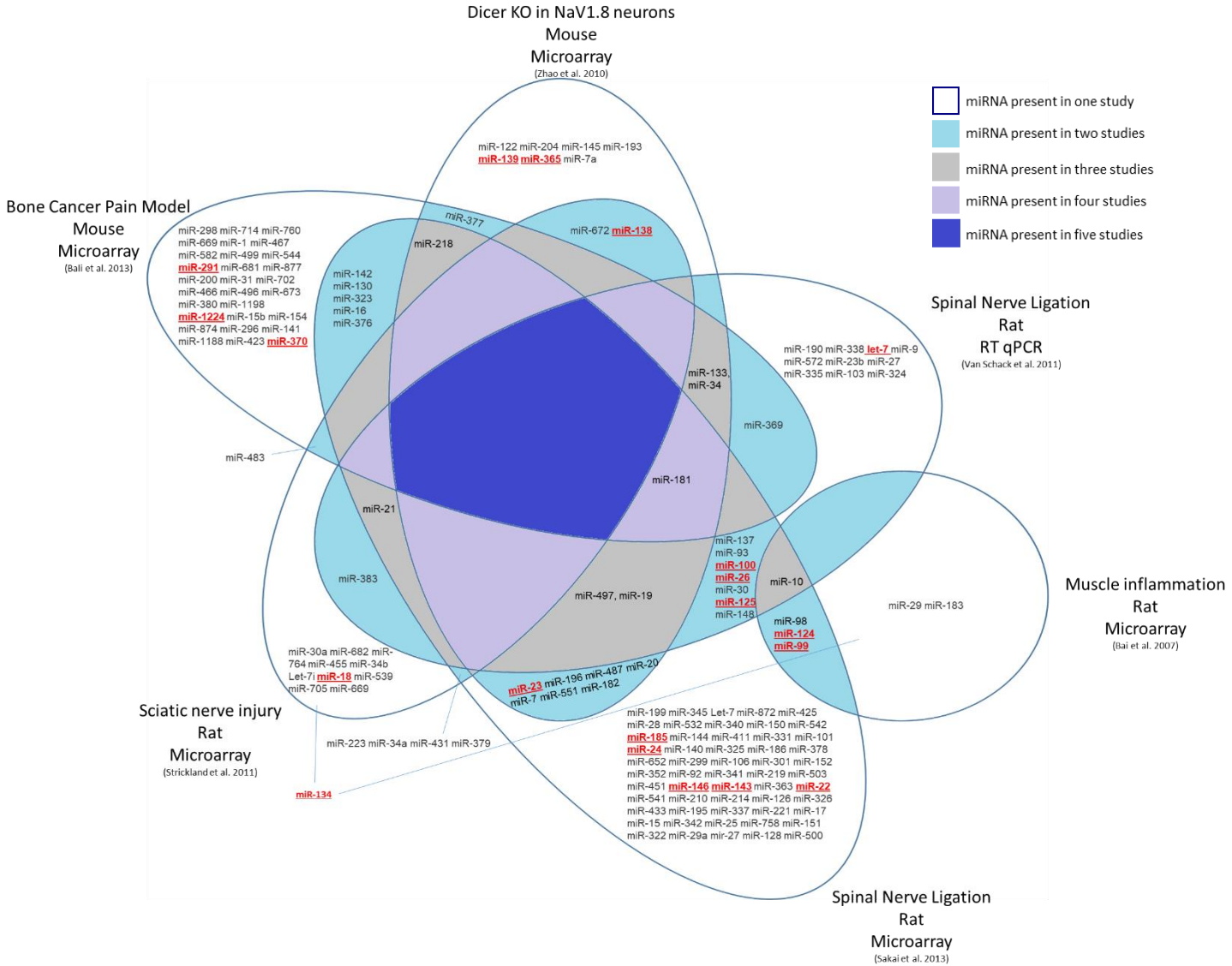


Figure 3.2.3. Published studies of miRNA levels within sensory ganglia in models of pain, and comparison to the microarray of miRNA levels in hyperalgesic priming.

Available literature was searched for examples of extensive miRNA sequencing or arrays performed on the RNA extracted from sensory ganglia which were affected within models of pain. miRNA are shown as being "similar" between studies if the same miRNA family demonstrated changes in expression level (either up or down regulation) in the studies shown.

Those miRNA which also demonstrated an expression level change in the microarray analysis of miRNA levels in hyperalgesic priming (detailed in this thesis) are highlighted in red text.

3.2.2 qPCR investigation of miR-138 through the priming protocol

In order to validate the observed increase in the microarray data of miR-138-5p, and to build a profile of miR-138-5p expression throughout the hyperalgesic priming process levels of miR-138-5p were assessed through qPCR. RNA was extracted from DRG at key stages in the hyperalgesic priming model: days 2, 7 and 14. These time points represent specific stages of pain behaviour, with day 2 animals suffering from acute inflammatory pain, day 7 animals having baseline pain responses following the acute insult, and day 14 animals having entered the chronic phase of pain after second injection of inflammatory agent (figure 3.2.4, a).

An interesting pattern of miR-138-5p expression is observed throughout the hyperalgesic priming protocol (Figure 3.2.4, c-d). At day two, following the initial inflammatory insult, a significant increase of miR-138-5p in Carrageenan primed samples is observed compared to saline (figure 3.2.4, c). Following resolution of the inflammatory pain response caused by this initial insult, miR-138-5p returns to basal levels with no significant difference between saline control and carrageenan primed samples, or compared to levels at day 2 in the saline primed sample (Figure 3.2.4, c). This dynamic regulation appears to follow the inflammatory process and pain behaviour in the model, with miR-138-5p levels increasing in response to acute inflammatory insult, and resolving to baseline when inflammatory response and the associated pain has subsided.

On Day 14, once the secondary PGE_2 inflammatory insult was applied to both saline control and carrageenan primed animals, a large trend towards an increase in miR-138-5p is observed in primed animals compared to those animals which were saline primed (Figure 3.2.4, d). This suggests that the initial inflammatory insult of carrageenan may produce longer term effects, leading to an increased average level of miR-138-5p occurring following secondary inflammation.

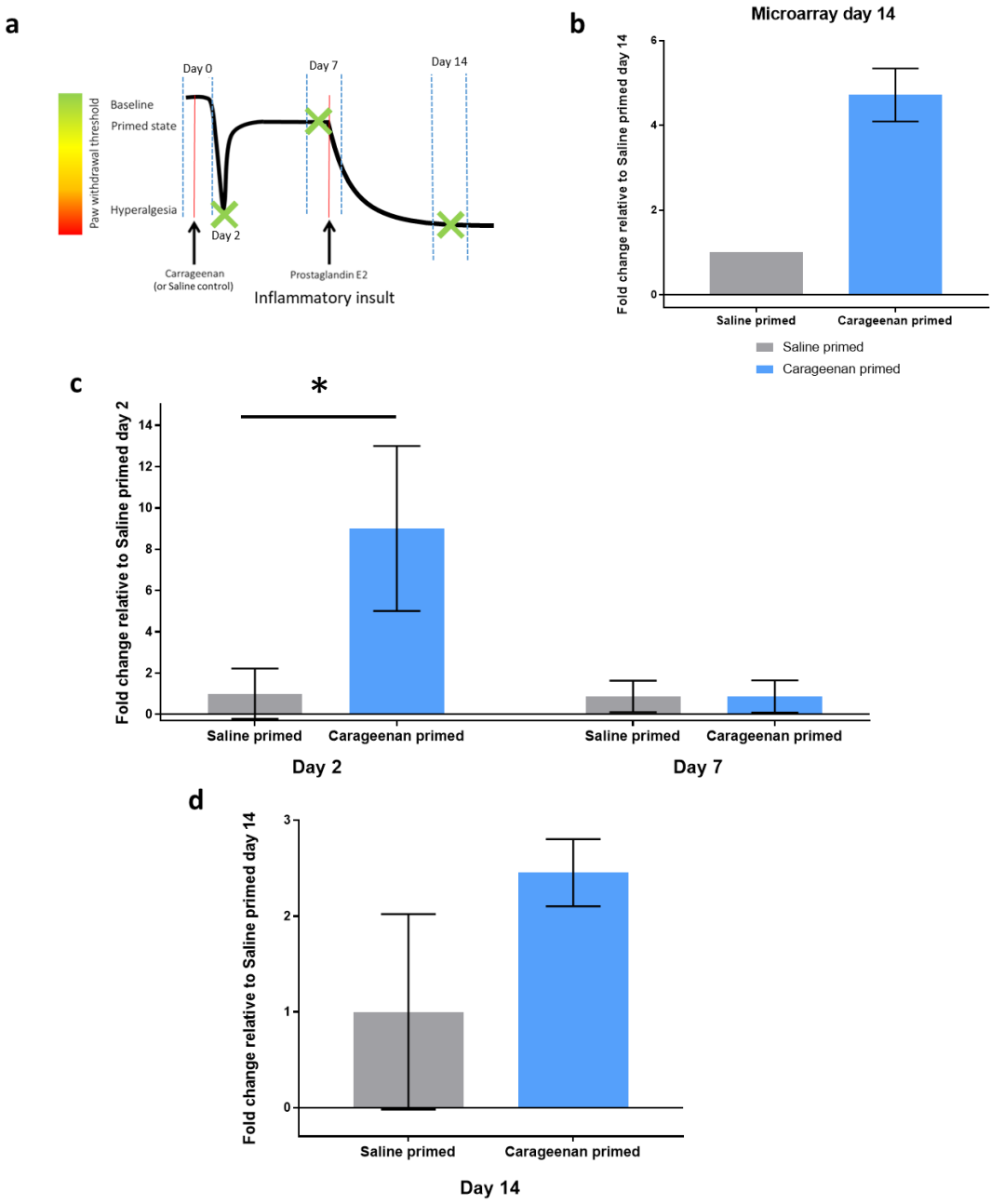


Figure 3.2.4. Levels of miR-138-5p as assessed through microarray and qPCR throughout the hyperalgesic priming protocol.

(a) Schematic of the hyperalgesic priming protocol with relevant tissue collections indicated by green crosses at day 2, day 7 and day 14 following initial priming insult. **(b)** Result of the initial microarray demonstrating the observed increase in miR-138-5p expression in carrageenan primed DRG (n=2) compared to saline primed control (n=1) at day 14. **(c)** qPCR of miR-138-5p levels following initial inflammatory insult. On day 2 following the initial insult a significant increase of miR-138-5p is observed in the carrageenan primed DRG samples (n=8) compared to that of saline primed samples (n=7), *p=0.04 by Bonferroni multiple comparisons following two-way ANOVA. On day 7 following the initial insult saline primed and carrageenan primed samples return to levels not significantly different to that of Day 2 saline primed samples or each other. **(d)** qPCR of miR-138-5p levels following secondary inflammatory insult. On day 14 of the priming protocol, miR-138-5p demonstrates an insignificant increase in carrageenan primed DRG (n=6), compared to the average levels observed in time point matched saline primed DRG (n=6). p=0.2 as determined by students unpaired t-test. All data is shown as mean +/- SEM.

From the qPCR data, a 2.58 fold increase in miR-138-5p was observed compared to the saline matched control at day 14, compared to a 5.34 fold increase observed from the initial microarray (Figure 2.4.3, b, d).This highlights the importance of validating the initial microarray data through qPCR, as the low sample size for the initial array may cause inaccuracies. The large variations in the expression level of miR-138 observed in the samples which underwent qPCR are not unexpected when it is considered that this assay was carried out using samples from an in vivo experiment which will have natural biological variation between animals.

What is not possible from this data is the absolute quantification of miR-138 levels. This is a limitation of the ΔCt method of qPCR quantification (Bustin 2002), as results are comparative rather than absolutely quantitative. Subsequent assays could be carried out in order to modify this data and carry out these comparisons.

From the observed miR-138-5p pattern of expression throughout the hyperalgesic priming protocol, it was concluded that miR-138-5p is likely to play a role in the progression of inflammatory pain. This could possibly be through the direct targeting of mRNAs involved in inflammatory processes.

3.2.3 Identification of functionally relevant targets for miR-138-5p

The predicted capacity of miR-138-5p to act as a potential regulator of inflammatory processes in the DRG prompted us to search for functional candidates that could mediate the actions of miR-138-5p in inflammatory pain. In order to identify possible novel targets for miR-138-5p which are relevant to this model, a bioinformatics approach was used. For this, a work-flow of target prediction algorithms and Gene Ontology analysis was employed to aid this search (Figure 3.2.4).

A range of target prediction algorithms are available for the identification of miRNA (Betel et al. 2008; Thadani & Tammi 2006). Among these, miRgate allows simultaneous access to multiple prediction algorithms (Andrés-León et al. 2015). When the predicted targets for miR-138-5p are retrieved from miRgate, a set of 5524 predicted target transcript IDs is generated. This set includes a level of redundancy

through the presence of multiple transcripts from the same gene, or multiple target sites within the same transcript. To remove any possible duplications such as these the resulting transcripts were converted to gene IDs through the Ensembl Biomart converter, resulting in a set of 3634 genes. Whilst this gives a clearer vision of the gene number that miR-138 is predicted to target the resulting gene set of 3634 genes was still considered too large to comprehend a manual analysis of sufficient detail in order to select target candidates.

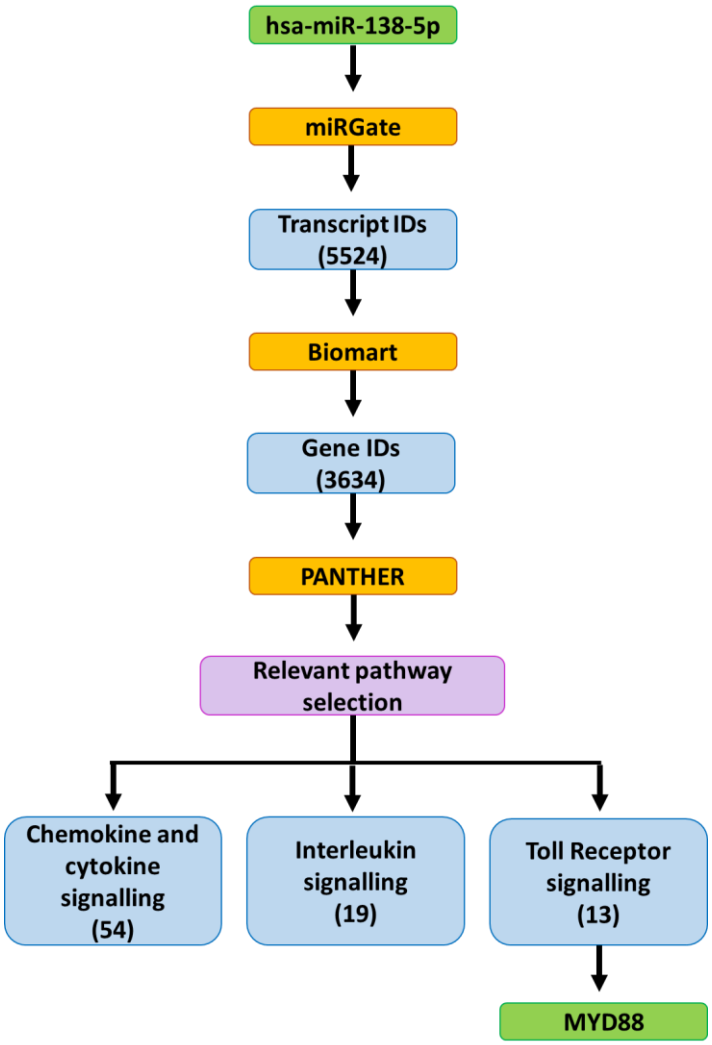


Figure 3.2.5 Bioinformatics workflow for miRNA target identification.
A Process of target predictions and gene ontology sorting was undertaken to identify targets of miR-138-5p applicable to the model of hyperalgesic priming. Predicted target transcript IDs for miR-138-5p were extracted from the miRgate prediction algorithm and converted to gene IDs by Biomart. Gene IDs were sorted through PANTHER Gene ontology data base and relevant pathway ontologies were extracted. From this, MYD88 appeared as a functionally relevant target for further study.

The use of Gene Ontology databases such as PANTHER (Mi et al. 2013) which are designed to classify proteins and their genes allow for the sorting and identification of the functionally relevant targets within this data set. The relevant pathways of chemokine and cytokine signalling, interleukin signalling and toll receptor signalling were selected. This produced a candidate list of 86 predicted target genes (figure 3.2.4).

The resulting list of 86 predicted targets was of a small enough size to manually select target candidates. One of the options for a candidate target which appeared interesting and relevant to the model of hyperalgesic priming was the Myeloid Differentiation primary response 88 protein (MYD88). This target candidate was selected from the gene lists resulting from the outlined filtering approach based upon searches of the literature which highlighted MYD88 as a key player in inflammatory processes.

MYD88 was first identified in 1990 as a response gene to the inflammatory cytokine interleukin 6 (IL6) (Lord et al. 1990) MYD88 is now known to be the central node in a core "bow-tie" network of inflammatory pathways (Oda & Kitano 2006 figure 3.2.5), acting as a downstream mediator of the Toll-like Receptor family (TLR) and Interleukin-1 Receptor (IL1-R) pathways. MYD88 activation as a result of TLR or IL1-R signalling leads to subsequent induction of the IL-1R associated kinase (IRAK) family (Oda & Kitano 2006). This family of kinases has many downstream effects to induce inflammation (Deguine & Barton 2014). For example, the activation of Nuclear Factor Kappa B (NFκB) and Mitogen-activated protein kinase (MAPK) (figure 3.2.5). As MYD88 can be seen as a central node in a network of inflammation (Oda & Kitano 2006) if miR-138-5p does in fact target MYD88, this has the potential to have downstream effects on a wide range of inflammatory processes.

MYD88 has also previously been demonstrated as playing a role in pain models. Following Chronic Constriction Injury in the rat, MYD88 is increased within the Dorsal Horn and the DRG (Liu et al. 2017). This increase in MYD88 can be reversed, along with the associated hyperalgesia, through application of an MYD88 inhibitory

peptide (Liu et al. 2017). MYD88 knockout mice show reduced inflammatory pain response as a result of injection of the inflammatory activator lipopolysaccharide (LPS), as well as reduced production of inflammatory mediators and pronociceptive cytokines such as TNFα (Calil et al. 2014). These observations of MYD88 knockout are similar to those observed from a TLR4 mutant mouse model (Calil et al. 2014) demonstrating MYD88 having a central role in TLR4 mediated inflammatory pain.

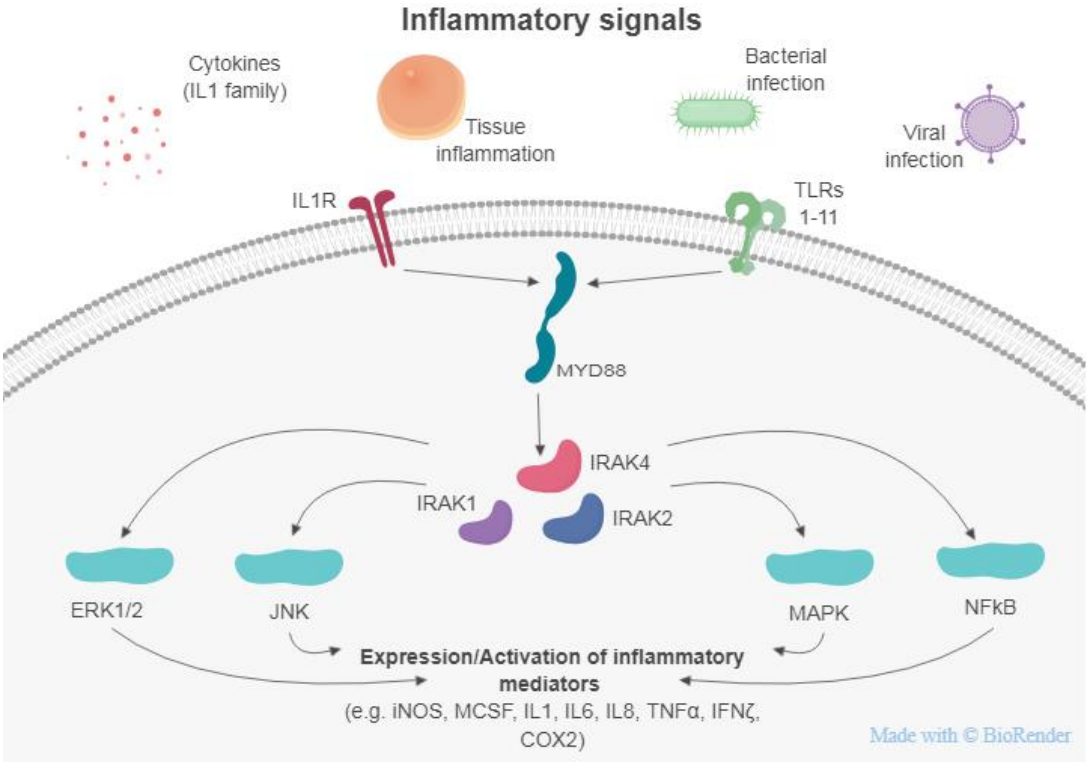


Figure 3.2.6 MYD88 as a central node in inflammatory signalling
MYD88 is a downstream adaptor of TLR receptors and the IL1 receptor which are responsible for the sensing of multiple inflammatory signals. Through activation of IRAKs MYD88 can activate an amplified downstream cascade of inflammatory signalling leading to the expression of proinflammatory genes and activation of inflammatory mediators. Diagram created from data within (Oda & Kitano 2006).

In regards to a sensory neuron specific role of MYD88, a conditional knockout of MYD88 in NaV1.8+ sensory neurons demonstrated the importance of MYD88 in chronic pain signalling (Liu et al. 2016). In these mice, acute inflammatory pain appears to remain as in wild type animals, however late phase inflammatory or neuropathic pain is attenuated (Liu et al. 2016).

Whilst the remainder of this chapter focuses on MYD88 as a relevant and interesting target for miR-138-5p it is important to note that other targets were selected from this target prediction filtering approach however they did not produce positive results in further tests (such as the luciferase assay, data not shown). For instance these selections included the Acid Sensing Ion Channel 4 (ASIC4) a member of the ASIC family which has been implicated in pain sensation (Wemmie et al. 2013), however the function of ASIC4 itself is unclear (Schwartz et al. 2015).

3.2.4 Validation of MYD88 as a target for miR-138-5p

Following the identification of MYD88 as a predicated target for miR-138-5p, it was important to provide a first step in the functional validation of this potential target. For this, a luciferase assay was carried out in order to confirm the interaction of miR-138-5p with the predicted target sites within the MYD88 3'UTR. Three predicted target sites for miR-138-5p are present within the 3'UTR of MYD88 (figure 3.2.6 a). All of these predicated target sites for miR-138-5p in MYD88 were investigated for the capacity to act as true functional targets using luciferase assays (figure 3.2.6 b). The luciferase assay allows, through the use of a specifically designed construct, for the confirmation of miRNA interaction with a predicted target site (Chapter 1.14).

Of the sites which were predicted to be targeted by miR-138-5p, only site three demonstrated significant reduction in luciferase signal in the presence of miR-138 mimic, and was therefore carried forward for mutagenesis recovery (figure 3.2.6). In

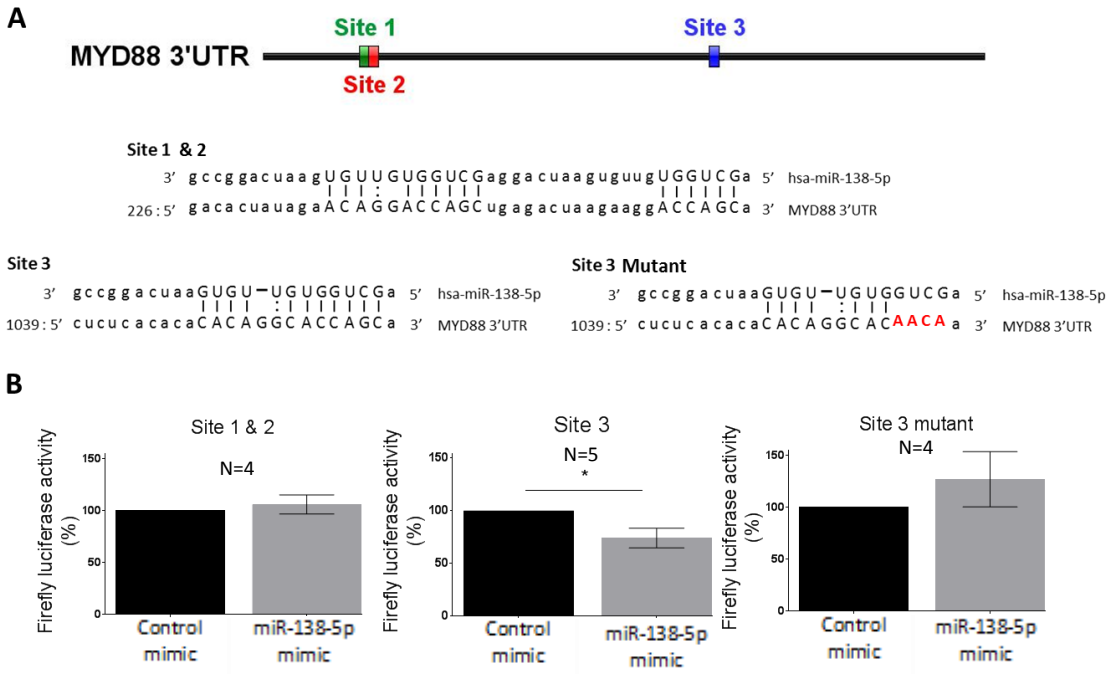


Figure 3.2.7. Luciferase assay confirmation of MYD88 as a target of miR-138-5p
(a) Three target sites are present within the 3'UTR of MYD88. Constructs inserted into pmiRglo vector are shown with their alignment to miR-138-5p. Site one and Site two are present within the same locus in the 3'UTR, and were therefore combined into one construct for luciferase assay **(b)** Results of the firefly luciferase activity within HEK293T cells upon transfection with reporter plasmid containing target sites as indicated. Site 3 saw significant reduction in firefly luciferase activity when transfected alongside miR-138-5p mimic compared to when transfected alongside a non-targeting mimic control. Site Directed Mutagenesis (SDM) of the site 3 seed sequence (Site 3 mutant) leads to recovery of this reduction. * $p<0.05$ as determined by Students paired t-test. Data is shown as mean +/- SEM.

mutagenesis recovery, nucleotides within the seed sequence section of the miRNA recognition site are replaced. If the miRNA was truly targeting the predicted site then recovery of luciferase levels should be observed as a result of this. Site three was thus confirmed as a true functional target for miR-138-5p following seed sequence mutagenesis recovery of the luciferase signal (Figure 3.2.6).

The luciferase assay provides us with further evidence for MYD88 as a true target of miR-138-5p, however it does not absolutely confirm the targeting within the desired model. Here the human miR-138-5p mimic and predicted target sites for luciferase assay have been assessed. In order to apply this to the hyperalgesic priming model used here, predicted miR-138-5p target sites in the context of the rat MYD88 3'UTR should also be validated through luciferase assay.

The targeting of MYD88 by miR-138-5p may be involved in the processes of inflammatory pain seen in the hyperalgesic model. MYD88 has been previously shown as a target of miR-203 (Wei et al. 2013). In this study it was demonstrated miR-203 is able to directly target the 3'UTR of MYD88, and downregulation of MYD88 levels through transfection of miR-203 into a macrophage cell line undergoing inflammation can lead to subsequent reduction in the levels of inflammatory mediators such as NFkB, TNFα, and IL6 (Wei et al. 2013). Results presented in this thesis demonstrate, the ability of miR-138-5p to target the 3'UTR of MYD88, which may allow miR-138-5p to have a similar effect within the DRG during inflammatory pain conditions.

Despite the demonstration here that miR-138 can target MYD88, it is also important to consider that other predicted or functional mRNA targets have been previously described (figure 3.2.4, Liu et al. 2013; X. Zhou et al. 2016) of which MYD88 is only one. Alternative approaches can be taken to validate the functioning of a miRNA within entire biological systems, which may not validate direct miRNA-target interactions, but could indicate a miRNA playing a general role in inflammatory pain processes. For example, there are commercially available cytokine arrays (Huang

2004), which allow for the simultaneous detection of multiple cytokine expression levels.

3.3 Conclusions and future directions

This work demonstrated how miRNAs are dysregulated during hyperalgesic priming, and provided a list of candidate miRNAs which could play a role in the processes of chronic inflammatory pain (figure 3.2.2). Future work could focus on assessing the relevance of this dysregulated miRNA profile in other models of pain, or on the functions of the individual miRNA identified.

One candidate was chosen, miR-138-5p, this miRNA was further investigated through qPCR to demonstrate expression levels throughout the hyperalgesic priming protocol (figure 3.2.3). This demonstrated that miR-138-5p levels appear to correlate with an increase in pain response. This implicated miR-138-5p as a novel modulator of inflammatory pain processes, and made miR-138-5p an interesting candidate for further investigation in chronic pain. As discussed, further profiling of miR-138-5p levels within the hyperalgesic priming protocol or within other models of pain could be carried out.

Through bioinformatics, a number of predicted targets for miR-138-5p which were relevant to inflammation and pain were identified (figure 3.2.4). One of these, MYD88, was confirmed to be a functional target for miR-138-5p through a luciferase reporter assay (figure 3.2.6). Future work should assess if the targeting of MYD88 by miR-138-5p is relevant to the model of hyperalgesic priming. In addition to this, investigation of the overall effects of miR-138-5p on the DRG during hyperalgesic priming could be undertaken.

The work contained within this chapter demonstrates that miRNAs are dysregulated in the process of hyperalgesic priming, and these miRNAs have the potential to function as key mediators of inflammation and pain. In order to further investigate the mechanistic function of miRNA we sought to establish an appropriate *in vitro* model.

Chapter 4. *In vitro* modelling of nociception

4.1 Introduction

In order to investigate the molecular mechanisms through which miRNAs may be acting within the DRG during nociceptive processes, it was essential to establish an appropriate *in vitro* model. The primary culture of neurons is a powerful tool through which to tightly regulate and accurately observe environmental and cellular changes. Considerations in respect to the localised processes the researcher wants to explore must however be taken.

4.1.1 *In vitro* assessment of nociception

As nociception is the sensory nervous system's response to potentially harmful painful stimuli, an important consideration is how neuronal activity can be assessed *in vitro*. In this study, we achieve this via calcium signalling imaging. Calcium is a key intracellular signalling molecule, where a rise in calcium ions leads to downstream effects on multiple cell processes, from gene transcription to cell cycle regulation (Berridge et al. 2003). Calcium indicator dyes (Paredes et al. 2008) and genetically encoded calcium indicators (Looger & Griesbeck 2012) have been developed in order to allow researchers to visually monitor intracellular calcium ion levels through fluorescent signals as an indicator of biological processes. Calcium entry into neurons is also a useful indicator of membrane depolarisation, and the generation of an action potential (Simms & Zamponi 2014). Through use of a calcium indicator dye, transient rises in intracellular Ca^{2+} levels can be measured in response to an applied stimulus, acting as indirect indicator of action potential firing (Grienberger & Konnerth 2012).

As previously discussed, the sensory neurons which are present within the DRG are made up of multiple subtypes (table 3.1.1.), and the *in vitro* investigation of nociception would require the presence of the pain sensing C and Aδ fibres. In previous studies, it was shown that the nociceptive peptidergic and non-peptidergic c-fibres (table 3.1.1) specify postnatally *in vivo* (Marmigère & Ernfors 2007). This would theoretically mean that nociceptor subtypes would not be fully specified when the DRG are removed from the embryo before culturing. The suitability of the

cultures for the study of nociception based upon the presence of these subtypes was also to therefore be assessed through calcium imaging.

The capsaicin receptor, TRPV1 is present on the nociceptive neurons responsible for the transduction of thermal and mechanical pain (Brenneis et al. 2013) and is considered a key player in the sensing of painful stimuli and the development of sensitivity (Adcock 2009). A calcium response indicative of axon potential firing in response to *in vitro* application of capsaicin would therefore provide an indication of the presence of cell subtypes which express TRPV1, and are capable of sensing painful stimuli.

4.1.2 Modelling of the nociceptive circuit

The cell bodies of sensory neurons reside within the DRG just outside of the spinal cord (figure 3.1.1), and possess a distinctive pseudounipolar structure; each neuron extending one process into the dorsal horn of the spinal cord, and another extremely long process to the periphery (figure 3.1.1). This morphology is key to their function of relaying sensory information from the different tissues and organs to the CNS (Marmigère & Ernfors 2007). When establishing an *in vitro* model, it is therefore important to note that the peripheral and central systems responsible for the processing of pain reside in distinctly different regions of the body (figure 3.1.1) and also demonstrate differential gene expression (Gumy et al. 2011).

DRG neurons also demonstrate differential expression of mRNAs between cell body and axonal compartments (Gumy et al. 2011). For example, some sensory neurons in the adult rat express a novel 3' UTR-extended isoform of CaMK4 that is associated with its localisation to axons (Harrison et al. 2014). This differential localisation of CaMK4 may play a role in the plasticity and function of this sensory neuron subtype (Harrison et al. 2014). It has been shown that chronic pain induction mechanisms differ between the cell body and axon (Ferrari, Araldi, et al. 2015) and it is believed that a concerted action of both cell body and axon is important in the establishment and maintenance of chronic pain (Ferrari, Bogen, et al. 2015). In a model of the transition of acute to chronic pain, hyperalgesic priming, it has been shown that

peripheral administration of translation inhibitors can reverse and prevent chronic pain (Ferrari et al. 2013). Local translation in the axon is therefore a key factor in the maintenance of chronic pain, and it is important to understand the expression of candidate miRNAs and mRNAs in these different cellular compartments.

Classic culture of sensory neurons in a dissociated bath culture, whereby the cell body and axon exist in the same environment, and are subject to the same environmental cues, is therefore not an accurate representation of the anatomical and physiological environment in which they exist *in vivo*. Two culture techniques were implemented which allow for the compartmentalised culture of DRG neurons: microfluidic device chambers, and culture on porous membranes.

4.1.3 Microfluidic devices

Microfluidic devices provide an experimental platform within which the *in vivo* environmental and physical compartmentalisation of cell body and axon can be mimicked *in vitro*. Various microfluidics based platforms have been devised which allow for the construction of nervous system circuits *in vitro,* for the study of the molecular basis of central and peripheral nervous system physiology and disorders (Saliba et al. 2018). Here we have established the culture of sensory neurons within microfluidic devices in order to better recapitulate the *in vivo* environment.

The devices used consist of two channels separated by microgrooves (figure 4.1.1). Cell bodies are unable to pass through the microgrooves, spatially isolating them from the axons which can extend through the microgrooves (figure 4.1.1). If a volume difference is established between the media wells supplying the channels either side of the microgrooves, then fluidic isolation can be achieved, allowing for the creation of different microenvironments in the two channels (Taylor et al. 2005). These devices, or similar, have previously been used in the culture of sensory neurons (Neto et al. 2014; Silva et al. 2017; Tsantoulas et al. 2013). The culture of DRG neurons within microfluidic devices was in particular established in order to allow a better *in vitro* representation of the *in vivo* environment of the sensory neurons.

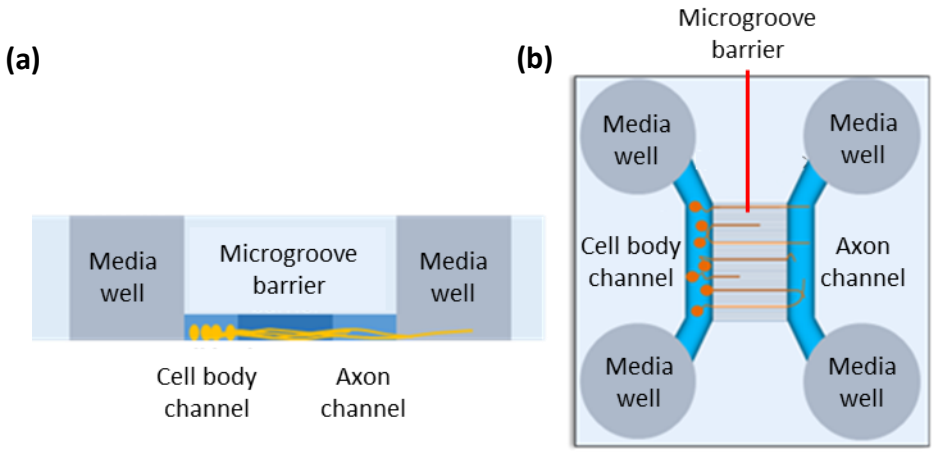


Figure 4.1.1 Microfluidic devices
Schematics of the microfluidic devices used for the culture of neurons. Side **(a)** and above **(b)** view illustrations of the microfluidic devices which allow for the culture of neuronal cells. The device is constructed from moulded PDMS. Media is provided to the culture through the indicated media wells. If a volume difference is established between the wells supplying the channels separated by microgrooves fluidic isolation can be achieved between the channels. This induced fluidic isolation allows for the two channels to represent different media environments within the same culture, which better recapitulates *in vitro* the differing environments the cell body and axon can exist within *in vivo*.

In addition to allowing the recreation of the different environments encountered by cell body and axon *in vivo*, the microfluidic culture system also permits the study the DRG cultures functionally through calcium imaging (Tsantoulas et al. 2013). One of the aims of this work was to demonstrate that through the culture of embryonic DRG neurons in microfluidic chambers, we could develop a functional assay. This functional assay would require nociceptive sensory neurons to extend axons into the fluidically isolated channel. This would then allow the axon to be stimulated to produce a response observable through calcium imaging. The development of such a system would allow the study of nociceptive signals in controlled environment, which could be adapted to mimic those found in inflammatory processes.

4.1.4 Culture of DRG on porous membranes

Culture of DRG on porous membranes (colloquially known as Twiss chambers based on the first user of the developed protocol for DRG culture (Zheng et al. 2001)) allows for the spatial separation of DRG cell bodies from axons (figure 4.1.2). It has been shown previously that the separated isolated compartments extracted from

the cultures can be used for immunofluorescence or molecular biology based analysis (Unsain et al. 2014). It was sought therefore to establish these cultures of DRG, and to assess whether the RNA extracted from the axonal side of culture was free of cell body contamination, and of enough quality for downstream qPCR analysis. This would then allow for the confident assessment of the levels of miRNA or mRNAs within the cell body and/or axons of the DRG neurons within the model.

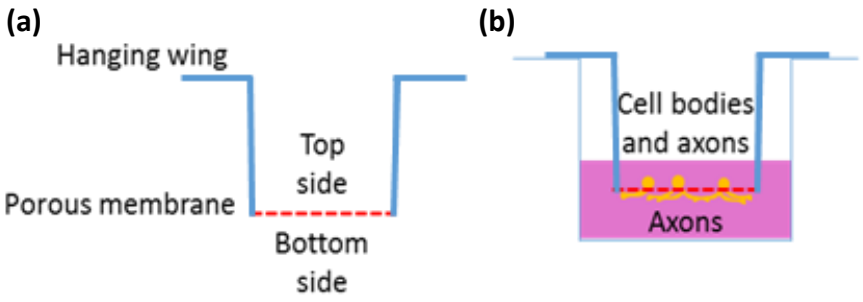


Figure 4.1.2 Porous membrane culture inserts.
These inserts consist of a hanging basket designed to be placed into the wells of a standard cell culture dish (a) the bottom of this basket consists of a porous membrane through which axons can extend and adhere to the underside of the membrane. (b) When placed into the well of a cell culture plate, cell bodies and axons can therefore be spatially separated within the same culture.

4.1.5 Experimental aims

In order to develop appropriate *in vitro* models through which to assess nociceptive processes and the role of miRNAs it was undertaken to:

- Demonstrate the presence of relevant functional cell subtypes within the culture of embryonic DRG through calcium imaging.
- Establish the culture of embryonic DRG within microfluidic devices for the assessment of nociceptive processes.
- Evaluate the use of porous membrane culture of DRG for fractionated RNA extraction from cell body and axon.

4.2 Results and discussion

4.2.1 Embryonic DRG cultures demonstrate subtypes relevant to nociception through calcium imaging

An important aspect of developing an *in vitro* model through which to investigate inflammatory modulation of nociceptive processes, was the ability to assess the excitability of the cells in response to applied stimuli.

First, the cultured DRG cells were stimulated by addition of potassium chloride. Potassium channels have been shown to play a prominent role in nociceptive processing, particularly in chronic pain states, where the neurons demonstrate abnormal excitability which is underpinned by potassium channel dysfunction (Tsantoulas & McMahon 2014). A significant fluorescent calcium indicator response of the cells to application of potassium was observed, with a mean peak fluorescence fold change of 2.6 that of baseline (figure 4.2.1, a). Interestingly, it was found that the peak in fluorescence shows a correlation with cell body size, with larger cells showing a smaller peak in fluorescence (figure 4.2.1, c). Potassium is however a general depolarising stimuli, and is therefore not useful in the distinguishing of those neurons which are involved in nociceptive processes from other sensory neuron subtypes.

Next, the TRPV1 antagonist capsaicin was used to stimulate the cells. TRPV1 is a key mediator in inflammatory sensitization (Adcock 2009) and its expression within sensory neuron subtypes has been shown to be critical in nociception (Brenneis et al. 2013). As shown in figure 4.2.1, the cultured DRG cells demonstrate an increase in intracellular calcium levels in response to application of capsaicin, with two distinct populations based on their fluorescent fold change becoming apparent (Figure 4.2.1, b). The highly responsive cells to capsaicin appear to only be a portion of those cells present within the culture, suggesting the existence of heterogeneity of DRG cell types within the cultures, and thus a good representation of the diversity seen *in vivo*. The response to capsaicin, as with potassium, is correlated to the cell body size (Figure 4.2.1, d), however, two distinct populations become apparent. The cells of small cell body diameter representing the highly responsive cells (figure 4.2.1, d).

Interestingly, this again could be representative of *in vivo* observations, where the small diameter Aδ fibres express TRPV1 (Brenneis et al. 2013).

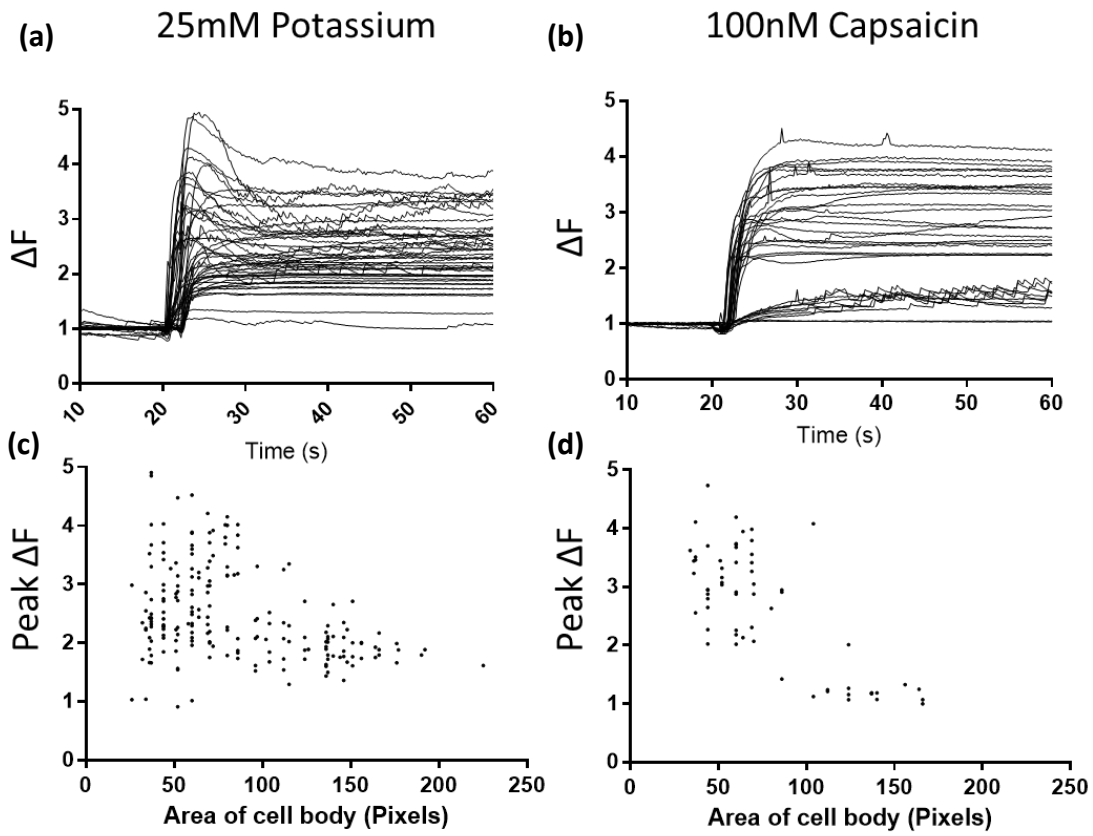


Figure 4.2.1 Subsets of cells relevant to pain processes are present in embryonic DRG cultures based on their calcium responses

Dissociated embryonic DRG cultures loaded with Fluo5 calcium indicator dye were treated with 25mM KCl **(a)** or 100nM Capsaicin **(b)** whilst recordings of fluorescent intensity were taken. Single region of interest traces of change in fluorescence (ΔF) compared to baseline unstimulated fluorescence are shown. Each trace is representative of a single cell. Two sets of responders become apparent based upon the individual cells ΔF to Capsaicin **(b)** which are not apparent in KCl treated cultures **(a)**. When peak ΔF is plotted in comparison to cell body area, the intensity of response to capsaicin **(d)**, shown by cells is more strongly related to cell body size compared to the response to KCl **(c)**. In **(d)** two clear groupings can be seen where high ΔF responders show a smaller cell body area. Traces are collated from three separate cultures. n=213 cells for KCl, n=66 cells for capsaicin.

It is important to note that in these tests the cultures contain both neuronal and non-neuronal cells. The non-neuronal cell population is diminished in the cultures through the addition of the anti-mitotic Aphidocolin (Chapter 2.2.1), however it is

not completely eliminated. Every care is taken to select those cells which appear morphologically to be neuronal.

The finding that within the *in vitro* culture, a proportion of DRG cells have differentiated to respond to the nociceptive stimuli of TRPV1 validates the approach of culturing embryonic DRG cells. Since the nociceptive non-peptidergic (IB4 binding) subpopulation of DRG neurons are dependent on the presence of Glial Derived Neurotrophic Factor (GDNF) in early postnatal life (Molliver et al. 1997), the addition of GDNF to the embryonic cultures may be a key contributing factor for the specification of capsaicin responsive neurons *in vitro*.

So far, the recordings of calcium responses shown (figure 4.2.1) were performed in the classical bath culture of dissociated DRG neurons. As stated above, this culture method does not accurately recapitulate the environment within which the neuron exists *in vivo,* where the axon exists in an environment removed from the cell body. In addition to this, stimulation of the bath culture leads to stimulation of the entire cell, whereas *in vivo* only the peripheral nociceptor terminal would be exposed to the sensory stimulus, and in most cases, the inflammatory mediators involved in the progression of pain.

4.2.2 Microfluidic devices allow for the culture and functional analysis of DRG neurons

Microfluidic culture chambers allow the spatial and fluidic isolation of axons from cell bodies, allowing simulation of the differing environments seen *in vivo* (figure 4.2.2). The culture of DRG neurons within microfluidic devices therefore allows for a more physiologically relevant *in vitro* model.

The embryonic DRG cultures were successfully set up within the microfluidic devices. As can be seen in (figure 4.2.2) DRG derived sensory neurons extend axons through the microgrooves into the axonal compartment. The correct functioning of the microfluidics was confirmed through the use of a lipophilic tracer dye, DiO. This dye is taken up and incorporated into the membrane of cells, and can then diffuse throughout the cell membrane. This dye, when applied to the axonal side of the culture, will therefore be taken up by axons and transported to their cell bodies, where the dye will fluoresce at high levels. As can be seen from the images (figure 4.2.2, c) this does occur, demonstrating the crossing of live axons through the microgrooves. However, cell bodies can also be identified which do not show fluorescence, meaning that their axons do not extend to the other side, and demonstrating that fluidic isolation between the cell body and axonal compartments has been achieved (figure 4.2.2, c).

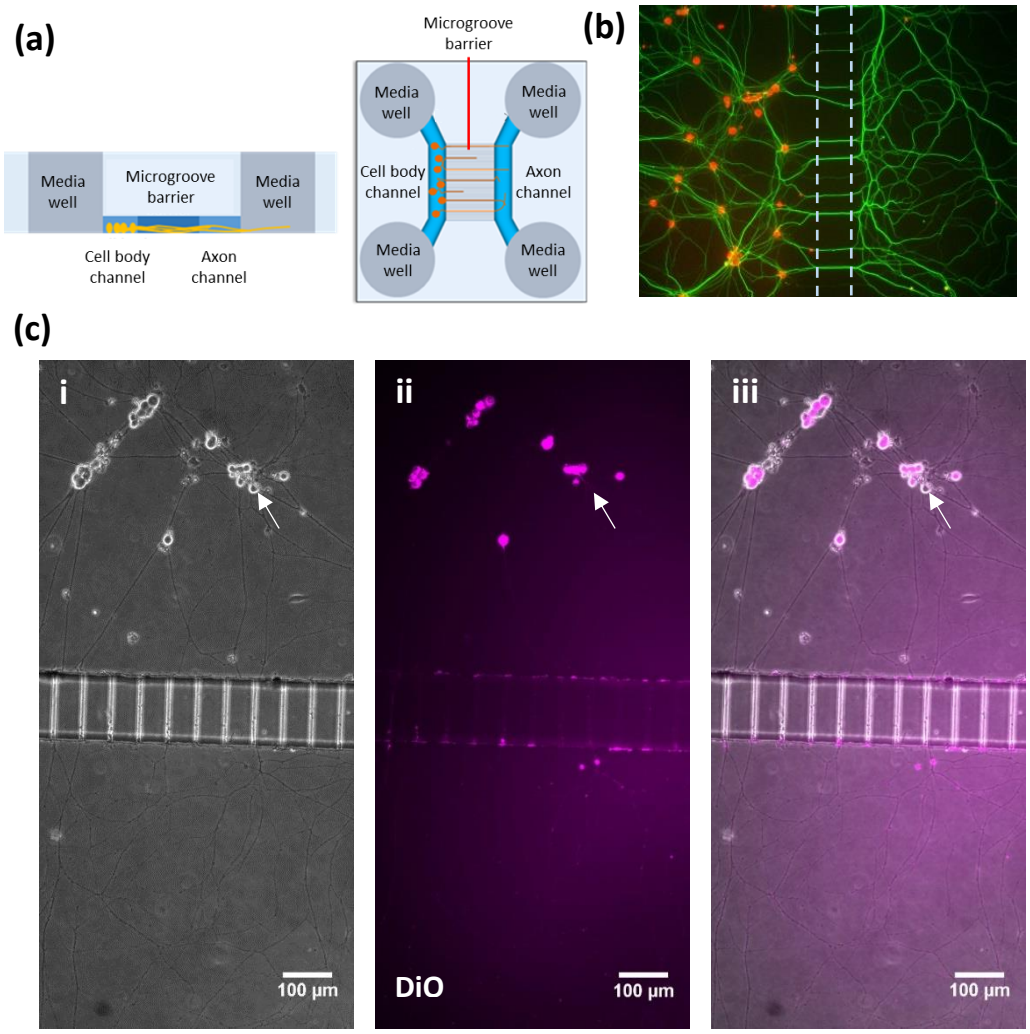


Figure 4.2.2 Microfluidic devices
(a) Side and above view illustrations of the microfluidic devices which allow for the culture of neuronal cells. Axon and cell body channels are moulded from PDMS, connected by a microgroove barrier. Media is provided to the channels through the adjacent media wells. **(b)** Dissociated dorsal root ganglia were cultured within the device prior to immunocytochemistry. Acetylated Tubulin (green) shows the cytoskeleton of axonal projections. DAPI nuclear stain shown in red. Dashed white line demonstrates the microgroove barrier region. **(c)** Dissociated dorsal root ganglia cultures imaged live within the microfluidic device. **(i)** Bright field image displays the positioning of cell bodies and axons within the device. **(ii)** DiO cell permeable dye is applied to the axonal side of the device, axons take up the dye and transport to the cell body. **(iii)** Merged image, arrowhead indicates live DRG neuronal cell body which does not have an axon extending into the adjacent channel and has therefore not taken up DiO.

An important factor of the microfluidic devices is the potential to selectively stimulate the axon in isolation, as it would be stimulated *in vivo,* and the response to stimulus of the axon can then be recorded through calcium imaging of the cell bodies of the DRG neurons (figure 4.2.3). Cell bodies in these cultures demonstrate a significant response to capsaicin as a result of axonal stimulation, with a mean fluorescence increase to 2.3 times that of the baseline (figure 4.2.3). An interesting

observation of the calcium response observed here, compared to that in 4.2.1, is the transient nature of the calcium peak. This suggests a more accurate recapitulation of the *in vivo* action potential response to stimulus.

Non-neuronal cells would not extend processes of significant length through the microgrooves. As only the axonal compartment was subject to stimulus, and responses within the cell bodies were observed, this validates that capsaicin responsive neurons are present within the culture, and that these extend functional capsaicin responsive axons to the axonal channel of the device. The presence of nociceptor-like sensory neuron subtype, and the ability for the isolated stimulation of the axon as seen *in vivo* is a key component of the *in vitro* assessment of nociception.

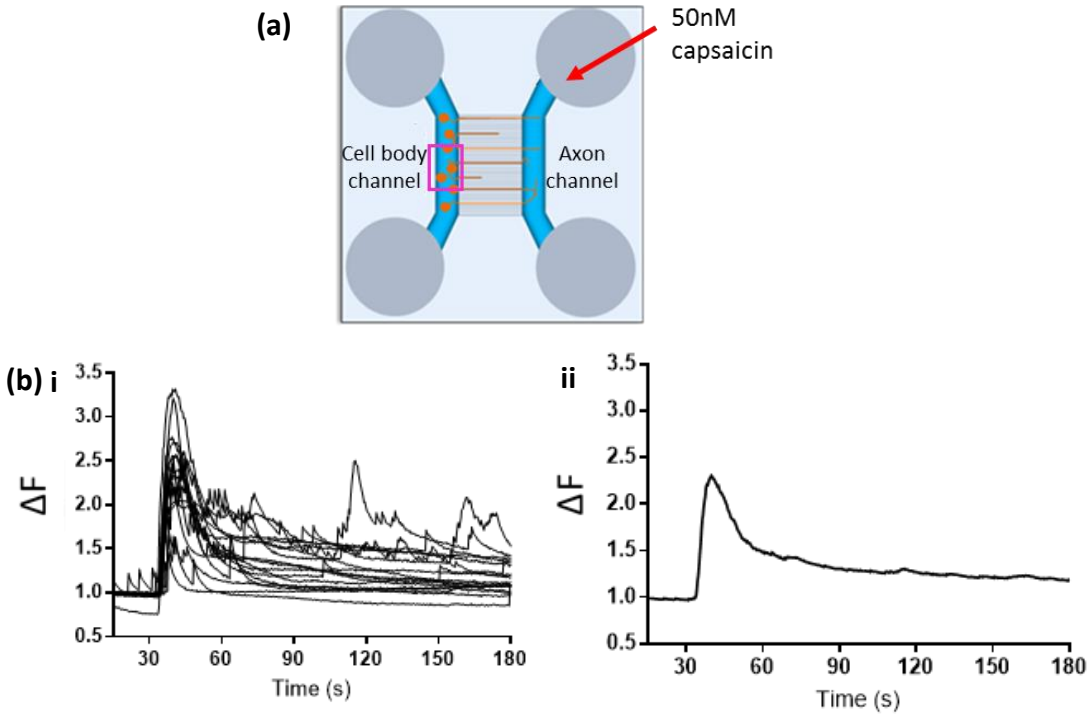
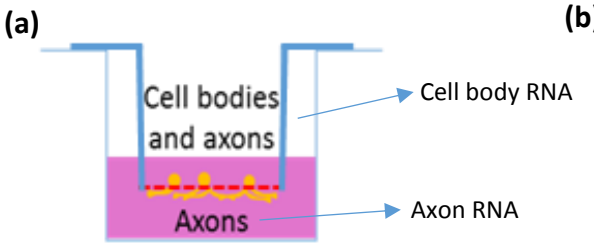


Figure 4.2.3 Capsaicin responsive DRG cells extend functional axons through microgrooves
(a) Illustration of the microfluidic device culture of dissociated DRG cultures. Neurons extend axons to the axon chamber where they are spatially and environmentally separated from their cell bodies. **(b)** Example traces from a microfluidic device culture. When dissociated DRG cells are cultured within a microfluidic device, stimulants can be applied to the axons alone, better representing the *in vivo* environment. Dissociated embryonic DRG cultures loaded with Fluo5 calcium indicator dye were treated with 50nM Capsaicin, whilst recordings of fluorescent intensity were taken from the cell bodies (pink box in a). Single cell traces from a representative cultures are shown in **i** and an average of responses is shown in **ii**. n=17 cells

The fluidic isolation of axon from cell body (4.2.2), and ability to assess the functionality of the sensory neurons responsible for nociception (4.2.3), are key beneficial aspects to the culture of DRG in microfluidic devices. However, the ability to extract RNA from these cultures is hindered by the high cost of the devices, and low RNA yield which results from extraction. As such, the culture of DRG on porous membranes was assessed for this.

4.2.3 Culture of DRG on porous membrane allows for the extraction of RNA from cell body and axon

The use of porous membrane devices allows the culture of DRG in a compartmentalised format, where axons extend to the underside of a membrane and cell bodies remain above (figure 4.2.4). This method of culture is useful for the fractionated extraction of cellular components, however does not allow for fluidic isolation.



(b)

DIV	Fraction	RNA yield (ug)
3	Cell Body	3.858
	Axon	2.65
6	Cell Body	5.113
	Axon	3.933
9	Cell Body	4.415
	Axon	1.046
12	Cell Body	4.847
	Axon	7.681

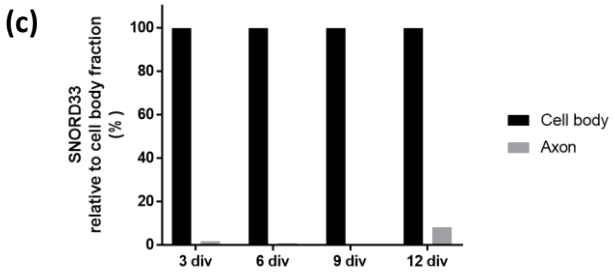


Figure 4.2.4 Porous membrane cultures show effective physical separation of DRG axons from cell bodies to allow for RNA extraction
(a) Schematic of the chamber culture set up demonstrating how cell bodies are separated from their axons by a porous membrane. This allows for RNA extraction from the separated culture compartments for downstream analysis. **(b)** Quantities of RNA extracted from respective fractions of the porous membrane cultures shown DIV: Days *in vitro* **(c)** qPCR of the nuclear RNA SNORD33 in RNA extractions from porous membrane DRG cultures at different time points post-plating. Levels are shown relative to the SNORD33 levels of the cell body fraction of RNA at each time point. Axonal fraction levels of SNORD33 range from 0.4% to 8% of their respective cell body fractions.

Once the DRG neurons had grown for the indicated time points (figure 4.2.4, b), RNA was extracted from cell body and axonal fractions of the culture. The average yield of axon sample was 3.8µg, and of cell body 4.6µg (figure 4.2.4, b). Since only a 5ng/µl concentration of RNA is required for miRNA qPCR, this is more than sufficient in quantity for subsequent qPCR. The quality of RNA was also deemed sufficient (based on 260/280 ratios) to carry forward for qPCR assessment of cell body and axon separation (figure 4.2.4 c).

Importantly, negligible levels of cell body contamination within the axonal fraction of the culture are seen, as confirmed through qPCR of the small nucleolar RNA, SNORD33 (Figure 4.2.4, c). SNORD33 is a C/D box small nucleolar RNA, which contain the C/D box motif which is necessary, and sufficient, to direct RNA targeting to the nucleolar compartment in yeast and mammals (Samarsky et al. 1998). A selection of C/D box SNORs were used for initial assessment through qPCR and of these, SNORD33 demonstrated the highest levels of expression within embryonic DRG cultures (data not shown). Therefore, SNORD33 was utilised as a marker for cell body presence within the RNA samples. Consistently low levels of SNORD33 were found in the axonal RNA samples, with levels on average 2.75% of that observed from the cell body fraction (figure 4.2.4 c).

The culture of DRG on porous membranes through the method described (Chapter 2.2.7) allows for the culture of entire ganglia, which reduces the processing of the cells which occurs in dissociated culture. This creates a culture of cells which are growing in an environment which is more representative of their state *in vivo* than dissociated cultures. However, the culture of dissociated DRG neurons would allow for the more efficient application of agents such as cell permeable miRNA inhibitors, and also morphological assessment of the cell bodies through methods such as immunocytochemistry. If the culture of dissociated sensory neurons is required for future experiments, further characterisation of the purity of the axonal fraction would need to be assessed, as the dissociation may allow the passing of small cell bodies, now separated from the ganglia, through the membrane.

As stated previously, this culture method does not allow for the fluidic isolation of cell body from axon, meaning the cell body and axon are existing in the same media environment. This is not an accurate representation of the *in vivo* environment, where the axon exists in a different cellular environment to the cell body. Other labs have begun to develop the use of methods in these cultures which, when applied to the culture, allow for the sealing of the porous membrane holes (unpublished data). These methods would prevent media flow between the two compartments, and potentially allow for the culture of cell body and axon in different media environments.

The culture of DRG on porous membranes was shown as a useful method through which differential RNA expression between the cell body and axon can be assessed (figure 4.2.4). This has potential useful applications in the study of miRNA in sensory neuron function and nociception.

4.3 Conclusions and future directions

The aim of the work contained within this chapter was to establish appropriate *in vitro* systems through which to investigate the function of miRNA in nociception.

With the view to assessing their suitability for the study of nociceptive processes, it was established that embryonic DRG neuron cultures demonstrate heterogeneity of cell types. This was through demonstration that these cells elicit a response to capsaicin, indicative of the presence of nociceptive sensory neurons (figure 4.2.1, 4.2.3). Future studies should be carried out to further characterise the cultures for their use in the study of pain processes. This would require a combination of immunocytochemical and functional assessments of the cultures. For example, as in (Barabas et al. 2012) where they have characterised the populations of mechanical and cold sensitive TRPA1-responsive sensory neuron subtypes through functional calcium imaging, and via staining with commonly used peptidergic (CGRP) and non-peptidergic (IB4) sensory neuron markers (Barabas et al. 2012). The subtypes and characteristics of the culture required however will depend on the direction of future studies, and the necessary characteristics required to assess the relevant processes.

It was demonstrated that dissociated embryonic DRG cultures can be successfully cultured within a microfluidic device which allows for the fluidic isolation of the cell body from the axon (figure 4.2.2). Calcium imaging demonstrated the presence of capsaicin responsive DRG neurons within the cultures, which extend functional axons to the axonal compartment of the microfluidic device (figure 4.2.3). It was also demonstrated that porous membrane cultures can be used to extract a high yield of RNA for downstream analysis, which shows a low level of cell body contamination in the axonal fraction (figure 4.2.4). This would allow us to identify the spatial expression of miRNA or mRNA of interest in downstream studies of the effects of miRNA on the culture.

The porous membrane and microfluidic cultures should be used in conjunction with each other for future studies. As the microfluidic cultures (whilst being a better model in regards to recapitulating the spatial and environmental separation of cell body from axon *in vivo)*, do not allow us to regularly extract fractionated RNA of a high yield, as in the porous membrane cultures. In further studies the question of which aspects of these two culture techniques is most desirable should be addressed.

These culture methods can also allow for the co-culture of the DRG neurons with other cell types which are present in the pain circuit. For example, the DRG cultures can be grown in conjunction with macrophages which are an important cell type involved in inflammatory processes. The microfluidic devices, such as those used here, are in fact being used currently as potential platforms for the generation of *in vitro* circuits through co-culture of different interacting cell types (Saliba et al. 2018). A benefit of the porous membrane cultures is the potential mobility of the cultures themselves (i.e. the baskets can be transferred between wells of a six well plate). This would allow for the transfer of the cultures into cultures of interacting cell types. For example, a culture of DRG on the porous membrane could be transferred into a culture of macrophages. This would allow for the assessment of the interaction of DRG neurons with interacting cell types, and the subsequent assessment of the changes associated with this.

For future studies of miRNA effects on the *in vitro* cultures the ability to transfect these cells with reagents such as miRNA mimics or inhibitors and siRNA would be useful. Currently, the optimisation of transfection of the *in vitro* DRG cultures has proven difficult. Previous groups have stated the difficulty which is faced in the transfection of the primary DRG cultures using classical techniques (Yu et al. 2015) and reasonable efforts were made within this project to successfully transfect the DRG neurons using the common transfection reagent Lipofectamine, and the techniques of microinjection and electroporation to no useful avail (data not shown). Cell permeable miRNA inhibitors and siRNA constructs are commercially available, which will allow for inhibition of the target miRNA or mRNA without the need for transfection. This will prove useful in the context of population studies which can be carried out using calcium imaging or qPCR. Unfortunately the constraints of my personal study limited the investigation of miR-138 and MYD88 within these cultures, as at this stage of the project the decision was made to focus efforts on the *Drosophila* work being carried out in parallel which is outlined in future chapters, however further work on this side of the project is to be carried out within the group to investigate this.

In summary, the *in vitro* culture of embryonic DRG cultures was demonstrated to be suitable for the future investigation of miRNAs in nociceptive processes: the relevant cell types appear to be present; are able to be functionally assessed through calcium imaging; and a suitable method through which to extract fractionated RNA was devised. These culture methods would allow for the future investigation of the functional mechanisms of miRNAs (for example miR-138-5p which was identified as a candidate in chapter 3) in inflammatory and nociceptive processes.

Part II – Investigation of miRNAs and their role in the development and ageing in the nervous system of *Drosophila* melanogaster

Chapter 5. Identification of miRNAs with a role in nervous system development

5.1 Introduction

Despite the increasing knowledge of the importance of miRNAs in the development and function of the nervous system, the localisation and cellular mechanisms for the majority of miRNAs is not known. To date, individual miRNA have been shown to play important roles in key stages of nervous system development, and some examples of these were described in the introduction to this thesis (Chapter 1.13-15). Here, the suitability of the model system chosen in this part of the thesis through which to investigate novel functions of miRNA in the nervous system: *Drosophila melanogaster* is discussed.

5.1.1 *Drosophila* melanogaster as an experimental model

The fruit fly, *Drosophila*, has established a prominent place in modern science, being the chosen model in research that has led to eight Nobel prizes to date, and used by labs across the world for over a century. Many key discoveries of gene regulation and developmental genetics originated from work in the fly, and it is estimated that around three-quarters of identified disease causing genes in humans have functional orthologues in *Drosophila* (Reiter et al. 2001). Indeed, much of the internal organ structure of the fly demonstrates a degree of homology to humans (Ugur et al. 2016). As a result, this has led to the creation of many disease models in *Drosophila*, which are easily applicable for genetic or therapeutic investigation (Pandey & Nichols 2011).

There are many practical reasons behind the choice to use *Drosophila* as a model organism (Prokop & Root 2013). Firstly, their ease to obtain and maintain in comparison to mammalian models, allowing experiments to be carried out at a low relative cost with fewer ethical and regulatory barriers. The life-cycle of *Drosophila* is also dramatically shorter compared to mammalian models, with a genetic cross

yielding embryos within hours, and adults within ten days. This allows for outputs to be greatly increased within a given timeframe in comparison to mammalian models. *Drosophila* tools also allow the easy maintenance of mutant chromosomes, and therefore stocks of a desired genotype, as the males demonstrate a lack of recombination, and the use of balancer chromosomes allows the researcher to prevent recombination in females and to track heritability (Ashburner et al. 2005).

Work in 1910 by T.H.Morgan on chromosomal heritability, and the subsequent public release of the mutants generated from the study, was a key landmark in *Drosophila*'s research history (Rubin & Lewis 2000; Ashburner et al. 2005). From this landmark study, *Drosophila* as a model system in research has gone from strength to strength, with a basis in the informal collaboration of Drosophilists through the use of publicly available stock centres. For example, the Bloomington and Kyoto centres, where researchers deposit created lines for use by others. There is now an expansive availability of *Drosophila* stocks to the researcher, including gene mutations and knockouts. These strengths of *Drosophila* as an experimental model system lends to its use in large scale genetic screens (St Johnston 2002), which can identify genes or mutations which are important in developmental processes, or functional mechanisms in health and disease conditions.

5.1.2 Gal4/UAS

Whilst gene mutations and knockout animals are useful, in order to determine the temporal and tissue specific roles of genes, targeted expression models are required. One such tool in *Drosophila* which is utilised in this work is the Gal4/Upstream Activating Sequence (Gal4/UAS) system. The Gal4/UAS system allows for the expression of specific genes in a cell type, and developmental time point specific manner. For this, the GAL4 gene encodes the yeast transcriptional activator protein, Gal4, which will recognise an Upstream Activation Sequence (UAS) that drives the expression of downstream genes (figure 5.1.1, Brand & Perrimon 1993). There are extensive stocks available, which allow for the expression of Gal4 in many different tissues and at specific developmental time points, along with UAS stocks which allow for the expression of genes of interest.

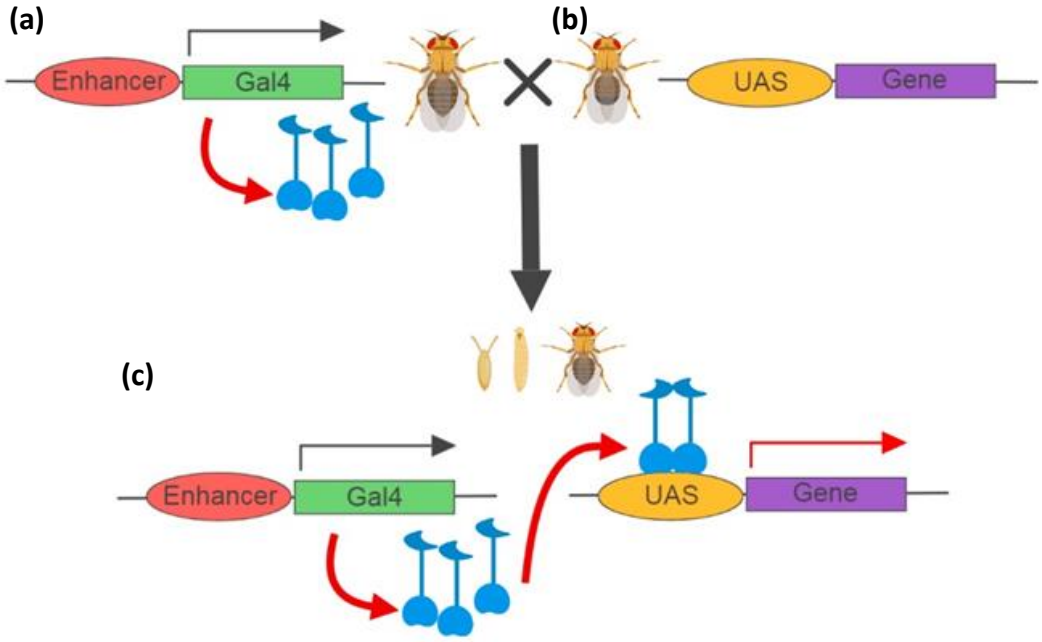


Figure 5.1.1 The Gal4/UAS enhancer trap system
(a) An enhancer placed upstream of the Gal4 gene, or the Gal4 gene placed downstream of an enhancer, allows for Gal4 to be expressed within specific tissues or time points. **(b)** The Upstream Activation Sequence (UAS) can be placed upstream of a gene or construct of interest and inserted into the *Drosophila* genome. **(c)** In the progeny resulting from a cross, Gal4, where expressed, can recognise the UAS, triggering expression of a gene of interest which is under the control of UAS. Figure constructed in BioRender.

5.1.3 Nervous system development in *Drosophila* melanogaster

Drosophila as an experimental model is highly versatile, and is widely recognised as a useful tool in the research of nervous system disorders (Jeibmann & Paulus 2009; Gatto & Broadie 2011). Clear parallels can be drawn between *Drosophila* and mammalian nervous systems, allowing translation of findings. Some example diagrams and antibody staining of the structures of the developing and mature *Drosophila* nervous system are shown (figure 5.1.2).

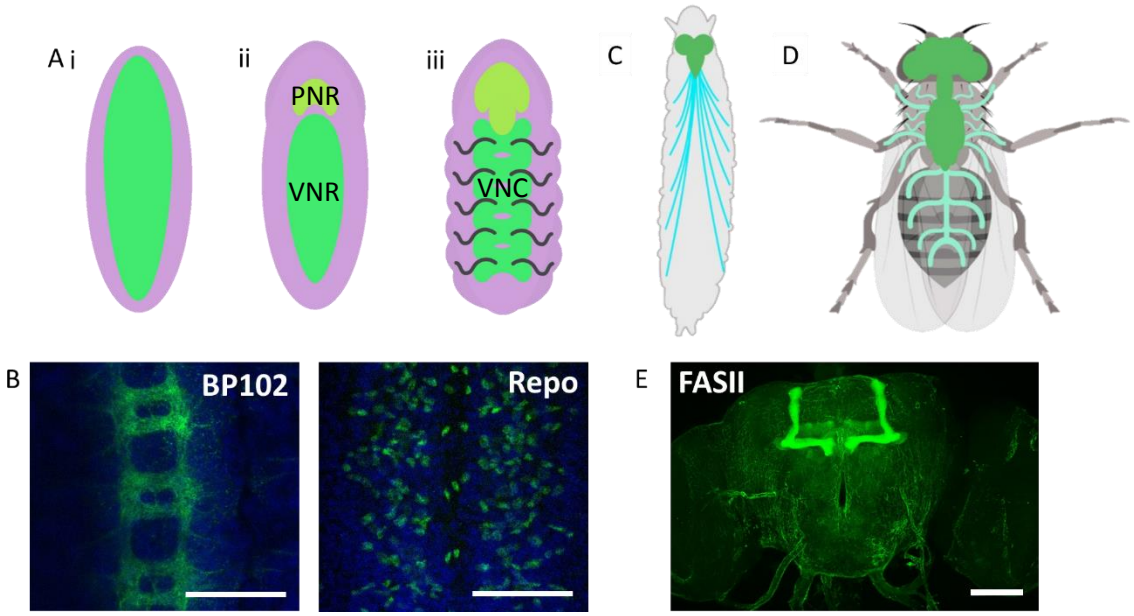


Figure 5.1.2 Nervous system development in *Drosophila*
(a) Schematics of the ventral portion of *Drosophila* embryos are shown to demonstrate stages of central nervous system development. Schematics shown here are based upon those found in (Campos-Ortega & Hartenstein 1997). **(i)** In the early embryo, the neurogenic regions are specified within the ectoderm (green) **(ii)** The cells within the neurogenic region give rise to the neuroblasts of the ventral nerve cord in the ventral neurogenic region (VNR) and the brain in the pro-cephalic neurogenic region (PNR) **(iii)** Neuroblasts delaminate from the ectoderm in later stages, and are arranged into the stereotypical segmented structure of the ventral nerve cord (VNC) from which motor neurons extend axons to the periphery, and sensory neurons extend axons to the VNC from the periphery of the embryo (in black). **(b)** Elements of the embryonic nervous system can be revealed through antibody staining. BP102 highlights the axons of the CNS, revealing the stereotypical segmented structure, and Repo stains the nuclei of all glial cells. The basic structures of the nervous system established within the embryo persist in **(c)** the larvae and **(d)** the adult, where further differentiation and reorganisation occurs. The adult brain of *Drosophila* can also be stained with antibodies revealing the specific neuronal lobes. For instance **(e)** FasiculinII (FASII) staining in green reveals the lobed structure of the mushroom bodies. Scale bars: 50µm.

The use of a model system such as *Drosophila* to investigate the development of the nervous system allows us to gain a greater understanding of normal function, and the underlying causes of dysfunction and disease. Below, some examples of *Drosophila* as a tool to dissect conserved elements of the nervous system are discussed.

5.1.4 Differentiation of nervous system cells

As in mammals, the *Drosophila* nervous system develops from precursor cells, or neuroblasts. Neuroblasts, through a series of interdependent signalling cascades, generate neural precursor cells, which further differentiate into mature nervous system cells (Figure 5.1.2 a, Campos-Ortega & Hartenstein 1997). Each neuroblast expresses a distinct profile of genes, and contributes a specific lineage of cells to the nervous system, demonstrating how nervous system patterning begins at these early stages of development (Harris et al. 2015). A series of activating proneural genes, and inhibitory neurogenic genes, control the formation and patterning of neuroblasts (Urbach & Technau 2003; Sprecher et al. 2007), many of which are conserved to mammals. For an example, the transcription factor Dachshund (*dac*) (Mardon et al. 1994) demonstrates a distinct pattern of expression in individual, or clusters, of neuroblasts throughout nervous system development in *Drosophila.* Dac is expressed in a pattern overlapping, but not completely correlated with the Pax6 homologue *eyeless* (Urbach & Technau 2003; Sprecher et al. 2007). *Dac* mutants in *Drosophila* display abnormalities in the development of nervous system structures, for example the mushroom bodies of the *Drosophila* brain (figure 5.1.2,e, Noveen et al. 2000). The mammalian homologue of *dac*, DACH1, demonstrates expression within the developing CNS and eye in mice, again with overlapping expression with Pax6, as in *Drosophila* (Hammond et al. 1998). Although mouse mutants of DACH1 do not present any gross abnormalities in early nervous system development, they show postnatal lethality within 24 hours (Backman et al. 2003), suggesting an underlying developmental defect. This is one example of the differentiation and cell specification regulators which are conserved to *Drosophila* which allow for the conserved study of their molecular processes.

5.1.5 Axon growth and pathfinding

The relative simplicity of the *Drosophila* nervous system allows the assessment of axon growth and branching through techniques such as imaging of highly stereotyped axonal structures. For example many antibodies are available for the axon tracts of the embryonic ventral midline (Evans & Bashaw 2010), or axon fascicles that form the mushroom body lobes of the brain (Crittenden et al. 1998). In

addition to this, more recently, the *in vitro* culture of *Drosophila* neurons has been developed to allow for more molecularly detailed assessment of axon growth (Prokop et al. 2012; Egger et al. 2013). Beyond the technical accessibility, many elements of axon growth and pathfinding are common between *Drosophila* and mammals, and as such *Drosophila* is a widely used model system to investigate axon growth and pathfinding.

As in mammals, the leading process of an extending *Drosophila* axon consists of the growth cone. The growth cone is a dynamic cytoskeletal and membrane structure, which possesses the ability to respond to a vast array of cues, guiding the growth of the axon to the correct target (Sánchez-Soriano et al. 2010). Many of the cytoskeletal regulators involved in growth cone dynamics are conserved between *Drosophila* and mammals (Prokop et al. 2013). This conservation allows the battery of genetic tools available in *Drosophila* to be applied to the study of axon growth, and growth cone dynamics. As an example, a comprehensive study of the role of the *Drosophila* actin linker molecule, Short Stop (*Shot*) and its mammalian homologue, ACF7 demonstrated the role of both in the formation of filipodia at the growth cone (Sánchez-Soriano et al. 2009). Similar effects of the mutation or knockdown of this gene were observed across *Drosophila* and mouse in three separate *in vitro* models (Sánchez-Soriano et al. 2009), demonstrating a crucial conservation of function. Again, this is but one example of the many conserved elements of axon growth and pathfinding found in *Drosophila* which aid in its tractability as a model system.

5.1.6 Synapse development

Drosophila also provides us with an accessible model for the study of synapse formation and function, for instance in the neuromuscular junction (NMJ) of the larvae (Menon et al. 2013). The NMJ of *Drosophila* is a glutamatergic synapse, as opposed to its cholinergic mammalian counterpart, however it remains a genetically tractable system through which to study synapse formation and function. Similar to vertebrates, the formation of the NMJ in *Drosophila* is characterised by an initial overgrowth of the synapse, followed by pruning to the mature synapse(Menon et al. 2013; Sanes & Lichtman 1999), in an activity dependent process (Buffelli et al. 2003;

Jarecki & Keshishian 1995). Post-synaptic glutamate receptors at the *Drosophila* NMJ show a tendency to preferentially cluster at active zones, where there is a higher level of glutamate release from the presynaptic terminal (Marrus & DiAntonio 2004). This allows for the *Drosophila* NMJ to be used as a tractable model for the role of presynaptic activity in postsynaptic receptor clustering. Although the mammalian NMJ is not glutamatergic, it has been shown that glutamatergic neuromuscular synapses can be induced through the co-culture of glutamatergic neurons with myotubules (Ettorre et al. 2012). These studies of the *Drosophila* NMJ are therefore applicable in the field of synapse specificity research, and in research surrounding the processes governing the maturation of synapses.

5.1.7 Using *Drosophila* to investigate non-conserved biological paradigms

The examples outlined above emphasise the tractability of *Drosophila* as a model system, and how it can be used in the study of multiple neurodevelopmental mechanisms (Okray & Hassan 2013; Gatto & Broadie 2011). Some examples of conserved neurodevelopmental processes and genes in *Drosophila* were described (Chapter 5.1.4-7). In addition to this, non-conserved aspects of the nervous system in *Drosophila* can still be utilised to elucidate the overall function of key systems. For example, the *Drosophila* olfactory circuitry is a widely used system to study the specificity of neuronal network formation (Hong & Luo 2014). This is despite being mediated by receptors that are unique to insects, thought to be the key to insects intense sense of smell (Spehr & Munger 2009; Getahun et al. 2013); and possessing an overall arrangement of the olfactory system which is different to mammals (Spehr & Munger 2009). This demonstrates how *Drosophila* can be used to investigate biological paradigms that are applicable to mammalian models, even if not absolutely conserved.

In summary, the conservation of basic processes of nervous system development and signalling cascades in *Drosophila* allow for parallels to be drawn to the mammalian nervous system. Whilst the relative simplicity of the nervous system, and availability of genetic tools, provides a model through which observations of alterations can be more easily made. In the context of this work, the model of the

Drosophila compound eye was used to conduct an initial investigation into the effects miRNAs can have on nervous system development.

5.1.8 The *Drosophila* compound eye

The *Drosophila* eye is made of approximately 800 highly organised repeated units called ommatidia (figure 5.1.3). Each one of these units is comprised of a precisely formed structure of pigment cells, lens secreting cone cells, and eight photoreceptors (Thomas & Wassarman 1999). The development of these structures is tightly organised, and very rarely disrupted in the wild type fly, making this a stable system through which to observe developmental defects. In addition to this, from a practical point of view, the fact that the eye is an external structure makes it amenable for observation and analysis via simple visualisation techniques (Mishra & Knust 2013).

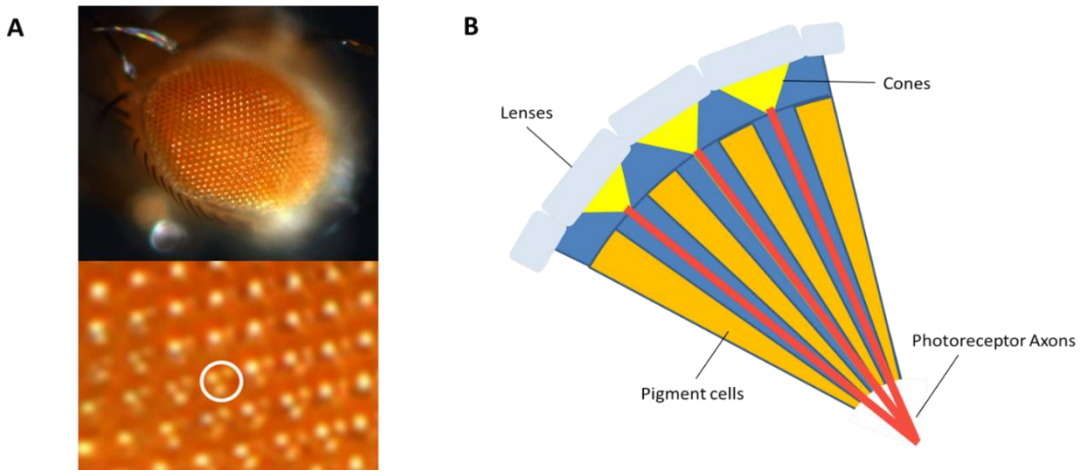


Figure 5.1.3 The *Drosophila* compound eye
(a) A photograph of a wild type *Drosophila* eye, showing the highly ordered patterning of ommatidia. Inset: a close up of the eye structure where the organised repetitive pattern of ommatidia can be seen. **(b)** A diagram of a transverse section of the *Drosophila* eye, showing how the ommatidia are comprised of a structure of photoreceptor axons, pigment cells, cones and lenses.

For the eye to develop, as with other nervous system structures, it requires the concerted action of many regulatory events, and the expression of multiple genes. So far, over 500 mutants have been characterised that result in the disruption of the patterning of the eye, with cellular and molecular mechanisms that fall into multiple categories (Call et al. 2007). In figure 5.1.4 a section of the identified *Drosophila*

retinal determination network is outlined (Kumar 2009), along with the conserved mammalian counterparts. It has been estimated that approximately two-thirds of the 3200 vital genes in *Drosophila* are required for assembly and neuronal connectivity of the eye (Thaker & Kankel 1992). Despite extensive studies into the development of the *Drosophila* eye, many components of eye development are therefore yet to be functionally defined.

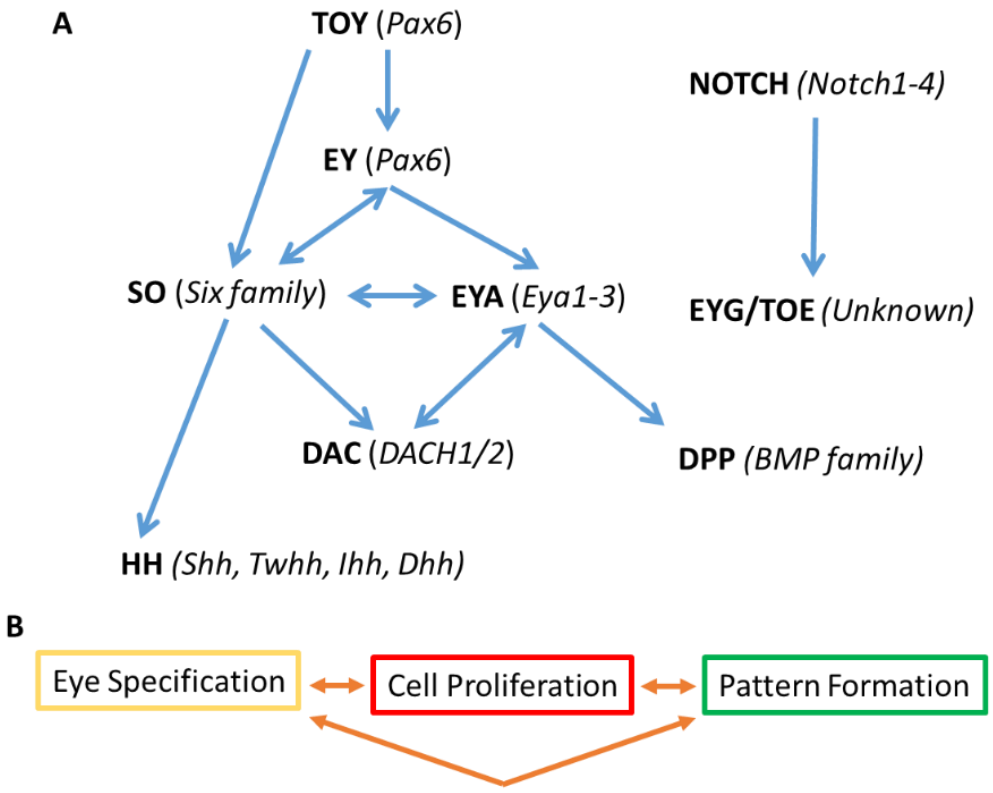


Figure 5.1.4 The *Drosophila* retinal determination network
(a) An example section of the Retinal determination network of the *Drosophila* eye. Example regulatory genes are shown with their mammalian homologues in brackets. **(b)** The processes of eye specification, cell proliferation and pattern formation all work in an interconnected way to form the *Drosophila* compound eye

As the *Drosophila* compound eye is a highly studied model of nervous system development, a battery of genetic tools are also readily available for use in this system. A range of Gal4 stocks have been developed for targeted expression of

genes within the eye (Thomas & Wassarman 1999). The sevenless and Glass Multiple Receptor (GMR) gal4 drivers are widely used to target expression of a UAS transgene to the developing photoreceptors of the eye, and the differentiated cells of the eye disc respectively (Ray & Lakhotia 2015). Here, the *eyeless* (ey) gal4 driver is used. *Eyeless* is the *Drosophila* homologue to Pax6, and demonstrates expression within eye disc progenitors starting in early development (Quiring et al. 1994). *Eyeless* expression then persists throughout eye development, to terminally differentiated larval and adult photoreceptors (Sheng et al. 1997). The importance of *ey* in the development of the eye structures is demonstrated through the ability of *ey* to induce ectopic eye formation (Halder et al. 1995). Eyeless expression is also found in other structures of the nervous system throughout development, for example, in the neurons of the developing mushroom body (Callaerts et al. 2001).

5.1.9 *Drosophila* melanogaster as a model to study miRNA

As with other model systems, miRNAs have been shown to function as regulators of multiple cell processes in *Drosophila* (Carthew et al. 2017). A comprehensive investigation of *Drosophila* miRNAs and their predicted targets showed an enrichment of target genes which are involved in both the development and maintenance of the nervous system (Enright et al. 2003). This study suggested that, as in mammals, miRNAs are key regulators of nervous system processes in *Drosophila* (Enright et al. 2003). In fact, many of the previously described examples of miRNAs that have been shown to be involved in nervous system development have their roots in *Drosophila* work (Chapter 1.12-16), which highlights the potential of this model system in further miRNA research.

When taking into account the conservation of miRNAs and their roles in *Drosophila* it is important to consider the existence of a two-layered model of conservation. First, the conservation of the miRNA itself must be considered, and secondly, the conservation of the miRNA targets. Bioinformatics tools are available to establish the level of conservation between *Drosophila* miRNAs and other species. One such tool is miRviewer (Kiezun et al. 2012), which analyses miRNA conservation across 50 species in relation to a consensus sequence. All miRNAs present in miRBase v.16 (Kozomara

& Griffiths-Jones 2014) are represented, along with newly predicted miRNAs found with miRNAminer (Artzi et al. 2008). The sequence conservation is provided as a numerical score, which is comparable across species, thus providing an easily accessible conservation metric. In addition to the conservation of a miRNAs whole mature sequence, as determined by tools such as miRviewer, miRNAs with similarities in seed sequence can also be considered. For example in the case of miR-1000/miR-137 previously discussed (Verma et al. 2015, Chapter 1.16), which share a similar seed sequence, and have been demonstrated to regulate glutamatergic signalling in *Drosophila* and mouse respectively.

There are however many *Drosophila* specific miRNAs. In these situations the use of *Drosophila* as a model system is still relevant in the demonstration of the capacity of miRNAs to regulate nervous system function. As an example, the first miRNA which was found to control neuronal patterning was discovered in another common model system: *C.elegans*. The *C.elegans* Lys6 miRNA controls factors which govern the asymmetrical development of taste receptor neurons (Johnston & Hobert 2003). Although this is a non-conserved miRNA, this study provided the first evidence of the paradigm that a single miRNA can control the patterning and development of the nervous system. Another particularly relevant example in the context of this work is the function of miR-279/996 cluster in Notch signalling (Kavaler et al. 2018). It has been shown that through the targeting of a Notch signalling repressor, Insensible, in non-neuronal cells miR279/996 can regulate neuronal cell fate determination in sensory organs (Kavaler et al. 2018). Although this is a miRNA only found in *Drosophila*, it provides an example of the mechanisms through which miRNA can potentially modulate signalling pathways. In this context, it is possible to anticipate that any disruptions to the *Drosophila* nervous system function and development due to alterations in miRNA levels could be replicable in mammalian systems, if not through the exact same miRNA, then possibly through a similar pathway.

The battery of experimental tools available in *Drosophila* research also lend themselves to the study of miRNA function (Iftikhar et al. 2017). In particular, there are stocks available for both overexpression of miRNAs (Bejarano et al. 2012;

Schertel et al. 2012) and inhibition of miRNAs (Fulga et al. 2015) with the Gal4/UAS system, along with a cohort of knockout mutant stocks (Chen et al. 2014).

In this work the UAS-miRNA expression stock resource described in Bejarano et al. (2012) is used. This study produced two stock collections, with individual miRNAs placed downstream of the UAS sequence. One collection inserted the UAS constructs with the P-element insertion method, which delivered random positioning of the UAS constructs throughout the genome (Bejarano et al. 2012). The other stock resource, which is utilised here, was generated through site directed insertions of the UAS-miRNA constructs. This created a collection of stocks where all UAS constructs were inserted at the same specified genomic location (Bejarano et al. 2012). This site directed insertion allows for direct comparisons to be made between stocks, without questions of the effect of genomic insertion site being raised.

The *ey* Gal4 driver, which we use here, was previously used to assess the effect of an alternative UAS-miRNA resource on eye development (Schertel et al. 2012), this provides us with an alternative resource against which to validate this investigation. The information which is available from this study is not however very detailed, and showed a very low level of successful phenotype identification (~10%).

In later parts of our study (Chapter 6-7), the miRNA sponge collection described in Fulga et al. (2015) is used. miRNA sponges are transgenes which encode for multiple copies of miRNA target sites of perfect, or near perfect, complementarity to the target miRNA (Ebert & Sharp 2010). These act as functional inhibitors, sequestering the miRNA, and preventing it's binding to miRNA recognition sites present within target genes (Ebert & Sharp 2010). These UAS-miRNA sponge lines have been shown to produce effects that closely resemble null or hypomorphic alleles when ubiquitously expressed (Fulga et al. 2015). The UAS-miRNA sponge collection made available utilises site specific integration of UAS-miRNA sponge sequences (Fulga et al. 2015). Whilst miRNA knockout lines are available (Chen et al. 2014), these do not allow for the tissue or time-point specific knockdown of miRNA activity, and the

miRNA sponge lines have been shown to be capable of this when combined with a Gal4 of interest (Loya et al. 2009).

5.1.10 Experimental aims

There is a growing recognition that the development of the nervous system can be regulated by individual miRNAs. However, the full understanding of these processes is far from complete and, there is a clear need to broaden the knowledge of miRNA regulatory pathways in nervous system development. Both at the level of identification of miRNAs which are involved in nervous system development, and mechanistic understanding of miRNAs targets and overall function. The overarching aim of the work presented in this chapter was to identify those miRNAs with potential roles in nervous system development. For this we divided the work in three specific objectives.

- Overexpression of 100 individual UAS miRNA lines within the developing *Drosophila* eye using the *ey*Gal4 driver, which will lead to overexpression of the miRNA in the eye throughout development.
- Phenotypical assessment of abnormalities in eye development, through the analysis of the size and patterning of the external structures of the eye.
- Prioritisation of the miRNAs investigated, based on the severity of effects observed, and the conservation of the miRNA sequences between *Drosophila* and mammals.

5.2 Results and discussion

As a first approach to tackle the identification of miRNAs which may play a role in nervous system development, overexpression of 100 individual UAS-miRNA constructs was carried out in the developing *Drosophila* eye using the *ey*GAL4 driver. The effects of combining *ey*Gal4 with the individual UAS-miRNA lines on the adult eye morphology was thus analysed.

5.2.1 Eye size defects after overexpression of miRNAs in the developing eye

Overexpression of individual miRNAs within the developing eye had the potential to disrupt multiple morphological characteristics. Disruptions in the size of the eye were first assessed, as this approach has previously been used in studies of genetic factors that regulate cell proliferation and differentiation in the developing eye (Richard & Hoch 2015).

As a control, heterozygotes of the *ey*Gal4 driver were assessed. These were initially compared to a random selection of heterozygote UAS-miRNA flies and white eyed mutant background flies, as a test of the control selection and area measurement approach. Importantly, the relatively small variations in eye size in the control flies showed no significant differences between groups, and were similar to those observed in previously published studies (Figure 5.2.1, Richard & Hoch 2015) .

From the 100 UAS-miRNA lines that were tested, only 22 demonstrated significant reductions in eye size when combined with *ey*Gal4 (Figure 5.2.1, c). Of these, some miRNAs which were previously linked to nervous system development were present. For example, the previously identified regulator of neuronal differentiation, miR-7 (Caygill & Brand 2017; Li & Carthew 2005), demonstrated a mean reduction in eye size of 39% (figure 5.2.1, d). The most severe reduction in eye size was that observed as a result of miR-79 expression, where on average the size of the eye was reduced by 65% (figure 5.2.1, d). The role of miR-79 in the nervous system has been previously studied in *C.elegans*, where it's role in the homeostasis of proteoglycans is shown to be crucial in the correct migration of neurons (Pedersen et al. 2013).

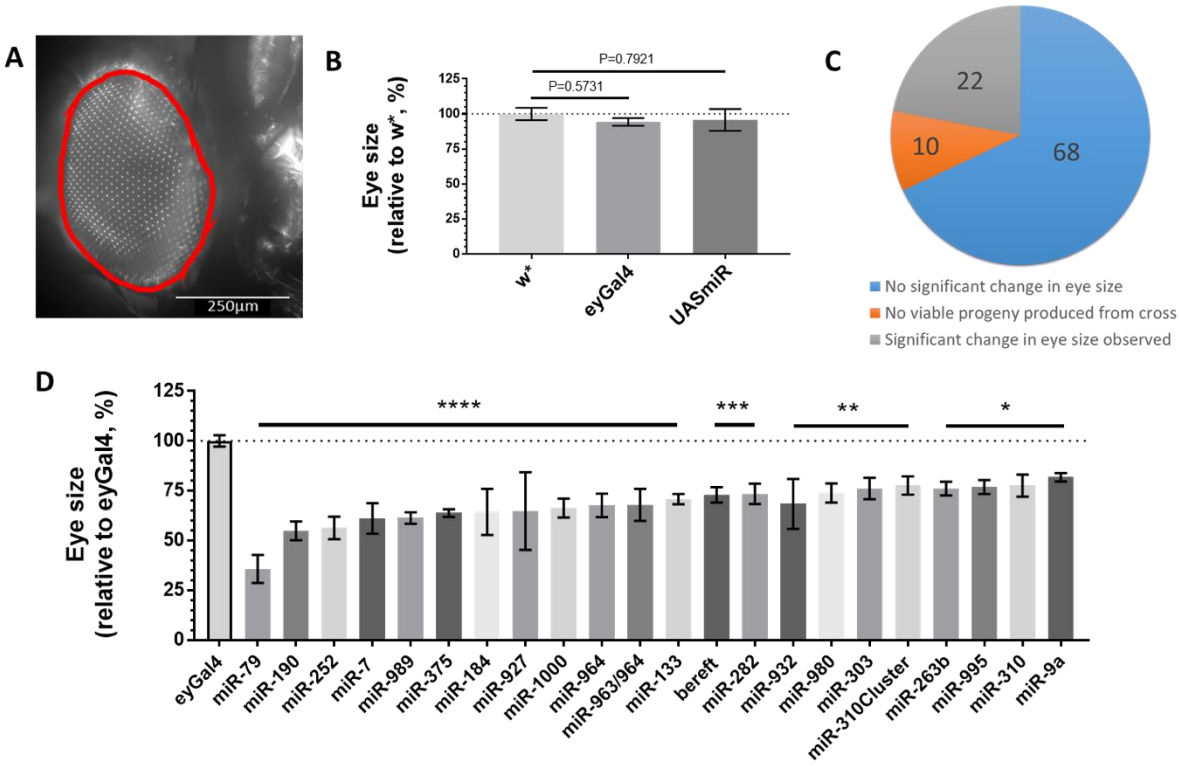


Figure 5.2.1 Overexpression of miRNA can produce defects in eye size
(a) Example image of a *Drosophila* eye with the eye boundary highlighted in red. **(b)** Control populations eye area comparison. No significance seen following one way ANOVA. **(c)** Pie chart to show the proportion of miRNA lines which demonstrated a significant change in eye size. **(d)** miRNA which produce significant changes in eye size are shown. Significance compared to *ey*GAl4 control population as determined by Dunnett's multiple comparisons following one way ANOVA. *(p≤.05) ** (p≤.01) *** (p≤.001) **** (p≤.0001). The number of images analysed for each genotype ranged from 8 to 15, with a median of 12. Error bars show mean +/- SEM.

Interestingly, miR-79 has been identified as a homologue to miR-9, but miR-9a produces a much smaller effect on the size of the eye (figure 5.2.1 c). The presence of miRNAs which have been previously identified to play a role in nervous system development within those which produced significant effects on eye size here, served to validate the experimental model as a relevant approach for the identification of miRNAs involved in nervous system development.

Despite examples of miRNAs with previously known neuronal function, some miRNAs seen here have not been previously investigated as to their role in the development of the nervous system. This included those with the most severe defects in eye size, such as miR-190 (figure 5.2.1).

The analysis of eye size can answer questions about the potential role of a miRNA in the differentiation or proliferation of cells within the developing *Drosophila* eye. We decided however to develop a separate readout in order to identify miRNAs which may have an alternative effect on eye and therefore nervous system development.

5.2.2 Defects in ommatidia patterning after overexpression of miRNA in the developing eye

The incorrect development of the *Drosophila* eye can also be determined visually from the disruption of the normally perfect patterning of the ommatidia centres (figure 5.1.3). The disruption of the lattice of ommatidia is referred to as a "rough eye" phenotype. This disruption can be caused by defects in the development of single cells of the ommatidia, or patterning of the ommatidia. This phenotype can be an indication of defects in the specification or arrangement of cells within the eye, including the photoreceptor neurons.

Whilst automated quantitative methods of the scoring of the eye have been previously developed, for example the flynotyper algorithm (Iyer et al. 2016), we devised a visual method of scoring the disruptions in ommatidia patterning (chapter 2.3.5, figure 5.2.2, a). This visual scoring of the images was found to be a less variable method here, as the flynotyper software did not produce consistent scores for control eyes, or representative scores for test experimental images, when tested. It is important to note that in this study the scoring of eyes was only conducted by one researcher to produce the data shown, however subsets of the images were independently scored to verify the scoring method and all image were scored blind (i.e. images were numbered so the genotype was not known at time of scoring).

The control genotypes (as with eye size in figure 5.2.1) were scored for ommatidia disruption, and demonstrated a consistent scoring of 0, with no variation (data not shown). This again validated the control selection, and the scoring method for the organisation of the ommatidia. After overexpression in the developing eye, 30 miRNAs produced a pattern of significantly disrupted ommatidia (fig. 5.2.2, b).

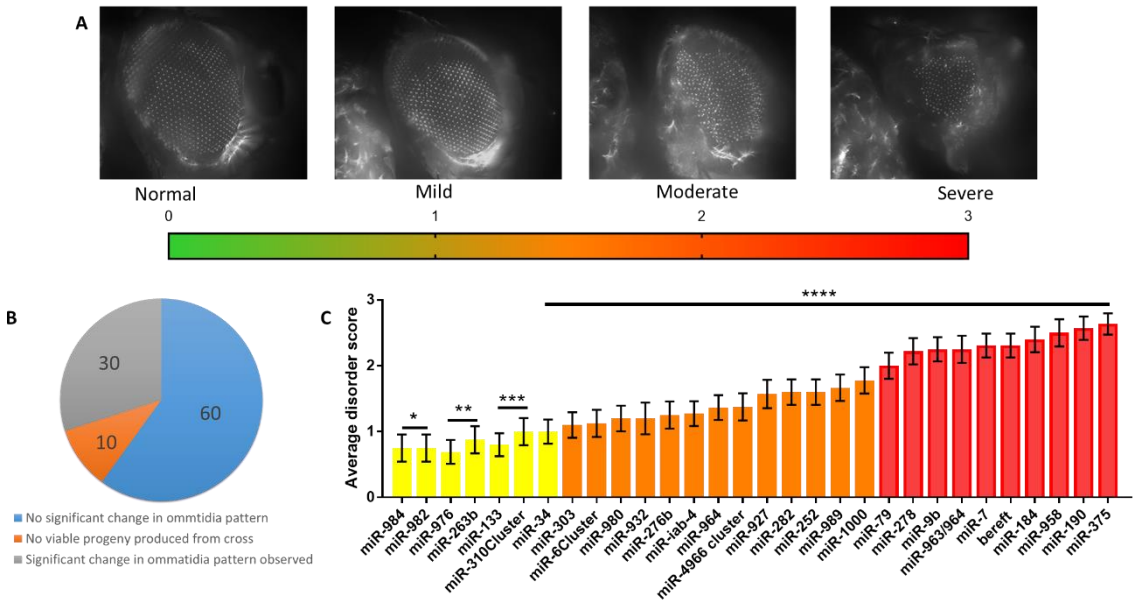


Figure 5.2.2 Overexpression of miRNA can produce defects in ommatidia patterning
(a) Example images of *Drosophila* eyes with indicated disorder scores. **(b)**Pie chart to show the proportion of miRNA which produced a significant effect on ommatidia pattern when overexpressed in the eye **(c)** miRNA which produce significant average disorder scores compared to eyGal4 alone. EyGal4 alone produced a consistent score of zero (not shown). Significance compared to eyGAl4 control population as determined by Dunnett's multiple comparisons following one way ANOVA. *(p≤.05) ** (p≤.01) *** (p≤.001) **** (p≤.0001). The number of images analysed for each genotype ranged from 8 to 15, with a median of 12. Error bars show mean +/- SEM.

As was shown for the eye size, some previously identified miRNAs involved in nervous system development were among those with significant effects. For example miR-79, as discussed previously, and one of its homologues, miR-9b, demonstrate similar and severe patterning disruption with mean scores of 2.25 and 2 respectively (figure 5.2.2, b). miR-9 has been previously identified as a miRNA involved in axon growth and branching during the development of the nervous system (Dajas-Bailador et al. 2012). This is interesting in contrast to the measurement of eye size, where miR-79 demonstrated a much more significant effect (figure 5.2.1, c). This indicates that the two scoring methods employed here are able to identify miRNAs which may be affecting different processes of nervous system development.

Again, as with eye size, the assessment of ommatidia patterning also identified miRNAs which have not been previously implicated in nervous system development,

with miR-190 again demonstrating severe pattern disruption with a mean score of 2.571 (figure 5.2.2, b).

From the data shown (figure 5.2.1-2), it was demonstrated that, through the overexpression of miRNAs in the developing *Drosophila* eye, specific miRNAs which are able to disrupt development can be found. From the assessment of eye size and ommatidia patterning of the *Drosophila* eye after overexpression of individual miRNAs, 19 candidate miRNAs showed statistically significant disruption using both analytical methods, with 3 miRNAs producing significant effects on size alone and 11 on the patterning of the eye only (figure 5.2.3). This observation rate of a phenotype as a result of miRNA expression demonstrates a higher level of success compared to similar screens (Schertel et al. 2012), which may be due to the more detailed quantitative assessment of phenotype used here. A large proportion (57%), of the

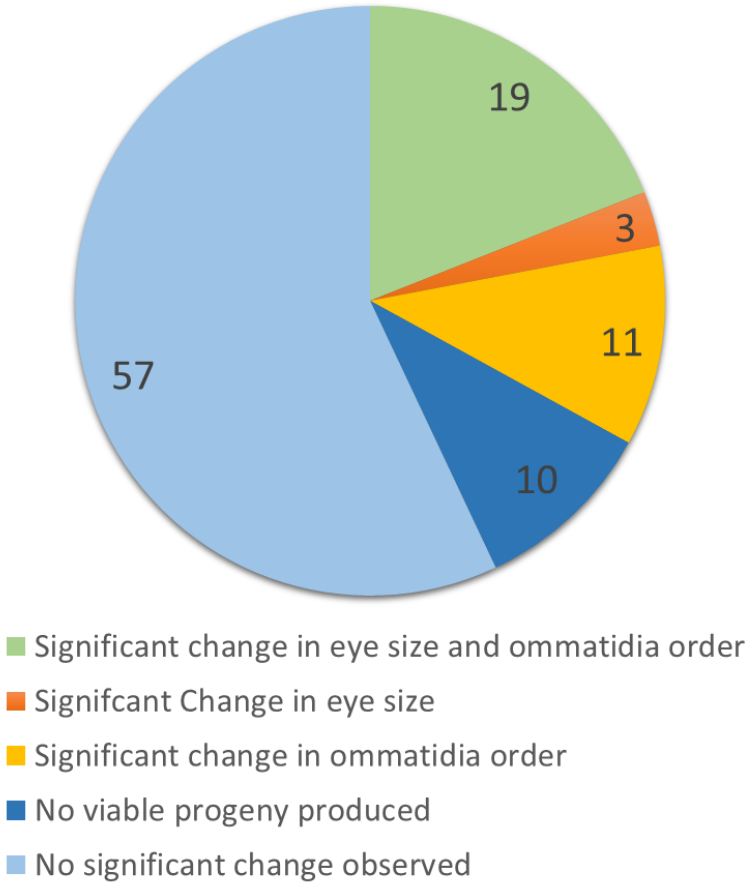


Figure 5.2.3 Summary of the miRNA overexpression screen in the developing eye
Summary of the frequency of the developmental defects assayed in the screen. Significant changes were observed as a result of overexpression of miRNA within the developing *Drosophila* eye.

UAS-miRNA lines studied did not produce any significant effect on the development of the eye (figure 5.2.3 a). This is promising in terms of the validity of the screening approach, as the results obtained are most likely a reflection of specific miRNA function, rather than the overwhelming of the miRNA-RISC complex system, or the non-specific detrimental effect of increased production of RNA in the developing eye.

Interestingly, although it has been previously observed that the eye structure is dispensable for the viability of adult *Drosophila* (hence the naming of the *eyeless* gene, from the phenotype induced from mutation), a lethal phenotype was observed as a result of overexpression of ten individual miRNAs (figure 5.2.3 a). The lethality is not an artefact of the use of the UAS resource described in Bejarano et al. (2012), as lethality as a result miRNA overexpression through a different UAS resource in the *ey* Gal4 driver pattern has also been previously observed (Schertel et al. 2012). *Ey* has been shown to be expressed within other centres of the nervous system in previous studies (Callaerts et al. 2001). Therefore, it could be possible that the lethality is a result of the miRNA expression in these centres, rather than within the eye. Another possibility is that the expressed miRNA may be secreted from the *ey*Gal4 expressing cells. For example, one of the miRNAs which produces a lethal effect, miR-92b, has shown presence in extracellular vesicles in previous studies of brain cancer samples (Bronisz et al. 2016). This would lead to the miRNA being able to be taken up, and exhibit an effect on, cells surrounding the *ey*Gal4 expressing cells (for instance the cells of the developing brain), which could lead to the observed lethality.

The majority of the miRNAs which showed a significant effect in eye development demonstrated changes in both size and patterning (5.2.3, a). This is to be expected, as the development of the eye is due to complex signalling networks which interconnect the processes of cell proliferation, pattern formation and cell type specification (Kumar 2009). There are a few exceptions to this however, mainly those which only significantly alter the patterning of the eye, and not the size. This could be due to the lower variability observed in the patterning control. This may also be due to the method used to score the disruption of the ommatidia, which, being a

discrete scale, as opposed to a continuous measurement (5.2.2, a), could allow for slight alterations to produce a larger effect on the overall average. This allows us to identify those miRNA which may be producing a mild effect due to overexpression.

This investigation utilised an overexpression approach to identify miRNAs for further study. Overexpression screens allow for the removal of some confounding factors, such as the possibility of effects of downregulation only being apparent within small subsets of cells; or the redundancy of a miRNA in the tissue being observed. Overexpression may however cause effects that are not relevant to the physiological levels of the miRNA, and the large concentration of the miRNA resulting from overexpression may cause its association with target transcripts that it would not interact with normally. Additionally, since this screen was not accompanied by data regarding the expression of miRNAs in the developing eye, miRNAs that are ectopically expressed in these regions, might be targeting transcripts that are not normally part of their regulatory system. For this reason, for most of the follow up studies that were carried out after the screen we decided to also use a stock resource of miRNA-sponge UAS lines, which allows for an inhibitory effect to be tested via the sequestering of a chosen miRNA within a specific tissue (Fulga et al. 2015).

5.2.3 Conservation of miRNA sequences

With the aim to identify miRNAs for further study in the development and function of the nervous system, those miRNAs which demonstrated a high level of conservation from *Drosophila* to human were desirable candidates. The previously described miRviewer tool was therefore used to assess the conservation of miRNA sequence from Drosophila to Human (Kiezun et al. 2012). This tool provides numerical scores for miRNA conservation, this score is based upon the similarity of the species specific miRNA sequence compared to a consensus sequence for the miRNA. The consensus sequence is based upon an average from all species which possess the miRNA in question. For example, if a miRNA has the exact same sequence in all species, then the conservation score will be 1 for all species. However, if one species had a miRNA sequence which only demonstrated 80%

homology to the consensus sequence, the conservation score returned would be 0.8 for that species. It is therefore possible to compare the conservation scores between the *Drosophila* and human miRNAs to provide an indication of the sequence conservation between them. A ratio of the human to *Drosophila* conservation scores was therefore created as a measure of sequence conservation. These ratios are shown for all miRNA which produced a significant change in eye size or pattern when overexpressed in the developing eye, and those miRNA which caused lethality when overexpressed in the developing eye (figure 5.2.4).

miRNA	mean eye size (% of control)	p value	mean ommatidia order score	p value	miRviewer conservation ratio		
					Hsa score	Dme score	Ratio
bereft	72.92	***	2.31	****	na		na
miR-1000	66.32	****	1.78	****	0	1	∞
miR-133	70.79	****	0.80	***	1	0.78	0.78
miR-184	64.37	****	2.40	****	0.99	0.64	0.65
miR-190	54.81	****	2.57	****	1	0.74	0.74
miR-252	56.33	****	1.60	****	0	1	∞
miR-263b	76.07	*	0.88	**	0	1	∞
miR-276b	90.74	na	1.25	****	0	1	∞
miR-278	88.98	na	2.22	****	0	1	∞
miR-282	73.41	***	1.60	****	0	1	∞
miR-303	76.15	**	1.10	****	0	1	∞
miR-310	77.63	**	0.33	na	0	1	∞
miR-310Cluster	77.7	*	1.00	***	0	1	∞
miR-34	116.8	na	1.00	****	1	0.65	0.65
miR-375	63.78	****	2.64	****	1	0.53	0.53
miR-4966 cluster	80.68	na	1.38	****	na		na
miR-6Cluster	94.73	na	1.13	****	0	1	∞
miR-7	61.04	****	2.31	****	1	0.73	0.73
miR-79	35.67	****	2.00	****	0.95	0.77	0.81
miR-927	64.78	****	1.57	****	0	1	∞
miR-932	68.35	**	1.20	****	0	1	∞
miR-958	92.26	na	2.50	****	0	1	∞
miR-963/964	67.9	****	2.25	****	0	1	∞
miR-964	67.67	****	1.36	****	0	1	∞
miR-976	87.92	na	0.69	**	0	1	∞
miR-980	73.87	**	1.20	****	0	1	∞
miR-982	85.9	na	0.75	*	0	1	∞
miR-984	81.55	na	0.75	*	0	1	∞
miR-989	61.27	****	1.67	****	0	1	∞
miR-9b	85.93	na	2.25	****	0	0.73	∞
miR-iab-4	84.79	na	1.27	****	na		na
miR-995	76.88	*	0.25	na	0	1	∞
miR-9a	81.79	*	0.05	na	1	0.74	0.74

miRNA	miRviewer conservation ratio		
	Hsa score	Dme score	Ratio
miR-1	1	0.66	0.66
miR-1012	0	1	∞
miR-124	1	0.86	0.86
miR-274	0	1	∞
miR-318	0	1	∞
miR-8	0	1	∞
miR-92b	1	0.55	0.55
miR-986	0	1	∞
miR-993	0	1	∞
miR-9cCluster	0	1	∞

Figure 5.2.4 Conservation of miRNA sequences of those miRNA which produced a significant result in the *Drosophila* eye screen.

(a) miRNA which produced significant effects on either size or ommatidia disorder. **(b)** miRNA which resulted in reduced viability of the progeny.

For each miRNA the corresponding results of overexpression on the size and ommatidia order of the Drosophila eye are shown (not applicable to (b)) *($p \leq 0.05$) ** ($p \leq 0.01$) *** ($p \leq 0.001$) **** ($p \leq 0.0001$) as determined by Dunnett's multiple comparisons following one way ANOVA.

The miRNAs miRviewer conservation scores for human (hsa) and Drosophila (dme) are also shown. Conservation is represented in (a) and (b) as a ratio of the Human (Hsa) to *Drosophila* (Dme) miRviewer scores.

Of the candidates which produced an effect within the eye, 11 of them are predicted to be conserved between *Drosophila* and human based on sequence similarity by miRviewer (figure 5.2.3 b, c). These are miR- 124, 79, 133, 190, 9a, 7, 1, 34, 184, 92b, and 375, in order of conservation ratio (figure 5.2.3, figure 5.2.4). However, this does not necessarily indicate that the targets of these miRNAs are also conserved, and further investigation of this is required to determine the conservation of the miRNA regulatory processes. As previously discussed however (Chapter 5.1.9), the lack of sequence conservation of a miRNA does not necessarily preclude the potential for further investigation. The 11 candidates which were predicted to be conserved between *Drosophila* and human are summarised in graph form in figure 5.2.5, with their associated results from overexpression in the eye size and ommatidia disorder assessments.

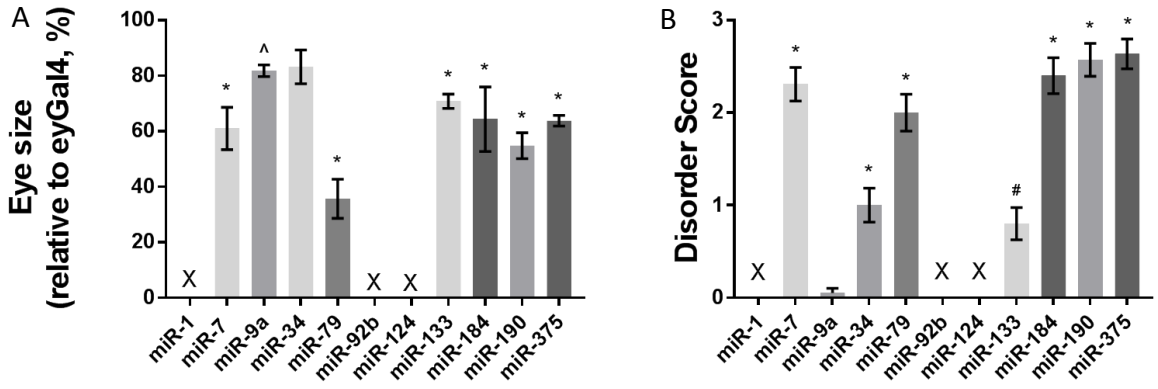


Figure 5.2.5 Summarisation of conserved miRNA results from the eye screen
Eye size **(a)** and disorder **(b)** scores of miRNAs conserved from *Drosophila* to human from miRviewer comparison. Those which did not produce viable progeny to score eye phenotypes from, are marked with an X in absence of data. (*)P≤0.0001, (#) p≤0.001, (^) p≤0.05. Error bars show mean +/- SEM. Data presented is a repetition of that shown in figures 5.2.1-3.

5.3 Conclusions and future directions

Results presented in this chapter demonstrate that overexpression of individual miRNAs within the developing *Drosophila* eye can lead to developmental defects observable through the assessment of the size and patterning of the external eye structures. The results also provide detailed assessment of the phenotypic effects of individual miRNAs overexpression which can be accessed for future investigation.

The future use of the data obtained from this screen depends on the needs of the researcher. As previously discussed, the *Drosophila* eye is a model of developmental regulation applicable across many systems, from cancer progression to the nervous system. In the context of this thesis, the identified candidate miRNA will be carried forward into tests on their role in nervous system processes, however future work could use these results in multiple developmental or disease process investigations.

The expression of 100 separate UAS-miRNA lines within the *Drosophila* compound eye has produced a useful data set of miRNAs that could have an effect on nervous system developmental processes (Figure 5.2.1-3). Of those which produced an effect on the eye, 11 demonstrate sequence conservation from *Drosophila* to Human: miR-124, 79, 133, 190, 9a, 7, 1, 34, 184, 92b and 375, and it was from these a candidate miRNA for further investigation here was to be selected (Figure 5.2.3-4).

Chapter 6. Investigation of miR-190 in nervous system development

6.1 Introduction

Following the identification of those well conserved miRNAs which produced a significant effect in the initial *Drosophila* eye screen (Chapter 5), miR-190 was chosen for further investigations into its role in the nervous system. To arrive at this conclusion, findings of the study in the *Drosophila* eye were complemented with a systematic assessment of published literature. This assessment included the identification of validated mRNA targets, expression patterns, and functional studies.

6.1.1 miR-190 conservation

First identified in mouse (Lagos-Quintana et al. 2003), and later in human and *Drosophila* studies (Landgraf et al. 2007; J. Graham Ruby et al. 2007), miR-190 is a conserved miRNA that shows high sequence homology across species, with the predominant mature miRNA being produced from the 5' end of the stem loop (figure 6.1.1 a, Kiezun et al. 2012). Despite this conservation from *Drosophila* to human, miR-190 has not however been shown to be present in *C.elegans*, which instead expresses a similar family member miR-50 (J. Graham Ruby et al. 2007).

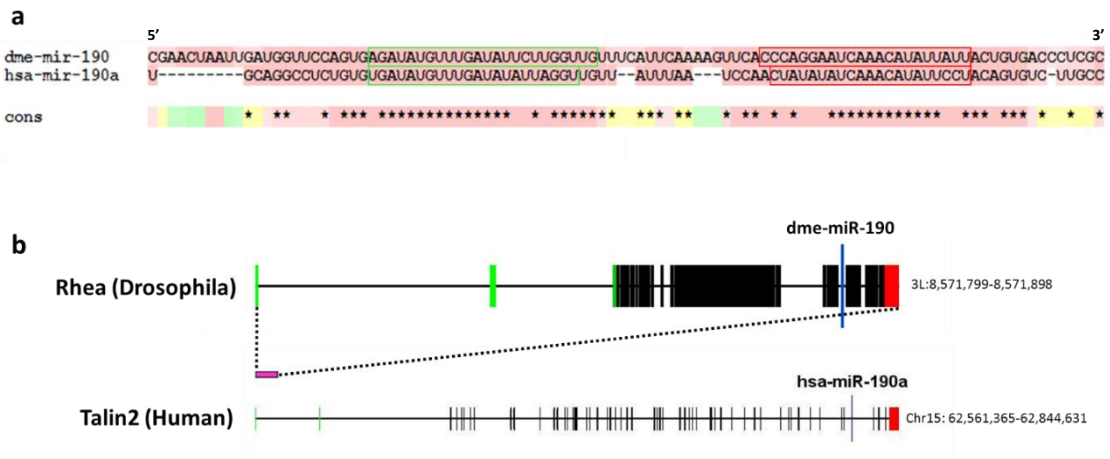


Figure 6.1.1 Sequence conservation of miR-190 from *Drosophila* to human
(a) T-Coffee alignment of pre-miR-190 sequences from *Drosophila* and human. Asterisks below indicate conserved residues. High sequence conservation is observed in the respective 5' (green box) and 3' (red box) miRNA sequences. **(b)** Schematic of locations of miR-190 genes. In *Drosophila* miR-190 resides within an intron of the Rhea locus, the homologue to mammalian talins. In Human, miR-190 resides within an intron of Talin2. Pink box indicates scale of *Drosophila* locus compared to human. Green bands indicate the 5'UTR of the gene and Red bands indicate the 3'UTR of the gene.

In mammals, miR-190a resides within an intron of Talin2, and this localisation is also observed in *Drosophila*, within the intronic region of the talin homologue gene locus, Rhea (6.1.1 b). In mammals, it has been shown that miR-190 levels are linked to the levels of transcription of its host gene (Zheng , et al. 2010c).

6.1.2 Identified functions of miR-190

Unlike some miRNAs, research into the function of miR-190 has been limited, with findings suggesting a role for miR-190 in the progression of cancers (Yu et al. 2018; Beezhold et al. 2011; Almog et al. 2013), angiogenesis (Hao et al. 2014; De Lella Ezcurra et al. 2016) and opioid tolerance (Zheng, et al. 2010a; Zheng, et al. 2010b).

Much of the work so far has been focused the expression profile and role of miR-190 in cancers. This is particularly relevant to studies in the development and function of the nervous system, as many gene regulatory networks and mechanistic processes are common among nervous system processes and cancers. This includes processes such as: the cytoskeletal dynamics of cancer cell metastasis and neuronal motility (Heine et al. 2015); the ability of cancer and neuronal cells to adapt to their localised microenvironment (Maguire et al. 2015); and the cellular responses of cancer and neuronal cells to guidance cues (Duman-Scheel 2009).

In the case of miR-190, it has been shown to be downregulated in breast cancers, and to target SMAD2 (Yu et al. 2018). SMAD2 is a positive regulator of the epithelial to mesenchymal transition, which, in the context of cancer, means that miR-190 downregulation can promote metastasis (Yu et al. 2018). SMAD2 has also been shown to be involved in nervous system development, mice which have a conditional knockout of SMAD2 in the central nervous system demonstrate with developmental and behavioural abnormalities (Wang et al. 2011).

Arsenic exposure is associated with increased occurrence of lung cancers. miR-190 has been shown to be upregulated upon application of arsenic, in conjunction with its host gene, Talin2 (Beezhold et al. 2011). This leads to downregulation of the miR-190 direct target PHLPP, activating Akt signalling (Beezhold et al. 2011). Again, Akt

signalling is a pathway which is implicated in nervous system processes, and dysregulation of Akt signalling is the root of many neurodevelopmental disorders (Wang et al. 2017). The miR-190 target identified, PHLPP, is abundant in developing and mature hippocampal neurons (Jackson et al. 2010).

Increased levels of miR-190 have also been associated with tumour dormancy in otherwise fast-growing glioblastomas and osteosarcomas (Almog et al. 2013), with subsequent studies suggesting that miR-190 may limit the progression of tumours generated in mice from a human colon cancer cell line through miR-190 targeting of angiogenic factors (Hao et al. 2014). This study found that miR-190 can supress angiogenesis in *in vivo* models of ischaemia and tumour angiogenesis, with miR-190 inhibitors promoting the formation of blood vessels in these models (Hao et al. 2014). They also identified a group of angiogenic genes which were targets of miR-190 which centre around the VEGF pathway (Hao et al. 2014). This study of miR-190 in angiogenesis may also have implications in the role of miR-190 in the nervous system, as VEGF is a key mediator of nervous system processes, both through the regulation of blood vessel formation in the nervous system, and direct roles in nervous system cells (Rosenstein et al. 2010).

In *Drosophila*, miR-190 overexpression promotes the formation of tracheal branches in response to hypoxia (De Lella Ezcurra et al. 2016). This demonstrates a possible conserved function in hypoxia as in tumour angiogenesis, however this action is through a non-conserved target mRNA, the hypoxia-inducible factor suppressor Fatigia (De Lella Ezcurra et al. 2016). Again, as with angiogenesis factors acting within the mammalian nervous system, it has been shown that there are parallel functions for *Drosophila* tracheal development factors in the developing nervous system (Long et al. 2014). No direct associations for the miR-190 target identified, Fatiga, to nervous system development have been demonstrated however.

One interesting set of papers which regard miR-190 directly in the context of the nervous system are those which focus on its role in opioid tolerance. Rat hippocampal cultures treated with fentanyl show a reduced level of miR-190, and

this reduction leads to a subsequent increase in levels of one of the identified miR-190 targets, NeuroD (Zheng2010b). This pathway has been shown to be important in the maintenance of dendritic spines, where artificially increasing levels of miR-190, and therefore reducing NeuroD, can lead to reduction in spine density and volume (Zheng, et al. 2010a). This indicates a possible role for miR-190 within the nervous system, however these targets are not conserved in *Drosophila* and similar mechanisms have not been suggested.

6.1.3 Identified target genes of miR-190

From the literature, a number of targets have been found for miR-190 across multiple organisms (table 6.1.1). Although these could be applied to nervous system processes as previously discussed, none of the targets which have been previously identified in mammals are predicted to be conserved to *Drosophila*.

Identified target(s)	Species	Reference
SMAD2	Human	(Yu et al. 2018)
FOXP2	Human	(Jia et al. 2016)
Fatiga	*Drosophila*	(De Lella Ezcurra et al. 2016)
TP53INP1	Human	(Cramer et al. 2014)
TCF4, Smad2, Smad4, IGF1, HGF, K-Ras, JAK2, VEGF	Human	(Hao et al. 2014)
IGF-1 (190b)	Human	(Hung et al. 2014)
Kcnq5	Human	(Li et al. 2014)
PHLPP1	Mouse	(Yu et al. 2014)
NeuroD	Rat	(Zheng, Zeng, Zhang, et al. 2010)

Table 6.1.1 Summary of targets previously identified for miR-190 validated through luciferase assay
Previously identified targets for miR-190 which have been validated through luciferase assay are shown. Host species and references are indicated. All mammalian targets shown are targeted by miR-190a, except for IGF-1 which is a target for miR-190b.

Even if the 3'UTR targeting of miR-190 is not conserved, it is however important to consider the conservation of pathway targeting. For example, the suggested roles for miR-190 in mammalian angiogenesis and *Drosophila* tracheal development previously discussed.

6.1.4 Expression pattern of miR-190

The first indication of the expression pattern of miR-190 in *Drosophila* was displayed in the first paper which identified miR-190 in *Drosophila* (J. Graham Ruby et al. 2007). In this study, they utilised computational methods to identify novel miRNAs within the *Drosophila* genome, followed by RNA sequencing of the miRNAs at different developmental stages and tissues (J. Graham Ruby et al. 2007). They demonstrated the existence of miR-190, and observed enhanced levels of miR-190 expression within imaginal discs, adult heads, and late stage embryos (J. Graham Ruby et al. 2007). This suggests an expression of miR-190 within structures of the nervous system, as the adult head is composed mainly of the neural structures of the brain, antenna and eye, and the nervous system becomes more developed in late stage embryos (figure 5.1.1, a).

There are no indications however of the cellular expression pattern of miR-190 in the developing tissue of the fly embryo, as one of the last studies to tackle miRNA expression patterns in *Drosophila* embryos (Aboobaker et al. 2005) was published before the identification of miR-190 in 2007 (J. Graham Ruby et al. 2007). It has however been shown previously that knockout of the miR-190 gene in *Drosophila* is larval lethal (Chen et al. 2014). This would suggest significant expression, and a role of miR-190, in structures vital to development such as the nervous system.

One interesting paper which may be linked to miR-190 expression previously demonstrated differential expression of the RNA and protein products of the miR-190 host gene during *Drosophila* embryogenesis (Brown et al. 2002). It was shown that *in situ* hybridisation for the mRNA reveals strong expression in the region of the ventral nerve cord, however, antibodies for the Rhea protein do not indicate protein expression in this region (Brown et al. 2002). This indicates a possible requirement

for the RNA products of the Rhea locus, including miR-190, in the ventral nerve cord of the developing nervous system.

Whilst there are currently no direct indications of miR-190 expression patterns in developing mammalian models, the altered expression of miR-190 in nervous system disorders/trauma has been indicated in previous papers. In a model of traumatic brain injury in the mouse, miR-190 was shown as one of the most downregulated miRNAs following injury (Meissner et al. 2016). In qRT-PCR analysis of miRNA levels in Alzheimer's disease patient brains, miR-190 was shown to be upregulated in the hippocampal and cerebellar regions (Cogswell et al. 2008). This may suggest a role for miR-190 in the injury response, or degenerative nervous system processes, whilst also indicating a presence of miR-190 within the mammalian nervous system.

6.1.5 Experimental aims

The initial screen of miRNAs in *Drosophila* eye development highlighted miR-190 as a promising candidate for further exploration. There are early indications in the existing literature of a role of miR-190 in the nervous system. However, its function and expression pattern during embryonic development in *Drosophila* is not fully elucidated, along with the effects of alterations to miR-190 levels on nervous system development. A conserved role for miR-190 in the nervous system has also not been made clear.

In order to characterise the involvement of miR-190 in the development of the nervous system we undertook the following:

- Determine the expression pattern of miR-190 throughout *Drosophila* embryonic development.
- Observe the effect on development of miR-190 expression changes in the nervous system.
- Establish if there may be a conserved effect of miR-190 between *Drosophila* and mammalian neurodevelopment.

- Identify if there may be conserved targets or target pathways which could mediate any functional effects observed in *Drosophila* and mammalian nervous system development.

6.2 Results and discussion

6.2.1 smiFISH of miR-190 in *Drosophila* embryos

As described in the previous section, miR-190 emerged as an interesting candidate from an overexpression screen in the *Drosophila* eye. Whilst this is a useful approach through which to identify possible modulators of biological processes, the expression pattern of miR-190 within developing *Drosophila* is not currently described. In order to investigate this, a modified fluorescent *in situ* protocol was utilised to observe the expression of miR-190 within the *Drosophila* embryo. Small molecule inexpensive fluorescent in situ hybridisation (smiFISH), allows the visualisation of the expression of a target RNA in a tissue. This is achieved through the hybridisation of target RNAs with sequence specific probes and a secondary fluorescently flagged probe to allow imaging through microscopy (Tsanov et al. 2016). The probes used here are designed to target the primary-miRNA sequence, as this is the longest form of the miRNA transcript before cleavage (figure 1.3). This allows for a stronger signal to be created, as a larger number of probes can hybridise to a longer sequence, however, this does limit the analysis to the nuclear regions, and does not give a clear picture of sub-cellular localisation of the mature miRNA.

As the probes for miR-190 were purposefully designed for this project in collaboration with the Ronshaugen lab in Manchester (Chapter 2.4.2), it was important to validate their specific binding capacity based upon the probe sequence. In order to show this, the same embryos were probed for miR-190 and miR-184 in parallel. Importantly, the probes for miR-184 did not show any overlapping pattern of expression with the probes designed for miR-190, suggesting that the miR-190 probes are specifically hybridising with their target sequence (figure 6.2.1). In addition to this, embryos were probed simultaneously for miR-79 and miR-375 in separate *Drosophila* embryos, and these also did not demonstrate a pattern similar to that seen with miR-190 probes (data not shown). This provided us with sufficient evidence that the probes for miR-190 were specifically hybridising with their target sequence, and the patterning observed was not due to non-specific binding of the probes.

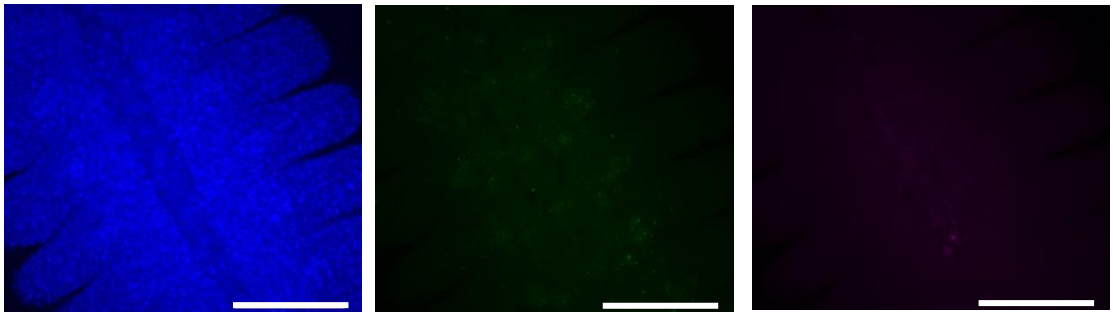


Figure 6.2.1 Confirmation of specific hybridisation of miR-190 probes
Drosophila embryos were simultaneously probed for miR-190 (green) and miR-184 (magenta). The probes did not demonstrate similar patterns of hybridisation. DAPI staining (Blue) is shown for the context of the whole embryo. Maximum intensity projections of confocal z-stacks of *Drosophila* embryo are shown. Scale bars 50µm.

Following the confirmation that the designed probes were not hybridising in a non-specific manner, the expression profile of miR-190 pri-miRNA in the *Drosophila* embryos was investigated (figure 6.2.2).

In early embryos, (defined here as encompassing the blastoderm to gastrulation stages), no expression of miR-190 could be observed through smiFISH (figure 6.2.2, a). Upon completion of gastrulation, miR-190 expression becomes apparent on the ventral side of the embryo. An image of the ventral side of the embryo around stage 8 is shown (figure 6.2.2 b), once gastrulation has completed, where fluorescent spots are visible in individual cells indicating pri-miR-190 expression. This pattern of expression correlates with previous observations of miR-190 abundance within the *Drosophila* embryo (J. Graham Ruby et al. 2007), where expression was seen to be increased in later stages of development. The expression of pri-miR-190 continues across the ventral portion of the embryo until later stages of development, where patterning of the expression can be observed on the ventral side of the embryo (figure 6.2.2, c).

An image of the ventral side of an embryo of around stage 16 is shown (figure 6.2.2 c), where the germband has fully retracted. The pri-miR-190 expression pattern corresponds to wide bands of expression across the segments of the embryo, which centre on the approximate region of the ventral nerve cord. This expression pattern also correlates with previous observations of the expression of Rhea (Talin), the miR-190 host locus mRNA, (Brown et al. 2002). Interestingly, this later study shows that

while Rhea mRNA expression is detected within the developing nervous system, there is no expression of protein. This suggests a role for the rhea mRNA alone in the nervous system, which may directly linked to the required processing of miR-190 (Brown et al. 2002).

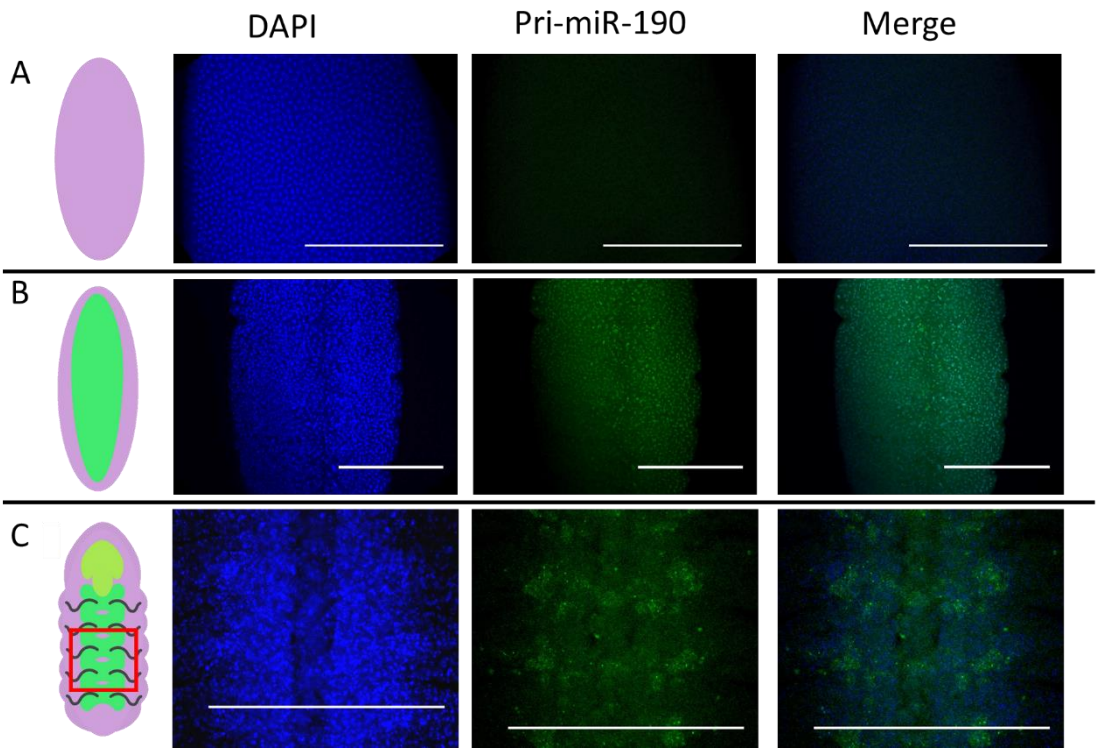


Figure 6.2.2 smiFISH of miR-190 in *Drosophila* embryos
Expression of miR-190 within *Drosophila* embryos of differing stages, approximate stages are indicated in diagrams to the left. All views are of the ventral portion of the embryos. DAPI stain for cell nuclei is shown in blue to the left, and miR-190 smiFISH in green in the central panels, merged images are to the right. **(a)** Representative images of an early stage embryo, no regions of miR-190 expression were observed. **(b)** Representative images of the ventral portion of an embryo of around stage 8, bright puncta can be observed in these ventral cells indicating miR-190 expression. **(c)** Representative images of the ventral portion of an embryo of around stage 13. Regions of miR-190 expression can be seen in an ordered segmental pattern. Red box indicates approximate area shown in image. Scale bars: 100µm

In figure 5.1.2 some example embryonic nervous system markers were shown for context. BP102, which strongly stains for the axons of the CNS, and demonstrates the repetitive segmented structure of the *Drosophila* CNS; and Repo, which stains the nuclei of all glia (except midline glia) which indicates the spread of nervous system cells across the ventral portion of the embryo. Whilst the images of miR-190 expression shown may indicate a presence of miR-190 in cells of the nervous system,

future co-staining with nervous system markers such as BP102 or Repo would give a better indication of the exact expression of miR-190. This includes the possible confirmation of expression in the nervous system, along with identification of the cell types miR-190 is expressed within.

The data here does however indicate that pri-miR-190 is expressed within or around the regions of the developing embryonic nervous system, which suggests a role of miR-190 in the development and function of the nervous system.

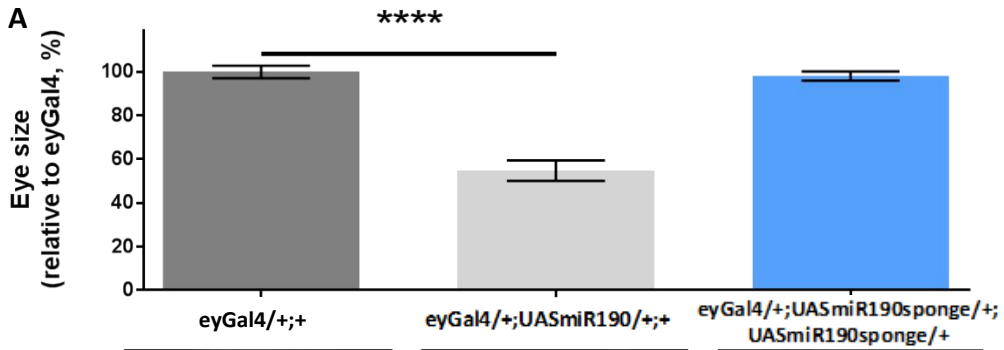
6.2.2 Modulation of miR-190 effect on *Drosophila* development

Following the observations of the effect of miR-190 overexpression in the developing *Drosophila* eye, and the expression pattern detected in the embryo, it was decided to carry out further tests to investigate the possible role of miR-190 in the overall development of the nervous system. For this, miR-190 was again over-expressed and inhibited within the developing eye, and throughout the developing nervous system. In order to overexpress miR-190, the previously described UAS-miR190 constructs were utilised (Bejarano et al. 2012). Inhibition of miR-190 was carried out through the use of a genetically encoded sponge construct under the control of UAS (Fulga et al. 2015). As a control for the inhibition of miR-190 with the sponge construct, an RNA of equal length, with a scrambled sequence not complementary to any known miRNA, can be used (Fulga et al. 2015).

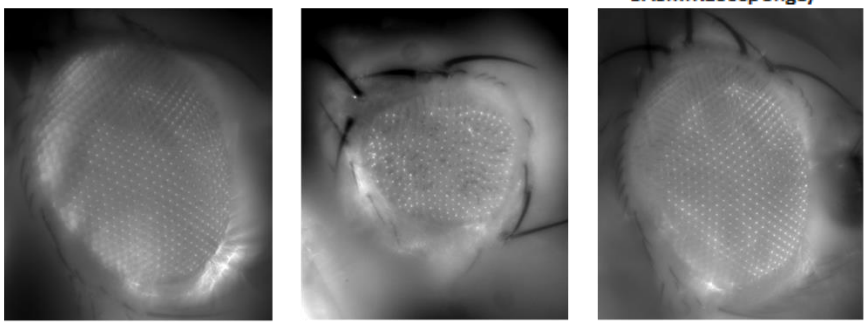
The Gal4 driver used here to express the UAS constructs throughout the developing neurons is Embryonic lethal, abnormal vision (ElaV). This has been reported to drive expression in post-mitotic neurons after stage 12 of embryonic development, and is widely used as a post-mitotic neuron marker (Robinow & White 1991). Some more recent studies have observed expression of elaV in earlier stages of development, including transient expression of elaV in embryonic glia and neuroblasts (Berger et al. 2007). Loss of ElaV does not however cause any observed effects in glial number or patterning, suggesting the expression within non-neuronal cells is not of significance (Berger et al. 2007).

As in the experiments presented previously (Chapter 5.2) overexpression of miR-190 through eyGal4 driven expression of a UAS-miR-190 construct caused significant disruption to eye development. Overexpression of miR-190 with the ElaV Gal4 driver caused an extreme effect on the viability of *Drosophila*, with no hatched feeding larvae being observed (figure 6.2.3, c). This is in concurrence with the effect observed within the *Drosophila* eye, where over expression of miR-190 is detrimental to eye development. This effect could be due to differentiation or cell death defects caused by the overexpression of miR-190, or severe abnormalities of the later development of the neurons in processes such as axon growth.

Inhibition of miR-190 in *ey*Gal4 pattern did not however lead to any observed disruption in the development of the external eye structures (Figure 6.2.3 a, b). In addition to this, no effect on the viability of developing *Drosophila* was observed with the inhibition of miR-190 throughout the neurons of the developing nervous system (table 6.2.3, c). Additional preliminary investigations of the effect of inhibition of miR-190 on the development of the glutamatergic motor neurons of *Drosophila* larvae were also carried out, and did not indicate any gross abnormalities in development or function due to this (Appendix VI). This indicates that the previous observations of larval lethality as a result of miR-190 knockout (Chen et al. 2014), may not be due to miR-190 expression being required within neurons. This does not preclude the role of miR-190 in finer aspects of neuron development however, which may not be elucidated through the methods used here.



B



C

Gal 4 line	UAS	Larvae Feeding?	Pupation rate (%)	Emerging adult rate (%)		
				Total	Male	Female
elaV	None	✓	92	96	51	49
	miR-190	×	-	-	-	-
	Scramble sponge	✓	91	97	57	43
	miR-190 sponge	✓	94	92	58	42

Figure 6.2.3 Developmental effects due to miR-190 level modulation in the nervous system
(a) miR-190 was either overexpressed (UASmiR190) or downregulated (miR190sponge) in the *Drosophila* eye, and the effects on eye size were recorded. There is a significant reduction in eye size when miR-190 is overexpressed **** P< 0.0001 as calculated by Dunnett's multiple comparisons following one way ANOVA. n>10 for all genotypes **(b)** Representative images of the eyes of indicated genotypes **(c)**Indicated UAS lines were crossed with elaVGal4 to drive expression of constructs throughout the nervous system. Progeny from crosses were then monitored to observe presence of larvae feeding, rate of pupation, and rate of emerging adults and ratio of emerging adult genders. All results are shown as an average of three separate crosses and progeny collections. n=150 larvae collected per genotype

These results indicated that miR-190 overexpression is detrimental to the development of the nervous system in *Drosophila*. Whereas the endogenous role of miR-190 in the nervous system appears to be more subtle during development. In order to determine if the effect observed here is conserved from *Drosophila* to mammalian models, the effect of miR-190 modulation on a model of mammalian nervous system development was investigated.

6.2.3 Effect of miR-190 modulation on murine cortical cultures

Mammalian models do not lend themselves easily to assessment of whole animal viability with targeted gene modulation as previously used in *Drosophila* (figure 6.2.3 c), therefore a different approach was used to investigate the possible conserved function of miR-190 in mammalian neuron development. A classical model of mammalian neuron development is the culture of rodent cortical neurons (Dotti et al. 1988; Takano et al. 2015), and this is used here.

Embryonic murine cortical neurons were cultured *in vitro*, and transfected with the appropriate constructs to either overexpress, or inhibit, miR-190 action in the cells. This was achieved through transfection with modified oligonucleotides (Chapter 1.10). Transfections of miR-190 mimic, inhibitor, or appropriate controls, were carried out alongside a GFP plasmid, to allow identification and morphological assessment of transfected neurons.

Two measurements of neuron development were used to assess the cultures following transfection. Firstly, the length of axons which had developed was measured, to provide us with an indication of appropriate neuron morphology development; secondly, the number of neurons which successfully survived forty-eight hours following transfection was observed.

Inhibition of miR-190 in the cortical cultures did not produce any significant effects on the axon growth, or viability of neurons within the cultures (figure 6.2.4 a, c). The mean number of surviving neurons shows a high level of variability in these cultures, and the result is not statistically significant despite an average reduction in mean neuron survival percentage to 78% of control. This suggests that further repeats may be required, or an alternative measure of neuron viability should be implemented in order to determine the effect of miR-190 inhibition on neuron survival in these cultures. These results however do correlate with those observed in *Drosophila*, as any significant abnormalities in neuron development through inhibition of miR-190 were not expected.

There was a significant increase of axon length observed when miR-190-5p mimic was transfected into the cortical neurons, and increase of on average 14% compared to the mimic control (Figure 6.2.4 b). This increase could suggest disrupted control of axon pathfinding and extension, leading to overgrowth of the axon. A significant decrease in the number of surviving neurons in cultures where miR-190-5p is overexpressed was also observed, with levels falling to 73% of the levels observed in the control (figure 6.2.4 d). This suggests that the effects observed here correlate with those observed in the *Drosophila* eye and viability tests (Figure 6.2.3), as the observed effects in *Drosophila* may be due to large abnormalities in axon extension and pathfinding, or due to cell death occurring in the miR-190 overexpressing neurons.

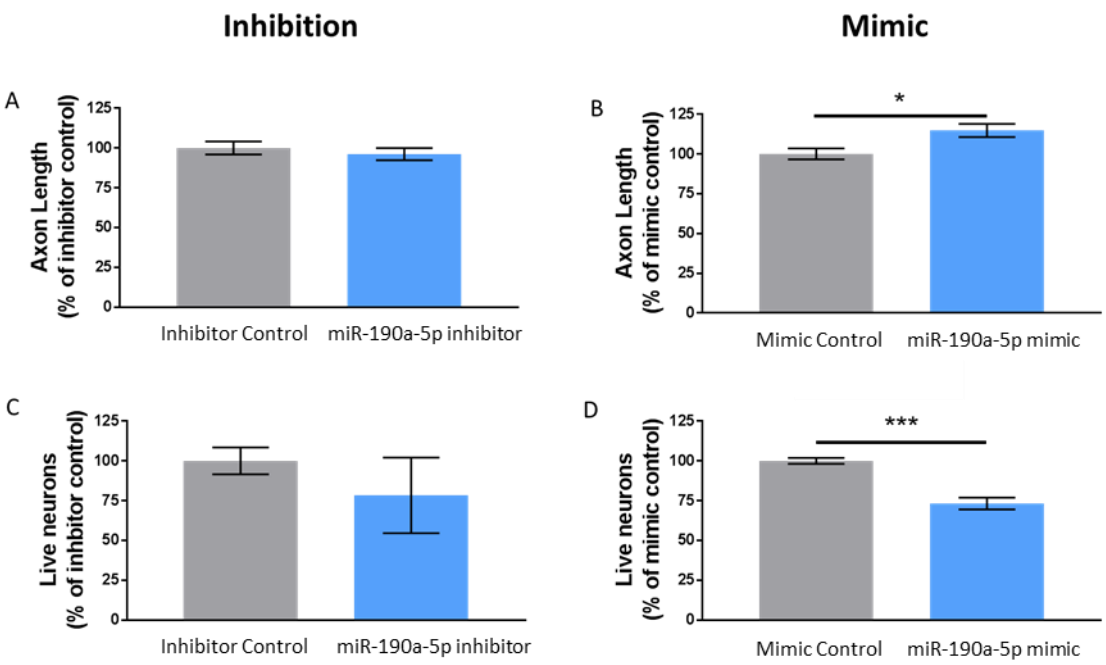


Figure 6.2.4 Effect of miR-190 mimic and inhibitor in mouse cortical cultures
Mouse cortical cultures were transfected with a miR-190a-5p inhibitor **(A, C)** or mimic **(B, D)** 24 hours after plating. 48 hours following transfection, cultures were fixed and assessed for the length of axons **(A, B)** and live neurons proportional to dead cells **(C, D).** No significant changes were observed in the axon length **(a)** or viability of cultures **(c)** between the non-targeting inhibitor and miR-190 inhibitor. When miR-190a-5p mimic is applied to the cultures, a significant increase in axon length is observed **(b)**, and a significant decrease of the proportion of live neurons **(d)**. *P<0.05, ***P<0.001 as determined by students t test. Error bars show mean +/- SEM. Data shown is as a result of three separate biological repetitions of all experiments.

From these results (Figure 6.2.3, 6.2.4) it can be concluded that overexpression of miR-190 appears to be having a negative effect on the development of neurons in *Drosophila* and *in vitro* mammalian cells. In order to determine if miR-190-5p may be acting upon the same pathways in the context of the nervous system in *Drosophila* and mouse, the predicted targets of miR-190-5p which may explain the effects seen here were identified.

6.2.4 Identification of conserved miR-190 targets

In order to identify conserved targets of miR-190 between *Drosophila* and mammals a bioinformatics approach was utilised, similar to that in 3.2.3. The availability of target prediction tools for *Drosophila* miRNA is less than that of mammalian systems, and the miRgate curated database tool is thus not usable as in 3.2.3. Instead, the miRanda target prediction database was used. miRanda is equipped with an algorithm that models the alignment of a miRNA with a transcripts 3'UTR, and numerically scores alignments based on certain desirable sequence features (Enright et al. 2003). This algorithm has previously been used to identify *Drosophila* miRNA targets (Enright et al. 2003) and 1482 predicted target genes for dme-miR-190-5p were generated from this (figure 6.2.5).

As well as the lower availability of target prediction algorithms for targets of *Drosophila* miRNA, the PANTHER gene ontology database used previously in this work was also determined to be unsuitable for the identification of targets. This was due to the high level of redundancy observed when the resulting gene list from miRanda is input into the PANTHER database, despite the database being capable of recognising *Drosophila* genes. When the resulting list of 1482 predicted genes is directly input to PANTHER, only 850 genes are returned as able to be recognised (57%), and this level of redundancy could lead to potentially relevant targets being lost. There are alternative methods for the gene ontology investigation of *Drosophila* gene sets, for instance the FlyBase query builder (Tweedie et al. 2009) and FlyMine (Lyne et al. 2007).

In order to identify genes from this data set which were relevant to this project however, it was decided to reference back to the initial screen in the *Drosophila* eye (Chapter 5) and select for genes which may be involved. This method of target identification ensured that targets which were relevant to the systems through which effects were already observed were selected. Previous publications provide us with example networks of genes which underlie eye development in *Drosophila*, or the "retinal determination network" (Kumar 2009; Şahin & Çelik 2013) and these were used to compile a shortlist of genes against which to compare the predicted targets. From this comparison, eyeless (*ey*), sine occulis (so), decapentaplegic (*dpp*), and dachshund (*dac*) were identified as predicted targets for miR-190-5p in *Drosophila* which are also implicated in the development of the eye (figure 6.2.5).

To confirm the possibility of these target genes for miR-190-5p also being relevant to mammalian models, the homologues of these genes in mouse and human were then investigated as having target sites for miR-190-5p within their 3'UTR. These were again identified using the miRanda database target prediction tool (6.2.5). From this, *dac* and *ey* emerged as targets for miR-190-5p which are conserved from *Drosophila* to both mouse and human as DACH1 and Pax6 respectively (figure 6.2.5). This however does not discredit those predicted targets which were identified as not being conserved. It has been previously proposed that miRNA targeting multiple components of the same pathway could be a mechanism to avoid redundancy (Ben-Hamo & Efroni 2015; Krishnan et al. 2013; Wu et al. 2014). The conservation of multiple targets of these pathways in each species is therefore promising for a conserved function of miR-190 in regulating this network.

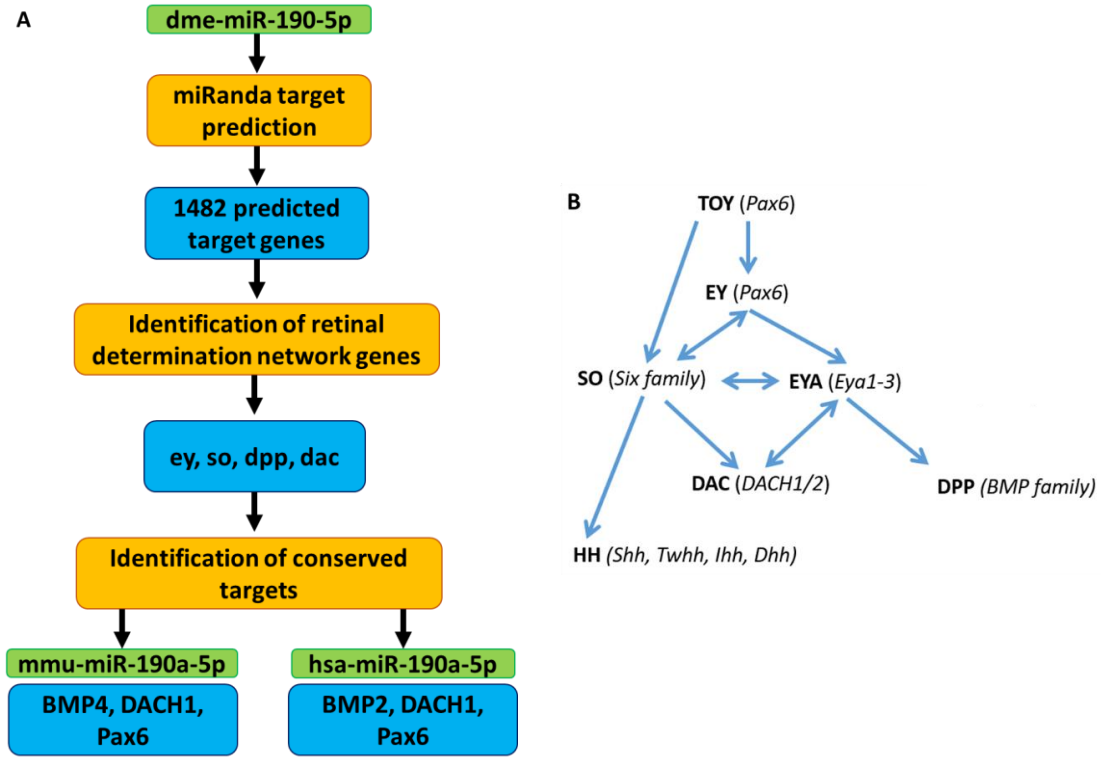


Figure 6.2.5 Identification of relevant conserved targets of miR-190
(a) Workflow of identification of conserved targets of miR-190 relevant to used models. *Drosophila* (Dme) miR-190a-5p produces 1482 predicted targets through miRanda target prediction. From this, genes present from within the retinal determination network were identified. The mouse (mmu) and human (Hsa) homologues to these target genes were then investigated through miRanda target search for target sites for the respective miR-190 homologues **(b)** Section of the Retinal Determination network demonstrating the predicted targets interactions.

6.2.5 Functional validation of predicted miR-190 target sites

As Pax6 and DACH1 were identified as conserved target candidates for miR-190-5p which may explain the effects previously observed, we tested for these putative interactions via luciferase reporter assay.

Initially, Pax6 appeared to be a target for miR-190-5p from the luciferase assay, and was therefore carried forward to site directed mutagenesis recovery to confirm this (figure 6.2.6, a). However, mutation of the miRNA target site did not reverse the reduction in luciferase signal seen, and additional repeats of the assay lead to the initial observed reduction becoming not statistically significant (figure 6.2.6 a).

DACH1 was however positively identified as a target for miR-190, with a significant reduction in luciferase activity being observed when the second predicted target site is inserted into the 3'UTR, and transfected alongside miR-190-5p mimic (figure 6.2.6 b). This reduction is subsequently rescued through mutagenesis of the miR-190 target site seed sequence within the 3'UTR (figure 6.2.6 b).

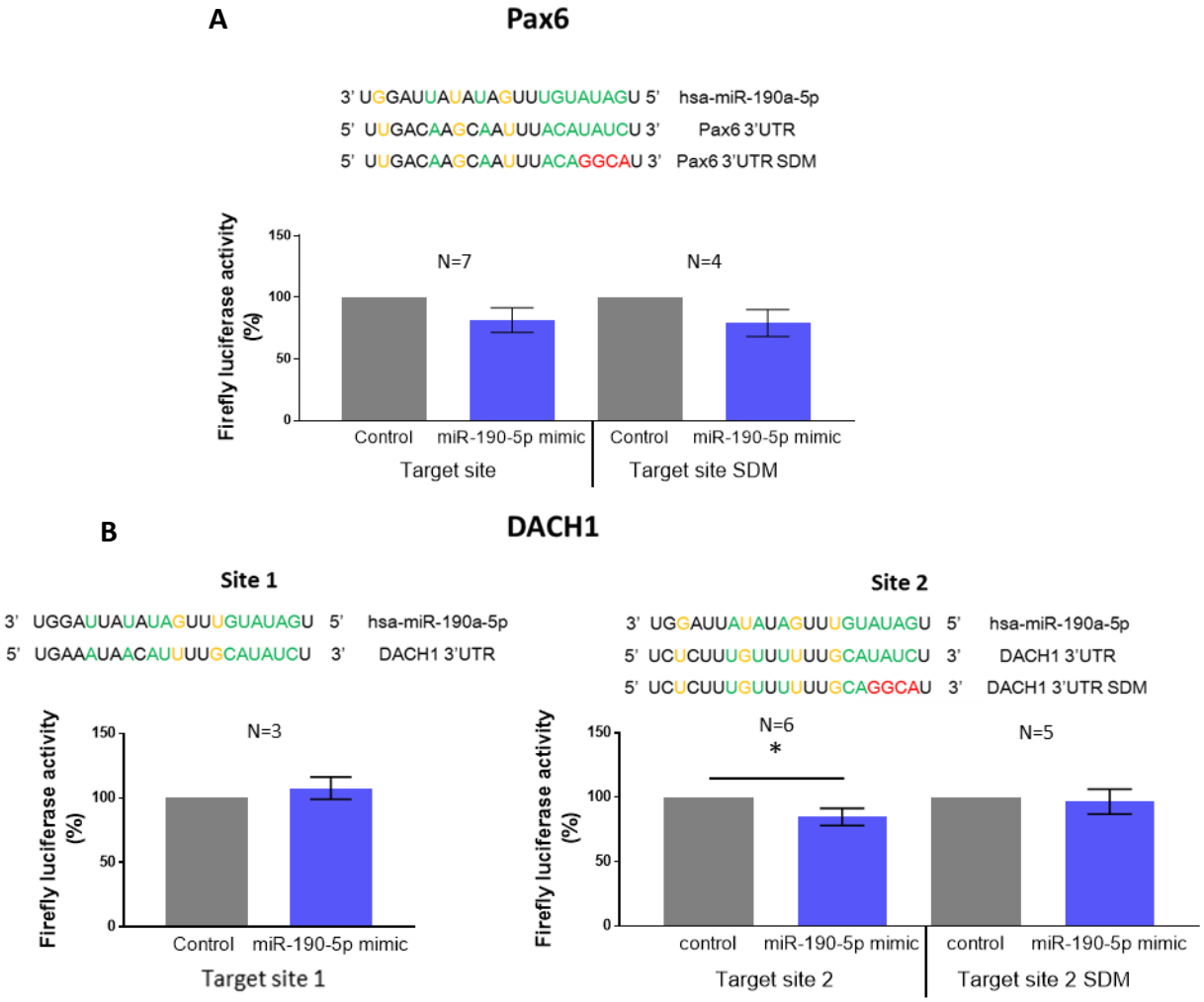


Figure 6.2.6 Luciferase assays to determine probable novel targets of miR-190a-5p
Results of the firefly luciferase activity within HEK293T cells upon transfection with reporter plasmid containing predicated target sites of miR-190a-5p as indicated. **(a)** Pax6 3'UTR possesses one predicated target site which saw an insignificant reduction in luciferase activity which was not rescued by site directed mutagenesis. **(b)**DACH1 3'UTR possesses two predicted target sites. Site 2 saw significant reduction in firefly luciferase activity in presence of miR-190a-5p mimic. Site Directed Mutagenesis of this site (Target Site 2 SDM) leads to recovery of this reduction. All luciferase assays performed with 50nM mimic and 50ng plasmid * $p<0.05$ as determined by students paired t test. Error bars show mean +/- SEM. Sequences shown for miRNA and target site interaction- Green: complementary nucleotides, Orange: G:U pairings, Red: Mutated nucleotides for SDM.

The targeting of DACH1 by miR-190-5p is predicted to be conserved to *Drosophila*, where miR-190 can target the DACH1 homologue dac. As previously described, the luciferase targeting system used here is designed around the validation of mammalian miRNA target identification. In order to confirm targeting of the *dac* 3'UTR in *Drosophila* by miR-190-5p, an alternative luciferase assay would need to be carried out. This would ideally be within a *Drosophila* cell line and using plasmids designed to express *Drosophila* miR-190 and *dac* target sites. A similar approach is used in previous papers, either for miR-190-5p itself (De Lella Ezcurra et al. 2016) or alternative miRNA (Verma et al. 2015). It is important to use the complementary synthetic miRNA sequence and predicted target site for the species being investigated, alongside a cell line derived from, as it has been shown that sequence features of the entire mature miRNA are important for the miRNA targeting of a 3'UTR, not simply the 5' seed sequence (Steinkraus et al. 2016).

6.2.6 Indications of conserved targeting of *dac* by miR-190 in *Drosophila*

In addition to the luciferase assay to confirm the targeting of *dac* by miR-190 in *Drosophila*, alternative *in vivo* indications of miR-190 targeting *dac* in *Drosophila* were explored.

As an initial indication of miR-190 targeting *dac* in *Drosophila*, a previously published observation of the role of *dac* in the development of the mushroom bodies was used (Noveen et al. 2000). The mushroom bodies are higher processing centres in the *Drosophila* brain which are key in learning and memory. It has been observed that null mutations in *dac* lead to malformation of the mushroom bodies, which can be visualised through immunohistochemistry of the brain (Noveen et al. 2000).

Overexpression of miR-190 in the developing mushroom bodies of *Drosophila* was achieved with the previously used UAS-miRNA line (Bejarano et al. 2012) and the OK^{ey107} Gal4 driver. This Gal4 driver is a modified form of the eyGal4 driver which is preferentially expressed in the developing mushroom bodies (Adachi et al. 2003). The resulting adult *Drosophila* brains were imaged through immunohistochemistry

with the FASII antibody. FASII stains strongly for the α and β lobes of the mushroom body, with weak staining in the γ lobes (Crittenden et al. 1998). FasII is used in the original paper demonstrating the effect of *dac* mutants on mushroom body development (Noveen et al. 2000). It was anticipated that if miR-190 does in fact target and downregulate *dac* in the nervous system of *Drosophila*, that the overexpression of miR-190 in the mushroom bodies would produce similar effects to those observed with null mutations of dac.

When miR-190 was overexpressed in the *Drosophila* mushroom bodies, a loss of FasII staining of the α lobes in all brains imaged was observed (figure 6.2.7). In 30% of brains, the β lobes also lost staining of FasII, and all brains show malformations in β lobes similar to those shown in figure 6.2.7 if the staining was not completely lost.

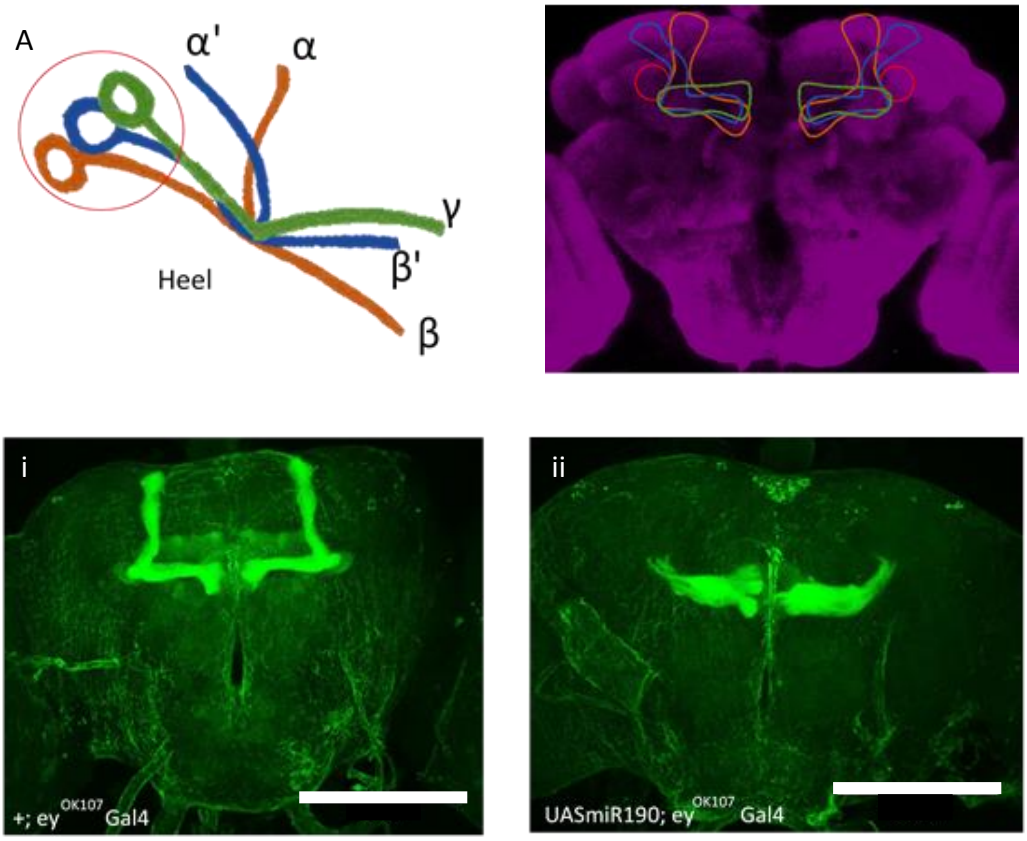


Figure 6.2.7 Effect of miR-190 overexpression on mushroom body development
(a) Schematic diagram of the *Drosophila* mushroom body lobes and position within the brain. (b) Confocal images of adult *Drosophila* brains stained with FASII which reveals the mushroom bodies. (i) eyOK107 drives expression of Gal4 in the mushroom bodies and when combined with a UAS-miR-190 construct (ii) leads to loss of the α lobes and malformation of the β lobes. Scale bars: 100um. N=13

This effect is similar to that observed in the *dac* loss-of-function mutants (Noveen et al. 2000).

It is important to note that FasII does not stain for all 5 lobes of the mushroom body, but only the α and β lobes of the mushroom body, and weakly the γ lobes. Therefore, the loss of staining observed here may be due to misrouting of the axons to alternative lobes, or due to complete loss of the neurons. A subsequent paper on the role of *dac* in mushroom body formation demonstrated that the null mutation of *dac* results in misrouting of the axons from the α/β lobes to the α'/β' lobes (Martini & Davis 2005). Therefore, future experiments to verify the similar effects of miR-190 overexpression would involve co-expression of the miRNA with a marker such as GFP. This would allow us to determine if the apparent loss of the α lobes and malformation of the β lobes is due to misrouting of the axons which form these, as shown in (Martini & Davis 2005), or due to the complete loss of the neurons or axons.

The effect observed here in the *Drosophila* mushroom body is a result of the Gal4 driven overexpression of miR-190. These effects may therefore be a result of ectopic expression of the miRNA, and miR-190 may not target *dac* endogenously *in vivo*. This may be due to the relative changes in *dac* levels caused by miR-190 inhibition being negligible, or due to miR-190 not being expressed within the same cells as *dac* endogenously. Previous indications were not found in the literature of the effect of *dac* overexpression in the mushroom bodies, therefore inhibition of miR-190 in this system would not provide us with further indications of the targeting of *dac* by miR-190.

In order to demonstrate that the targeting of *dac* by miR-190 *in vivo* is possible, a clearer indication of the expression patterns of miR-190 and *dac* was required. To further explore the targeting of *dac* by miR-190 in *Drosophila,* an initial co-stain for Dac alongside smiFISH for miR-190 was performed in the *Drosophila* embryo to observe the interacting expression patterns. It is expected, if miR-190 does in fact

target dac it will lower the expression of Dac protein. Therefore areas of high miR-190 expression will correlate with lower levels of Dac.

From the co-stain for miR-190 and Dac in the *Drosophila* embryos it was observed that pri-miR-190 and Dac do not demonstrate overlapping patterns of expression (figure 6.2.7). As has been previously published, Dac is expressed within neuroblasts of the developing *Drosophila* nervous system (Urbach & Technau 2003; Sprecher et al. 2007) and pri-miR-190 expression is strongest in the regions outside of this Dac expression, suggesting that pri-miR-190 is not expressed within these nervous system progenitors. Again, the smiFISH protocol stains for the pri-miRNA, therefore this does not indicate expression of mature miR-190, but strongly suggests that miR-190 does not appear to be actively expressed within the Dac expressing cells.

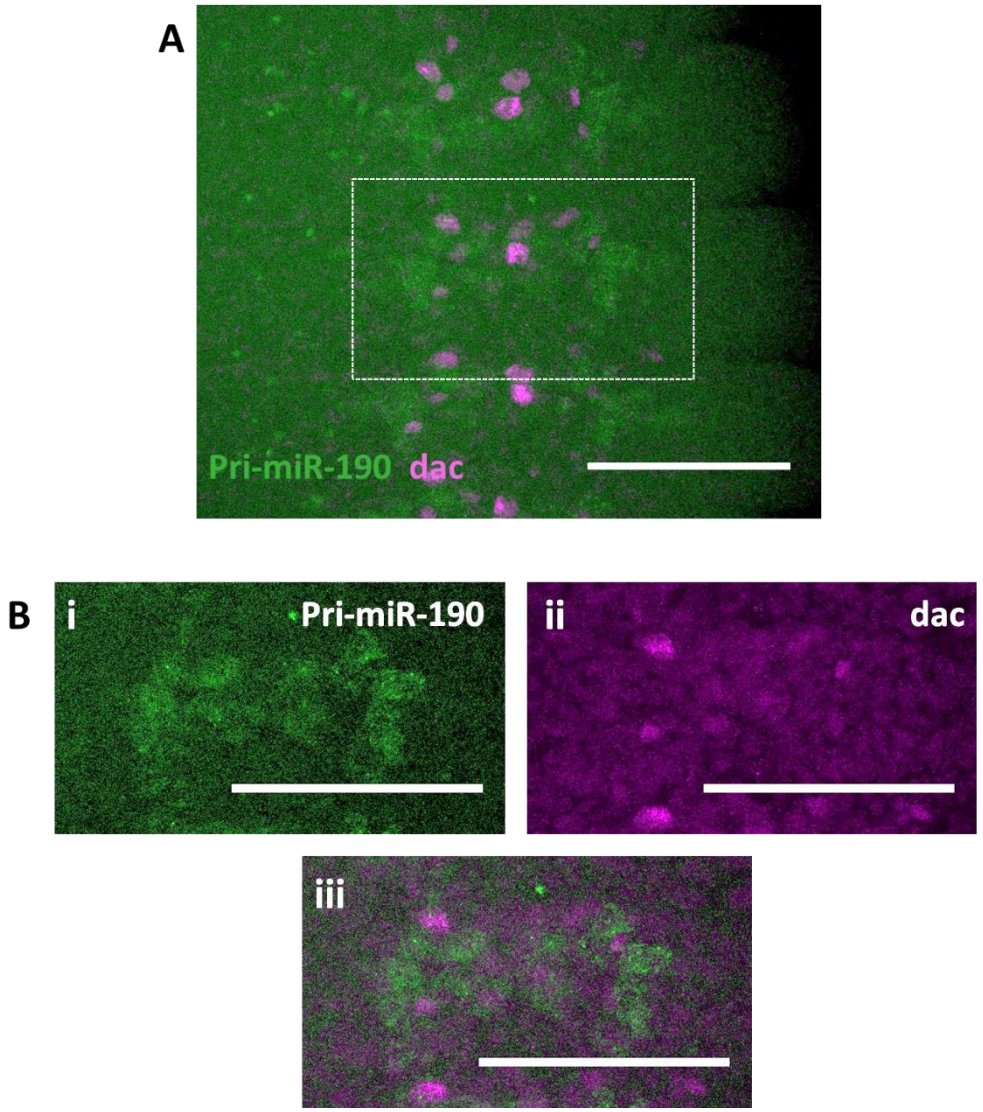


Figure 6.2.8 miR-190 expression suggests conserved targeting of DACH1
smiFISH of miR-190 within late stage *Drosophila* embryo combined with staining for *dac* demonstrates the expression pattern of miR-190 and dac.(a) maximum intensity projection of a confocal z stack of ventral portion of the embryo showing the expression of miR-190 and *dac* in the context of the embryo. White box indicates the region shown in b. (b) maximum intensity projection of subsection of z stack shown in a. Scale bars: 50µm.

The expression pattern observed here suggests miR-190 is not actively expressed within those cells which require the expression of Dac protein. This pattern of expression would be anticipated if miR-190 is in fact targeting dac, as the presence of miR-190 would lower the levels of dac protein expression.

This could also however suggest that miR-190 is expressed within non-neural or non-neuronal cells, as expression within these cells has yet to be shown. This could explain why inhibition of miR-190 in the developing neurons does not appear to cause gross abnormalities in development which impact upon the viability of the animal. Again, future co-stainings for miR-190 with additional nervous system markers may enable the identification of the miR-190 expressing cells.

An important aspect to note of this approach is that the antibody recognises the protein Dac, whereas miRNA are regulators at the level of mRNA. Therefore, an alternative method through which to assess the expression patterns of miR-190 and its target, the *dac* mRNA, would be to carry out an in situ hybridisation for *dac* mRNA alongside miR-190 smiFISH. It is important to note however, that miRNAs can function as inhibitors of translation, in addition to promoting mRNA decay, so therefore the observation of the protein levels is more representative of the action of a miRNA.

As a key regulator of cell fate, *dac* expression is underpinned by an extensive signalling network to prevent mis-expression (Anderson et al. 2006). One possible explanation for the role of miR-190 in the development of the nervous system is that of conferring an extra level of regulation to this robust signalling network, and preventing mis-expression of *dac* protein. miRNAs have been previously described as regulators of biological robustness (Ebert & Sharp 2012; Pelaez & Carthew 2012). In fact, many miRNAs in *Drosophila* do not exhibit effects which appear to be essential under normal conditions (Pelaez & Carthew 2012). For example, the function of miR-7 in eye development appears to only be essential in conditions of heat stress, where it functions as a buffer of differentiation (Caygill & Brand 2017). This may again explain why inhibition of miR-190 does not produce a strong effect in these results.

6.3 Conclusions and future directions

miR-190 emerged as a strong candidate from the initial eye screen (Chapter 5), and existing literature suggested a probable role for miR-190 in the development and function of the nervous system which had not been previously uncovered (Chapter 6.1). Despite some indications of miR-190 expression levels in *Drosophila* (J. Graham Ruby et al. 2007), there was no existing data showing the cellular expression pattern of miR-190 in *Drosophila* development. smiFISH demonstrated pri-miR-190 expression in *Drosophila* embryos in a pattern indicative of a nervous system linked expression (figure 6.2.2). Therefore, it was decided that the role of miR-190 in nervous system development and processes was to be further investigated. Further experiments should be conducted to demonstrate the exact localisation of pri-miR-190 expression, for example by co-staining for nervous system markers alongside smiFISH for pri-miR-190.

Although homozygous miR-190 knockout had previously been shown to be lethal (Chen et al. 2014). There were no previous indications in the literature of the effect that modulation of miR-190 levels specifically within the nervous system would have. It was shown here that overexpression of miR-190 in both *Drosophila* and mouse neurons had detrimental effects (figure 6.2.3-4), suggesting that endogenously miR-190 levels may need to be tightly controlled during development. However, inhibition of miR-190 did not produce any observed effects on the gross development of either *Drosophila* or mouse neurons (figure 6.2.3-4 Appendix VI). Alternative assays are carried out in Chapter 7 in order to determine the role that miR-190 inhibition plays in the function of the mature nervous system.

Relevant targets for miR-190 in mammals in regards to the nervous system have been previously identified (table 6.1.2), but most were not shown, or predicted to be, conserved to *Drosophila*. Despite this, the transcription factor Dac/DACH1, which is involved in eye and nervous system development, was identified as a conserved predicted target for *Drosophila*, mouse, and human miR-190-5p. DACH1 was further confirmed as a target for miR-190-5p through luciferase assay (Figure 6.2.6). In

future studies, luciferase assays should also be conducted to confirm the targeting of *dac* by miR-190-5p in *Drosophila*.

Indications that miR-190-5p targets *dac* in *Drosophila* were also found. Namely: the recapitulation of developmental defects of *dac* null mutations in the mushroom bodies by overexpression of miR-190 (figure 6.2.7); and the expression patterns of *dac* and pri-miR-190 in *Drosophila* embryos being indicative of miR-190 targeting dac (figure 6.2.8). In addition to luciferase assay, this targeting could be further confirmed through observing the effect on *dac* expression caused by modulation of the levels of miR-190-5p. Future work should focus on complementary modulation of DACH1/dac levels in order to observe that the effects caused are logical in conjunction with miR-190 effects.

Overall, it was demonstrated that miR-190 could play a conserved role in the development of the nervous system through the regulation of dac/DACH1 levels, however future work is required to further validate this interaction in both *Drosophila* and mammalian models.

Chapter 7. Investigation of miR-190 in mature nervous system function

7.1 Introduction

The function of the nervous system is underpinned by the formation and maintenance of the correct circuitry, and by the ability to appropriately modulate this circuitry throughout the lifespan of an organism. The connections between neurons within the nervous system circuitry are called synapses, and the formation and maintenance of these, and their adaptability, allows the nervous system to function (Chapter 1.4). These are processes which have been shown to be regulated previously by miRNAs (Chapter 1.16-19). The use of *Drosophila* as a model of the mature nervous system allows for parallels to be drawn to mammals due to a high level of conservation, genetically, anatomically, and functionally. The model also provides useful behavioural assays which allow for the assessment of neuronal circuit function. For this reason, and following on from the studies of miR-190 in early development (Chapter 6), the function of miR-190 was also assessed in the mature nervous system of *Drosophila*.

7.1.1 The mature nervous system of *Drosophila*

Alongside the conserved elements found in the development of the nervous system (Chapter 5.1), many parallels can be drawn between the neuroanatomy of the adult nervous system of *Drosophila* and mammalian models. For instance, the adult CNS of *Drosophila* can be subdivided into two processing bodies, the brain and the thoracicoabdominal ganglion (THA), which can, to a certain level, be compared to the mammalian brain and spinal cord respectively. Much like their mammalian counterparts, the brain of *Drosophila* is comprised of structured lobe regions, which are specialised for their biological function, and the THA ganglion is a segmented structure which extends down the body of the fly, receiving, transmitting and processing information to and from the brain and periphery of the animal. Certain aspects of *Drosophila* neuroanatomy are not conserved however, for instance the cell bodies of *Drosophila* sensory neurons reside within the periphery of the animal, as opposed to just outside the spinal cord as in mammals. This is because sensory neurons in *Drosophila* do not possess the distinctive pseudounipolar morphology of

their mammalian counterparts. Instead, *Drosophila* possess multidendritic sensory neurons (Grueber et al. 2002).

In addition to the conserved aspects in the neuroanatomy of *Drosophila*, the signalling molecules which mediate the nervous system circuit are generally well conserved from *Drosophila* to mammals. Interneurons in *Drosophila* utilise the neurotransmitters acetylcholine (Ach) at cholinergic synapses, gamma-aminobutyric acid (GABA) at GABAergic synapses and glutamate (Glut) at the Glutamatergic synapses (Clark et al. 2018). *Drosophila* also possess nervous system subtypes which utilise the monoamines such as serotonin and dopamine at the synapse (Denno et al. 2015). This conservation allows for the dissection of the mechanistic pathways at these synapses within the model system of *Drosophila*, even in contexts where the precise neuroanatomy is not conserved.

Drosophila models for multiple neurodegenerative diseases have thus been developed based on exploiting the tractability of the system, and utilising the conserved elements of the nervous system (Marsh & Thompson 2006; Bilen & Bonini 2005). Although many of these diseases do not occur naturally within *Drosophila*, models have been created through the "humanisation" of the *Drosophila* model with the expression of human genes within the nervous system. For example, using the Gal4/UAS experimental approach, for modelling Alzheimer's disease (Bouleau & Tricoire 2015). Upon expression in *Drosophila* of these human genes and mutant versions of these genes, that are implicated in some of the cellular processes observed in Alzheimer's disease, it has been possible to recapitulate some of the characteristics that occur in Alzheimer's disease in *Drosophila*. For instance, the visible degeneration of the brain, deposits of protein aggregates, reduction in lifespan, and learning and behavioural defects (Moloney et al. 2010). Although these models are not a perfect representation of the regulatory networks in mammals, they have contributed important knowledge of the disease pathologies in a system that has greater access to genetic tools, and can be more easily manipulated and observed than the mammalian counterpart.

7.1.2 Adult behavioural assays in *Drosophila*

There are multiple behavioural assays which have been developed as a measurement of the appropriate function of the mature nervous system in adult *Drosophila*. One example of particular prominence is the behavioural assays of the circadian clock (Tataroglu & Emery 2014) (which were the basis of the 2017 Nobel prize in Physiology and Medicine awarded to *Drosophila* researchers). In this chapter, the assays of climbing ability and longevity were used in order to assess the correct functioning of the mature nervous system in adult *Drosophila*.

The climbing ability of *Drosophila* can be assessed through a negative geotaxis assay (Madabattula et al. 2015). This assay utilises innate escape response behaviour in the fly, which is initiated though the tapping of flies to the bottom of a container and causes them to quickly climb upwards. The efficiency of this behaviour is measured through the flies' ability to climb past a predetermined benchmark (Madabattula et al. 2015). When the nervous system circuits which underlie this behaviour are disrupted, the ability of the flies to climb past this benchmark will be inhibited. It has previously been shown that this behavioural test can be used to assess and dissect the mechanisms of models of neurodegenerative disease which manifest with locomotive defects, such as Parkinson's disease (Madabattula et al. 2015).

Assessment of the lifespan and survivorship of *Drosophila* can be used as a measurement of enhanced deterioration of the nervous system as a result of genetic manipulation in nervous system structures (Linford et al. 2013). These are experiments which are more easily and quickly assessed in *Drosophila* than in mammalian counterparts, due to the higher availability of test subjects, and the short relative lifespan of *Drosophila*. Defects in the aging of the nervous system will lead to an increase in mortality or a reduction of the average lifespan. This test has therefore been used to dissect mechanisms of nervous system dysfunction, in particular in the assessment of Alzheimer's disease models (Moloney et al. 2010).

7.1.3 Experimental aims

Experiments were undertaken to determine if miR-190 has a role in the function of the mature nervous system in *Drosophila*.

- Firstly, miR-190 function was inhibited within the neurons of adult *Drosophila,* and the effect of this on the lifespan of the animals was assessed.
- Subsequently, to investigate in more detail the mechanism of action for miR-190. miR-190 function was selectively inhibited within cholinergic or glutamatergic neuronal subsets, and the effect of this was assessed on motor ability in a climbing assay, and on lifespan in a survivorship assay.
- Target genes which may explain the observed effects of these assays were also predicted.

7.2 Results and Discussion

7.2.1 miR-190 inhibition in neurons leads to a reduction in *Drosophila* lifespan

In order to assess whether inhibition of miR-190 within neurons would lead to an observable effect in the function of the mature nervous system, a genetically encoded miR-190 sponge was used. This will, when expressed under the Gal4 UAS system, sequester miR-190 and inhibit its function (Fulga et al. 2015).

First, expression of this sponge throughout the whole nervous system was driven with the previously used ElaVGal4 driver, which expresses Gal4 in post mitotic neurons (Robinow & White 1991). It was demonstrated previously, that inhibition of miR-190 in neurons in this manner does not lead to a significant effect on the survivorship of *Drosophila* in early development (figure 6.2.1). Additional preliminary observations also demonstrated that the inhibition of miR-190 in glutamatergic motor neurons does not lead to abnormalities in the development of synapses, or function of the developing larval nervous system (Appendix VI). The lifespan of adult *Drosophila* with miR-190 inhibited in the pattern of ElaV was subsequently assessed as an indicator of nervous system function and degeneration (figure 7.2.1).

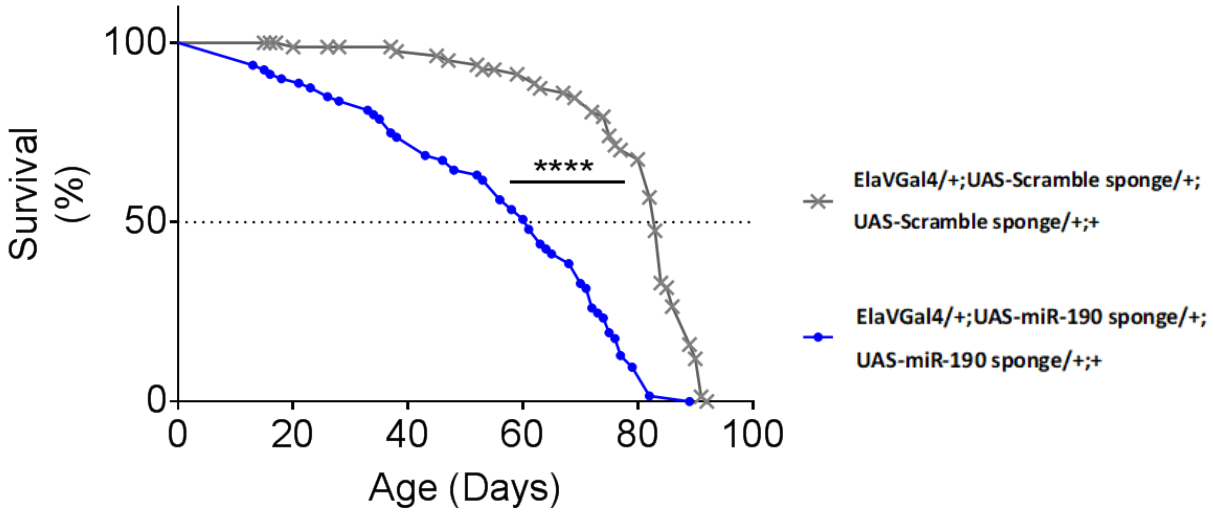


Figure 7.2.1 Inhibition of miR-190 throughout the nervous system leads to a reduction of lifespan
miR-190 sponge or scramble RNA was expressed throughout the nervous system with the ElaV Gal4 driver. ElaVGal4: Gal4 expression driven in post-mitotic neurons, Scramble sponge: non-targeting scramble miRNA sponge under control of UAS. miR-190 sponge: miR-190 miRNA sponge under control of UAS. Adult *Drosophila* were monitored for their survivorship until entire cohorts were deceased. A significant reduction in the survival of *Drosophila* when miR-190 was inhibited throughout the nervous system was observed. ****P<0.0001 as determined by Mantel-Cox log-rank test. N=80 for both genotypes.

The survivorship of the adult *Drosophila* was significantly reduced with the inhibition of miR-190 in the post-mitotic neurons (figure 7.2.1). With the median survival of *Drosophila* expressing the miR-190 sponge throughout the nervous system being 61 days (figure 7.2.1). This is a significant reduction when compared to the survival of those flies expressing the non-targeting scramble sponge, which demonstrated a median survival of 83 days (figure 7.2.1). This result suggests miR-190 plays a role in nervous system maintenance and function with an age related effect, and inhibition of miR-190 may cause enhanced nervous system degeneration.

There have been indications of miR-190 having a function in the aging or degeneration of the nervous system in mammalian models. It has been previously shown that miR-190 is significantly downregulated following traumatic brain injury in the mouse (Meissner et al. 2016), and that miR-190 is upregulated in brain regions of Alzheimer's disease patients (Cogswell et al. 2008). These indications are however demonstrating the dysregulation of miR-190 in disease states in mammals. Whereas the result seen here (figure 7.2.1) suggests an endogenous role of miR-190 in the maintenance of the *Drosophila* nervous system.

7.2.2 Inhibition of miR-190 in the nervous system and assessment of climbing ability

Following the results of the initial tests on the role of miR-190 in the function and aging of the nervous system (figure 7.2.1), it was then sought to determine if miR-190 inhibition could also produce an effect on the climbing ability of adult *Drosophila*. Previously, preliminary results suggested that the locomotor behaviour of the *Drosophila* larvae was unaffected by inhibition of miR-190 (Appendix VI). In order to observe if an age related effect could be observed, the effects of miR-190 inhibition were assessed through climbing assays on both one day old and 45 day old adult flies.

In addition to age related decline in climbing, we wished to observe if an effect could be mediated by miR-190 acting upon a specific neuronal subtype. It has been previously found that the cholinergic and glutamatergic neuronal subtypes are

important in *Drosophila* larval locomotion circuitry, cholinergic interneurons within the CNS innervate the glutamatergic neurons which form the NMJ (Landgraf & Thor 2006; Kohsaka et al. 2017). Action of miR-190 was also therefore inhibited in the cholinergic neurons through the use of a ChaTGal4 driver, and the glutamatergic neurons through the use of a VGlutGal4 driver. These manipulations were made in order to determine whether miR-190 exerts a mechanism of action specific to one of these neuronal subtypes.

First, a climbing assay was conducted on adult *Drosophila* one day post eclosion, to determine if inhibition of miR-190 in nervous system subtypes would cause an effect on the climbing ability of young *Drosophila*. Climbing behaviour was seen here to be significantly impaired in one day old *Drosophila* when miR-190 sponge expression was driven by the ElaV gal4 driver (Figure 7.2.2 a). However, the same effect was not seen when miR-190 sponge expression was driven by the ChAT or VGluT Gal4 drivers (figure 7.2.2 a). This suggests that miR-190 may be playing a role in the functioning of the nervous system at this stage, however this effect is not necessarily associated with a specific neuronal subtype. It is important to note that this test (7.2.2 a) was conducted when the adult flies were one day old. If miR-190 is playing a role in the aging of the nervous system (as the results in 7.2.1 suggest), the inhibition of miR-190 may produce greater effects on the climbing assay in aged flies.

To assess whether miR-190 had an age related effect on adult *Drosophila* climbing ability, the climbing assay was repeated when the flies were 45 days old (figure 7.2.2 b). In this assay, it was found that when Gal4 was expressed without the presence of a UAS construct, Gal4 appeared to be having a detrimental effect on the functioning of the nervous system (figure 7.2.2 b). All Gal4 expression patterns used led to a significant decrease in climbing ability compared to when assessed at day 1. This would be expected due to the natural aging of the flies. However, this reduction was of a much greater magnitude than that seen with the combination of the Gal4 driver and the Scramble miRNA UAS construct (figure 7.2.2 b). Similar toxic effects of high levels of Gal4 expression on locomotor activity have been observed, due to Gal4 protein aggregate-induced neuronal cell death (Rezával et al. 2007).

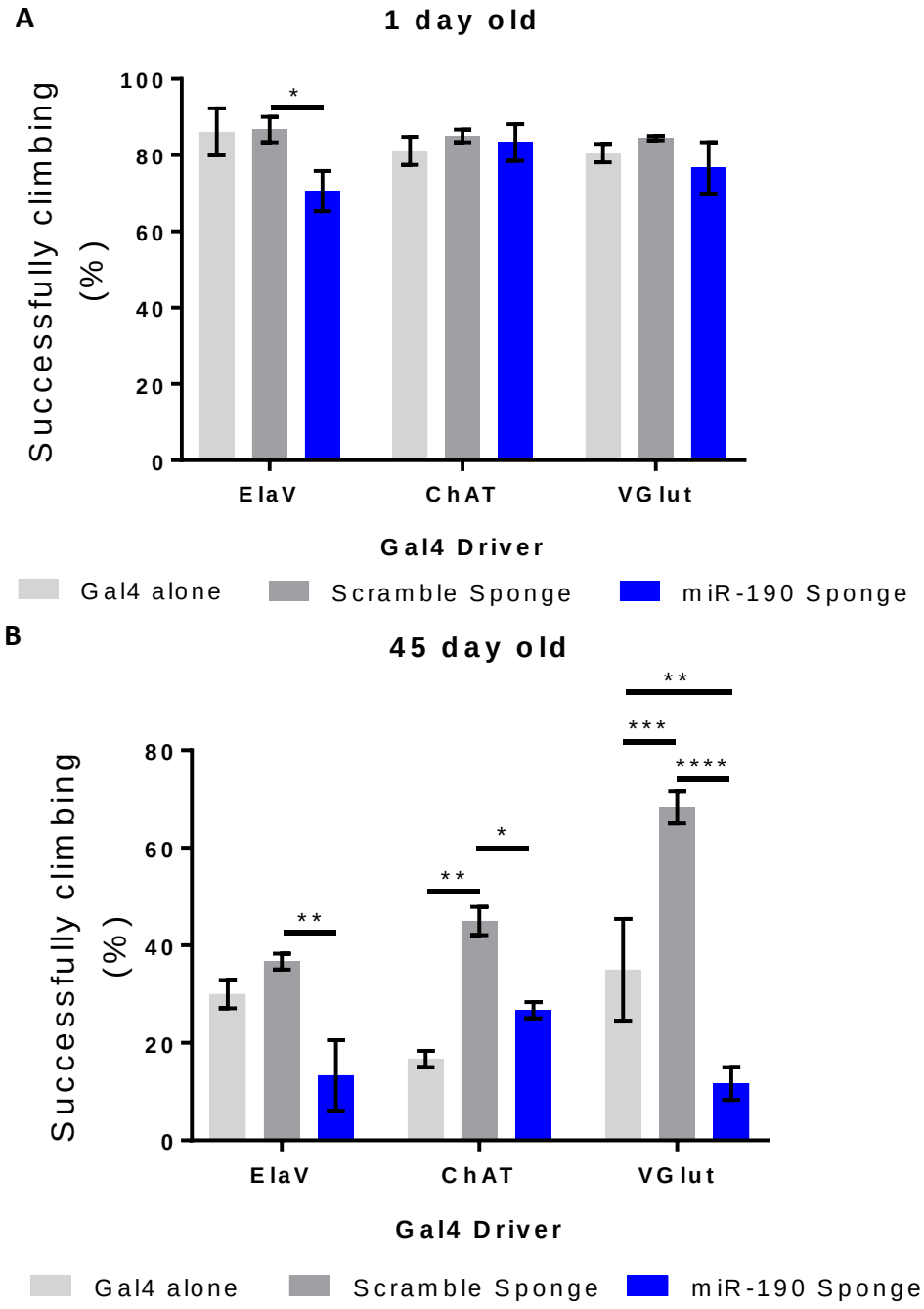


Figure 7.2.2 miR-190 inhibition effect on climbing ability in adult flies
The climbing ability of adult *Drosophila* at **(a)** one day post eclosion and **(b)** 45 days post eclosion with indicated genotypes was assessed through negative geotaxis assay. **ElaV**: Gal4 expression in postmitotic neurons. ElaVGal4/w[*];+;+ **ChAT**: Gal4 expression in cholinergic neurons. [w*];+;ChATGal4/+ **VGlut**: Gal4 expression in glutamatergic neurons. w[1118];VGlutGal4/+;+ **Scramble sponge**: non-targeting scramble miRNA sponge under control of UAS. w[*];UAS-Scramble Sponge/+; UAS-Scramble Sponge/+ **miR-190 sponge**: miR-190 miRNA sponge under control of UAS. w[*];UAS-miR-190 Sponge/+;UAS-miR-190 Sponge/+
*P<0.05, **P<0.01, ***P<0.001, ****P<0.0001 as determined by Bonferroni multiple comparisons following 2 way ANOVA. All genotypes n=60. 3 separate groups of 20 flies were assayed for all genotypes. Error bars show mean +/- SEM.

When direct comparison is conducted of the climbing ability of flies expressing either the scramble-sponge or miR-190-sponge, a significant reduction in the climbing ability of those flies expressing miR-190 sponge results. This was seen as a result of combination with the ElaV, ChaT and VGlut Gal4 drivers (figure 7.2.2 b). This result suggests that miR-190 is endogenously performing a role in the functioning of the aged nervous system. However, as the results seen from the Gal4 controls are variable, this result cannot be completely relied upon.

Previously published observations have demonstrated that the methodology used here to assess climbing ability (Madabattula et al. 2015) can produce highly variable results, which impact upon the significance of differences observed. High throughput methodologies which assess negative geotaxis such as the modified RING assay could instead be used to validate these results (Gargano et al. 2005).

Due to the possible age-related decline of climbing ability observed in this assay, and the initial observation that miR-190 inhibition throughout the nervous system lead to defects in survivorship, the effect of miR-190 inhibition within nervous system subsets was then assessed through a survivorship assay.

7.2.3 Inhibition of miR-190 within the nervous system and assessment of lifespan

Here, as in 7.2.2 a genetically encoded sponge for miR-190 was expressed in post-mitotic neurons, and within the cholinergic and glutamatergic nervous system subsets. The effect of this on the proportion of flies which survived to 45 days was then assessed in a survivorship assay.

It has been shown that selective inhibition of nervous system subtypes can also, as with locomotion, impact on the longevity of *Drosophila*. In fact, many pesticides selectively inhibit Acetylcholinesterase, which lead to a build-up of acetylcholine, which is lethal to the animal. Additionally, it has been observed that selective inhibition of Glutamatergic neurons can lead to reductions of the lifespan of *Drosophila* (Verma et al. 2015).

Although significantly detrimental effects of Gal4 expression in absence of an UAS construct were observed on the climbing ability of *Drosophila* (figure 7.2.2), this effect was not seen to as great an extent in the survivorship assay. There is a slight reduction in survivorship when Gal4 is expressed in absence of a UAS construct (figure 7.2.3), however this is not significant when compared to the expression of Gal4 when in the presence of the scramble sponge UAS construct.

Significant reduction of the survivorship of flies when miR-190 was inhibited through elaVgal4 driven expression of the miR-190 sponge was observed again, with only 79% of flies surviving to 45 days (figure 7.2.3). This further demonstrates that endogenous miR-190 may be playing a role in either the function, or the maintenance of, the nervous system.

VGlut gal4 driven expression of miR-190 sponge produced no effect on the survival of the flies however. This is interesting, as previous papers demonstrate that modulation of the activity of glutamatergic neurons can in fact lead to a reduction in lifespan (Verma et al. 2015). This may however be due to the time point at which we are assessing survivorship in this assay and greater effects may be seen later in life. At 45 days however, the survivorship of the flies is only reduced on average by 2% (figure 7.2.3).

ChAT gal4 driven miR-190 sponge expression does however lead to a significant decrease in survivorship, with only 75% of flies surviving to 45 days on average (figure 7.2.3). This suggests miR-190-inhibition is producing an effect on the cholinergic neurons in this assay. These results therefore predict that endogenous miR-190 has a function in the aging nervous system, particularly in the functionality and maintenance of the cholinergic system. As such, relevant predicted targets for miR-190-5p in this context were to be identified.

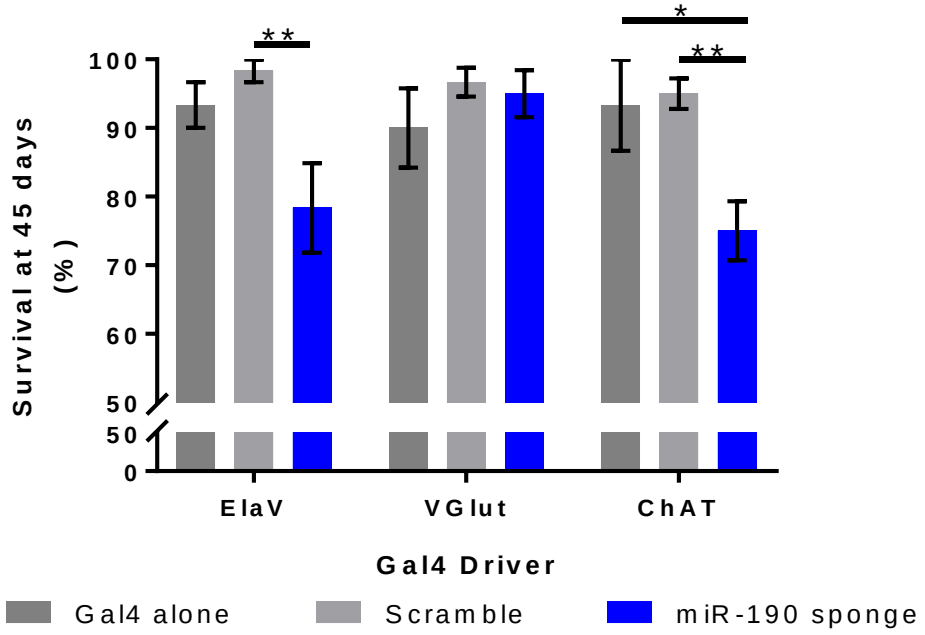


Figure 7.2.3 miR-190 sponge effect on lifespan expressed in nervous system subsets
Survival of flies of indicated genotypes to 45 days was recorded. **ElaV**: Gal4 expression in postmitotic neurons. ElaVGal4/w[*];+;+ **ChAT**: Gal4 expression in cholinergic neurons. [w*];+;ChATGal4/+ **VGlut**: Gal4 expression in glutamatergic neurons. w[1118];VGlutGal4/+;+ **Scramble sponge**: non-targeting scramble miRNA sponge under control of UAS. w[*];UAS-Scramble Sponge/+; UAS-Scramble Sponge/+ **miR-190 sponge**: miR-190 miRNA sponge under control of UAS. w[*];UAS-miR-190 Sponge/+;UAS-miR-190 Sponge/+
*P<0.05, **P<0.01 as determined by Bonferroni multiple comparisons following 2 way ANOVA. 6 groups of ten flies were assayed for each genotype. Error bars show mean +/- SEM.

7.2.4 Identification of targets of miR-190 which may indicate a role in nervous system function

In order to predict targets for miR-190 which may explain the effect of inhibition on lifespan, the previously compiled list of predicted targets from the miRanda database was used (figure 6.2.5). Again, as in chapter 6.2.3 a manual identification method of relevant targets, informed by previous results, was used. As previously discussed, when working with *Drosophila* gene datasets, a large number of genes are discounted in our previously used automated database methods, therefore informed manual analysis can be a better option in this context. Using previous indications from results presented in this thesis that miR-190-5p may have a specific role in cholinergic neuron subsets (figure 7.2.3), genes were identified within the predicted target data set which may influence the turnover of acetylcholine or perform a function at the cholinergic synapse. This was simply conducted through an initial

summarization from the literature of genes which are involved in cholinergic neuron function in *Drosophila* and a subsequent search of the predicted target genes for the presence of these in the dataset.

Three genes implicated in the cholinergic pathway were identified as possible targets of miR-190-5p: Acetylcholinesterase (AchE), Cholineacetyltransferase (ChAT) and Vesicular acetylcholine transporter (VAChT) (figure 7.2.4).

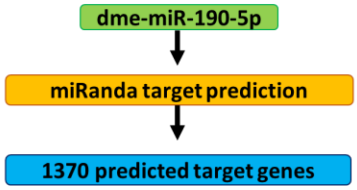
The identified predicted targets of VAChT, AChE and ChAT all function at the cholinergic synapse, and work in concert for the transport and turnover of Ach (figure 7.2.4). VAChT is a vesicular transporter of Ach, which is required for the loading of Ach into synaptic vesicles for release into the synaptic cleft. AChE catalyses the degradation of Ach, into choline and an acetyl group, preventing it's binding to Ach receptors, and allowing reuptake of choline into the pre-synapse. ChAT synthesises Acetylcholine from Choline and activated Acetyl groups. If miR-190 targets these genes, this would implicate miR-190 in the homeostasis of protein levels at the cholinergic synapse, indicating a significant role for miR-190-5p in the functioning of the mature nervous system.

The possible regulation of the cholinergic system by miR-190-5p targeting multiple components of acetylcholine turnover is an example of an interesting paradigm, as it has been previously suggested that a class of miRNA, "CholinomiRs" may be regulators of cholinergic pathways (Simchovitz et al. 2017; Nadorp & Soreq 2014). These CholinomiRs have been suggested as possible targets or treatments for a personalised medicine approach of the treatment of neuroinflammatory disorders such as Alzheimer's disease (Simchovitz et al. 2017).

This predicted targeting of cholinergic genes by miR-190-5p is not however conserved outside of *Drosophila*. This perhaps not unexpected, as it has been previously observed that predicted targeting of Ach processing genes by miRNA is not well conserved, including many which are primate specific (Nadorp & Soreq 2014). If miR-190 does in fact target regulators of cholinergic signalling in the

Drosophila nervous system, it may prove as a novel and useful model through which to investigate the effects of moderation of cholinergic pathways through a miRNA.

A



B **Ace**

3' guUGGuUcUUAUagUUUGUAUAGa 5' dme-miR-190-5p
5' auAUUuAuAAUGcaAAACAUAUCa 3' Ace 3'UTR

3' GuugGUUcuUAUAGUU--UGUAUAGa 5' dme-miR-190-5p
5' UcugUAAucGUAUUAAagGCAUAUCa 3' Ace 3'UTR

C **VAChT**

3' guUGGUUCUUAUAGUU - UGUAUAGa 5' dme-miR-190-5p
5' caACCAAG - GUAACGAUACAUAUCa 3' VAChT 3'UTR

3' guugGUUCUUAUA--GUUUGUAUAGa 5' dme-miR-190-5p
5' auggCAUCCAUAUCGCAGACAUAUCa 3' VAChT 3'UTR

3' guugguucuUAUAG---UUUGUAUAGa 5' dme-miR-190-5p
5' agacuuucuAUAUCCGUAAACAUAUCa 3' VAChT 3'UTR

3' guuggUUCUUAUAGUUUGUAUAGa 5' dme-miR-190-5p
5' uauagACGUUUGUGUUACAUAUCu 3' VAChT 3'UTR

D **ChaT**

3' guUGG--UUCUUAUAGUUUGUAUAGa 5' dme-miR-190-5p
5' ccACCAGAAAAAAAAAAAACAUAUCa 3' Cha 3'UTR

3' guUGG--UUCUUAUAGUUUGUAUAGa 5' dme-miR-190-5p
5' ccACCAGAAAAAAAAAAAACAUAUCa 3' Cha 3'UTR

3' guuGGUUCU-UAUAGUU-UGUAUAGa 5' dme-miR-190-5p
5' gacUUGAGACGUAACAAUACAUAUCa 3' Cha 3'UTR

3' guugguucuuauaguuUGUAUAGa 5' dme-miR-190-5p
5' gcaacccauucgcuuuACAUAUCc 3' Cha 3'UTR

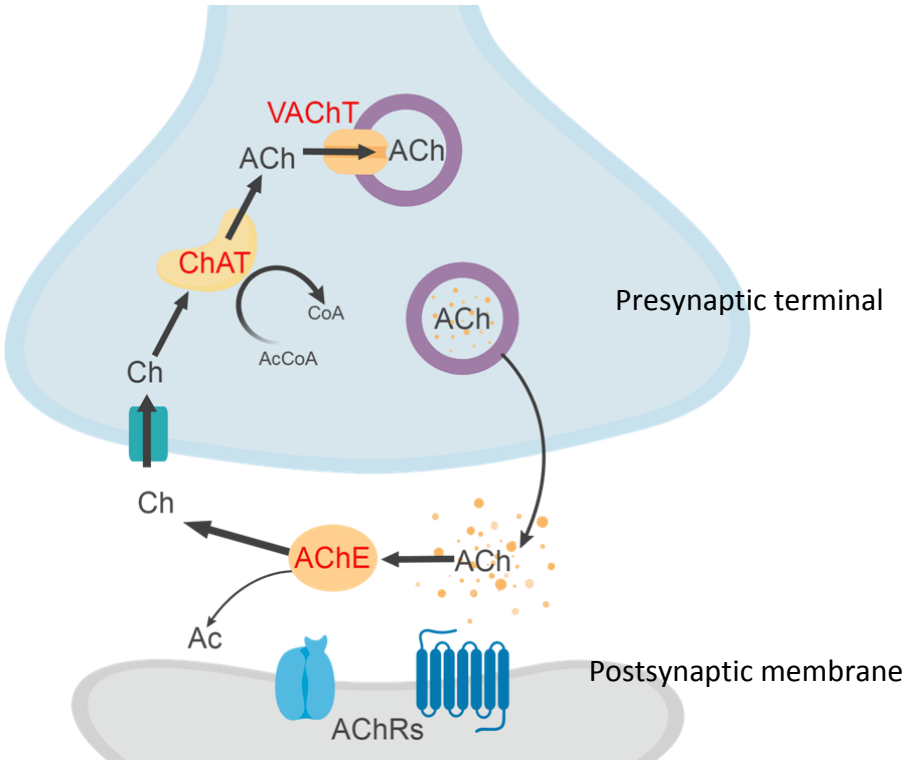


Figure 7.2.4 Identification of predicted target genes for miR-190 which can modulate neuronal function

(a) miRanda target prediction produced a set of 1370 predicted target genes for dme-miR-190-5p. This data set was investigated for genes with a known function in nervous system function. This yielded three candidate genes which all function in the cholinergic synapse. **(b)** Two predicted target sites are present in the 3'UTR of the ace gene transcript, which encodes the enzyme Acetylcholinesterase (AChE). **(c)** Four target sites are present within the 3'utR of VAChT, which encodes the Vesicular Acetylcholine Transporter (VAChT) **(d)** Four Target sites are present within the 3'UTR of the Cha gene locus, which encodes for the Choline Acetyltransferase (ChaT) **(e)** Schematic diagram of how the predicted miR-190 targets of AChE, ChAT and VAChT function in the cholinergic synapse (indicated in red). (Made in Biorender)

7.3 Conclusions and future directions

A role for miR-190 in the functioning of the mature nervous system was shown through climbing and longevity assays. Inhibition of miR-190 within postmitotic neurons leads to a reduction of the lifespan of *Drosophila* (figure 7.2.1). Further to this, inhibition of miR-190 within postmitotic neurons, and cholinergic and glutamatergic neuronal subsets, leads to a possible age related decline in climbing ability (figure 7.2.2). These results indicate a role for miR-190 in the functioning and aging of the mature nervous system. Further tests to determine the specific effect of miR-190 on the nervous system should be carried out, for example immunohistochemistry, or functional tests of nervous system signalling.

Inhibition of miR-190 within cholinergic subsets of neurons, but not glutamatergic, also leads to reduction in the survivorship of the adult flies (figure 7.2.3). The results of these survivorship assays (figure 7.2.3) suggest a function of miR-190 specific to cholinergic neuron subsets. It was shown, through bioinformatics analysis, that miR-190 is predicted to target multiple genes which function within the cholinergic synapse (figure 7.2.4). Whilst the targeting of these genes by miR-190 is not predicted to be conserved outside of *Drosophila*, this work provides an interesting *in vivo* indication of the action of "CholinomiRs" in *Drosophila,* which has not been shown previously. As a result of this, miR-190 may prove as a miRNA through which the action and potential of "CholinomiRs" can be assessed within the highly tractable model of *Drosophila*. Future work should focus on identifying these genes as true targets of miR-190-5p, for example through luciferase assay, and the effect of miR-190 on cholinergic signalling in *Drosophila*.

Chapter 8. Final Conclusions

The nervous system is a complex network of multiple cell types, each specialised for their individual functions (Chapter 1.1-2). In particular, the neurons, which form the underlying circuitry of the nervous system, are morphologically differentiated in a polarised structure with specialised cellular sub compartments. Through variations in neuronal structure, and specification of neuronal subtypes, the neurons are able to attain great diversity of function. This complexity is achieved during development, and maintained throughout the life of the organism through the controlled expression of proteins in a spatial and temporal manner, with translation playing a particularly relevant role (Chapter 1.5-7). A class of translational regulators, miRNAs, have been implicated in protein level control in the nervous system (Chapter 1.8). Although a selection of individual miRNAs have been characterised as to their specific roles within the nervous system, there is still much scope for the identification of novel roles for miRNAs (Chapter 1.13-16).

The objective of this project was the identification of novel functions of individual miRNAs in the development and function of the nervous system. This overarching hypothesis was investigated in two separate parts using independent experimental paradigms.

8.1 Identification of miRNAs which could regulate nervous system function in chronic nociception and pain

The sensation and processing of pain is a critical function of the nervous system, which is performed by a precise neuronal circuit. This circuit requires the controlled expression of proteins, which can be modulated at the level of translation in a spatial and temporal manner (Kays et al. 2018; Jimé Nez-Díaz et al. 2008; Ferrari et al. 2013). When this circuitry is disturbed, for instance by inflammation or injury, chronic pain can result (Xu & Yaksh 2011). As potential modulators of translation in chronic pain processes, levels of miRNAs, and their possible functions, were to be investigated in a model of the transition from acute to chronic inflammatory pain – hyperalgesic priming. This model was chosen based upon the ability to observe the

progression from acute to chronic pain, and previous observations of the importance of peripheral local translation.

Although previous studies had investigated the disrupted levels of miRNAs in various other models of pain processes, these studies demonstrate great variability (figure 3.1.2). Due to the high degree of variability observed in these previous studies, and the lack of study of miRNA profiles in Hyperalgesic priming, it was important to assess the miRNA profile of our chosen model.

We demonstrated, through microarray, that individual miRNAs are dysregulated within the DRG in hyperalgesic priming (figure 3.2.1-3). This is a finding that has not been previously shown in the current literature. Crucially, the findings obtained here demonstrated dysregulation of some miRNAs which were present in the previous analysis of the existing literature, and previously implicated in pain processes, reinforcing the validity of the experimental approach. This work also identified other miRNAs which may be novel potential modulators of pain.

One miRNA, which became the focus of this work, miR-138-5p, was characterised throughout the model of hyperalgesic priming using qPCR. miR-138-5p exhibited a distinctive expression profile within the DRG throughout the hyperalgesic priming protocol, which implicated miR-138-5p in inflammatory pain processes (figure 3.2.3). It was then demonstrated, through a combination of bioinformatics and luciferase reporter assays, that miR-138-5p functions as a probable regulator of the inflammatory mediator, MYD88. This therefore indicated a novel function for miR-138-5p within inflammatory pain (figure 3.2.4-5). Another miRNA, miR-203, has been shown previously to target MYD88 (Wei et al. 2013), and transfection of inflammatory macrophages with miR-203 can lead to a reduction of inflammatory mediators. This suggests that miR-138 may be able to elicit a similar response through targeting of MYD88 within the sensory ganglia. Future experiments should seek to characterise the effect of miR-138 expression on inflammatory mediators, especially when you consider target predictions shown within this thesis (figure 3.2.4), and previous studies which have predicted or identified other targets for miR-

138 (Liu et al. 2013, X. Zhou et al. 2016) which may implicate this miRNA in inflammatory processes.

In order to further characterise the mechanisms that might be controlled by these miRNAs, this project developed *in vitro* models within which to study these processes with greater cellular and molecular detail. The presence of nociceptive sensory neuron subtypes within the embryonic sensory ganglia cultures used in our lab was an important validation of our work. This is especially relevant when considering previous literature, which suggests that embryonic sensory neuron cultures will not possess the relevant nociceptive sensory neuron subtypes (Marmigère & Ernfors 2007). The presence of the relevant sensory neuron subtypes was demonstrated through functional calcium imaging (Figure 4.2.1). Further to this, the recapitulation of the *in vivo* environment of the sensory neuron (i.e. the cell body and peripheral axon existing within different environments) through the use of microfluidic culture methods was also achieved (Figure 4.2.3). This method has been described previously (Neto et al. 2014; Silva et al. 2017; Tsantoulas et al. 2013), and the protocols contained with these previous studies formed the basis of the methodology implemented within this thesis. It was demonstrated additionally that within our cultures the functional assessment of the sensory neuron cultures is possible, and that the embryonic sensory neuron cultures extend functional capsaicin responsive axons through the microgrooves to allow stimulation via TRPV1 to elicit a response observable through calcium imaging. A similar approach was taken in a previous paper (Tsantoulas et al. 2013) however this was conducted on postnatal and adult DRG cultures.

Relevant to the assessment of miRNAs within the sensory neuron, and the independent functionalities and locations of the cell body and axon *in vivo*, the extraction of RNA samples from subcellular fractions was also required (figure 4.2.4). This was achieved through culture of DRG upon porous membranes which had been used previously to culture sensory neurons (Unsain et al. 2014), from which fractionated RNA can be extracted. Importantly, the suitability of the RNA for downstream qPCR analysis, and the absence of cell body contamination in the axonal

fraction was demonstrated in this work (figure 4.2.4). The culture of the sensory neuron cultures on porous membranes does not offer the fluidic isolation of the microfluidic culture method, however this will provide a useful complementary method when used in conjunction with the microfluidic culture method, as the extraction of RNA from the culture sub compartments of microfluidic devices has not yet been optimised.

Overall, this part of the thesis provides the first evidence of the dysregulation of miRNAs in hyperalgesic priming model of the transition from acute to chronic pain. It specifically analysed the potential role that these might have in the function the DRG, which lay at the basis of neuronal sensitisation processes. A novel role of miR-138 within this chronic inflammatory pain model was also proposed, through the targeting of MYD88. The work also paved the way for further investigation of miR-138 function, by establishing *in vitro* models that recapitulate neuronal compartmentalisation, and permit the more accurate study of inflammatory and nociceptive processes.

8.2. Investigation of individual miRNAs that control nervous system processes in *Drosophila* melanogaster

The development and function of the nervous system is a sophisticated process which requires the spatial and temporal control of protein expression. This can be controlled at the level of translation (Di Liegro et al. 2014; Jung et al. 2012; Sotelo-Silveira et al. 2006). As regulators of translation, which had already been implicated in the development and function of the nervous system, miRNAs were investigated within the model system of *Drosophila* as to their roles in the nervous system.

The Drosophila eye is an established model through which to investigate the developmental defects gene expression changes can induce in the nervous system (Thomas & Wassarman 1999). An initial screen of miRNAs that affect eye development in *Drosophila* made it possible to identify a list of miRNAs that could potentially regulate neuronal function and development (Chapter 5). This screen produced promising results for candidate miRNAs for further study, and when

compared to a previous similar screen of miRNA overexpression effects in the developing eye (Schertel et al. 2012) this study produced similar results, but with a higher rate of phenotype identification.

In the context of this work, a candidate from these identified miRNA, miR-190, was carried forward for further investigation. This candidate was selected based upon systematic assessment of existing targets (table 6.1.1), expression patterns (6.1.4) and previously published functions in non-neuronal models (Chapter 6.1.2). Whilst literature surrounding miR-190 implicated this miRNA in the development and functioning of the nervous system, there had been no explicit study in *Drosophila* as to the role or function of miR-190 in the nervous system.

A novel potential role for miR-190 in the development of the nervous system was uncovered. Overexpression of miR-190 within assays of the developing nervous system of *Drosophila* and mouse appeared to demonstrate miR-190 in high levels as detrimental to the developing nervous system (figure 6.2.3), whereas inhibition of miR-190 did not appear to lead to any gross developmental defects (figure 6.2.3). It was also demonstrated, through bioinformatics and luciferase assay, that miR-190 has the potential to function as an evolutionarily conserved regulator of Dac/DACH1 (figure 6.2.4-5). Previously published studies which sought to identify targets of miR-190 failed to uncover any targets which were conserved from *Drosophila* to mammals (table 6.1.1), this is therefore the first indication of a conserved target for miR-190 with a function in nervous system development. Overall, it was decided that the role uncovered for miR-190 in nervous system development might be that of an additional layer of control to the robust biological network which underlies the function of dac.

Beyond the potential role uncovered for miR190 in early development, a novel function for miR-190 within the mature nervous system circuitry was also demonstrated. Constitutive inhibition of miR-190 throughout postmitotic neurons leads to defects in the aged climbing ability and lifespan of *Drosophila* (figure 7.2.1-3). It was further shown that inhibition of miR-190 in cholinergic neurons alone can

lead to a reduction in the survivorship of adult *Drosophila*, implicating miR-190 as a possible regulator of the cholinergic system (7.2.3). Through bioinformatics, predicted targets for miR-190 which function within the cholinergic synapse were identified (figure 7.2.4). These results could highlight the cholinergic system as an overall regulatory target for miR-190 (figure 7.2.4). The identification of miR-190 as a probable modulator of the cholinergic system may in the future allow the use of miR-190 in *Drosophila* as a model for the investigation of the action of "cholinomiRs" (Nadorp & Soreq 2014; Simchovitz et al. 2017). As yet, a *Drosophila* model of these poorly conserved cholinergic system regulators has not been identified.

The proposed novel functions of miR-190 as both a developmental regulator, and mediator of aging in the nervous system of *Drosophila*, demonstrate the ability of an individual miRNA to function, dependent upon their spatial and temporal expression, as a regulator of multiple cell processes.

8.3 Future directions

Whilst the specific functions of the miRNA identified in this work will still require further investigation, the potential for miRNA research is vast, particularly as future biomarkers or therapeutic targets of disease.

Expression profiles of individual, or groups of, miRNAs have been suggested as potential biomarkers for disease states such as cancers (Scheffer et al. 2014), Alzheimer's disease (Cogswell et al. 2008) or even pain (Andersen et al. 2014). Levels of miRNAs can be detected in tissues affected by disease or disorder, or as circulating biomarkers in blood. One particularly interesting use of miRNAs as biomarkers is in the context of traumatic brain injury (Pietro et al. 2018). In this study the differential expression profiles of miRNAs in mild and severe traumatic brain injury were assessed, and the miRNA profiles observed were able to differentiate between the severity of the injury (Pietro et al. 2018). The profiling of miRNA signatures in disease may become a useful diagnostic tool. These approaches are suggested as an alternative to techniques which are complicated by a patient who may be presenting with potential life threatening condition, or traditional more invasive techniques.

miRNAs have shown great scope as possible therapeutics, as an alternative to targeting pathogenic proteins with small molecule inhibitors (van Rooij & Kauppinen 2014). One of the most prevalent cases is the use of miRavirsen (a miR-122 inhibitor) which has been in Phase II clinical trials for the treatment of Hepatitis C virus (HCV) since 2017 (Janssen et al. 2013). In the context of this work, miRNAs have also been identified as possible novel therapeutics in inflammation and pain, for example the case of miR-199 (Q. Zhou et al. 2016). Irritable bowel syndrome (IBS) is a condition which can present with abdominal pain and visceral hypersensitivity. It has been demonstrated that miR-199 levels decrease in both the colon and DRG in IBS cases, and this decrease correlates with an increase in TRPV1, a target of miR-199 (Q. Zhou et al. 2016). Intraperitoneal injection of miR-199 precursor in a rat model of visceral hypersensitivity leads to a decrease in TRPV1 expression and subsequent relief of visceral hypersensitivity (Q. Zhou et al. 2016). The miRNAs which were identified in this work could therefore in the future potentially be used as novel therapeutics in nervous system disorders.

8.4 General findings

The potential for the discovery of novel miRNA functions within the nervous system was demonstrated through two independent projects. Each initiated with the aim of identifying novel relevant miRNAs, either through microarray (Chapter 3) or a genetic screening process (Chapter 5). Both of these approaches provided a list of candidate miRNAs for further investigation, from which those for further study within this work were selected.

From this work, the novel roles which two miRNAs, miR-138 and miR-190, could play in the nervous system were investigated. miR-138-5p as a mediator of inflammatory pain, and miR-190 as a mediator of nervous system development and mature nervous system function. This work therefore demonstrates the scope of miRNA research.

In summary, this work identified novel roles for miRNAs in processes that regulate nervous system development and function. This work therefore contributes valuable knowledge to our current understanding of how the nervous system can develop and function.

9. Bibliography

Aboobaker, A. et al., 2005. Drosophila microRNAs exhibit diverse spatial expression patterns during embryonic development. *PNAS*, 102(50), pp.18017–18022.

Adachi, Y. et al., 2003. Conserved cis-regulatory modules mediate complex neural expression patterns of the eyeless gene in the Drosophila brain. *Mechanisms of Development*, 120(10), pp.1113–1126.

Adcock, J.J., 2009. TRPV1 receptors in sensitisation of cough and pain reflexes. *Pulmonary Pharmacology & Therapeutics*, 22(2), pp.65–70.

Afonso-Grunz, F. & Muller, S., 2015. Principles of miRNA-mRNA interactions: beyond sequence complementarity. *Cellular and molecular life sciences : CMLS*, 72(16), pp.3127–3141.

Agarwal, V. et al., 2015. Predicting effective microRNA target sites in mammalian mRNAs. *eLife*, 12(4), pp.1–38.

Aley, K.O. et al., 2000. Chronic hypersensitivity for inflammatory nociceptor sensitization mediated by the epsilon isozyme of protein kinase C. *The Journal of neuroscience*, 20(12), pp.4680–4685.

Almog, N. et al., 2013. Transcriptional changes induced by the tumor dormancy-associated microRNA-190. *Transcription*, 4(4), pp.177–191.

Ambros, V. et al., 2003. A uniform system for microRNA annotation. *RNA*, 9(3), pp.277-9.

Andersen, H.H., Duroux, M. & Gazerani, P., 2014. MicroRNAs as modulators and biomarkers of inflammatory and neuropathic pain conditions. *Neurobiology of disease*, 71, pp.159–168.

Anderson, J., Salzer, C.L. & Kumar, J.P., 2006. Regulation of the retinal determination gene dachshund in the embryonic head and developing eye of Drosophila. *Developmental Biology*, 297(2), pp.536–549.

Andrés-León, E. et al., 2015. miRGate: a curated database of human, mouse and rat miRNA-mRNA targets. *Database : the journal of biological databases and curation*, 2015, pp.1–9.

Aranha, M.M. et al., 2011. miR-34a Regulates Mouse Neural Stem Cell Differentiation. *PLOS ONE*, 6(8), p.e21396.

Artzi, S., Kiezun, A. & Shomron, N., 2008. miRNAminer: A tool for homologous

microRNA gene search. *BMC Bioinformatics*, 9(1), p.39.

Ashburner, M., Golic, K.G. & Hawley, R.S., 2005. *Drosophila. A laboratory handbook.* 18th ed., Cold Spring Harbor, New York: Cold Spring Harbor Laboratory Press.

Ataman, B. et al., 2008. Rapid activity-dependent modifications in synaptic structure and function require bidirectional Wnt signaling. *Neuron*, 57(5), pp.705–718.

Austin, P.J., Wu, A. & Moalem-Taylor, G., 2012. Chronic constriction of the sciatic nerve and pain hypersensitivity testing in rats. *Journal of visualized experiments : JoVE*, (61).

Azevedo, F.A.C. et al., 2009. Equal numbers of neuronal and nonneuronal cells make the human brain an isometrically scaled-up primate brain. *The Journal of Comparative Neurology*, 513(5), pp.532–541.

Backman, M. et al., 2003. Targeted disruption of mouse Dach1 results in postnatal lethality. *Developmental dynamics : an official publication of the American Association of Anatomists*, 226(1), pp.139–144.

Bahassi el M., Stambrook, P.J, 2014. Next-generation sequencing technologies: breaking the sound barrier of human genetics. *Mutagenesis,* 29(5) pp.303-10

Bai, G. et al., 2007. Downregulation of selective microRNAs in trigeminal ganglion neurons following inflammatory muscle pain. *Molecular Pain*, 3, p.15.

Bajjalieh, S.M., 1999. Synaptic vesicle docking and fusion. *Current opinion in neurobiology*, 9(3), pp.321–328.

Bali, K.K. et al., 2013. Genome-wide identification and functional analyses of microRNA signatures associated with cancer pain. *EMBO Molecular Medicine*, 5(11), pp.1740–1758.

Banerjee, A. & Roy, J.K., 2018. Bantam regulates the axonal geometry of Drosophila larval brain by modulating actin regulator enabled. *Invertebrate neuroscience : IN*, 18(2), p.7.

Barabas, M.E., Kossyreva, E.A. & Stucky, C.L., 2012. TRPA1 is functionally expressed primarily by IB4-binding, non-peptidergic mouse and rat sensory neurons. *PloS one*, 7(10), p.e47988.

Barnes, A.P. & Polleux, F., 2009. Establishment of axon-dendrite polarity in developing neurons. *Annual review of neuroscience*, 32, pp.347–381.

Bartel, D.P., 2004. MicroRNAs: Genomics, Biogenesis, Mechanism, and Function. *Cell*,

116(2), pp.281–297.

Bartel, D.P., 2009. MicroRNAs: target recognition and regulatory functions. *Cell*, 136(2), pp.215–233.

Batista, A.F.R. & Hengst, U., 2016. Intra-axonal protein synthesis in development and beyond. *International Journal of Developmental Neuroscience*, 55, pp.140–149.

Baud, V. & Karin, M., 2001. Signal transduction by tumor necrosis factor and its relatives. *Trends in cell biology*, 11(9), pp.372–377.

Beezhold, K. et al., 2011. miR-190-mediated downregulation of PHLPP contributes to arsenic-induced Akt activation and carcinogenesis. *Toxicological sciences : an official journal of the Society of Toxicology*, 123(2), pp.411–420.

Bejarano, F. et al., 2012. A genome-wide transgenic resource for conditional expression of Drosophila microRNAs. *Development (Cambridge, England)*, 139(15), pp.2821–2831.

Ben-Hamo, R. & Efroni, S., 2015. MicroRNA regulation of molecular pathways as a generic mechanism and as a core disease phenotype. *Oncotarget*, 6(3), pp.1594–604.

Berger, C. et al., 2007. The commonly used marker ELAV is transiently expressed in neuroblasts and glial cells in the Drosophila embryonic CNS. *Developmental dynamics : an official publication of the American Association of Anatomists*, 236(12), pp.3562–3568.

Berridge, M.J., Bootman, M.D. & Roderick, H.L., 2003. Calcium signalling: dynamics, homeostasis and remodelling. *Nature reviews. Molecular cell biology*, 4(7), pp.517–529.

Betel, D. et al., 2008. The microRNA.org resource: Targets and expression. *Nucleic Acids Research*, 36(SUPPL. 1), pp.149–153.

Bhattacharyya, S.N. et al., 2006. Relief of microRNA-mediated translational repression in human cells subjected to stress. *Cell*, 125(6), pp.1111–1124.

Bilen, J. & Bonini, N.M., 2005. Drosophila as a model for human neurodegenerative disease. *Annual review of genetics*, 39, pp.153–171.

Bliim, N. et al., 2016. Transcriptional regulation of long-term potentiation. *Neurogenetics*, 17(4), pp.201–210.

Bouleau, S. & Tricoire, H., 2015. Drosophila models of Alzheimer's disease: advances,

limits, and perspectives. *Journal of Alzheimer's disease : JAD*, 45(4), pp.1015–1038.

Bouvier, D.S. & Murai, K.K., 2015. Synergistic actions of microglia and astrocytes in the progression of Alzheimer's disease. *Journal of Alzheimer's disease : JAD*, 45(4), pp.1001–14.

Brand, A.H. & Perrimon, N., 1993. Targeted gene expression as a means of altering cell fates and generating dominant phenotypes. *Development (Cambridge, England)*, 118(2), pp.401–415.

Brennecke, J. et al., 2003. bantam encodes a developmentally regulated microRNA that controls cell proliferation and regulates the proapoptotic gene hid in Drosophila. *Cell*, 113(1), pp.25–36.

Brenneis, C. et al., 2013. Phenotyping the function of TRPV1-expressing sensory neurons by targeted axonal silencing. *The Journal of neuroscience : the official journal of the Society for Neuroscience*, 33(1), pp.315–326.

Bronisz, A., Godlewski, J. & Chiocca, E.A., 2016. Extracellular Vesicles and MicroRNAs: Their Role in Tumorigenicity and Therapy for Brain Tumors. *Cellular and molecular neurobiology*, 36(3), pp.361–376.

Brown, N.H. et al., 2002. Talin Is Essential for Integrin Function in Drosophila. *Developmental Cell*, 3(4), pp.569–579.

Buffelli, M. et al., 2003. Genetic evidence that relative synaptic efficacy biases the outcome of synaptic competition. *Nature*, 424, p.430.

Bustin, S.A., 2002. Quantification of mRNA using real-time reverse transcription PCR (RT-PCR): trends and problems. *Journal of molecular endocrinology*, 29(1), pp.23–39.

Busto, G.U. et al., 2015. Micrornas that promote or inhibit memory formation in drosophila melanogaster. *Genetics*, 200(2), pp.569–580.

Byrne, F.M. et al., 2015. Characterisation of pain responses in the high fat diet/streptozotocin model of diabetes and the analgesic effects of antidiabetic treatments. *Journal of diabetes research*, 2015, p.752481.

Cai, X., Hagedorn, C.H. & Cullen, B.R., 2004. Human microRNAs are processed from capped, polyadenylated transcripts that can also function as mRNAs. *RNA (New York, N.Y.)*, 10(12), pp.1957–1966.

Cajigas, I.J. et al., 2012. The local transcriptome in the synaptic neuropil revealed by deep sequencing and high-resolution imaging. *Neuron*, 74(3), pp.453–466.

Calil, I.L. et al., 2014. Lipopolysaccharide induces inflammatory hyperalgesia triggering a TLR4/MyD88-dependent cytokine cascade in the mice paw. *PLoS ONE*, 9(3), pp.2–9.

Call, G.B. et al., 2007. Genomewide Clonal Analysis of Lethal Mutations in the Drosophila melanogaster Eye: Comparison of the X Chromosome and Autosomes. *Genetics*, 177(2), pp.689–697.

Callaerts, P. et al., 2001. Drosophila Pax-6/eyeless is essential for normal adult brain structure and function. *Journal of neurobiology*, 46(2), pp.73–88.

Campbell, D.S. & Holt, C.E., 2001. Chemotropic responses of retinal growth cones mediated by rapid local protein synthesis and degradation. *Neuron*, 32(6), pp.1013–1026.

Campos-Ortega, J.A. & Hartenstein, V., 1997. *The Embryonic Development of Drosophila melanogaster* 2nd ed., Berlin/Heidelberg: Springer-Verlag.

Carr, F.B. & Zachariou, V., 2014. Nociception and pain: lessons from optogenetics. *Frontiers in behavioral neuroscience*, 8, p.69.

Carthew, R.W., Agbu, P. & Giri, R., 2017. MicroRNA function in Drosophila melanogaster. *Seminars in Cell & Developmental Biology*, 65, pp.29–37.

Caygill, E.E. & Brand, A.H., 2017. miR-7 Buffers Differentiation in the Developing Drosophila Visual System. *Cell Reports*, 20(6), pp.1255–1261.

Chaplan, S.R. et al., 1994. Quantitative assessment of tactile allodynia in the rat paw. *Journal of Neuroscience Methods*, 53(1), pp.55–63.

Chen, K. & Rajewsky, N., 2006. Natural selection on human microRNA binding sites inferred from SNP data. *Nature genetics*, 38(12), pp.1452–1456.

Chen, Y. et al., 2014. Resource Systematic Study of Drosophila MicroRNA Functions Using a Collection of Targeted Knockout Mutations. *Developmental Cell*, 31(6), pp.784–800.

Cheng, J.-K. & Ji, R.-R., 2008. Intracellular signaling in primary sensory neurons and persistent pain. *Neurochemical research*, 33(10), pp.1970–1978.

Chi, S.W. et al., 2009. Argonaute HITS-CLIP decodes microRNA-mRNA interaction maps. *Nature*, 460(7254), pp.479–486.

Clark, M.Q. et al., 2018. Neural circuits driving larval locomotion in Drosophila. *Neural development*, 13(1), p.6.

Clayton, K.A., Van Enoo, A.A. & Ikezu, T., 2017. Alzheimer's Disease: The Role of Microglia in Brain Homeostasis and Proteopathy. *Frontiers in Neuroscience*, 11, p.680.

Cogswell, J.P. et al., 2008. Identification of miRNA changes in Alzheimer's disease brain and CSF yields putative biomarkers and insights into disease pathways. *Journal of Alzheimer's disease : JAD*, 14(1), pp.27–41.

Cosker, K.E. & Segal, R.A., 2014. Neuronal signaling through endocytosis. *Cold Spring Harbor Perspectives in Biology*, 6(2), pp.1–16.

Cramer, E.M. et al., 2014. miR-190 is upregulated in Epstein-Barr Virus type I latency and modulates cellular mRNAs involved in cell survival and viral reactivation. *Virology*, 464–465, pp.184–195.

Crittenden, J.R. et al., 1998. Tripartite Mushroom Body Architecture Revealed by Antigenic Markers. *Learning & Memory*, 5(1), pp.38–51.

Dajas-Bailador, F. et al., 2012. microRNA-9 regulates axon extension and branching by targeting Map1b in mouse cortical neurons. *Nature Neuroscience*, 15(5), pp.697–699.

Dani, A. et al., 2010. Superresolution imaging of chemical synapses in the brain. *Neuron*, 68(5), pp.843–856.

Daou, I. et al., 2016. Optogenetic silencing of NaV1.8-positive afferents alleviates inflammatory and neuropathic pain. *eneuro*.

Deguine, J. & Barton, G.M., 2014. MyD88: a central player in innate immune signaling. *F1000Prime Reports*, 6, p.97.

Delcroix, J.-D. et al., 2003. NGF Signaling in Sensory Neurons. *Neuron*, 39(1), pp.69–84.

Denno, M.E., Privman, E. & Venton, B.J., 2015. Analysis of neurotransmitter tissue content of Drosophila melanogaster in different life stages. *ACS chemical neuroscience*, 6(1), pp.117–123.

Derry, M.C. et al., 2006. Regulation of poly(A)-binding protein through PABP-interacting proteins. *Cold Spring Harbor symposia on quantitative biology*, 71, pp.537–543.

Didiano, D. & Hobert, O., 2006. Perfect seed pairing is not a generally reliable predictor for miRNA-target interactions. *Nat Struct Mol Biol*, 13.

Dotti, C.G., Sullivan, C.A. & Banker, G.A., 1988. The establishment of polarity by hippocampal neurons in culture. *The Journal of neuroscience : the official journal of the Society for Neuroscience*, 8(4), pp.1454–1468.

Douglas, P. M., & Cyr, D. M., 2010. Interplay between protein homeostasis networks in protein aggregation and proteotoxicity. *Biopolymers*, 93(3), pp.229-36.

Duman-Scheel, M., 2009. Netrin and DCC: axon guidance regulators at the intersection of nervous system development and cancer. *Current drug targets*, 10(7), pp.602–610.

Eacker, S.M. et al., 2011. Neuronal activity regulates hippocampal miRNA expression. *PLoS ONE*, 6(10).

Ebert, M. & Sharp, P., 2012. Roles of miRNAs in conferring robustness to biological processes. *Cell*, 149(3), pp.515–524.

Ebert, M.S. & Sharp, P.A., 2010. MicroRNA sponges: progress and possibilities. *RNA (New York, N.Y.)*, 16(11), pp.2043–2050.

Edbauer, D. et al., 2010. Regulation of Synaptic Structure and Function by FMRP-Associated MicroRNAs miR-125b and miR-132. *Neuron*, 65(3), pp.373–384.

Edelstein, A.D. et al., 2014. Advanced methods of microscope control using μManager software. *Journal of Biological Methods*, 1(2), p.e10.

Egger, B. et al., 2013. In vitro imaging of primary neural cell culture from Drosophila. *Nature Protocols*, 8(5), pp.958–965.

Enright, A.J. et al., 2003. MicroRNA targets in Drosophila. *Genome biology*, 5(1), p.R1.

Ettorre, M. et al., 2012. Glutamatergic Neurons Induce Expression of Functional Glutamatergic Synapses in Primary Myotubes P. Wenner, ed. *PLoS ONE*, 7(2), p.e31451.

Eulalio, A., Helms, S., et al., 2009. A C-terminal silencing domain in GW182 is essential for miRNA function. *RNA (New York, N.Y.)*, 15(6), pp.1067–1077.

Eulalio, A., Huntzinger, E., et al., 2009. Deadenylation is a widespread effect of miRNA regulation. *RNA (New York, N.Y.)*, 15(1), pp.21–32.

Eulalio, A., Huntzinger, E. & Izaurralde, E., 2008. GW182 interaction with Argonaute is essential for miRNA-mediated translational repression and mRNA decay.

Nature structural & molecular biology, 15(4), pp.346–353.

Evans, T.A. & Bashaw, G.J., 2010. Axon guidance at the midline: of mice and flies. *Current Opinion in Neurobiology*, 20(1), pp.79–85.

Fabian, M.R. et al., 2009. Mammalian miRNA RISC recruits CAF1 and PABP to affect PABP-dependent deadenylation. *Molecular cell*, 35(6), pp.868–880.

Fabian, M.R. et al., 2011. miRNA-mediated deadenylation is orchestrated by GW182 through two conserved motifs that interact with CCR4-NOT. *Nature structural & molecular biology*, 18(11), pp.1211–1217.

Fabian, M.R. & Sonenberg, N., 2012. The mechanics of miRNA-mediated gene silencing: A look under the hood of miRISC. *Nature Structural &Molecular Biology*, 19(6), pp.586–593.

Fatt, P. & Katz, B., 1952. Spontaneous subthreshold activity at motor nerve endings. *The Journal of Physiology*, 117(1), pp.109–128.

Fayaz, A. et al., 2016. Prevalence of chronic pain in the UK: a systematic review and meta-analysis of population studies. *BMJ Open*, 6(6), p.e010364.

Fenton, B.W., Shih, E. & Zolton, J., 2015. The neurobiology of pain perception in normal and persistent pain. *Pain management*, 5(4), pp.297–317.

Ferrari, L.F., Bogen, O., et al., 2015. Accounting for the Delay in the Transition from Acute to Chronic Pain: Axonal and Nuclear Mechanisms. *The Journal of Neuroscience*, 35(2), pp.495–507.

Ferrari, L.F. et al., 2013. Peripheral administration of translation inhibitors reverses increased hyperalgesia in a model of chronic pain in the rat. *Journal of Pain*, 14(7), pp.731-738.

Ferrari, L.F., Araldi, D. & Levine, J.D., 2015. Distinct Terminal and Cell Body Mechanisms in the Nociceptor Mediate Hyperalgesic Priming. *The Journal of Neuroscience*, 35(15), pp.6107–6116.

Fiore, R. & Schratt, G., 2007. MicroRNAs in synapse development: tiny molecules to remember. *Expert Opinion on Biological Therapy*, 7(12), pp.1823–1831.

Fiorenza, A. et al., 2016. Blocking miRNA Biogenesis in Adult Forebrain Neurons Enhances Seizure Susceptibility, Fear Memory, and Food Intake by Increasing Neuronal Responsiveness. *Cerebral cortex*, 26(4), pp.1619–1633.

Flexner, J.B., Flexner, L.B. & Stellar, E., 1963. Memory in mice as affected by

intracerebral puromycin. *Science*, 141(3575), pp.57–59.

Frost, R.J.A. & Olson, E.N., 2011. Control of glucose homeostasis and insulin sensitivity by the Let-7 family of microRNAs. *Proceedings of the National Academy of Sciences*, 108(52), pp.21075–21080.

Fulga, T.A. et al., 2015. A transgenic resource for conditional competitive inhibition of conserved Drosophila microRNAs. *Nature Communications*, 6(7279).

Funakoshi, Y. et al., 2007. Mechanism of mRNA deadenylation: Evidence for a molecular interplay between translation termination factor eRF3 and mRNA deadenylases. *Genes and Development*, 21(23), pp.3135–3148.

Gargano, J.W. et al., 2005. Rapid iterative negative geotaxis (RING): A new method for assessing age-related locomotor decline in Drosophila. *Experimental Gerontology*, 40(5), pp.386–395.

Gatto, C.L. & Broadie, K., 2011. Drosophila Modeling of Heritable Neurodevelopmental Disorders. *Current Opinion in Neurobiology*, 21(6), pp.834–841.

Getahun, M.N. et al., 2013. Insect odorant response sensitivity is tuned by metabotropically autoregulated olfactory receptors. *PloS one*, 8(3), p.e58889.

Ghahramani Seno, M.M. et al., 2011. Gene and miRNA expression profiles in autism spectrum disorders. *Brain research*, 1380, pp.85–97.

Giraldez, A.J. et al., 2005. MicroRNAs regulate brain morphogenesis in zebrafish. *Science*, 308(5723), pp.833–838.

Grienberger, C. & Konnerth, A., 2012. Imaging Calcium in Neurons. *Neuron*, 73(5), pp.862–885.

Grimson, A. et al., 2007. MicroRNA targeting specificity in mammals: determinants beyond seed pairing. *Molecular cell*, 27(1), pp.91–105.

Grueber, W.B., Jan, L.Y. & Jan, Y.N., 2002. Tiling of the Drosophila epidermis by multidendritic sensory neurons. *Development (Cambridge, England)*, 129(12), pp.2867–78.

Guhaniyogi, J. & Brewer, G., 2001. Regulation of mRNA stability in mammalian cells. *Gene*, 265(1–2), pp.11–23.

Gumy, L.F. et al., 2011. Transcriptome analysis of embryonic and adult sensory axons reveals changes in mRNA repertoire localization. *RNA*, 17(1), pp.85–98.

Gunthorpe, M.J. et al., 2002. The diversity in the vanilloid (TRPV) receptor family of ion channels. *Trends in pharmacological sciences*, 23(4), pp.183–191.

Ha, M. & Kim, V.N., 2014. Regulation of microRNA biogenesis. *Nature Reviews Molecular Cell Biology*, 15(8), pp.509–524.

Halder, G., Callaerts, P. & Gehring, W.J., 1995. Induction of ectopic eyes by targeted expression of the eyeless gene in Drosophila. *Science*, 267(5205), pp.1788–1792.

Hammond, K.L. et al., 1998. Mammalian and Drosophila dachshund genes are related to the Ski proto-oncogene and are expressed in eye and limb. *Mechanisms of Development*, 74(1), pp.121–131.

Hao, Y. et al., 2014. The synergistic regulation of VEGF-mediated angiogenesis through miR-190 and target genes. *RNA*, 20(8), pp.1328–1336.

Harris, R.M. et al., 2015. Neuron hemilineages provide the functional ground plan for the Drosophila ventral nervous system L. C. Griffith, ed. *eLife*, 4, p.e04493.

Harris, W. a, Holt, C.E. & Bonhoeffer, F., 1987. Retinal axons with and without their somata, growing to and arborizing in the tectum of Xenopus embryos: a time-lapse video study of single fibres in vivo. *Development (Cambridge, England)*, 101(1), pp.123–133.

Harrison, B.J. et al., 2014. IB4-binding sensory neurons in the adult rat express a novel 3′ UTR-extended isoform of CaMK4 that is associated with its localization to axons. *The Journal of comparative neurology*, 522(2), p.10.1002/cne.23398.

Hartenstein, V. & Brody, T., 1999. Atlas of Drosophila development. *The interactive fly:gene networks development and the internet*. Available at: http://www.sdbonline.org/sites/fly/atlas/00atlas.htm.

Heine, P., Ehrlicher, A. & Kas, J., 2015. Neuronal and metastatic cancer cells: Unlike brothers. *Biochimica et biophysica acta*, 1853(11 Pt B), pp.3126–3131.

Hershey, J.W.B., Sonenberg, N. & Mathews, M.B., 2012. Principles of translational control: An overview. *Cold Spring Harbor Perspectives in Biology*, 4(12), pp.1–10.

Hetz, C., & Glimcher, L. H., 2011. Protein homeostasis networks in physiology and disease. *Current opinion in cell biology*, 23.

Hipfner, D.R., Weigmann, K. & Cohen, S.M., 2002. The bantam gene regulates

Drosophila growth. *Genetics*, 161(4), pp.1527–1537.

Hong, W. & Luo, L., 2014. Genetic control of wiring specificity in the fly olfactory system. *Genetics*, 196(1), pp.17–29.

Hu, Z. & Li, Z., 2017. miRNAs in synapse development and synaptic plasticity. *Current opinion in neurobiology*, 45, pp.24–31.

Huang, R.P., 2004. Cytokine protein arrays. *Methods in Molecular Biology*, 264, pp.215–231.

Hung, T.-M. et al., 2014. Up-regulation of microRNA-190b plays a role for decreased IGF-1 that induces insulin resistance in human hepatocellular carcinoma. *PloS one*, 9(2), p.e89446.

Hutvagner, G. et al., 2004. Sequence-specific inhibition of small RNA function. *PLoS biology*, 2(4), p.e98.

Iftikhar, H. et al., 2017. The in vivo genetic toolkit for studying expression and functions of Drosophila melanogaster microRNAs. *RNA Biology*, 14(2), pp.179–187.

Iyer, A.N., Bellon, A. & Baudet, M.-L., 2014. microRNAs in axon guidance. *Frontiers in cellular neuroscience*, 14(8), p.78.

Iyer, J. et al., 2016. Quantitative Assessment of Eye Phenotypes for Functional Genetic Studies Using Drosophila melanogaster. *G3 (Bethesda, Md.)*, 6(5), pp.1427–37.

Jackson, T.C. et al., 2010. PHLPP1 splice variants differentially regulate AKT and PKCalpha signaling in hippocampal neurons: characterization of PHLPP proteins in the adult hippocampus. *Journal of neurochemistry*, 115(4), pp.941–955.

Janssen, H.L.A. et al., 2013. Treatment of HCV infection by targeting microRNA. *The New England journal of medicine*, 368(18), pp.1685–1694.

Jarecki, J. & Keshishian, H., 1995. Role of neural activity during synaptogenesis in Drosophila. *The Journal of neuroscience : the official journal of the Society for Neuroscience*, 15(12), pp.8177–8190.

Jeibmann, A. & Paulus, W., 2009. Drosophila melanogaster as a model organism of brain diseases. *International Journal of Molecular Sciences*, 10(2), pp.407–440.

Ji, R.-R. et al., 2018. Neuroinflammation and Central Sensitization in Chronic and Widespread Pain. *Anesthesiology*, 129(2), p.1.

Ji, R.R. et al., 2003. Central sensitization and LTP: Do pain and memory share similar mechanisms? *Trends in Neurosciences*, 26(12), pp.696–705.

Jia, W.-Z. et al., 2016. MicroRNA-190 regulates FOXP2 genes in human gastric cancer. *OncoTargets and therapy*, 9, pp.3643–3651.

Jiang, N. et al., 2014. The microRNA bantam regulates a developmental transition in epithelial cells that restricts sensory dendrite growth. *Development (Cambridge, England)*, 141(13), pp.2657–2668.

Jimé Nez-Díaz, L. et al., 2008. Local Translation in Primary Afferent Fibers Regulates Nociception. *PLoS ONE*, 3(4), p.e1961.

Jin, Y. et al., 2013. Evaluating the microRNA targeting sites by luciferase reporter gene assay. *Methods in molecular biology (Clifton, N.J.)*, 936, pp.117–127.

Johnston, R.J. & Hobert, O., 2003. A microRNA controlling left/right neuronal asymmetry in Caenorhabditis elegans. *Nature*, 426(6968), pp.845–849.

Jung, H., Yoon, B.C. & Holt, C.E., 2012. Axonal mRNA localization and local protein synthesis in nervous system assembly, maintenance and repair. *Nature Reviews Neuroscience*, 13(7), pp.514–514.

Kandasamy, R. & Price, T.J., 2015. The pharmacology of nociceptor priming. *Handbook of experimental pharmacology*, 227, pp.15–37.

Kapur, M., Monaghan, C.E. & Ackerman, S.L., 2017. Regulation of mRNA Translation in Neurons—A Matter of Life and Death. *Neuron*, 96(3), pp.616–637.

Kavaler, J. et al., 2018. miRNA suppression of a Notch repressor directs nonneuronal fate in Drosophila mechanosensory organs. *Journal of Cell Biology*, 217(2), pp.571–583.

Kays, J. et al., 2018. Peripheral Synthesis of an Atypical Protein Kinase C Mediates the Enhancement of Excitability and the Development of Mechanical Hyperalgesia Produced by Nerve Growth Factor. *Neuroscience*, 371, pp.420–432.

Kedde, M. et al., 2010. A Pumilio-induced RNA structure switch in p27-3' UTR controls miR-221 and miR-222 accessibility. *Nature cell biology*, 12(10), pp.1014–1020.

Kedersha, N. et al., 2005. Stress granules and processing bodies are dynamically linked sites of mRNP remodeling. *The Journal of cell biology*, 169(6), pp.871–884.

Kertesz, M. et al., 2007. The role of site accessibility in microRNA target recognition. *Nature Genetics*, 39, p.1278.

Kevenaar, J.T. & Hoogenraad, C.C., 2015. The axonal cytoskeleton: from organization to function. *Frontiers in Molecular Neuroscience*, 14(8), p.44..

Khvorova, A., Reynolds, A. & Jayasena, S.D., 2003. Functional siRNAs and miRNAs exhibit strand bias. *Cell*, 115(2), pp.209–216.

Kiezun, A. et al., 2012. miRviewer: a multispecies microRNA homologous viewer. *BMC Research Notes*, 5, p.92.

Kishino T. et al., (1997). UBE3A/E6-AP mutations cause Angelman syndrome. *Nat. Genet*. 15(1), pp.70–73.

Koenig, E. et al., 2000. Cryptic peripheral ribosomal domains distributed intermittently along mammalian myelinated axons. *The Journal of neuroscience : the official journal of the Society for Neuroscience*, 20(22), pp.390–400.

Kohsaka, H., Guertin, P.A. & Nose, A., 2017. Neural Circuits Underlying Fly Larval Locomotion. *Current Pharmaceutical Design*, 23(12), pp.1722–1733.

Koritzinsky, M. et al., 2006. Gene expression during acute and prolonged hypoxia is regulated by distinct mechanisms of translational control. *EMBO Journal*, 25(5), pp.1114–1125.

Kos, A. et al., 2016. MicroRNA-181 promotes synaptogenesis and attenuates axonal outgrowth in cortical neurons. *Cellular and molecular life sciences : CMLS*, 73(18), pp.3555–3567.

Kozomara, A. et al., 2014. Target Repression Induced by Endogenous microRNAs: Large Differences, Small Effects. *PLOS ONE*, 9(8), p.e104286.

Kozomara, A. & Griffiths-Jones, S., 2014. MiRBase: Annotating high confidence microRNAs using deep sequencing data. *Nucleic Acids Research*, 42(D1), pp.68–73.

Krishnan, K. et al., 2013. MicroRNA-182-5p targets a network of genes involved in DNA repair. *RNA,* 19(2), pp.230–242.

Kumar, J.P., 2009. The Molecular Circuitry Governing Retinal Determination. *Biochimica et biophysica acta*, 1789(4), pp.306–314.

Kusuda, R. et al., 2011. Differential expression of microRNAs in mouse pain models.

Molecular Pain, 7, p.17.

Kye, M.J. et al., 2011. NMDA mediated contextual conditioning changes miRNA expression. *PLoS ONE*, 6(9), pp.1–15.

Lagos-Quintana, M. et al., 2003. New microRNAs from mouse and human. *RNA*, 9(2), pp.175–179.

Lai, Y.-W. et al., 2016. Drosophila microRNA-34 Impairs Axon Pruning of Mushroom Body γ Neurons by Downregulating the Expression of Ecdysone Receptor. *Scientific Reports*, 6, p.39141.

Landgraf, M. & Thor, S., 2006. Development of Drosophila motoneurons: Specification and morphology. *Seminars in Cell and Developmental Biology*, 17(1), pp.3–11.

Landgraf, P. et al., 2007. A mammalian microRNA expression atlas based on small RNA library sequencing. *Cell*, 129(7), pp.1401–1414.

Latremoliere, A. & Woolf, C.J., 2009. Central Sensitization: A Generator of Pain Hypersensitivity by Central Neural Plasticity. *The journal of pain : official journal of the American Pain Society*, 10(9), pp.895–926.

Lee, H. et al., 2016. Biogenesis and regulation of the let-7 miRNAs and their functional implications. *Protein and Cell*, 7(2), pp.100–113.

Lee, I. et al., 2009. New class of microRNA targets containing simultaneous 5'-UTR and 3 '-UTR interaction sites. *Genome Research*, 19, pp.1175–1183.

Lee, R.C., 1993. The C . elegans Heterochronic Gene lin-4 Encodes Small RNAs with Antisense Complementarity to & II-14. *Cell*, 75, pp.843–854.

Lee, S.-K. & Hollenbeck, P.J., 2003. Organization and translation of mRNA in sympathetic axons. *Journal of cell science*, 116(Pt 21), pp.4467–4478.

Lee, T. et al., 2015. Dosage and temporal thresholds in microRNA proteomics. *Molecular & cellular proteomics : MCP*, 14(2), pp.289–302.

Lee, Y. et al., 2004. MicroRNA genes are transcribed by RNA polymerase II. *The EMBO journal*, 23(20), pp.4051–4060.

Lehmann, S.M. et al., 2012. An unconventional role for miRNA: let-7 activates Toll-like receptor 7 and causes neurodegeneration. *Nature Neuroscience*, 15(6), pp.827–835.

Lei, L. et al., 2005. The zinc finger transcription factor Klf7 is required for TrkA gene

expression and development of nociceptive sensory neurons. *Genes & development*, 19(11), pp.1354–1364.

Leitman J, et al., 2014. ER Stress-Induced eIF2-alpha Phosphorylation Underlies Sensitivity of Striatal Neurons to Pathogenic Huntingtin. *PloS one,* 9(3): e90803.

De Lella Ezcurra, A.L. et al., 2016. miR-190 Enhances HIF-Dependent Responses to Hypoxia in Drosophila by Inhibiting the Prolyl-4-hydroxylase Fatiga. *PLoS genetics*, 12(5), p.e1006073.

Lewis, B.P., Burge, C.B. & Bartel, D.P., 2005. Conserved seed pairing, often flanked by adenosines, indicates that thousands of human genes are microRNA targets. *Cell*, 120(1), pp.15–20.

Lewis, T.L., Courchet, J. & Polleux, F., 2013. Cell biology in neuroscience: Cellular and molecular mechanisms underlying axon formation, growth, and branching. *The Journal of cell biology*, 202(6), pp.837–48.

Li, S.S. et al., 2014. MicroRNA-190 regulates hypoxic pulmonary vasoconstriction by targeting a voltage-gated K(+) channel in arterial smooth muscle cells. *Journal of cellular biochemistry*, 115(6), pp.1196–1205.

Li, X. & Carthew, R.W., 2005. A microRNA mediates EGF receptor signaling and promotes photoreceptor differentiation in the Drosophila eye. *Cell*, 123(7), pp.1267–1277.

Li, Y. et al., 2017. Dorsal root ganglion neurons become hyperexcitable and increase expression of voltage-gated T-type calcium channels (Cav3.2) in paclitaxel-induced peripheral neuropathy. *PAIN*, 158(3), pp.417-429.

Di Liegro, C.M., Schiera, G. & Di Liegro, I., 2014. Regulation of mRNA transport, localization and translation in the nervous system of mammals. *International Journal of Molecular Medicine*, 33(4), pp.747–762.

Lin, Y.-C. & Koleske, A.J., 2010. Mechanisms of synapse and dendrite maintenance and their disruption in psychiatric and neurodegenerative disorders. *Annual review of neuroscience*, 33, pp.349–378.

Linford, N.J. et al., 2013. Measurement of Lifespan in Drosophila melanogaster. *Journal of Visualized Experiments*, (71), pp.1–9.

Lippi, G. et al., 2011. Targeting of the Arpc3 actin nucleation factor by miR-29a/b regulates dendritic spine morphology. *The Journal of Cell Biology*, 194(6), p.889-

904.

Liu, C. G. et al., 2004. An oligonucleotide microchip for genome-wide microRNA profiling in human and mouse tissues. *PNAS*, 101(26), 9740-4.

Liu, C.-M. et al., 2013. MicroRNA-138 and SIRT1 form a mutual negative feedback loop to regulate mammalian axon regeneration. *Genes & development*, 27(13), pp.1473–1483.

Liu, F. et al., 2017. Suppression of MyD88-dependent signaling alleviates neuropathic pain induced by peripheral nerve injury in the rat. *Journal of neuroinflammation*, 14(1), p.70.

Liu, N. et al., 2012. The microRNA miR-34 modulates ageing and neurodegeneration in Drosophila. *Nature*, 482(7386), pp.519–523.

Liu, X.-J. et al., 2016. TLR signaling adaptor protein MyD88 in primary sensory neurons contributes to persistent inflammatory and neuropathic pain and neuroinflammation. *Scientific Reports*, 6, p.28188.

Long, S.K.R. et al., 2014. A Comparison of Midline and Tracheal Gene Regulation during Drosophila Development. *PLOS ONE*, 9(1), p.e85518.

Looger, L.L. & Griesbeck, O., 2012. Genetically encoded neural activity indicators. *Current Opinion in Neurobiology*, 22(1), pp.18–23.

Lord, K.A., Hoffman-Liebermann, B. & Liebermann, D.A., 1990. Nucleotide sequence and expression of a cDNA encoding MyD88, a novel myeloid differentiation primary response gene induced by IL6. *Oncogene*, 5(7), pp.1095–1097.

Lowery, L.A. & Van Vactor, D., 2009. The trip of the tip: understanding the growth cone machinery. *Nature reviews. Molecular cell biology*, 10(5), pp.332–343.

Loya, C.M. et al., 2009. Transgenic microRNA inhibition with spatiotemporal specificity in intact organisms. *Nature methods*, 6(12), pp.897–903.

Lu, C.S. et al., 2014. MicroRNA-8 promotes robust motor axon targeting by coordinate regulation of cell adhesion molecules during synapse development. *Philosophical Transactions of the Royal Society B: Biological Sciences*, 369(1652), p.20130517.

Lu, Y.C. et al., 2014. ELAVL1 modulates transcriptome-wide miRNA binding in murine macrophages. *Cell reports*, 9(6), pp.2330–2343.

Lugli, G. et al., 2008. Expression of microRNAs and their precursors in synaptic

fractions of adult mouse forebrain. *Journal of Neurochemistry*, 106(2), pp.650–661.

Luo, Y., Na, Z. & Slavoff, S.A., 2018. P-Bodies: Composition, Properties, and Functions. *Biochemistry*, 57(17), pp.2424–2431.

Lyne, R. et al., 2007. FlyMine: An integrated database for Drosophila and Anopheles genomics. *Genome Biology*, 8(7), p.R129.

Lytle, J.R., Yario, T.A. & Steitz, J.A., 2007. Target mRNAs are repressed as efficiently by microRNA-binding sites in the 5' UTR as in the 3' UTR. *Proceedings of the National Academy of Sciences*, 104(23), pp.9667–9672.

Maccioni, R.B., Muñoz, J.P. & Barbeito, L., 2001. The molecular bases of Alzheimer's disease and other neurodegenerative disorders. *Archives of Medical Research*, 32(5), pp.367–381.

Madabattula, S.T. et al., 2015. Quantitative Analysis of Climbing Defects in a Drosophila Model of Neurodegenerative Disorders. *Journal of Visualized Experiments*, (100), pp.1–9.

Maday, S. et al., 2014. Axonal Transport: Cargo-Specific Mechanisms of Motility and Regulation. *Neuron*, 84(2), pp.292–309.

Maguire, L.H., Thomas, A.R. & Goldstein, A.M., 2015. Tumors of the neural crest: Common themes in development and cancer. *Developmental dynamics : an official publication of the American Association of Anatomists*, 244(3), pp.311–322.

Mardon, G., Solomon, N.M. & Rubin, G.M., 1994. dachshund encodes a nuclear protein required for normal eye and leg development in Drosophila. *Development*, 120(12), p.3473-3486.

Mardones, P., Martínez, G. & Hetz, C., 2015. Control of systemic proteostasis by the nervous system. *Trends in Cell Biology*, 25(1), pp.1–10.

Marmigère, F. & Ernfors, P., 2007. Specification and connectivity of neuronal subtypes in the sensory lineage. *Nature reviews. Neuroscience*, 8(2), pp.114–127.

Marrus, S.B. & DiAntonio, A., 2004. Preferential localization of glutamate receptors opposite sites of high presynaptic release. *Current biology : CB*, 14(11), pp.924–931.

Marsh, J.L. & Thompson, L.M., 2006. Drosophila in the Study of Neurodegenerative Disease. *Neuron*, 52(1), pp.169–178.

Martin, H.C. et al., 2014. Imperfect centered miRNA binding sites are common and can mediate repression of target mRNAs. *Genome Biology*, 15(3), pp.1–22.

Martini, S.R. & Davis, R.L., 2005. The dachshund gene is required for the proper guidance and branching of mushroom body axons in Drosophila melanogaster. *Journal of neurobiology*, 64(2), pp.133–144.

McMahon, S.B. et al., 2013. *Wall & Melzack's Textbook of Pain* 6th ed., Elsevier/Saunders.

McWilliams, D.F. & Walsh, D.A., 2017. Pain mechanisms in rheumatoid arthritis. *Clinical and experimental rheumatology*, 35 Suppl 107(5), pp.94–101.

Meissner, L. et al., 2016. Temporal Profile of MicroRNA Expression in Contused Cortex after Traumatic Brain Injury in Mice. *Journal of neurotrauma*, 33(8), pp.713–720.

Meister, G. et al., 2004. Sequence-specific inhibition of microRNA- and siRNA-induced RNA silencing. *RNA*, 10(3), pp.544–550.

Menon, K.P., Carrillo, R.A. & Zinn, K., 2013. Development and plasticity of the Drosophila larval neuromuscular junction. *Wiley interdisciplinary reviews. Developmental biology*, 2(5), pp.647–670.

El Mestikawy, S. et al., 2011. From glutamate co-release to vesicular synergy: vesicular glutamate transporters. *Nature reviews. Neuroscience*, 12(4), pp.204–216.

Metzker, M.L., 2010. Sequencing technologies - the next generation *Nature Reviews Genetics,* 11(1), pp.31-46

Meza-Sosa, K.F., Pedraza-Alva, G. & Perez-Martinez, L., 2014. microRNAs: key triggers of neuronal cell fate. *Frontiers in Cellular Neuroscience*, 25(8), p.175.

Mi, H. et al., 2013. Large-scale gene function analysis with the PANTHER classification system. *Nature protocols*, 8(8), pp.1551–66.

Miller, A.C. & Pereda, A.E., 2017. The electrical synapse: Molecular complexities at the gap and beyond. *Developmental neurobiology*, 77(5), pp.562–574.

Mishra A., Godavarthi S. K., Maheshwari M., Goswami A., Jana N. R. (2009b). The ubiquitin ligase E6-AP is induced and recruited to aggresomes in response to

proteasome inhibition and may be involved in the ubiquitination of Hsp70-bound misfolded proteins. *J. Biol. Chem.* 284(16), pp.10537–10545.

Mishra, M. & Knust, E., 2013. Analysis of the Drosophila compound eye with light and electron microscopy. *Methods in molecular biology (Clifton, N.J.)*, 935, pp.161–182.

Molliver, D.C. et al., 1997. IB4-binding DRG neurons switch from NGF to GDNF dependence in early postnatal life. *Neuron*, 19, pp.849–861.

Moloney, A. et al., 2010. Alzheimer's disease: insights from Drosophila melanogaster models. *Trends in Biochemical Sciences*, 35(4), pp.228–235.

Morgado, A.L. et al., 2015. MicroRNA-34a Modulates Neural Stem Cell Differentiation by Regulating Expression of Synaptic and Autophagic Proteins. *Molecular neurobiology*, 51(3), pp.1168–1183.

Murray, R.M. et al., 2017. 30 Years on: How the Neurodevelopmental Hypothesis of Schizophrenia Morphed Into the Developmental Risk Factor Model of Psychosis. *Schizophrenia Bulletin*, 43(6), pp.1190–1196.

Nadorp, B. & Soreq, H., 2014. Predicted overlapping microRNA regulators of acetylcholine packaging and degradation in neuroinflammation-related disorders. *Frontiers in molecular neuroscience*, 7, p.9.

Nelson, P.T. et al., 2004. Microarray-based, high-throughput gene expression profiling of microRNAs. *Nature Methods,* 1(2), pp.155-61.

Nesler, K.R. et al., 2013. The miRNA pathway controls rapid changes in activity-dependent synaptic structure at the Drosophila melanogaster neuromuscular junction. *PloS one*, 8(7), p.e68385.

Neto, E. et al., 2014. Sensory neurons and osteoblasts: close partners in a microfluidic platform. *Integrative biology : quantitative biosciences from nano to macro*, 6(6), pp.586–595.

Neumann, E. et al., 2015. Expression changes of microRNA-1 and its targets Connexin 43 and brain-derived neurotrophic factor in the peripheral nervous system of chronic neuropathic rats. *Molecular Pain*, 11, p.39.

Nichols, C.D., Becnel, J. & Pandey, U.B., 2012. Methods to Assay Drosophila Behavior. *Journal of Visualized Experiments : JoVE*, (61), p.3795.

Nicoll, R.A., 2017. A Brief History of Long-Term Potentiation. *Neuron*, 93(2), pp.281–

290.

Noveen, A., Daniel, A. & Hartenstein, V., 2000. Early development of the Drosophila mushroom body: the roles of eyeless and dachshund. *Development (Cambridge, England)*, 127(16), pp.3475–3488.

Oda, K. & Kitano, H., 2006. A comprehensive map of the toll-like receptor signaling network. *Molecular Systems Biology*, 2, p.2006.0015.

Okray, Z. & Hassan, B.A., 2013. Genetic approaches in Drosophila for the study neurodevelopmental disorders. *Neuropharmacology*, 68, pp.150–156.

Olde Loohuis, N.F.M. et al., 2015. Elevated microRNA-181c and microRNA-30d levels in the enlarged amygdala of the valproic acid rat model of autism. *Neurobiology of disease*, 80, pp.42–53.

Ostroff, L.E. et al., 2002. Polyribosomes redistribute from dendritic shafts into spines with enlarged synapses during LTP in developing rat hippocampal slices. *Neuron*, 35(3), pp.535–545.

Owen, M.J. et al., 2011. Neurodevelopmental hypothesis of schizophrenia. *The British journal of psychiatry : the journal of mental science*, 198(3), pp.173–5.

Pandey, U.B. & Nichols, C.D., 2011. Human Disease Models in Drosophila melanogaster and the Role of the Fly in Therapeutic Drug Discovery E. L. Barker, ed. *Pharmacological Reviews*, 63(2), pp.411–436.

Paredes, R.M. et al., 2008. Chemical Calcium Indicators. *Methods (San Diego, Calif.)*, 46(3), pp.143–151.

Parker, R. & Sheth, U., 2007. P bodies and the control of mRNA translation and degradation. *Molecular cell*, 25(5), pp.635–646.

Parrish, J.Z. et al., 2009. The microRNA bantam functions in epithelial cells to regulate scaling growth of dendrite arbors in Drosophila sensory neurons. *Neuron*, 63(6), pp.788–802.

Pasquinelli, A.E. et al., 2000. Conservation of the sequence and temporal expression of let-7 heterochronic regulatory RNA. *Nature*, 408(6808), pp.86–89.

Pedersen, M.E. et al., 2013. An epidermal microRNA regulates neuronal migration through control of the cellular glycosylation state. *Science*, 341(6152), pp.1404–1408.

Pelaez, N. & Carthew, R.W., 2012. Biological robustness and the role of microRNAs: a

network perspective. *Current topics in developmental biology*, 99, pp.237–255.

Pereda, A.E., 2014. Electrical synapses and their functional interactions with chemical synapses. *Nature reviews. Neuroscience*, 15(4), pp.250–263.

Pietro, V. Di et al., 2018. MicroRNA signature of traumatic brain injury: From the biomarker discovery to the point-of-care. *Frontiers in Neurology*, 14(9), p.429.

Pillai, R.S., Artus, C.G. & Filipowicz, W., 2004. Tethering of human Ago proteins to mRNA mimics the miRNA-mediated repression of protein synthesis. *RNA (New York, N.Y.)*, 10(10), pp.1518–1525.

del Pino, I., Rico, B. & Marín, O., 2018. Neural circuit dysfunction in mouse models of neurodevelopmental disorders. *Current Opinion in Neurobiology*, 48, pp.174–182.

Poliseno, L. et al., 2010. Identification of the miR-106b~25 microRNA cluster as a proto-oncogenic PTEN-targeting intron that cooperates with its host gene MCM7 in transformation. *Science signaling*, 3(117), p.ra29.

Polleux, F. & Snider, W., 2010. Initiating and growing an axon. *Cold Spring Harbor perspectives in biology*, 2(4), pp.1–19.

Pritchard, C. C. et al. 2012. MicroRNA profiling: approaches and considerations. *Nature reviews. Genetics*, 13(5), pp.358-69.

Prokop, A. et al., 2013. Using fly genetics to dissect the cytoskeletal machinery of neurons during axonal growth and maintenance. *Journal of Cell Science*, 126(11), pp.2331–2341.

Prokop, A., Küppers-Munther, B. & Sánchez-Soriano, N., 2012. Using primary neuron cultures of drosophila to analyze neuronal circuit formation and function. In B. A. Hassan, ed. *Neuromethods*. Totowa, NJ: Humana Press, pp. 225–247.

Prokop, A. & Root, J., 2013. A rough guide to Drosophila mating schemes. *G3 (Bethesda, Md.)*, 3(2), p.Supplementary File 1: 1-30.

Quiring, R. et al., 1994. Homology of the eyeless gene of Drosophila to the Small eye gene in mice and Aniridia in humans. *Science*, 265(5173), pp.785–789.

Rajewsky, N., 2006. microRNA target predictions in animals. *Nature Genetics*, 38, p.S8.

Rajman, M. & Schratt, G., 2017. MicroRNAs in neural development: from master regulators to fine-tuners. *Development (Cambridge, England)*, 144(13),

pp.2310–2322.

Ray, M. & Lakhotia, S.C., 2015. The commonly used eye-specific sev-GAL4 and GMR-GAL4 drivers in Drosophila melanogaster are expressed in tissues other than eyes also. *Journal of Genetics*, 94(3), pp.407–416.

Reemst, K. et al., 2016. The Indispensable Roles of Microglia and Astrocytes during Brain Development. *Frontiers in human neuroscience*, 10, p.566.

Reichling, D.B. & Levine, J.D., 2009. Critical role of nociceptor plasticity in chronic pain. *Trends in neurosciences*, 32(12), pp.611–618.

Reiter, L.T. et al., 2001. A Systematic Analysis of Human Disease-Associated Gene Sequences In Drosophila melanogaster. *Genome Research*, 11(6), pp.1114–1125.

Ren, K. & Dubner, R., 1999. Inflammatory Models of Pain and Hyperalgesia. *ILAR journal*, 40(3), pp.111–118.

Rezával, C., Werbajh, S. & Ceriani, M.F., 2007. Neuronal death in Drosophila triggered by GAL4 accumulation. *European Journal of Neuroscience*, 25(3), pp.683–694.

Richard, M. & Hoch, M., 2015. Drosophila eye size is determined by Innexin 2-dependent Decapentaplegic signalling. *Developmental Biology*, 408(1), pp.26–40.

Robinow, S. & White, K., 1991. Characterization and spatial distribution of the ELAV protein during Drosophila melanogaster development. *Journal of neurobiology*, 22(5), pp.443–461.

Romero-Cordoba, S.L. et al., 2014. miRNA biogenesis: Biological impact in the development of cancer. *Cancer Biology & Therapy*, 15(11), pp.1444–1455.

van Rooij, E. & Kauppinen, S., 2014. Development of microRNA therapeutics is coming of age. *EMBO molecular medicine*, 6(7), pp.851–64.

Rosenstein, J.M., Krum, J.M. & Ruhrberg, C., 2010. VEGF in the nervous system. *Organogenesis*, 6(2), pp.107–114.

Rubin, G.M. & Lewis, E.B., 2000. A brief history of Drosophila's contributions to genome research. *Science*, 287(5461), pp.2216–2218.

Ruby, J.G. et al., 2007. Evolution, biogenesis, expression, and target predictions of a substantially expanded set of Drosophila microRNAs. *Genome Research*, 17(12),

pp.1850–1864.

Ruby, J.G., Jan, C.H. & Bartel, D.P., 2007. Intronic microRNA precursors that bypass Drosha processing. *Nature*, 448(7149), pp.83–86.

Saba, R. et al., 2012. Dopamine-Regulated MicroRNA MiR-181a Controls GluA2 Surface Expression in Hippocampal Neurons. *Molecular and Cellular Biology*, 32(3), p.619 LP-632.

Şahin, H.B. & Çelik, A., 2013. Drosophila Eye Development and Photoreceptor Specification. *eLS*, pp.1–12.

Sakai, A. et al., 2013. miR-7a alleviates the maintenance of neuropathic pain through regulation of neuronal excitability. *Brain*, 136(9), pp.2738–2750.

Sakai, A. & Suzuki, H., 2014. Emerging roles of microRNAs in chronic pain. *Neurochemistry International*, 77, pp.58–67.

Sakurai, K. et al., 2011. A role for human Dicer in pre-RISC loading of siRNAs. *Nucleic Acids Research*, 39(4), pp.1510–1525.

Saliba, J. et al., 2018. Development of microplatforms to mimic the in vivo architecture of CNS and PNS physiology and their diseases. *Genes*, 9(6), pp.1–29.

Samarsky, D.A. et al., 1998. The snoRNA box C/D motif directs nucleolar targeting and also couples snoRNA synthesis and localization. *The EMBO journal*, 17(13), pp.3747–3757.

Sambandan, S. et al., 2017. Activity-dependent spatially localized miRNA maturation in neuronal dendrites. *Science*, 355(6325), pp.634–637.

Sanabria-Castro, A., Alvarado-Echeverría, I. & Monge-Bonilla, C., 2017. Molecular Pathogenesis of Alzheimer's Disease: An Update. *Annals of neurosciences*, 24(1), pp.46–54.

Sánchez-Soriano, N. et al., 2010. Drosophila growth cones: A genetically tractable platform for the analysis of axonal growth dynamics. *Developmental Neurobiology*, 70(1), pp.58–71.

Sánchez-Soriano, N. et al., 2009. Mouse ACF7 and Drosophila Short stop modulate filopodia formation and microtubule organisation during neuronal growth. *Journal of Cell Science*, 122(14), pp.2534–2542.

Sanes, J.R. & Lichtman, J.W., 1999. Development of the vertebrate neuromuscular

junction. *Annual review of neuroscience*, 22, pp.389–442.

Sato, F. et al., 2009. Intra-Platform Repeatability and Inter-Platform Comparability of MicroRNA Microarray Technology K. Selvarajoo, ed. *PLoS ONE*, 4(5), p.e5540.

von Schack, D. et al., 2011. Dynamic changes in the microRNA expression profile reveal multiple regulatory mechanisms in the spinal nerve ligation model of neuropathic pain. *PloS one*, 6(3), p.e17670.

Schaefer, A. et al., 2007. Cerebellar neurodegeneration in the absence of microRNAs. *The Journal of Experimental Medicine*, 204(7), pp.1553–1558.

Scheffer, A.-R. et al., 2014. Circulating microRNAs in serum: novel biomarkers for patients with bladder cancer? *World journal of urology*, 32(2), pp.353–358.

Schelski, M. & Bradke, F., 2017. Neuronal polarization: From spatiotemporal signaling to cytoskeletal dynamics. *Molecular and cellular neurosciences*, 84, pp.11–28.

Schertel, C. et al., 2012. Functional characterization of Drosophila microRNAs by a novel in vivo library. *Genetics*, 192(4), pp.1543–1552.

Schindelin, J. et al., 2012. Fiji: an open-source platform for biological-image analysis. *Nature methods*, 9(7), pp.676–682.

Schratt, G., 2009. microRNAs at the synapse. *Nature reviews. Neuroscience*, 10(12), pp.842–849.

Schratt, G.M. et al., 2006. A brain-specific microRNA regulates dendritic spine development. *Nature*, 439(7074), pp.283–289.

Schwartz, V. et al, 2015. Acid-sensing ion channel (ASIC) 4 predominantly localizes to an early endosome-related organelle upon heterologous expression. *Scientific report*s, 15(5), p.18242.

Sheng, G. et al., 1997. Direct regulation of rhodopsin 1 by Pax-6/eyeless in Drosophila: Evidence for a conserved function in photoreceptors. *Genes and Development*, 11(9), pp.1122–1131.

Sheng, M. & Kim, E., 2011. The postsynaptic organization of synapses. *Cold Spring Harbor Perspectives in Biology*, 3(12), pp.1–20.

Shields, S.D. et al., 2012. Nav1.8 expression is not restricted to nociceptors in mouse peripheral nervous system. *Pain*, 153(10), pp.2017–2030.

Shin, C. et al., 2010. Expanding the microRNA targeting code: functional sites with

centered pairing. *Molecular cell*, 38(6), pp.789–802.

Siegert, S. et al., 2015. The schizophrenia risk gene product miR-137 alters presynaptic plasticity. *Nature Neuroscience*, 18(7), pp.1008-16..

Siksou, L., Triller, A. & Marty, S., 2011. Ultrastructural organization of presynaptic terminals. *Current opinion in neurobiology*, 21(2), pp.261–268.

Silva, D.I. et al., 2017. Dorsal root ganglion neurons regulate the transcriptional and translational programs of osteoblast differentiation in a microfluidic platform. *Cell Death & Disease*, 8(12), p.3209.

Sim, S.-E., Bakes, J. & Kaang, B.-K., 2014. Neuronal activity-dependent regulation of MicroRNAs. *Molecules and cells*, 37(7), pp.511–517.

Simchovitz, A., Heneka, M.T. & Soreq, H., 2017. Personalized genetics of the cholinergic blockade of neuroinflammation. *Journal of Neurochemistry*, 142, pp.178–187.

Simms, B.A. & Zamponi, G.W., 2014. Neuronal voltage-gated calcium channels: Structure, function, and dysfunction. *Neuron*, 82(1), pp.24–45.

Smith, R. & Taylor, J.P., 2011. Dissection and Imaging of Active Zones in the Drosophila Neuromuscular Junction. *JoVE*, (50), p.e2676.

Song, Y. et al., 2012. Regeneration of Drosophila sensory neuron axons and dendrites is regulated by the Akt pathway involving Pten and microRNA bantam. *Genes & Development*, 26(14), pp.1612–1625.

Sotelo-Silveira, J. et al., 2008. Myelinated axons contain beta-actin mRNA and ZBP-1 in periaxoplasmic ribosomal plaques and depend on cyclic AMP and F-actin integrity for in vitro translation. *Journal of neurochemistry*, 104(2), pp.545–557.

Sotelo-Silveira, J.R. et al., 2000. Neurofilament mRNAs are present and translated in the normal and severed sciatic nerve. *Journal of neuroscience research*, 62(1), pp.65–74.

Sotelo-Silveira, J.R. et al., 2006. RNA trafficking in axons. *Traffic (Copenhagen, Denmark)*, 7(5), pp.508–515.

Spehr, M. & Munger, S.D., 2009. Olfactory receptors: GPCRs and beyond. *Journal of neurochemistry*, 109(6), pp.1570–1583.

Sprecher, S.G., Reichert, H. & Hartenstein, V., 2007. Gene expression patterns in primary neuronal clusters of the Drosophila embryonic brain. *Gene expression*

patterns : GEP, 7(5), pp.584–595.

van Spronsen, M. et al., 2013. Developmental and Activity-Dependent miRNA Expression Profiling in Primary Hippocampal Neuron Cultures. *PLoS ONE*, 8(10).

St Johnston, D., 2002. the Art and Design of Genetic Screens: Drosophila Melanogaster. *Nature Reviews Genetics*, 3(3), pp.176–188.

Stark, K.L. et al., 2008. Altered brain microRNA biogenesis contributes to phenotypic deficits in a 22q11-deletion mouse model. *Nat Genet*, 40(6), pp.751–760.

Steinkraus, B.R., Toegel, M. & Fulga, T. a., 2016. Tiny giants of gene regulation: Experimental strategies for microRNA functional studies. *Wiley Interdisciplinary Reviews: Developmental Biology*, 5(3), pp.311–362.

Steward, O. & Levy, W.B., 1982. Preferential localization of polyribosomes under the base of dendritic spines in granule cells of the dentate gyrus. *The Journal of neuroscience : the official journal of the Society for Neuroscience*, 2(3), pp.284–291.

Steward, O. & Schuman, E.M., 2001. Protein Synthesis at Synaptic Sites on Dendrites. *Annual Review of Neuroscience*, 24(1), pp.299–325.

Strickland, I.T. et al., 2011. Axotomy-induced mir-21 promotes axon growth in adult dorsal root ganglion neurons. *PLoS ONE*, 6(8), pp.2–9.

Su, H. et al., 2011. Mammalian hyperplastic discs homolog EDD regulates miRNA-mediated gene silencing. *Molecular cell*, 43(1), pp.97–109.

Sutton, M.A. et al., 2006. Miniature neurotransmission stabilizes synaptic function via tonic suppression of local dendritic protein synthesis. *Cell*, 125(4), pp.785–799.

Svoboda, P., 2015. A toolbox for miRNA analysis. *FEBS Letters*, 589(14), pp.1694–1701.

Swanger, S.A. & Bassell, G.J., 2013. Dendritic protein synthesis in the normal and diseased brain. *Neuroscience*, 1(232), pp.106–127.

Takano, T. et al., 2015. Neuronal polarization. *Development*, 142(12), pp.2088–2093.

Tamariz, E. & Varela-Echavarría, A., 2015. The discovery of the growth cone and its influence on the study of axon guidance. *Frontiers in Neuroanatomy*, 15(9), p.51.

Tang, F. et al., 2006. 220-plex microRNA expression profile of a single cell. *Nature*

Protocols, 1(3), pp.1154-9

Tarantino, C. et al., 2010. miRNA 34a, 100, and 137 modulate differentiation of mouse embryonic stem cells. *FASEB journal : official publication of the Federation of American Societies for Experimental Biology*, 24(9), pp.3255–3263.

Tataroglu, O. & Emery, P., 2014. Studying circadian rhythms in Drosophila melanogaster. *Methods*, 68(1), pp.140–150.

Taylor, A.M. et al., 2005. A microfluidic culture platform for CNS axonal injury, regeneration and transport. *Nat Meth*, 2(8), pp.599–605.

Thadani, R. & Tammi, M.T., 2006. MicroTar: predicting microRNA targets from RNA duplexes. *BMC Bioinformatics*, 7(5), pp.1–9.

Thaker, H.M. & Kankel, D.R., 1992. Mosaic analysis gives an estimate of the extent of genomic involvement in the development of the visual system in Drosophila melanogaster. *Genetics*, 131(4), pp.883–894.

Thapar, R. & Denmon, A., 2013. Signaling Pathways That control mRNA Turnover. *Cell Signal*, 25(8), pp.1699–1710.

Thomas, B.J. & Wassarman, D.A., 1999. A fly's eye view of biology. *Trends in Genetics*, 15(5), pp.184–190.

Thomas, M.G. et al., 2014. Synaptic control of local translation: The plot thickens with new characters. *Cellular and Molecular Life Sciences*, 71(12), pp.2219–2239.

Thomson, J.M. et al, 2004. A custom microarray platform for analysis of microRNA gene expression. *Nature methods,* 1(1), pp.47-53.

Todd, A.J., 2010. Neuronal circuitry for pain processing in the dorsal horn. *Nature reviews. Neuroscience*, 11(12), pp.823–836.

Tsanov, N. et al., 2016. smiFISH and FISH-quant - a flexible single RNA detection approach with super-resolution capability. *Nucleic acids research*, 44(22), p.e165.

Tsantoulas, C. et al., 2013. Probing Functional Properties of Nociceptive Axons Using a Microfluidic Culture System Y. Yang, ed. *PLoS ONE*, 8(11), p.e80722.

Tsantoulas, C. & McMahon, S.B., 2014. Opening paths to novel analgesics: The role of potassium channels in chronic pain. *Trends in Neurosciences*, 37(3), pp.146–158.

Tweedie, S. et al., 2009. FlyBase: enhancing Drosophila Gene Ontology annotations. *Nucleic Acids Research*, 37(Database issue), pp.D555–D559.

Tymanskyj, S.R., Scales, T.M.E. & Gordon-Weeks, P.R., 2012. MAP1B enhances microtubule assembly rates and axon extension rates in developing neurons. *Molecular and cellular neurosciences*, 49(2), pp.110–119.

Ugur, B., Chen, K. & Bellen, H.J., 2016. Drosophila tools and assays for the study of human diseases. *Disease Models & Mechanisms*, 9(3), p.235 LP-244.

Unsain, N. et al., 2014. Production and Isolation of Axons from Sensory Neurons for Biochemical Analysis Using Porous Filters. *JoVE*, 89, p.e51795.

Upadhyay, A. et al., 2017. E3 Ubiquitin Ligases Neurobiological Mechanisms: Development to Degeneration. *Frontiers in Molecular Neuroscience*, 10, p.151.

Urbach, R. & Technau, G.M., 2003. Molecular markers for identified neuroblasts in the developing brain of Drosophila. *Development*, 130(16), p.3621 LP-3637.

Várallyay, E. et al., 2008. MicroRNA detection by northern blotting using locked nucleic acid probes. *Nature Protocols,* 3(2), pp.190-6.

de Vellis, J. & Carpenter, E., 1999. Cell lineages of the nervous system. In *Basic Neurochemistry: Molecular, Cellular and Medical Aspects. 6th edition.*

Verma, P. et al., 2015. A neuroprotective role for microRNA miR-1000 mediated by limiting glutamate excitotoxicity. *Nature Neuroscience*, 18(3), pp.379-85.

Wang, L. et al., 2017. Brain Development and Akt Signaling: the Crossroads of Signaling Pathway and Neurodevelopmental Diseases. *Journal of Molecular Neuroscience*, 61(3), pp.379–384.

Wang, L. et al., 2011. Smad2 protein disruption in the central nervous system leads to aberrant cerebellar development and early postnatal ataxia in mice. *Journal of Biological Chemistry*, 286(21), pp.18766–18774.

Wang, W. et al., 2007. RNA transport and localized protein synthesis in neurological disorders and neural repair. *Developmental neurobiology*, 67(9), pp.1166–1182.

Wei, J. et al., 2013. MyD88 as a target of microRNA-203 in regulation of lipopolysaccharide or Bacille Calmette-Guerin induced inflammatory response of macrophage RAW264.7 cells. *Molecular Immunology*, 55(3–4), pp.303–309.

Wemmie, J. A. et al., 2013. Acid-sensing ion channels in pain and disease. *Nature reviews. Neuroscience*, 14(7), 461-71.

Wiederhold, K. & Passmore, L.A., 2010. Cytoplasmic deadenylation: regulation of mRNA fate. *Biochemical Society Transactions*, 38(6), pp.1531–1536.

Wightman, B., Ha, I. & Ruvkun, G., 1993. Posttranscriptional regulation of the heterochronic gene lin-14 by lin-4 mediates temporal pattern formation in C. elegans. *Cell*, 75(5), pp.855–862.

Woolf, C.J., 2011. Central sensitization: Implications for the diagnosis and treatment of pain. *Pain*, 152(3 Suppl), pp.S2-15.

Woolf, C.J., 1983. Evidence for a central component of post-injury pain hypersensitivity. *Nature*, 306(5944), pp.686–688.

Woolf, C.J. & Ma, Q., 2007. Nociceptors-Noxious Stimulus Detectors. *Neuron*, 55(3), pp.353–364.

Wu, J. et al., 2014. MicroRNA-188 suppresses G1/S transition by targeting multiple cyclin/CDK complexes. *Cell Communication and Signaling*, 12(1), p.66.

Wu, X. & Brewer, G., 2012. The regulation of mRNA stability in mammalian cells: 2.0. *Gene*, 500(1), pp.10–21.

Xiao, W.H. & Bennett, G.J., 2008. Chemotherapy-evoked neuropathic pain: Abnormal spontaneous discharge in A-fiber and C-fiber primary afferent neurons and its suppression by acetyl-l-carnitine. *PAIN*, 135(3), pp.262-70.

Xu, Q. & Yaksh, T.L., 2011. A brief comparison of the pathophysiology of inflammatory versus neuropathic pain. *Current Opinion in Anaesthesiology*, 24(4), pp.400–407.

Yang, Y. et al., 2010. Identifying targets of miR-143 using a SILAC-based proteomic approach. *Molecular bioSystems*, 6(10), pp.1873–1882.

Yao, B. et al., 2011. Mapping of Ago2-GW182 functional interactions. *Methods in molecular biology (Clifton, N.J.)*, 725, pp.45–62.

Yao, J., Qi, J. & Chen, G., 2006. Actin-dependent activation of presynaptic silent synapses contributes to long-term synaptic plasticity in developing hippocampal neurons. *The Journal of neuroscience : the official journal of the Society for Neuroscience*, 26(31), pp.8137–8147.

Yu, L. et al., 2015. Highly efficient method for gene delivery into mouse dorsal root ganglia neurons. *Frontiers in Molecular Neuroscience*, 8, p.2.

Yu, Y. et al., 2018. miR-190 suppresses breast cancer metastasis by regulation of TGF-

beta-induced epithelial-mesenchymal transition. *Molecular cancer*, 17(1), p.70.

Yu, Y. et al., 2014. NF-kappaB1 p50 promotes p53 protein translation through miR-190 downregulation of PHLPP1. *Oncogene*, 33(8), pp.996–1005.

Zhang, J.-M. & An, J., 2007. Cytokines, inflammation, and pain. *International anesthesiology clinics*, 45(2), pp.27–37.

Zhao, J. et al., 2010. Small RNAs Control Sodium Channel Expression, Nociceptor Excitability, and Pain Thresholds. *The Journal of Neuroscience*, 30(32), pp.10860-10871.

Zheng, H., et al., 2010a. Modulations of NeuroD activity contribute to the differential effects of morphine and fentanyl on dendritic spine stability. *The Journal of neuroscience : the official journal of the Society for Neuroscience*, 30(24), pp.8102–8110.

Zheng, H., et al., 2010b. mu-Opioid receptor agonists differentially regulate the expression of miR-190 and NeuroD. *Molecular pharmacology*, 77(1), pp.102–109.

Zheng, H., 2010c. Yin Yang 1 phosphorylation contributes to the differential effects of mu-opioid receptor agonists on microRNA-190 expression. *The Journal of biological chemistry*, 285(29), pp.21994–22002.

Zheng, J.Q. et al., 2001. A functional role for intra-axonal protein synthesis during axonal regeneration from adult sensory neurons. *The Journal of neuroscience : the official journal of the Society for Neuroscience*, 21(23), pp.9291–9303.

Zheng, N. et al, 2017. Ubiquitin ligases: Structure, function, and regulation. *Annu Rev Biochem,* 20(86), pp.129–157.

Zeng, Y. and Cullen, B.R., 2003. Sequence requirements for micro RNA processing and function in human cells. *RNA,* 9(1), pp.112–23.

Zhou, Q. et al., 2016. Decreased miR-199 augments visceral pain in patients with IBS through translational upregulation of TRPV1. *Gut*, 65(5), pp.797–805.

Zhou, X. et al., 2016. MicroRNA-138 Inhibits Periodontal Progenitor Differentiation under Inflammatory Conditions. *Journal of dental research*, 95(2), pp.230–237.

Zipprich, J.T. et al., 2009. Importance of the C- Terminal domain of the human GW182 protein TNRC6C for translational repression. *RNA*, 15(5), pp.781–793.

Zivraj, K.H. et al., 2010. Subcellular profiling reveals distinct and developmentally

regulated repertoire of growth cone mRNAs. *The Journal of neuroscience : the official journal of the Society for Neuroscience*, 30(46), pp.15464–15478.

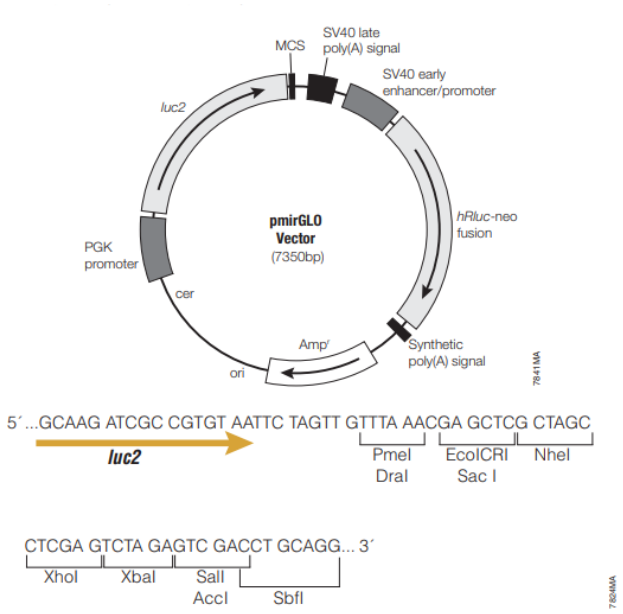
Zolessi, F.R. et al., 2006. Polarization and orientation of retinal ganglion cells in vivo. *Neural development*, 1(2), p.2.

10. Appendices

Appendix I. Plasmid maps

pmirGLO Dual-Luciferase miRNA Target Expression Vector

Original reference: (Zheng & Cullen 2003). Plasmid map shown here taken from Promega UK certificate of analysis.



pmaxGFP

Plasmid generated by Amaxa (Cologne, Germany). Plasmid map shown here taken from Amaxa Nucleofector II manual.

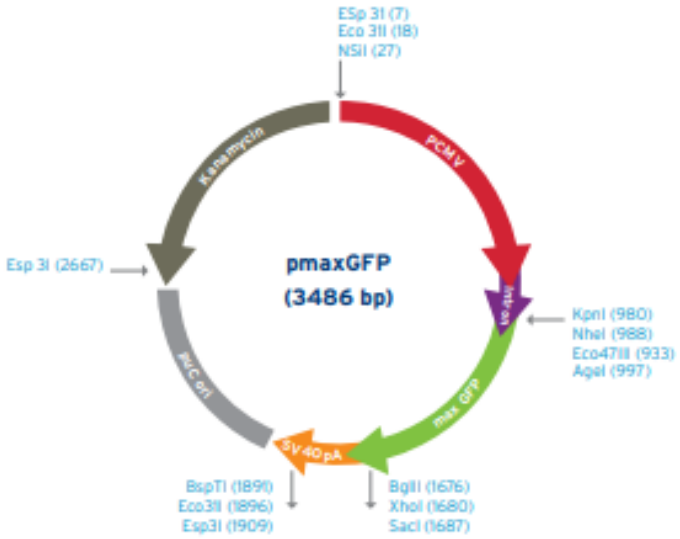


Fig. 8.

Appendix II - Hyperalgesic priming protocol

Taken verbatim from "Investigation into the Mechanisms of Hyperalgesic Priming" Submitted by James Spalton to the University of Nottingham for the degree Doctor of Philosophy 2016.

Animals

All procedures adhered to IASP and ARRIVE guidelines, were ethically approved and licenced by the UK Home Office. Experiments were all conducted upon male Sprague Dawley rats obtained from Charles River (Margate, UK). Animals were ordered in at a weight range of 179-199g so that they would be at a range of 200-250g upon commencing studies. During experiments animals were given free access to both food and water for the duration of the study and habituated to experimental equipment, and handled by the experimenter prior to experiments starting. Behavioural measurements were made between 0800 and 1700. The experimenter was blinded to the treatment of each animal.

Mechanical Paw Withdrawal Threshold

To measure the development of mechanical hyperalgesia animals were placed in a Perspex box with a mesh floor (Medical Engineering, University of Nottingham) where von Frey monofilaments were applied to the plantar surface of the hind paw exerting a bending force in grams (1, 2, 4, 6, 8, 10, 15 and 26g). Von Frey monofilaments were applied sequentially starting from 6g in increasing order to the plantar surface of both paws for three seconds until a withdrawal reflex was observed. This was defined as a rapid withdrawal of the paw from the stimulus, which was occasionally accompanied by slight shaking or licking of the paw. (Forces applied did not exceed 26g in any study). Each stimulus was applied for 3 seconds to the injured region of the paw, if no reflex was observed the next incremental filament was applied. Once a withdrawal reflex was observed, the next lower magnitude von Frey monofilament was used to test the paw to confirm no presence of a response (Calcutt et al., 1997). The lowest weight of monofilament used which elicited a reflex was taken to be the paw withdrawal threshold.

Induction of the Model of Hyperalgesic Priming

Solution Preparation

2.3.1.1 Carrageenan λ-Carrageenan (Sigma Aldrich, UK) was immersed in 0.9% saline and left in a water bath at 50°C for 24 hours to dissolve in the saline. The solution was then inverted several times within the tube to fully distribute the carrageenan throughout. Carrageenan when mixed in solution forms a thick emulsion. A concentration of 1% carrageenan was made for use in the induction of hyperalgesic priming. This concentration of carrageenan had been previously used in the generation of the hyperalgesic priming model (Aley et al., 2000).

2.3.1.2 TNFα TNFα (Sigma Aldrich) was dissolved in (0.9%) saline to make a stock solution of 100µg/ml. This was then diluted to a working concentration of 20µg/ml for injections. TNFα had also been used in several studies to induce hyperalgesic priming (Bogen et al., 2012).

2.3.1.3 PGE2 PGE2 (Cayman Chemicals, Cambridge Bioscience, UK) was dissolved in a solution of 99% of 0.9% saline and 1% ethanol to produce a stock solution of 1mg/ml. This was diluted to a working concentration of 0.2mg/ml. This was used to confirm that hyperalgesic priming had occurred.

58

Anaesthesia

Intraplantar administration of compounds was performed on animals while under brief isoflurane (Abbot, Kent, UK) anaesthesia. The anaesthetic system consisted of a Perspex induction box that received a delivery of 3% Isoflurane via an anaesthetic vaporiser, in a nitrous oxide and oxygen gas (BOC gases, UK) mixture in a ratio of 33:67 pressure controlled by 0-4 bar multistage gas ARC multistage regulators. Flow rate was maintained by Platon glass variable flow meters connected to a small animal nose cone through a non-rebreathable tubing system. An active extraction system (Fluo Vac) was used to remove exhaled gasses via an aldasorber (Harvard Apparatus).

2.3.3 Intraplantar Administration of Substances

Animals were placed within an induction box and anaesthetised as detailed in 2.3.2, upon the animal losing its righting reflex it was transferred to a small animal nose cone in prone position on a heating blanket. The animal's paws were positioned with the plantar surface facing up. The pedal reflex was tested to confirm the animal was areflexic. The plantar surface was disinfected with chlorhexidine (Hydrex) and a 28

gauge 0.3ml insulin syringe was used to administer a small 5µl bolus of noxious compound (carrageenan or, TNFα or, PGE2) into the plantar skin into the intradermal space. The needle was then twisted 180° to aid in skin closure and then immediately removed. Animal was then allowed to recover in a separate cage. Once the self-righting had returned the animal was transferred back to its home cage.

Appendix III. Chronic stage DRG microarray results

Results for all miRNA present on the microarray as summarised in 3.2. DRG 12: Saline primed control.

DRG9 and 16: Carrageenan primed samples. Values shown are relative fluorescent signal intensities.

Name	ID	DRG12(saline)	DRG9(Carra)	DRG16(Carra)
rno-let-7a-1-3p	MIMAT0017085			
rno-let-7a-2-3p	MIMAT0017086			
rno-let-7a-5p	MIMAT0000774	8.359973	96.912407	64.239094
rno-let-7b-3p	MIMAT0004705	26.609799	19.277725	32.405729
rno-let-7b-5p	MIMAT0000775	8.058657	86.379089	52.953525
rno-let-7c-1-3p	MIMAT0017087			
rno-let-7c-5p	MIMAT0000776	6.821093	117.582252	65.572362
rno-let-7d-3p	MIMAT0000563	16.340536	10.600784	9.407931
rno-let-7d-5p	MIMAT0000562		94.083155	46.113889
rno-let-7e-3p	MIMAT0004706			9.881403
rno-let-7e-5p	MIMAT0000777		21.082921	20.597064
rno-let-7f-1-3p	MIMAT0017089			
rno-let-7f-2-3p	MIMAT0017090			
rno-let-7f-5p	MIMAT0000778		20.662433	10.358079
rno-let-7i-3p	MIMAT0004707		10.40105	
rno-let-7i-5p	MIMAT0000779			
rno-miR-1-3p	MIMAT0003125			
rno-miR-1-5p	MIMAT0003162			
rno-miR-100-3p	MIMAT0017112		23.265985	
rno-miR-100-5p	MIMAT0000822	16.362438	43.154723	69.229569
rno-miR-101a-3p	MIMAT0000823			
rno-miR-101a-5p	MIMAT0004726			
rno-miR-101b-3p	MIMAT0000615			
rno-miR-101b-5p	MIMAT0017045			
rno-miR-103-1-5p	MIMAT0017114			
rno-miR-103-2-5p	MIMAT0017113			
rno-miR-103-3p	MIMAT0000824		26.056844	15.727879
rno-miR-105	MIMAT0012825			9.402176
rno-miR-106b-3p	MIMAT0004727			
rno-miR-106b-5p	MIMAT0000825			
rno-miR-107-3p	MIMAT0000826		22.22252	14.236834
rno-miR-107-5p	MIMAT0017115			
rno-miR-10a-3p	MIMAT0004709			
rno-miR-10a-5p	MIMAT0000782		10.355838	13.678401
rno-miR-10b-3p	MIMAT0017092			
rno-miR-10b-5p	MIMAT0000783			9.247407
rno-miR-1188-3p	MIMAT0017855	53.709537	48.277663	54.502482
rno-miR-1188-5p	MIMAT0017854	21.526514	25.046624	43.237514
rno-miR-1193-3p	MIMAT0017859			
rno-miR-1193-5p	MIMAT0017858			
rno-miR-1199-3p	MIMAT0031126	14.33137		18.426466
rno-miR-1199-5p	MIMAT0031125		29.912154	
rno-miR-122-3p	MIMAT0017116			
rno-miR-122-5p	MIMAT0000827			
rno-miR-1224	MIMAT0012827	1899.170441	380.903496	1071.76432
rno-miR-124-3p	MIMAT0000828	34.149902	136.027101	98.717315
rno-miR-124-5p	MIMAT0004728			
rno-miR-1249	MIMAT0017892	209.994328	132.807393	162.062569
rno-miR-125a-3p	MIMAT0004729	45.41776	39.75341	57.606403
rno-miR-125a-5p	MIMAT0000829	30.657333	60.142768	84.930222
rno-miR-125b-1-3p	MIMAT0004730		15.396513	10.306031
rno-miR-125b-2-3p	MIMAT0026467	8.546375		22.518709
rno-miR-125b-5p	MIMAT0000830	113.125792	304.592344	453.747803
rno-miR-126a-3p	MIMAT0000832			
rno-miR-126a-5p	MIMAT0000831			
rno-miR-126b	MIMAT0017843			
rno-miR-127-3p	MIMAT0000833		13.935313	28.843899
rno-miR-127-5p	MIMAT0017117			
rno-miR-128-1-5p	MIMAT0017118	34.470027	23.054282	32.388561
rno-miR-128-2-5p	MIMAT0017119	173.150506	189.562197	284.844352
rno-miR-128-3p	MIMAT0000834			

rno-miR-129-1-3p	MIMAT0017120	10.217979		12.236459
rno-miR-129-2-3p	MIMAT0000601	15.029952	13.124796	
rno-miR-129-5p	MIMAT0000600	8.85256	10.125151	11.703736
rno-miR-1298	MIMAT0025060			9.545159
rno-miR-1306-3p	MIMAT0024852	10.14638	11.868905	21.837195
rno-miR-1306-5p	MIMAT0024851	39.267068	25	45.332676
rno-miR-130a-3p	MIMAT0000836		12.402836	10.434118
rno-miR-130a-5p	MIMAT0017121			
rno-miR-130b-3p	MIMAT0000837			
rno-miR-130b-5p	MIMAT0017122			
rno-miR-132-3p	MIMAT0000838			
rno-miR-132-5p	MIMAT0017123			
rno-miR-133a-3p	MIMAT0000839	10.365228		13.832053
rno-miR-133a-5p	MIMAT0017124			
rno-miR-133b-3p	MIMAT0003126	18.297325	23.627456	24.749092
rno-miR-133b-5p	MIMAT0017205			
rno-miR-133c	MIMAT0017872	19.041162	25.967992	23.1683
rno-miR-134-3p	MIMAT0017125	51.065709	36.209934	58.94341
rno-miR-134-5p	MIMAT0000840	6.588977	16.403979	18.85051
rno-miR-135a-3p	MIMAT0004732	6.417665	22.890151	9.287415
rno-miR-135a-5p	MIMAT0000841			
rno-miR-135b-3p	MIMAT0017043			
rno-miR-135b-5p	MIMAT0000611			
rno-miR-136-3p	MIMAT0004733			
rno-miR-136-5p	MIMAT0000842			
rno-miR-137-3p	MIMAT0000843			
rno-miR-137-5p	MIMAT0017126			
rno-miR-138-1-3p	MIMAT0004734	12.389985		18.19852
rno-miR-138-2-3p	MIMAT0017127		10.241249	9.905044
rno-miR-138-5p	MIMAT0000844	25.786912	137.726333	105.488318
rno-miR-139-3p	MIMAT0004735	454.483164	127.763933	213.881533
rno-miR-139-5p	MIMAT0000845			
rno-miR-140-3p	MIMAT0000574	8.698012	10.742261	13.318502
rno-miR-140-5p	MIMAT0000573			
rno-miR-141-3p	MIMAT0000846			
rno-miR-141-5p	MIMAT0017128			
rno-miR-142-3p	MIMAT0000848			
rno-miR-142-5p	MIMAT0000847			
rno-miR-143-3p	MIMAT0000849		16.085754	29.255389
rno-miR-143-5p	MIMAT0017129	33.510496	73.966711	71.428111
rno-miR-144-3p	MIMAT0000850			
rno-miR-144-5p	MIMAT0017130			
rno-miR-145-3p	MIMAT0017131			
rno-miR-145-5p	MIMAT0000851		20.351912	31.676108
rno-miR-146a-3p	MIMAT0017132			
rno-miR-146a-5p	MIMAT0000852			
rno-miR-146b-3p	MIMAT0017334	7.705508	13.132469	18.346308
rno-miR-146b-5p	MIMAT0005595			
rno-miR-147	MIMAT0005297			
rno-miR-148b-3p	MIMAT0000579			
rno-miR-148b-5p	MIMAT0004645			
rno-miR-150-3p	MIMAT0017133	47.342002	30.706213	61.513198
rno-miR-150-5p	MIMAT0000853		16.021854	12.846516
rno-miR-151-3p	MIMAT0000614			8.359056
rno-miR-151-5p	MIMAT0000613		9.780301	
rno-miR-152-3p	MIMAT0000854			
rno-miR-152-5p	MIMAT0017134			
rno-miR-153-3p	MIMAT0000855			
rno-miR-153-5p	MIMAT0017135			
rno-miR-154-3p	MIMAT0017136			
rno-miR-154-5p	MIMAT0000856			
rno-miR-155-3p	MIMAT0030410			
rno-miR-155-5p	MIMAT0030409			
rno-miR-15b-3p	MIMAT0017093			
rno-miR-15b-5p	MIMAT0000784			
rno-miR-16-3p	MIMAT0017094			
rno-miR-16-5p	MIMAT0000785		23.377918	8.220598

rno-miR-17-1-3p	MIMAT0004710		15.934379	
rno-miR-17-2-3p	MIMAT0017295			
rno-miR-17-5p	MIMAT0000786			
rno-miR-181a-1-3p	MIMAT0000884			
rno-miR-181a-2-3p	MIMAT0017138			
rno-miR-181a-5p	MIMAT0000858		16.628666	18.545554
rno-miR-181b-1-3p	MIMAT0017139			
rno-miR-181b-2-3p	MIMAT0017140			
rno-miR-181b-5p	MIMAT0000859			
rno-miR-181c-3p	MIMAT0017137			
rno-miR-181c-5p	MIMAT0000857			
rno-miR-181d-3p	MIMAT0017296		12.0312	18.235229
rno-miR-181d-5p	MIMAT0005299			
rno-miR-182	MIMAT0005300		32.497572	12.652125
rno-miR-183-3p	MIMAT0017141	15.593387		20.788396
rno-miR-183-5p	MIMAT0000860		14.071148	8.592231
rno-miR-1839-3p	MIMAT0024844			
rno-miR-1839-5p	MIMAT0024843			
rno-miR-184	MIMAT0000861	7.936122	9.782959	9.920549
rno-miR-1843-3p	MIMAT0024848		18.215276	17.101646
rno-miR-1843-5p	MIMAT0024847			12.488871
rno-miR-185-3p	MIMAT0017142	8.607629		19.903161
rno-miR-185-5p	MIMAT0000862	7.592563	10.810916	23.642634
rno-miR-186-3p	MIMAT0017143			
rno-miR-186-5p	MIMAT0000863		11.910087	
rno-miR-187-3p	MIMAT0000864			
rno-miR-187-5p	MIMAT0017144	60.382318	22.957431	59.702542
rno-miR-188-3p	MIMAT0017297			
rno-miR-188-5p	MIMAT0005301	24.665629	51.221109	47.004695
rno-miR-18a-3p	MIMAT0017095	10.966828	12.665653	23.237503
rno-miR-18a-5p	MIMAT0000787			
rno-miR-190a-3p	MIMAT0017145			
rno-miR-190a-5p	MIMAT0000865			
rno-miR-190b-3p	MIMAT0017298			
rno-miR-190b-5p	MIMAT0005302			
rno-miR-1912-3p	MIMAT0017865			
rno-miR-1912-5p	MIMAT0017864			
rno-miR-191a-3p	MIMAT0017146			
rno-miR-191a-5p	MIMAT0000866		25.772287	27.756246
rno-miR-191b	MIMAT0017817			
rno-miR-192-3p	MIMAT0017147			
rno-miR-192-5p	MIMAT0000867			
rno-miR-193-3p	MIMAT0000868			
rno-miR-193-5p	MIMAT0004736			14.979929
rno-miR-194-3p	MIMAT0017148	27.580811	25.211572	37.558341
rno-miR-194-5p	MIMAT0000869			
rno-miR-1949	MIMAT0017852			
rno-miR-195-3p	MIMAT0017149			
rno-miR-195-5p	MIMAT0000870			
rno-miR-196a-3p	MIMAT0004737			
rno-miR-196a-5p	MIMAT0000871			
rno-miR-196b-3p	MIMAT0017171			
rno-miR-196b-5p	MIMAT0001082			
rno-miR-196c-3p	MIMAT0017299			
rno-miR-196c-5p	MIMAT0005303			
rno-miR-199a-3p	MIMAT0004738			
rno-miR-199a-5p	MIMAT0000872	13.537717	10.253118	18.700342
rno-miR-19a-3p	MIMAT0000789			
rno-miR-19a-5p	MIMAT0017098			
rno-miR-19b-1-5p	MIMAT0017096			
rno-miR-19b-2-5p	MIMAT0017097			
rno-miR-19b-3p	MIMAT0000788			
rno-miR-200a-3p	MIMAT0000874			
rno-miR-200a-5p	MIMAT0017151			
rno-miR-200b-3p	MIMAT0000875			
rno-miR-200b-5p	MIMAT0017152			
rno-miR-200c-3p	MIMAT0000873			

rno-miR-200c-5p	MIMAT0017150			10.984231
rno-miR-201-3p	MIMAT0017364			
rno-miR-201-5p	MIMAT0012846			
rno-miR-202-3p	MIMAT0017355			
rno-miR-202-5p	MIMAT0012822			
rno-miR-203a-3p	MIMAT0000876			
rno-miR-203a-5p	MIMAT0017153			
rno-miR-203b-3p	MIMAT0017800			
rno-miR-203b-5p	MIMAT0017799			
rno-miR-204-3p	MIMAT0004739	2248.942477	1878.029981	2367.599392
rno-miR-204-5p	MIMAT0000877	13.266715	25.375802	26.508162
rno-miR-205	MIMAT0000878			
rno-miR-206-3p	MIMAT0000879			
rno-miR-206-5p	MIMAT0017154			
rno-miR-207	MIMAT0003115	27.90215	17.755446	36.570495
rno-miR-208a-3p	MIMAT0000880			
rno-miR-208a-5p	MIMAT0017155	17.299549	23.463458	23.659713
rno-miR-208b-3p	MIMAT0017845			
rno-miR-208b-5p	MIMAT0017844			
rno-miR-20a-3p	MIMAT0000603			
rno-miR-20a-5p	MIMAT0000602			
rno-miR-20b-3p	MIMAT0003212			
rno-miR-20b-5p	MIMAT0003211			
rno-miR-21-3p	MIMAT0004711			
rno-miR-21-5p	MIMAT0000790			
rno-miR-210-3p	MIMAT0000881		11.183012	8.157594
rno-miR-210-5p	MIMAT0017156	15.050706	17.874065	25
rno-miR-211-3p	MIMAT0017157	225.396405	182.413276	264.647908
rno-miR-211-5p	MIMAT0000882		10.831835	9.242259
rno-miR-212-3p	MIMAT0000883	21.830218	66.639792	58.248974
rno-miR-212-5p	MIMAT0017158	7.914603		8.993491
rno-miR-214-3p	MIMAT0000885	262.333031	289.354348	406.795186
rno-miR-214-5p	MIMAT0017159			
rno-miR-215	MIMAT0003118			
rno-miR-216a-3p	MIMAT0017160			
rno-miR-216a-5p	MIMAT0000886			
rno-miR-216b-3p	MIMAT0017847			
rno-miR-216b-5p	MIMAT0017846			
rno-miR-217-3p	MIMAT0017161			
rno-miR-217-5p	MIMAT0000887			
rno-miR-218a-1-3p	MIMAT0017162			
rno-miR-218a-2-3p	MIMAT0004740			
rno-miR-218a-5p	MIMAT0000888			
rno-miR-218b	MIMAT0017838			
rno-miR-219a-1-3p	MIMAT0004741			
rno-miR-219a-2-3p	MIMAT0005446			
rno-miR-219a-5p	MIMAT0000889			
rno-miR-219b	MIMAT0017882			
rno-miR-22-3p	MIMAT0000791	46.979959	131.806913	184.908314
rno-miR-22-5p	MIMAT0003152			
rno-miR-221-3p	MIMAT0000890			
rno-miR-221-5p	MIMAT0017163			
rno-miR-222-3p	MIMAT0000891			
rno-miR-222-5p	MIMAT0017164		12.097361	
rno-miR-223-3p	MIMAT0000892	11.290874	11.071766	9.944336
rno-miR-223-5p	MIMAT0017165			
rno-miR-224-3p	MIMAT0017200			
rno-miR-224-5p	MIMAT0003119			
rno-miR-23a-3p	MIMAT0000792	18.426581	138.388691	61.081951
rno-miR-23a-5p	MIMAT0004712	42.483698	32.975404	58.304812
rno-miR-23b-3p	MIMAT0000793	30.530446	166.316209	89.152919
rno-miR-23b-5p	MIMAT0017099			
rno-miR-24-1-5p	MIMAT0003153			
rno-miR-24-2-5p	MIMAT0005441			
rno-miR-24-3p	MIMAT0000794	4728.305583	6671.221791	10680.27454
rno-miR-25-3p	MIMAT0000795			
rno-miR-25-5p	MIMAT0004713	62.093376	42.777776	52.559539

rno-miR-26a-3p	MIMAT0017100			
rno-miR-26a-5p	MIMAT0000796	11.703754	81.535887	60.651256
rno-miR-26b-3p	MIMAT0004714	10.998901		17.772205
rno-miR-26b-5p	MIMAT0000797		22.53445	
rno-miR-27a-3p	MIMAT0000799		34.884568	20.963176
rno-miR-27a-5p	MIMAT0004715			
rno-miR-27b-3p	MIMAT0000798		26.633266	19.816455
rno-miR-27b-5p	MIMAT0017101			
rno-miR-28-3p	MIMAT0004716			
rno-miR-28-5p	MIMAT0000800			
rno-miR-290	MIMAT0000893	22.786628	18.069438	9.999444
rno-miR-291a-3p	MIMAT0000895			
rno-miR-291a-5p	MIMAT0000894	58.915108	28.352168	27.083674
rno-miR-291b	MIMAT0017822			
rno-miR-292-3p	MIMAT0000897	8.613541		
rno-miR-292-5p	MIMAT0000896	19.593148	23.135788	32.956026
rno-miR-293-3p	MIMAT0017365			
rno-miR-293-5p	MIMAT0012847			
rno-miR-294	MIMAT0012848	10.342115		13.417522
rno-miR-295-3p	MIMAT0017366			
rno-miR-295-5p	MIMAT0012849	8.676328	14.26495	13.766168
rno-miR-296-3p	MIMAT0004742	96.891643	48.500841	80.509731
rno-miR-296-5p	MIMAT0000898	500.933463	326.945946	366.823996
rno-miR-297	MIMAT0000899			
rno-miR-298-3p	MIMAT0017166			
rno-miR-298-5p	MIMAT0000900	29.665187	43.720784	54.995857
rno-miR-2985	MIMAT0017891			
rno-miR-299a-3p	MIMAT0017167			
rno-miR-299a-5p	MIMAT0000901			
rno-miR-299b-3p	MIMAT0017834			
rno-miR-299b-5p	MIMAT0017833			
rno-miR-29a-3p	MIMAT0000802		59.018582	39.242933
rno-miR-29a-5p	MIMAT0004718			
rno-miR-29b-1-5p	MIMAT0005445			
rno-miR-29b-2-5p	MIMAT0004717			
rno-miR-29b-3p	MIMAT0000801		17.19594	8.468395
rno-miR-29c-3p	MIMAT0000803			
rno-miR-29c-5p	MIMAT0003154			
rno-miR-300-3p	MIMAT0000902		10.988324	
rno-miR-300-5p	MIMAT0004743			
rno-miR-301a-3p	MIMAT0000552	14.026598		
rno-miR-301a-5p	MIMAT0017026			
rno-miR-301b-3p	MIMAT0005304			
rno-miR-301b-5p	MIMAT0017300			
rno-miR-3065-3p	MIMAT0017840	180.387679	122.651486	147.526485
rno-miR-3065-5p	MIMAT0017839		11.949461	
rno-miR-3068-3p	MIMAT0024846	11.197905	33.222421	46.644759
rno-miR-3068-5p	MIMAT0024845			20.692035
rno-miR-3072	MIMAT0025071	189.776489	136.057822	160.312207
rno-miR-3074	MIMAT0017815			
rno-miR-3075	MIMAT0025057	30.298559	25.635012	35.805701
rno-miR-3085	MIMAT0017805	89.106883	50.298496	77.326052
rno-miR-3099	MIMAT0025048	9.907073		16.165023
rno-miR-30a-3p	MIMAT0000809			
rno-miR-30a-5p	MIMAT0000808		13.394399	18.538078
rno-miR-30b-3p	MIMAT0004721			11.789466
rno-miR-30b-5p	MIMAT0000806			
rno-miR-30c-1-3p	MIMAT0004719	91.704564	58.207343	87.895354
rno-miR-30c-2-3p	MIMAT0005442	23.415605		22.464738
rno-miR-30c-5p	MIMAT0000804		14.217803	9.791801
rno-miR-30d-3p	MIMAT0004722			
rno-miR-30d-5p	MIMAT0000807	25.723756	54.880718	50.056643
rno-miR-30e-3p	MIMAT0004720			
rno-miR-30e-5p	MIMAT0000805			8.377239
rno-miR-3102	MIMAT0025051	39.988865	33.427302	51.591411
rno-miR-3120	MIMAT0017900			
rno-miR-31a-3p	MIMAT0017102			

rno-miR-31a-5p	MIMAT0000810		11.464026	
rno-miR-31b	MIMAT0017816			
rno-miR-32-3p	MIMAT0017103			
rno-miR-32-5p	MIMAT0000811			
rno-miR-320-3p	MIMAT0000903	44.358865	40.651074	51.631401
rno-miR-320-5p	MIMAT0017168	12.681399	12.269591	26.640369
rno-miR-322-3p	MIMAT0000547			
rno-miR-322-5p	MIMAT0001619			
rno-miR-323-3p	MIMAT0000550		13.216764	
rno-miR-323-5p	MIMAT0004637	85.092807	121.657066	135.58993
rno-miR-324-3p	MIMAT0000554	45.435533	63.838473	72.520785
rno-miR-324-5p	MIMAT0000553	6.480624	9.961711	12.435795
rno-miR-325-3p	MIMAT0004639			
rno-miR-325-5p	MIMAT0000557			
rno-miR-326-3p	MIMAT0000560	16.439667	11.890413	19.287951
rno-miR-326-5p	MIMAT0017028	306.352506	274.33596	295.312451
rno-miR-327	MIMAT0000561	31.40786	44.204748	41.146325
rno-miR-328a-3p	MIMAT0000564	48.382708		41.79551
rno-miR-328a-5p	MIMAT0017029	971.989863	694.865462	1115.065402
rno-miR-328b-3p	MIMAT0017904	34.120793	31.639286	50.844927
rno-miR-329-3p	MIMAT0000566			8.84609
rno-miR-329-5p	MIMAT0017031			
rno-miR-33-3p	MIMAT0017104			
rno-miR-33-5p	MIMAT0000812		20.250863	
rno-miR-330-3p	MIMAT0000568	8.920528	25.211409	22.146752
rno-miR-330-5p	MIMAT0004641		10.527804	12.19315
rno-miR-331-3p	MIMAT0000570	9.376602		15.265915
rno-miR-331-5p	MIMAT0017033			
rno-miR-335	MIMAT0000575			
rno-miR-336-3p	MIMAT0017034			
rno-miR-336-5p	MIMAT0000576	8.924079	9.648959	8.419571
rno-miR-337-3p	MIMAT0000577			
rno-miR-337-5p	MIMAT0017035			
rno-miR-338-3p	MIMAT0000581		16.371323	
rno-miR-338-5p	MIMAT0004646		10.285379	
rno-miR-339-3p	MIMAT0004648			7.993293
rno-miR-339-5p	MIMAT0000583	8.704574	15.346972	13.539688
rno-miR-340-3p	MIMAT0000585		17.085416	
rno-miR-340-5p	MIMAT0004650			
rno-miR-341	MIMAT0000587	10.943356	13.299779	17.250867
rno-miR-342-3p	MIMAT0000589	8.546023	16.131556	14.614529
rno-miR-342-5p	MIMAT0004652	9.102903	10.687442	12.746487
rno-miR-343	MIMAT0000591	21.024955	18.744483	19.615266
rno-miR-344a	MIMAT0017842			
rno-miR-344a-3p	MIMAT0000592			
rno-miR-344a-5p	MIMAT0004654	7.847613		13.312619
rno-miR-344b-1-3p	MIMAT0017894			
rno-miR-344b-2-3p	MIMAT0017812			
rno-miR-344b-5p	MIMAT0017811			
rno-miR-344g	MIMAT0025052			
rno-miR-344i	MIMAT0025049			
rno-miR-345-3p	MIMAT0004655			
rno-miR-345-5p	MIMAT0000594	25.489027	23.781488	27.895515
rno-miR-346	MIMAT0000596	23.342937	27.427193	29.313721
rno-miR-347	MIMAT0000598	62.638866	198.889948	192.470811
rno-miR-3473	MIMAT0024853	3942.746792	1491.28881	5282.03235
rno-miR-349	MIMAT0000599	9.328126	11.809039	12.363735
rno-miR-34a-3p	MIMAT0017106			
rno-miR-34a-5p	MIMAT0000815		17.358267	10.568267
rno-miR-34b-3p	MIMAT0017105			
rno-miR-34b-5p	MIMAT0000813			
rno-miR-34c-3p	MIMAT0004723			10.868938
rno-miR-34c-5p	MIMAT0000814			
rno-miR-350	MIMAT0000604			
rno-miR-351-3p	MIMAT0017041	160.259018	57.472169	116.371886
rno-miR-351-5p	MIMAT0000608	55.235369	39.523313	60.090329
rno-miR-352	MIMAT0000610			

rno-miR-3541	MIMAT0017795	143.359296	121.805856	114.210033
rno-miR-3542	MIMAT0017796			
rno-miR-3543	MIMAT0017797			
rno-miR-3544	MIMAT0017798	6.731891		13.041732
rno-miR-3546	MIMAT0017801			
rno-miR-3547	MIMAT0017802	31.889976	26.114615	33.762111
rno-miR-3548	MIMAT0017806		14.850553	
rno-miR-3549	MIMAT0017807			
rno-miR-3550	MIMAT0017808	10.658642		14.615208
rno-miR-3551-3p	MIMAT0017810			
rno-miR-3551-5p	MIMAT0017809			
rno-miR-3552	MIMAT0017813	16.131502	21.277445	17.157984
rno-miR-3553	MIMAT0017814			
rno-miR-3556a	MIMAT0017821			
rno-miR-3556b	MIMAT0017818			
rno-miR-3557-3p	MIMAT0017820	19.015257	16.014868	23.848937
rno-miR-3557-5p	MIMAT0017819			
rno-miR-3558-3p	MIMAT0017826			
rno-miR-3558-5p	MIMAT0017825	15.858267	12.773128	14.433592
rno-miR-3559-3p	MIMAT0017828			
rno-miR-3559-5p	MIMAT0017827			
rno-miR-3560	MIMAT0017829	48.358512	72.004826	91.663031
rno-miR-3561-3p	MIMAT0017831			
rno-miR-3561-5p	MIMAT0017830			
rno-miR-3562	MIMAT0017832	26.156043	19.447002	49.398384
rno-miR-3564	MIMAT0017837			17.296113
rno-miR-3566	MIMAT0017841			8.579931
rno-miR-3568	MIMAT0017848			
rno-miR-3569	MIMAT0017849	20.655262	21.069348	29.711998
rno-miR-3570	MIMAT0017850			
rno-miR-3571	MIMAT0017851			
rno-miR-3572	MIMAT0017853	15.196424	12.511293	15.605586
rno-miR-3573-3p	MIMAT0017857	229.017371	156.792784	155.073313
rno-miR-3573-5p	MIMAT0017856	18.935411	20.073751	27.56127
rno-miR-3574	MIMAT0017860			
rno-miR-3575	MIMAT0017861			
rno-miR-3576	MIMAT0017862			
rno-miR-3577	MIMAT0017863	31.048119	19.899718	31.863847
rno-miR-3578	MIMAT0017866			
rno-miR-3579	MIMAT0017867			
rno-miR-3580-3p	MIMAT0017869			
rno-miR-3580-5p	MIMAT0017868			
rno-miR-3583-3p	MIMAT0017874			
rno-miR-3583-5p	MIMAT0017873			
rno-miR-3584-3p	MIMAT0017876	10.321442	10.45059	18.845287
rno-miR-3584-5p	MIMAT0017875	198.336781	226.632945	316.273533
rno-miR-3585-3p	MIMAT0017879			
rno-miR-3585-5p	MIMAT0017878			
rno-miR-3586-3p	MIMAT0017881			
rno-miR-3586-5p	MIMAT0017880	7.079242		12.895576
rno-miR-3587	MIMAT0017883			
rno-miR-3588	MIMAT0017887			
rno-miR-3589	MIMAT0017888			
rno-miR-3590-3p	MIMAT0017890			
rno-miR-3590-5p	MIMAT0017889			
rno-miR-3591	MIMAT0017893			
rno-miR-3592	MIMAT0017895			
rno-miR-3593-3p	MIMAT0017897	129.345206	109.016626	120.934871
rno-miR-3593-5p	MIMAT0017896			
rno-miR-3594-3p	MIMAT0017899	38.076109	32.103445	49.545747
rno-miR-3594-5p	MIMAT0017898	110.676696	74.876472	118.396676
rno-miR-3595	MIMAT0017903			
rno-miR-3596a	MIMAT0017886			
rno-miR-3596b	MIMAT0017871			
rno-miR-3596c	MIMAT0017877			
rno-miR-3596d	MIMAT0017823			
rno-miR-361-3p	MIMAT0017199	70.038147	50.447018	52.779093

rno-miR-361-5p	MIMAT0003117		13.482597	10.776716
rno-miR-362-3p	MIMAT0017357			
rno-miR-362-5p	MIMAT0012828			
rno-miR-363-3p	MIMAT0003210			
rno-miR-363-5p	MIMAT0003209	23.73109	14.959437	22.572116
rno-miR-365-3p	MIMAT0001549	33.600704	16.177753	18.897849
rno-miR-365-5p	MIMAT0017184	284.340682	187.078317	447.18262
rno-miR-369-3p	MIMAT0003207			
rno-miR-369-5p	MIMAT0003206			
rno-miR-370-3p	MIMAT0003122	2453.486316	626.446728	3600.667596
rno-miR-370-5p	MIMAT0017202			
rno-miR-374-3p	MIMAT0017223			
rno-miR-374-5p	MIMAT0003208			
rno-miR-375-3p	MIMAT0005307			
rno-miR-375-5p	MIMAT0017301	618.82619	296.909496	359.475133
rno-miR-376a-3p	MIMAT0003198			
rno-miR-376a-5p	MIMAT0003197			
rno-miR-376b-3p	MIMAT0003196			
rno-miR-376b-5p	MIMAT0003195			
rno-miR-376c-3p	MIMAT0003194			
rno-miR-376c-5p	MIMAT0017219			
rno-miR-377-3p	MIMAT0003123			
rno-miR-377-5p	MIMAT0017203			
rno-miR-378a-3p	MIMAT0003379	24.970583	13.962559	32.64911
rno-miR-378a-5p	MIMAT0003378	30.783797	28.571544	37.747858
rno-miR-378b	MIMAT0024855	13.993134	16.657257	28.548857
rno-miR-379-3p	MIMAT0004791			
rno-miR-379-5p	MIMAT0003192			
rno-miR-380-3p	MIMAT0017302			
rno-miR-380-5p	MIMAT0005308			
rno-miR-381-3p	MIMAT0003199	9.358819	24.130667	14.697511
rno-miR-381-5p	MIMAT0017220			
rno-miR-382-3p	MIMAT0003202			
rno-miR-382-5p	MIMAT0003201			
rno-miR-383-3p	MIMAT0017197			
rno-miR-383-5p	MIMAT0003114			
rno-miR-384-3p	MIMAT0005310			
rno-miR-384-5p	MIMAT0005309		14.192819	
rno-miR-409a-3p	MIMAT0003205	9.601128		8.283531
rno-miR-409a-5p	MIMAT0003204			
rno-miR-409b	MIMAT0017870			
rno-miR-410-3p	MIMAT0005311			
rno-miR-410-5p	MIMAT0017303			
rno-miR-411-3p	MIMAT0017304			
rno-miR-411-5p	MIMAT0005312			
rno-miR-412-3p	MIMAT0003124	8.608603	13.090305	12.950595
rno-miR-412-5p	MIMAT0017204			
rno-miR-421-3p	MIMAT0017175			
rno-miR-421-5p	MIMAT0001320			
rno-miR-423-3p	MIMAT0005313	15.34099		16.247973
rno-miR-423-5p	MIMAT0017305	50.652941	47.608814	48.59452
rno-miR-425-3p	MIMAT0017306			
rno-miR-425-5p	MIMAT0005314	6.665604		10.678337
rno-miR-429	MIMAT0001538			
rno-miR-431	MIMAT0001626			
rno-miR-433-3p	MIMAT0001628			10.432506
rno-miR-433-5p	MIMAT0017192	16.267387	13.713743	9.600527
rno-miR-434-3p	MIMAT0005315			
rno-miR-434-5p	MIMAT0017307			
rno-miR-448-3p	MIMAT0001534			
rno-miR-448-5p	MIMAT0017177			
rno-miR-449a-3p	MIMAT0017181			
rno-miR-449a-5p	MIMAT0001543			
rno-miR-449c-3p	MIMAT0017804			
rno-miR-449c-5p	MIMAT0017803			9.166734
rno-miR-450a-3p	MIMAT0017183			
rno-miR-450a-5p	MIMAT0001547			

rno-miR-451-3p	MIMAT0017193			
rno-miR-451-5p	MIMAT0001633			
rno-miR-455-3p	MIMAT0017308			
rno-miR-455-5p	MIMAT0005316			
rno-miR-463-3p	MIMAT0005317			
rno-miR-463-5p	MIMAT0017309			
rno-miR-465-3p	MIMAT0017367			
rno-miR-465-5p	MIMAT0012850			
rno-miR-466b-1-3p	MIMAT0017285	12.035503	27.107164	18.571817
rno-miR-466b-2-3p	MIMAT0017286			
rno-miR-466b-5p	MIMAT0005278	10.404631	20.43355	19.052802
rno-miR-466c-3p	MIMAT0017287			8.095226
rno-miR-466c-5p	MIMAT0005279			
rno-miR-466d	MIMAT0017824			9.741276
rno-miR-471-3p	MIMAT0017310			
rno-miR-471-5p	MIMAT0005318			
rno-miR-483-3p	MIMAT0003121	47.849962	35.433941	54.0677
rno-miR-483-5p	MIMAT0017201	25	18.624452	51.584208
rno-miR-484	MIMAT0005319	28.433691	28.375448	24.654946
rno-miR-485-3p	MIMAT0017222	19.622349	15.22258	19.74687
rno-miR-485-5p	MIMAT0003203	7.779005	23.808734	11.12003
rno-miR-487b-3p	MIMAT0003200			
rno-miR-487b-5p	MIMAT0017221	7.816798		
rno-miR-488-3p	MIMAT0005341			
rno-miR-488-5p	MIMAT0017320			
rno-miR-489-3p	MIMAT0003113			
rno-miR-489-5p	MIMAT0017196			
rno-miR-490-3p	MIMAT0012823	7.001884		17.918323
rno-miR-490-5p	MIMAT0017356			
rno-miR-493-3p	MIMAT0003191			
rno-miR-493-5p	MIMAT0017217			
rno-miR-494-3p	MIMAT0003193	2040.482587	1758.939711	3831.592617
rno-miR-494-5p	MIMAT0017218	6.683008		
rno-miR-495	MIMAT0005320			
rno-miR-496-3p	MIMAT0012860			
rno-miR-496-5p	MIMAT0017372			
rno-miR-497-3p	MIMAT0017230			
rno-miR-497-5p	MIMAT0003383		11.768152	
rno-miR-499-3p	MIMAT0017227			
rno-miR-499-5p	MIMAT0003381			
rno-miR-500-3p	MIMAT0005321	11.513542	15.524317	12.966683
rno-miR-500-5p	MIMAT0017311			
rno-miR-501-3p	MIMAT0017198			
rno-miR-501-5p	MIMAT0003116			
rno-miR-503-3p	MIMAT0017224	10.682303		13.67875
rno-miR-503-5p	MIMAT0003213			
rno-miR-504	MIMAT0012830			
rno-miR-505-3p	MIMAT0003380	84.364138	72.434361	112.757474
rno-miR-505-5p	MIMAT0017226	21.661187	22.94766	28.484769
rno-miR-509-3p	MIMAT0024850			
rno-miR-509-5p	MIMAT0024849			
rno-miR-511-3p	MIMAT0017358			
rno-miR-511-5p	MIMAT0012829			
rno-miR-532-3p	MIMAT0005323	25.082451	36.359801	31.238045
rno-miR-532-5p	MIMAT0005322			
rno-miR-539-3p	MIMAT0017212			
rno-miR-539-5p	MIMAT0003176			
rno-miR-540-3p	MIMAT0003174	24.101145	23.185987	27.26826
rno-miR-540-5p	MIMAT0017211			
rno-miR-541-3p	MIMAT0017213			
rno-miR-541-5p	MIMAT0003177			
rno-miR-542-3p	MIMAT0003179			
rno-miR-542-5p	MIMAT0003178			
rno-miR-543-3p	MIMAT0003175			
rno-miR-543-5p	MIMAT0004787			
rno-miR-544-3p	MIMAT0012831			
rno-miR-544-5p	MIMAT0017359			

rno-miR-547-3p	MIMAT0012851			
rno-miR-547-5p	MIMAT0017368		10.742688	
rno-miR-551b-3p	MIMAT0005596	557.871452	345.175252	722.503613
rno-miR-551b-5p	MIMAT0017335			
rno-miR-568	MIMAT0012832			
rno-miR-582-3p	MIMAT0017360			
rno-miR-582-5p	MIMAT0012833		9.799975	
rno-miR-592	MIMAT0012834			
rno-miR-598-3p	MIMAT0005325			
rno-miR-598-5p	MIMAT0005324	13.267537	13.9281	13.477339
rno-miR-615	MIMAT0012835	136.981763	186.404749	187.306287
rno-miR-6215	MIMAT0024854	247.377298	782.228972	1054.972357
rno-miR-6216	MIMAT0024856	318.28257	239.789415	423.230855
rno-miR-628	MIMAT0012836			
rno-miR-6314	MIMAT0025047			
rno-miR-6315	MIMAT0025050	23.009036	27.490634	30.973573
rno-miR-6316	MIMAT0025053			
rno-miR-6317	MIMAT0025054	7.22399		12.070635
rno-miR-6318	MIMAT0025055	67.148331	29.774647	47.379604
rno-miR-6319	MIMAT0025056			
rno-miR-632	MIMAT0012837			
rno-miR-6320	MIMAT0025058			
rno-miR-6321	MIMAT0025059			
rno-miR-6322	MIMAT0025061			
rno-miR-6323	MIMAT0025062			
rno-miR-6324	MIMAT0025063			9.386855
rno-miR-6325	MIMAT0025064			
rno-miR-6326	MIMAT0025065			
rno-miR-6327	MIMAT0025066			
rno-miR-6328	MIMAT0025067	51.90217	29.023965	35.102634
rno-miR-6329	MIMAT0025068			
rno-miR-6330	MIMAT0025069			
rno-miR-6331	MIMAT0025070			
rno-miR-6332	MIMAT0025073	4263.785759	1150.286755	2149.391876
rno-miR-6333	MIMAT0025074			
rno-miR-6334	MIMAT0025075	23.248205	13.042009	23.155676
rno-miR-652-3p	MIMAT0005342			
rno-miR-652-5p	MIMAT0017321	65.052212	85.146214	83.191842
rno-miR-653-3p	MIMAT0017361			
rno-miR-653-5p	MIMAT0012838			
rno-miR-664-1-5p	MIMAT0017228	39.473544	24.916954	51.244302
rno-miR-664-2-5p	MIMAT0017229	31.66968	22.96861	50.226441
rno-miR-664-3p	MIMAT0003382	30.651892	38.142801	24.153417
rno-miR-665	MIMAT0012844	53.081816	56.760306	73.460378
rno-miR-666-3p	MIMAT0017371			
rno-miR-666-5p	MIMAT0012855	45.952458	31.772432	49.056993
rno-miR-667-3p	MIMAT0012852	41.197164	42.603611	49.497347
rno-miR-667-5p	MIMAT0017369	645.78869	364.073316	520.780671
rno-miR-668	MIMAT0012839	25.232387	22.762448	36.022927
rno-miR-671	MIMAT0005326	10.132489		8.749875
rno-miR-672-3p	MIMAT0017312			
rno-miR-672-5p	MIMAT0005327			
rno-miR-673-3p	MIMAT0017313			
rno-miR-673-5p	MIMAT0005328			
rno-miR-674-3p	MIMAT0005330	22.886162		9.515507
rno-miR-674-5p	MIMAT0005329			
rno-miR-675-3p	MIMAT0017363			
rno-miR-675-5p	MIMAT0012841	47.81242	17.998262	47.802144
rno-miR-678	MIMAT0012857	81.533164	71.307259	107.265348
rno-miR-679	MIMAT0025072			
rno-miR-702-3p	MIMAT0017885	35.380116	19.408904	32.11287
rno-miR-702-5p	MIMAT0017884	52.28994	30.173398	69.211348
rno-miR-708-3p	MIMAT0005332			
rno-miR-708-5p	MIMAT0005331	15.962511	11.864316	17.939673
rno-miR-711	MIMAT0012859	39.418446	26.196285	57.666621
rno-miR-741-3p	MIMAT0017902			
rno-miR-741-5p	MIMAT0017901			

rno-miR-742-3p	MIMAT0005333			
rno-miR-742-5p	MIMAT0017314			
rno-miR-743a-3p	MIMAT0005334			
rno-miR-743a-5p	MIMAT0017315			
rno-miR-743b-3p	MIMAT0005280			
rno-miR-743b-5p	MIMAT0017288			8.519086
rno-miR-7578	MIMAT0029579			
rno-miR-758-3p	MIMAT0005335		40.151243	
rno-miR-758-5p	MIMAT0017316			9.458603
rno-miR-759	MIMAT0012856			
rno-miR-760-3p	MIMAT0005337	89.481446	70.924506	109.215033
rno-miR-760-5p	MIMAT0005336	27.83668	54.773537	20.14302
rno-miR-761	MIMAT0012853		10.162299	
rno-miR-764-3p	MIMAT0017370	30.921482	30.796768	37.087085
rno-miR-764-5p	MIMAT0012854	14.077051		17.426745
rno-miR-770-3p	MIMAT0017317	93.74576	56.35516	112.232214
rno-miR-770-5p	MIMAT0005338	9.002946		10.703996
rno-miR-7a-1-3p	MIMAT0000607			
rno-miR-7a-2-3p	MIMAT0017091	8.092389		16.330587
rno-miR-7a-5p	MIMAT0000606			
rno-miR-7b	MIMAT0000780			
rno-miR-802-3p	MIMAT0017362			
rno-miR-802-5p	MIMAT0012840			
rno-miR-871-3p	MIMAT0017289			
rno-miR-871-5p	MIMAT0005281			
rno-miR-872-3p	MIMAT0005283			
rno-miR-872-5p	MIMAT0005282			
rno-miR-873-3p	MIMAT0017318			
rno-miR-873-5p	MIMAT0005339			
rno-miR-874-3p	MIMAT0005284	57.750742	57.380038	51.630265
rno-miR-874-5p	MIMAT0017290	60.23162	53.954235	46.718266
rno-miR-875	MIMAT0012842			
rno-miR-876	MIMAT0012843			
rno-miR-877	MIMAT0005285	35.097091	34.221657	54.68439
rno-miR-878	MIMAT0005286			
rno-miR-879-3p	MIMAT0017291			
rno-miR-879-5p	MIMAT0005287			
rno-miR-880-3p	MIMAT0005288			
rno-miR-880-5p	MIMAT0017292			
rno-miR-881-3p	MIMAT0005289			
rno-miR-881-5p	MIMAT0017293			
rno-miR-883-3p	MIMAT0005290			
rno-miR-883-5p	MIMAT0017294			
rno-miR-92a-1-5p	MIMAT0017107			
rno-miR-92a-2-5p	MIMAT0017108	1745.283839	833.576048	1454.082641
rno-miR-92a-3p	MIMAT0000816	8.07959	14.251704	
rno-miR-92b-3p	MIMAT0005340	9.54603	14.754224	9.886385
rno-miR-92b-5p	MIMAT0017319	908.974672	979.550157	1163.635639
rno-miR-93-3p	MIMAT0017109		11.073996	
rno-miR-93-5p	MIMAT0000817			
rno-miR-935	MIMAT0012845			
rno-miR-96-3p	MIMAT0017110			
rno-miR-96-5p	MIMAT0000818			
rno-miR-98-3p	MIMAT0017111			
rno-miR-98-5p	MIMAT0000819			
rno-miR-99a-3p	MIMAT0004724			8.564554
rno-miR-99a-5p	MIMAT0000820	21.84437	86.416434	102.65708
rno-miR-99b-3p	MIMAT0004725	9.381611		15.408498
rno-miR-99b-5p	MIMAT0000821		15.029896	24.249504
rno-miR-9a-3p	MIMAT0004708			
rno-miR-9a-5p	MIMAT0000781			
rno-miR-9b-3p	MIMAT0017836			
rno-miR-9b-5p	MIMAT0017835			

Appendix IV. UAS-miRNA *Drosophila* stock list

All stocks were obtained from the Bloomington *Drosophila* stock centre. Stocks were created as referenced in (Bejarano et al. 2012).

miR-1	w[1118]; P{y[+t7.7] w[+mC]=UAS-LUC-mir-1.T}attP2/TM3, Sb[1]
miR-124	w[1118]; P{y[+t7.7] w[+mC]=UAS-LUC-mir-124.T}attP2
miR-252	w[1118]; P{y[+t7.7] w[+mC]=UAS-LUC-mir-252.T}attP2
miR-2b-1	w[1118]; P{y[+t7.7] w[+mC]=UAS-LUC-mir-2b-1.T}attP2
miR-31b	w[1118]; P{y[+t7.7] w[+mC]=UAS-LUC-mir-31b.T}attP2
miR-992	w[1118]; P{y[+t7.7] w[+mC]=UAS-LUC-mir-992.T}attP2
miR-9b	w[1118]; P{y[+t7.7] w[+mC]=UAS-LUC-mir-9b.T}attP2
miR-133	w[1118]; P{y[+t7.7] w[+mC]=UAS-LUC-mir-133.T}attP2
bereft	w[1118]; P{y[+t7.7] w[+mC]=UAS-LUC-bft.T}attP2
miR-284	w[1118]; P{y[+t7.7] w[+mC]=UAS-LUC-mir-284.T}attP2
miR-310Cluster	w[1118]; P{y[+t7.7] w[+mC]=UAS-LUC-mir-310.mir-311.mir-312.mir-313.T}attP2/TM3, Sb[1]
miR-6Cluster	w[1118]; P{y[+t7.7] w[+mC]=UAS-LUC-mir-6-1.mir-6-2.mir-6-3.T}attP2
miR-7	w[1118]; P{y[+t7.7] w[+mC]=UAS-LUC-mir-7.T}attP2
miR-9a	w[1118]; P{y[+t7.7] w[+mC]=UAS-LUC-mir-9a.T}attP2
miR-9c	w[1118]; P{y[+t7.7] w[+mC]=UAS-LUC-mir-9c.T}attP2
miR-12	w[1118]; P{y[+t7.7] w[+mC]=UAS-LUC-mir-12.T}attP2
miR-303	w[1118]; P{y[+t7.7] w[+mC]=UAS-LUC-mir-303.T}attP2
miR-275	w[1118]; P{y[+t7.7] w[+mC]=UAS-LUC-mir-275.T}attP2
miR-276a	w[1118]; P{y[+t7.7] w[+mC]=UAS-LUC-mir-276a.T}attP2
miR-312	w[1118]; P{y[+t7.7] w[+mC]=UAS-LUC-mir-312.T}attP2
miR-79	w[1118]; P{y[+t7.7] w[+mC]=UAS-LUC-mir-79.T}attP2
miR-263b	w[1118]; P{y[+t7.7] w[+mC]=UAS-LUC-mir-263b.T}attP2
miR-279	w[1118]; P{y[+t7.7] w[+mC]=UAS-LUC-mir-279.T}attP2
miR-964	w[1118]; P{y[+t7.7] w[+mC]=UAS-LUC-mir-964.T}attP2
miR-976	w[1118]; P{y[+t7.7] w[+mC]=UAS-LUC-mir-976.T}attP2/TM3, Sb[1]
miR-33	w[1118]; P{y[+t7.7] w[+mC]=UAS-LUC-mir-33.T}attP2
miR-286	w[1118]; P{y[+t7.7] w[+mC]=UAS-LUC-mir-286.T}attP2
miR-305	w[1118]; P{y[+t7.7] w[+mC]=UAS-LUC-mir-305.T}attP2/TM3, Sb[1]
miR-92a	w[1118]; P{y[+t7.7] w[+mC]=UAS-LUC-mir-92a.T}attP2
miR-190	w[1118]; P{y[+t7.7] w[+mC]=UAS-LUC-mir-190.T}attP2
miR-310	w[1118]; P{y[+t7.7] w[+mC]=UAS-LUC-mir-310.T}attP2/TM3, Sb[1]
miR-9cCluster	w[1118]; P{y[+t7.7] w[+mC]=UAS-LUC-mir-9c.mir-306.mir-79.mir-9b.T}attP2
miR-932	w[1118]; P{y[+t7.7] w[+mC]=UAS-LUC-mir-932.T}attP2
miR-34	w[1118]; P{y[+t7.7] w[+mC]=UAS-LUC-mir-34.T}attP2
miR-308	w[1118]; P{y[+t7.7] w[+mC]=UAS-LUC-mir-308.T}attP2
miR-285	w[1118]; P{y[+t7.7] w[+mC]=UAS-LUC-mir-285.T}attP2
miR-318	w[1118]; P{y[+t7.7] w[+mC]=UAS-LUC-mir-318.T}attP2/TM3, Sb[1]
miR-276b	w[1118]; P{y[+t7.7] w[+mC]=UAS-LUC-mir-276b.T}attP2
miR-311	w[1118]; P{y[+t7.7] w[+mC]=UAS-LUC-mir-311.T}attP2
miR-280	w[1118]; P{y[+t7.7] w[+mC]=UAS-LUC-mir-280.T}attP2
miR-282	w[1118]; P{y[+t7.7] w[+mC]=UAS-LUC-mir-282.T}attP2
miR-100	w[1118]; P{y[+t7.7] w[+mC]=UAS-LUC-mir-100.T}attP2
miR-281-1/2	w[1118]; P{y[+t7.7] w[+mC]=UAS-LUC-mir-281-1.mir-281-2.T}attP2
miR-275/305	w[1118]; P{y[+t7.7] w[+mC]=UAS-LUC-mir-275.mir-305.T}attP2
miR-10	w[1118]; P{y[+t7.7] w[+mC]=UAS-LUC-mir-10.T}attP2/TM3, Sb[1]
miR-304	w[1118]; P{y[+t7.7] w[+mC]=UAS-LUC-mir-304.T}attP2
let-7	w[1118]; P{y[+t7.7] w[+mC]=UAS-LUC-let-7.T}attP2
miR-274	w[1118]; P{y[+t7.7] w[+mC]=UAS-LUC-mir-274.T}attP2

miR-iab-4	w[1118]; P{y[+t7.7] w[+mC]=UAS-LUC-mir-iab-4.T}attP2
miR-184	w[1118]; P{y[+t7.7] w[+mC]=UAS-LUC-mir-184.T}attP2
miR-92b	w[1118]; P{y[+t7.7] w[+mC]=UAS-LUC-mir-92b.T}attP2
miR-8	w[1118]; P{y[+t7.7] w[+mC]=UAS-LUC-mir-8.T}attP2
miR-281-1	w[1118]; P{y[+t7.7] w[+mC]=UAS-LUC-mir-281-1.T}attP2
miR-14	w[1118]; P{y[+t7.7] w[+mC]=UAS-LUC-mir-14.T}attP2
miR-210	w[1118]; P{y[+t7.7] w[+mC]=UAS-LUC-mir-210.T}attP2
miR-278	w[1118]; P{y[+t7.7] w[+mC]=UAS-LUC-mir-278.T}attP2
miR-309	w[1118]; P{y[+t7.7] w[+mC]=UAS-LUC-mir-309.T}attP2
miR-375	w[1118]; P{y[+t7.7] w[+mC]=UAS-LUC-mir-375.T}attP2
miR-927	w[1118]; P{y[+t7.7] w[+mC]=UAS-LUC-mir-927.T}attP2
miR-929	w[1118]; P{y[+t7.7] w[+mC]=UAS-LUC-mir-929.T}attP2/TM3, Sb[1]
miR-954	w[1118]; P{y[+t7.7] w[+mC]=UAS-LUC-mir-954.T}attP2
miR-955	w[1118]; P{y[+t7.7] w[+mC]=UAS-LUC-mir-955.T}attP2
miR-956	w[1118]; P{y[+t7.7] w[+mC]=UAS-LUC-mir-956.T}attP2
miR-961	w[1118]; P{y[+t7.7] w[+mC]=UAS-LUC-mir-961.T}attP2
miR-970	w[1118]; P{y[+t7.7] w[+mC]=UAS-LUC-mir-970.T}attP2
miR-973	w[1118]; P{y[+t7.7] w[+mC]=UAS-LUC-mir-973.T}attP2
miR-980	w[1118]; P{y[+t7.7] w[+mC]=UAS-LUC-mir-980.T}attP2
miR-982	w[1118]; P{y[+t7.7] w[+mC]=UAS-LUC-mir-982.T}attP2
miR-982/303	w[1118]; P{y[+t7.7] w[+mC]=UAS-LUC-mir-982.mir-303.T}attP2
miR-983-1	w[1118]; P{y[+t7.7] w[+mC]=UAS-LUC-mir-983-1.T}attP2
miR-987	w[1118]; P{y[+t7.7] w[+mC]=UAS-LUC-mir-987.T}attP2
miR-988	w[1118]; P{y[+t7.7] w[+mC]=UAS-LUC-mir-988.T}attP2
miR-993	w[1118]; P{y[+t7.7] w[+mC]=UAS-LUC-mir-993.T}attP2
miR-994	w[1118]; P{y[+t7.7] w[+mC]=UAS-LUC-mir-994.T}attP2
miR-995	w[1118]; P{y[+t7.7] w[+mC]=UAS-LUC-mir-995.T}attP2
miR-999	w[1118]; P{y[+t7.7] w[+mC]=UAS-LUC-mir-999.T}attP2
miR-1000	w[1118]; P{y[+t7.7] w[+mC]=UAS-LUC-mir-1000.T}attP2
miR-1001	w[1118]; P{y[+t7.7] w[+mC]=UAS-LUC-mir-1001.T}attP2
miR-1004	w[1118]; P{y[+t7.7] w[+mC]=UAS-LUC-mir-1004.T}attP2
miR-1006	w[1118]; P{y[+t7.7] w[+mC]=UAS-LUC-mir-1006.T}attP2
miR-1009	w[1118]; P{y[+t7.7] w[+mC]=UAS-LUC-mir-1009.T}attP2
miR-1010	w[1118]; P{y[+t7.7] w[+mC]=UAS-LUC-mir-1010.T}attP2
miR-1015	w[1118]; P{y[+t7.7] w[+mC]=UAS-LUC-mir-1015.T}attP2
miR-1017	w[1118]; P{y[+t7.7] w[+mC]=UAS-LUC-mir-1017.T}attP2/TM3, Sb[1]
miR-137	w[1118]; P{y[+t7.7] w[+mC]=UAS-LUC-mir-137.T}attP2
miR-1011	w[1118]; P{y[+t7.7] w[+mC]=UAS-LUC-mir-1011.T}attP2
miR-966	w[1118]; P{y[+t7.7] w[+mC]=UAS-LUC-mir-966.T}attP2
miR-978	w[1118]; P{y[+t7.7] w[+mC]=UAS-LUC-mir-978.T}attP2
miR-985	w[1118]; P{y[+t7.7] w[+mC]=UAS-LUC-mir-985.T}attP2
miR-1012	w[1118]; P{y[+t7.7] w[+mC]=UAS-LUC-mir-1012.T}attP2
miR-1013	w[1118]; P{y[+t7.7] w[+mC]=UAS-LUC-mir-1013.T}attP2
miR-963/964	w[1118]; P{y[+t7.7] w[+mC]=UAS-LUC-mir-963.mir-964.T}attP2
miR-984Cluster	w[1118]; P{y[+t7.7] w[+mC]=UAS-LUC-mir-984.mir-983-1.mir-983-2.T}attP2
miR-986	w[1118]; P{y[+t7.7] w[+mC]=UAS-LUC-mir-986.T}attP2
miR-989	w[1118]; P{y[+t7.7] w[+mC]=UAS-LUC-mir-989.T}attP2
miR-1003	w[1118]; P{y[+t7.7] w[+mC]=UAS-LUC-mir-1003.T}attP2
miR-1007	w[1118]; P{y[+t7.7] w[+mC]=UAS-LUC-mir-1007.T}attP2
miR-958	w[1118]; P{y[+t7.7] w[+mC]=UAS-LUC-mir-958.T}attP2
miR-4966 cluster	w[1118]; P{y[+t7.7] w[+mC]=UAS-LUC-mir-4966-1.mir-975.mir-976.mir-977.T}attP2
miR-984	w[1118]; P{y[+t7.7] w[+mC]=UAS-LUC-mir-984.T}attP2

Appendix V. smiFISH probe sequences

Sequences for indicated miRNA are shown as probes with attached FLAP sequence for hybridisation of secondary fluorophore tag. Sequences are shown in 5' to 3' orientation.

Pri-miR-184

2017.10.06 pre-mir184 siFISH X_1	CCT CCT AAG TTT CGA GCT GGA CTC AGT GAA TTC GCT GTA GCT GTC TTT
2017.10.06 pre-mir184 siFISH X_9	CCT CCT AAG TTT CGA GCT GGA CTC AGT GTT GCC AAA TCA CAT TCA GGG
2017.10.06 pre-mir184 siFISH X_17	CCT CCT AAG TTT CGA GCT GGA CTC AGT GAA TCA ACG CAG CTC CAG AAG
2017.10.06 pre-mir184 siFISH X_25	CCT CCT AAG TTT CGA GCT GGA CTC AGT GAT GGC TAG CAA AAC GCT TCT
2017.10.06 pre-mir184 siFISH X_33	CCT CCT AAG TTT CGA GCT GGA CTC AGT GTT GGT TTG ATG AAT TGG TGA
2017.10.06 pre-mir184 siFISH X_2	CCT CCT AAG TTT CGA GCT GGA CTC AGT GCT GCT GCA CGT TAT GAA TTT
2017.10.06 pre-mir184 siFISH X_10	CCT CCT AAG TTT CGA GCT GGA CTC AGT GAG TGG CAA TGT TGT TTA GGT
2017.10.06 pre-mir184 siFISH X_18	CCT CCT AAG TTT CGA GCT GGA CTC AGT GTA GGA TGC GGT CCG TAT AAA
2017.10.06 pre-mir184 siFISH X_26	CCT CCT AAG TTT CGA GCT GGA CTC AGT GCA GCT GTG AAA AGT TAC CCA
2017.10.06 pre-mir184 siFISH X_34	CCT CCT AAG TTT CGA GCT GGA CTC AGT GAT TCC TGT CGA TTC AAT GGG
2017.10.06 pre-mir184 siFISH X_3	CCT CCT AAG TTT CGA GCT GGA CTC AGT GTA CCA AGC TCC ATT TTC CAC
2017.10.06 pre-mir184 siFISH X_11	CCT CCT AAG TTT CGA GCT GGA CTC AGT GAG AGT TTT CCG TTG GGT TTC
2017.10.06 pre-mir184 siFISH X_19	CCT CCT AAG TTT CGA GCT GGA CTC AGT GTA AAT CAG CCG AGC ACA CAC
2017.10.06 pre-mir184 siFISH X_27	CCT CCT AAG TTT CGA GCT GGA CTC AGT GTT ACC CCA CGT TTC GAT TAC
2017.10.06 pre-mir184 siFISH X_35	CCT CCT AAG TTT CGA GCT GGA CTC AGT GCA AAG CTC CTC TTT GAC TCG
2017.10.06 pre-mir184 siFISH X_4	CCT CCT AAG TTT CGA GCT GGA CTC AGT GGC GGA TAT AAA CTG GGT TCC
2017.10.06 pre-mir184 siFISH X_12	CCT CCT AAG TTT CGA GCT GGA CTC AGT GTT CGT TCG AGT AGA GTC CAC
2017.10.06 pre-mir184 siFISH X_20	CCT CCT AAG TTT CGA GCT GGA CTC AGT GCA TTT GCA TGA CGC ATA TGT
2017.10.06 pre-mir184 siFISH X_28	CCT CCT AAG TTT CGA GCT GGA CTC AGT GGC ACA CTT TTC TTT ATA CAT
2017.10.06 pre-mir184 siFISH X_36	CCT CCT AAG TTT CGA GCT GGA CTC AGT GGC ACT TAT TTA CTC GAT TGT
2017.10.06 pre-mir184 siFISH X_5	CCT CCT AAG TTT CGA GCT GGA CTC AGT GCT CTG GTA ATA TAA TGC CCT
2017.10.06 pre-mir184 siFISH X_13	CCT CCT AAG TTT CGA GCT GGA CTC AGT GTG CTA ATT GAT TTA CTC GCC
2017.10.06 pre-mir184 siFISH X_21	CCT CCT AAG TTT CGA GCT GGA CTC AGT GCT GCC AAC TCA TGT GCA TAA
2017.10.06 pre-mir184 siFISH X_29	CCT CCT AAG TTT CGA GCT GGA CTC AGT GAG CCC AGT TAA TCC ACT GAT
2017.10.06 pre-mir184 siFISH X_37	CCT CCT AAG TTT CGA GCT GGA CTC AGT GTG TTT TCT ATT CAC GCT TTA
2017.10.06 pre-mir184 siFISH X_6	CCT CCT AAG TTT CGA GCT GGA CTC AGT GGA ATT CAA GTC CCA GTT CTA
2017.10.06 pre-mir184 siFISH X_14	CCT CCT AAG TTT CGA GCT GGA CTC AGT GTC AAA CGG TTT TTA GTT GCA
2017.10.06 pre-mir184 siFISH X_22	CCT CCT AAG TTT CGA GCT GGA CTC AGT GAA CTG AAG AGA AGC CCT TGG
2017.10.06 pre-mir184 siFISH X_30	CCT CCT AAG TTT CGA GCT GGA CTC AGT GAT AAG GGT ACG AAT GCA CCG
2017.10.06 pre-mir184 siFISH X_7	CCT CCT AAG TTT CGA GCT GGA CTC AGT GAA TTA GCT CTG TAT CCG CAT
2017.10.06 pre-mir184 siFISH X_15	CCT CCT AAG TTT CGA GCT GGA CTC AGT GAA CTG AAA AAC CCT TTG CCG
2017.10.06 pre-mir184 siFISH X_23	CCT CCT AAG TTT CGA GCT GGA CTC AGT GCT GGC GGA GGA GCA AAT GAA
2017.10.06 pre-mir184 siFISH X_31	CCT CCT AAG TTT CGA GCT GGA CTC AGT GGT CTT TAA GTG CAC ACG GGG
2017.10.06 pre-mir184 siFISH X_8	CCT CCT AAG TTT CGA GCT GGA CTC AGT GAA ATG CCA AGC GAG GCA TTT
2017.10.06 pre-mir184 siFISH X_16	CCT CCT AAG TTT CGA GCT GGA CTC AGT GCC CTT TAG TTC GCA CAA AGA
2017.10.06 pre-mir184 siFISH X_24	CCT CCT AAG TTT CGA GCT GGA CTC AGT GGG GGG AAG GTG TTG AAC AAC
2017.10.06 pre-mir184 siFISH X_32	CCT CCT AAG TTT CGA GCT GGA CTC AGT GCT TAT CAG TTC TCC GTC CAG

Pri-miR-190

2017.10.06 pre-mir190 siFISH X_1	CCT CCT AAG TTT CGA GCT GGA CTC AGT GGT TAG TTA TCA TTC ACC ATT
2017.10.06 pre-mir190 siFISH X_9	CCT CCT AAG TTT CGA GCT GGA CTC AGT GGA TCA CCA ATG GAA TTT AGT
2017.10.06 pre-mir190 siFISH X_17	CCT CCT AAG TTT CGA GCT GGA CTC AGT GCT CAG AGT TTG GAT TGG ACT
2017.10.06 pre-mir190 siFISH X_25	CCT CCT AAG TTT CGA GCT GGA CTC AGT GTT CTA TAG GCG TAC TCG GTG
2017.10.06 pre-mir190 siFISH X_2	CCT CCT AAG TTT CGA GCT GGA CTC AGT GAT TAG GAT GAG TTT TCA GTT
2017.10.06 pre-mir190 siFISH X_10	CCT CCT AAG TTT CGA GCT GGA CTC AGT GTT ACA TGG TGA CTT GAG GCG
2017.10.06 pre-mir190 siFISH X_18	CCT CCT AAG TTT CGA GCT GGA CTC AGT GTT GTC TGT GGA CTT GAT CAC
2017.10.06 pre-mir190 siFISH X_26	CCT CCT AAG TTT CGA GCT GGA CTC AGT GCA TGT TTC ATA CAT TGT TCT
2017.10.06 pre-mir190 siFISH X_3	CCT CCT AAG TTT CGA GCT GGA CTC AGT GGG ATA AAT CAA GCA CCG CTT
2017.10.06 pre-mir190 siFISH X_11	CCT CCT AAG TTT CGA GCT GGA CTC AGT GTC ATG TTT TCG TCG AGT TCA
2017.10.06 pre-mir190 siFISH X_19	CCT CCT AAG TTT CGA GCT GGA CTC AGT GTA AGC GAA TGT TCC TCC TCT
2017.10.06 pre-mir190 siFISH X_27	CCT CCT AAG TTT CGA GCT GGA CTC AGT GGC TGG TGC TTT CAA AGA CTA
2017.10.06 pre-mir190 siFISH X_4	CCT CCT AAG TTT CGA GCT GGA CTC AGT GGT TCG TTT TGA AGG GCA AGT
2017.10.06 pre-mir190 siFISH X_12	CCT CCT AAG TTT CGA GCT GGA CTC AGT GCT CCA AGA TCA TTT CGT CAA
2017.10.06 pre-mir190 siFISH X_20	CCT CCT AAG TTT CGA GCT GGA CTC AGT GTC GAC CAT CGA TGT GTT GAT
2017.10.06 pre-mir190 siFISH X_28	CCT CCT AAG TTT CGA GCT GGA CTC AGT GTC ATC TCA ATG CCA ATT TCT
2017.10.06 pre-mir190 siFISH X_5	CCT CCT AAG TTT CGA GCT GGA CTC AGT GAT ATC TCA CTG GAA CCA TCA
2017.10.06 pre-mir190 siFISH X_13	CCT CCT AAG TTT CGA GCT GGA CTC AGT GGT CGA TGA GCT CAC GCT GAG
2017.10.06 pre-mir190 siFISH X_21	CCT CCT AAG TTT CGA GCT GGA CTC AGT GGA TCG AGC GTT GAT CTC CTG
2017.10.06 pre-mir190 siFISH X_29	CCT CCT AAG TTT CGA GCT GGA CTC AGT GAT TGG TGC TTC AAT TTA GCA
2017.10.06 pre-mir190 siFISH X_6	CCT CCT AAG TTT CGA GCT GGA CTC AGT GAT TCC TGG GTG AAC TTT TGA
2017.10.06 pre-mir190 siFISH X_14	CCT CCT AAG TTT CGA GCT GGA CTC AGT GAA GAC GAG CGG CCG AAA TGA
2017.10.06 pre-mir190 siFISH X_22	CCT CCT AAG TTT CGA GCT GGA CTC AGT GAG TTC CTT TTC CTT ACG CAG
2017.10.06 pre-mir190 siFISH X_30	CCT CCT AAG TTT CGA GCT GGA CTC AGT GCC CAC ACC AGA TAT TAG AAC
2017.10.06 pre-mir190 siFISH X_7	CCT CCT AAG TTT CGA GCT GGA CTC AGT GGG CGA GGG TCA CAG TAA TAA
2017.10.06 pre-mir190 siFISH X_15	CCT CCT AAG TTT CGA GCT GGA CTC AGT GGG AAA TAA GCA TCT CCT CGG
2017.10.06 pre-mir190 siFISH X_23	CCT CCT AAG TTT CGA GCT GGA CTC AGT GCA TTC TTC AGA AGC TGA CGC
2017.10.06 pre-mir190 siFISH X_31	CCT CCT AAG TTT CGA GCT GGA CTC AGT GGG TTA CGT GTT AGA TTT GCT
2017.10.06 pre-mir190 siFISH X_8	CCT CCT AAG TTT CGA GCT GGA CTC AGT GAG TTC TTG AGC TGA GTG TTT
2017.10.06 pre-mir190 siFISH X_16	CCT CCT AAG TTT CGA GCT GGA CTC AGT GTT GCA GGC AAT TAG TAG CTG
2017.10.06 pre-mir190 siFISH X_24	CCT CCT AAG TTT CGA GCT GGA CTC AGT GAC TTT CGT CTG TGG TGA ATC
2017.10.06 pre-mir190 siFISH X_32	CCT CCT AAG TTT CGA GCT GGA CTC AGT GTG ATT AGA GGT TAG AGG AGA

Appendix VI. miR-190 role in *Drosophila* larval NMJ assessment

As preliminary results these suggest that inhibition of miR-190 within developing neurons does not lead to substantial or significant defects in NMJ function or morphology.

NMJ dissection and staining

Wandering 3rd instar larvae were collected and dissected as in (Smith & Taylor 2011). Before fixation in 4% PFA for 30 minutes at room temperature. Following fixation larval pelts were transferred to a glass staining dish and washed three times in 0.3% PBST and permeabilised for 20 minutes. Pelts were blocked in 10% NGST for one hour at room temperature or overnight at 4°C. Blocking solution was exchanged for primary antibody in 10% NGST, pelts were incubated overnight at 4°C in primary antibody. Pelts were washed through three ten minute washes in 0.3%PBST and secondary was applied for one hour at room temperature in 10% NGST. Excess antibody was washed from the pelts by 3 exchanges of 0.3%PBST followed by three 10 minute washes in PBST. Pelts were washed in PBS before mounting.

Larval NMJ active zone quantification

NMJ stained with nc82 demonstrate bright puncta of fluorescence at active zone sites, images of these were used to determine the number of active zones per NMJ area. Confocal Z stacks were converted to maximum intensity projections in FIJI. Thresholding was applied to each image to create a mask of the NMJ area. The puncta within this mask were then automatically counted using the “Analyse Particles” function.

Larval locomotion

Larval locomotion assay was carried out as indicated in (Nichols et al. 2012). Total distance travelled by larvae was calculated by placing 3rd instar larvae into a petri dish coated with a thin layer of 2% agarose placed on top of a 0.2cm^2 grid. The number of lines each larvae crossed in 30 seconds was recorded.

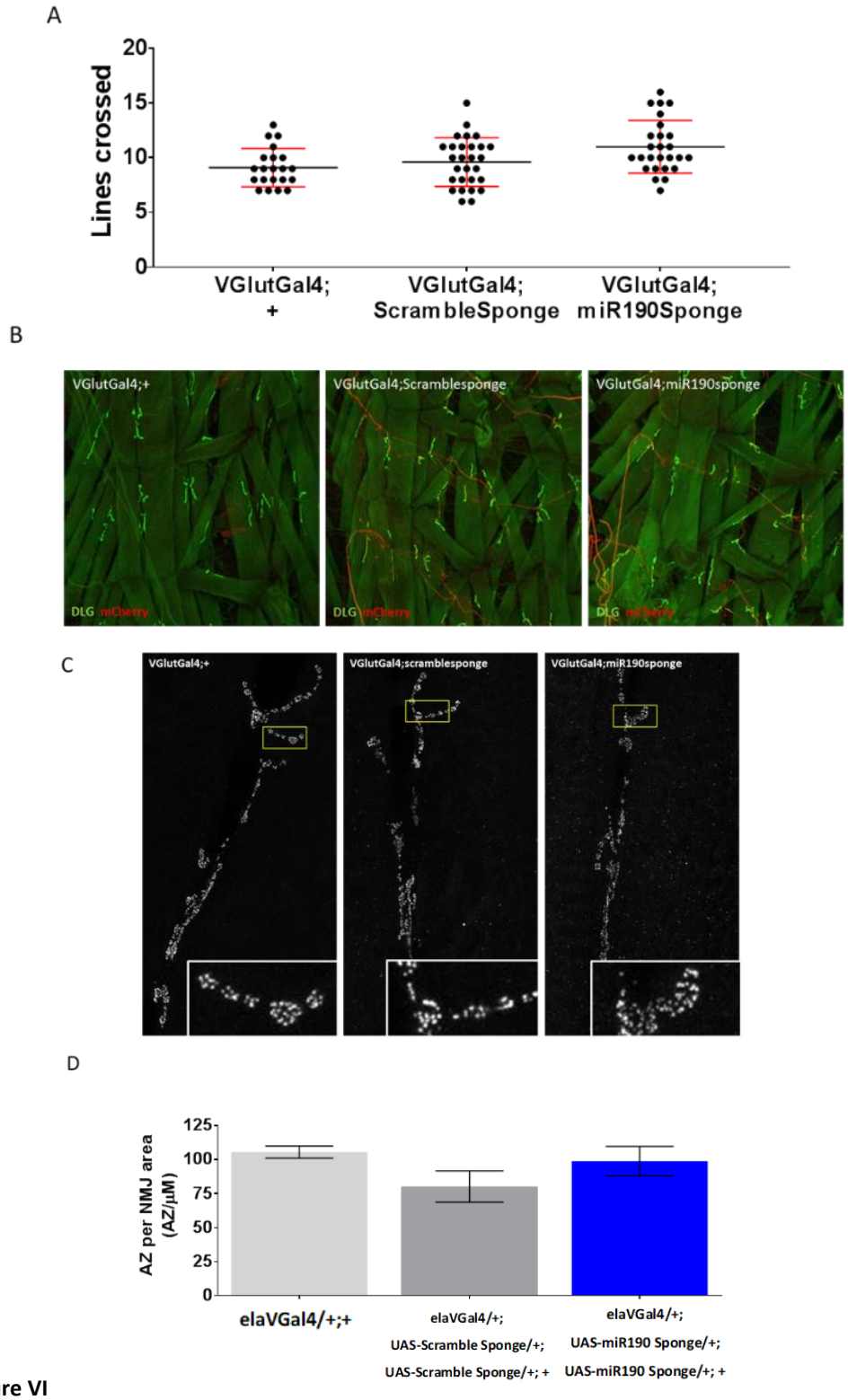


Figure VI

(a) Larval locomotion assay of *Drosophila* larvae of indicated genotypes. VGlutGal4 driven inhibition of miR-190 through the expression of a genetically encoded sponge does not produce significant defects in larval crawling distance. (b) DLG stain for postsynaptic active zones does not indicate any large scale disruptions in NMJ formation location or number with VGlutGal4 driven inhibition of miR-190 through the expression of a genetically encoded sponge. (c) Representative images of NMJ with nc82 stain for active zones (d) No significant alterations in active zone number are seen VGlutGal4 driven inhibition of miR-190 through the expression of a genetically encoded sponge
All error bars show mean +/- SEM.

Appendix VII. Professional internship for DTP student's reflection

As a requirement of the DTP studentship, I undertook a three month internship during the second year of my project, based within the volunteering department at the Marie Curie head office, London. Marie Curie is a charity which provides care and support to people living with a terminal illness.

During my internship at Marie Curie I engaged in two independent research projects for the volunteering team. One project was based on the development of new volunteer roles, which would enable Marie Curie to better support adolescents who are transitioning from child to adult palliative care systems. The other project was based upon the analysis of the volunteer engagement survey, and the development of the volunteering program to improve volunteer engagement and satisfaction based on the results of this.

Both of these projects involved communication and interaction with external organisations and individuals who had experience of palliative care. This helped me to develop skills in the presentation of myself as a representative of an organisation, whilst also remaining professional in light of challenging topics of conversation.

The placement was also in a completely different field to my own previous research and experience. This gave me a great chance to reinforce my existing skills in research, by going back to "stage one" and building up again. It highlighted to myself how much I had developed throughout the PhD programme, the skills which I possess and how these can be applied cross-discipline.

In addition to the experience working within a different sector, this internship placement also provided me with an opportunity to live and work in a different city. I found this challenging and I believe that the experience helped me to establish a better work/life balance, as I needed to form new social groups whilst working full time.

All in all I see the PIP as an important part of the BBSRC DTP studentship, through which I improved my study overall, mainly through strengthening existing skills, improving my confidence, and allowing me to experience a different working environment.